SIMPLE AND ENCAPSULATED TRANSITION METAL COMPLEXES OF SCHIFF BASES DERIVED FROM QUINOXALINE-2-CARBOXALDEHYDE AND DIAMINES: BIOLOGICAL AND CATALYTIC ACTIVITY STUDIES.

Thesis submitted to

Cochin University of Science and Technology

in partial fulfilment of the requirements for the degree of

Doctor of Philosophy

in

Chemistry

under the Faculty of Science

by

DIGNA VARGHESE

DEPARTMENT OF APPLIED CHEMISTRY

COCHIN UNIVERSITY OF SCIENCE AND TECHNOLOGY

KOCHI-682 022, KERALA, INDIA

August 2011

* *

"All wisdom is from the Lord, and with Him it remains forever."

* *

(The Holy Bible - Sirach 1/1)

Not just this thesis, but my whole life ….
is dedicated to my Pappa, Mummy and to
my Jesus Christ

Whose love and inspiration made me what
I am today…………

* *

Department of Applied Chemistry
Cochin University of Science and Technology
Kochi – 682 022

16-08-2011

Certificate

Certified that the thesis entitled **"Simple and encapsulated transition metal complexes of Schiff bases derived from quinoxaline-2-carboxaldehyde and diamines: biological and catalytic activity studies"** submitted by *Ms. Digna Varghese* is an authentic record of research work carried out by her under our supervision in partial fulfilment of the requirements for the degree of Doctor of Philosophy under the Faculty of Science of Cochin University of Science and Technology, and further that no part thereof has been presented before for any other degree.

Dr. P. A. Unnikrishnan   **Dr. K. K. Mohammed Yusuff**
(Co-Guide)   (Supervising Guide)

Declaration

I hereby declare that the work presented in the thesis entitled **"Simple and encapsulated transition metal complexes of Schiff bases derived from quinoxaline-2-carboxaldehyde and diamines: Biological and catalytic activity studies"** is entirely original and was carried out by me independently under the supervision of **Dr. K. K. Mohammed Yusuff** and **Dr. P. A. Unnikrishnan,** Department of Applied Chemistry, Cochin University of Science and Technology and has not been included in any other thesis submitted previously for the award of any other degree.

Kochi-22   **Digna Varghese**

16-08-2011

Acknowledgement ....

Any work can be perfect only by the cooperation and blessings of many people who have come along my life. I take this opportunity with much pleasure to remember all those people who have helped me through the course of my journey towards bringing out this thesis. First of all I stoop before my Lord Almighty for paving my way into the field of research and for the undeserving grace shown to me for completing this work. You have made my life more bountiful. May your name be exalted, honored, and glorified. Thank You for sharing all those wonderful people with me and for showing me Your love and care through them; the people who have contributed to the success of this thesis and to my personal growth as well.

The person to whom I am greatly indebted is my supervising guide Prof. K. K. Mohammed Yusuff for admitting me into the program. In my concept, the most important factor in research is to get a right person as the guide. I sincerely thank him for his guidance, inspiration, valuable suggestions and motivation. Apart from the subject of my research, I learnt a lot from him, which I am sure, will be useful in different stages of my life. His simplicity, moral ethics, patience, behaviour towards colleagues and students inspired me a lot. He has taught me group theoretical concepts when I have done M.Phil, which was helpful in my research field also. Sir, I consider it as a blessing to work under you. In this occasion I thank God for giving me an opportunity to work under him and I shall always cherish this association.

I invariably feel short of words to express my heartfelt gratitude and deep indebtedness to Dr. P. A. Unnikrishnan, my supervising co-guide for his efficient guidance through the awesome path of research with great patience. His constant encouragement and valuable suggestions at different stages were

really a great inspiration. I am greatly indebted to Prof. M.R. Prathapachandra Kurup for being my doctoral committee member.

With so much respect and admiration, I express my gratitude wholeheartedly to Prof. K. Sreekumar, Head of the Department, for providing all the facilities and support. I wish to express my sincere gratitude to Prof. K. Girish Kumar, Former Head, for the moral support and help offered at the time of joining and in the initial stages of my research.

The help and useful advice offered by the faculty members, Dr. S. Sugunan, Dr. S. Prathapan, Dr. N. Manoj, Dr. P. V.Mohanan and Dr. P. M. Sabura Begum, of this department during the crucial stages of my work and at times when I was confronted with chaos and confusion had been of much value and I am grateful to all of them for their kind heartedness. My deepest thanks go to all non teaching staff for always being there to assist with my needs.

I would like to express my deepest gratitude to Prof. M. V. Rajasekharan, Central University, Hyderabad, for giving me the opportunity to work in his research group, providing me with all necessary facilities and also for his invaluable guidance in crystal structure determination. I wish to express my warm and sincere thanks to Dr. Sarita G. Bhat, Head, Department of Biotechnology, CUSAT, Kochi, for helping me while doing DNA cleavage studies. I am greatly indebted to Dr. Ramadasan Kuttan, Research Director, Amala Cancer Research Centre, Thrissur, Kerala, for the cytotoxicity studies.

I would like to extend my sincere gratitude to Council of Scientific and Industrial Research (CSIR), New Delhi, for the award of a research fellowship during the tenure of this work. I would like to express my deepest gratitude to Department of Science and Technology (DST), India, for using the Sophisticated Analytical Instrumentation Facility (SAIF) at STIC Kochi, IIT

to share tons of fond memories and we had a lot of enjoyable moments during the evenings which made my CUSAT life so memorable. How many times we have spoken not only about magnetism and e.p.r., but also about dance!!! I am grateful to recall a lot of splendid memories I had with Anju, Manju, Seema, Nancy, Lorna chechi, Sheeja, Jinsa, Bibitha, Renjini, Asha, Sandhya and Suma in the hostel. Those days are so memorable and I would not like to miss them. I don't believe in goodbyes, only a long "I'll see you later". I will surely miss all our crazy and exciting times together but I know that someday our paths will cross again.

Where would I be without my family? My Pappa and Mummy deserve special mention for their unconditional support and prayers, for giving life in the first place, for educating me, with all the opportunities they could provide to explore my potentials and pursue my dreams ever since I was a child. As a typical parent in a middle class family, they worked industriously to support the family and did not spare any effort to provide the best possible environment for educating us. My Mummy is the one who sincerely raised me with her caring and constant prayers and she never failed to remind me to seek God's will in all things so that He will show you which path to take. Hence, this thesis is dedicated to them. I thank God Almighty for blessing me with such caring parents. My special thanks go to my brothers, Diji & Dixon and my sisters, Dimple & Dincy, for their love, support and motivation. I am also giving thanks to Beever, Christopher, Celine, Albert, Anna, Samuel and Sarah.

Digna Varghese

Preface

······❁······

Coordination chemistry is one of the most active research fields in chemistry today. It is mainly the chemistry of metal complexes derived from various types of ligands. The Schiff bases usually act as very effective coordinating ligands for the formation of mono-, di- or polynuclear complexes. In addition to their interesting ligational properties, both Schiff bases and their complexes have important biological and industrial applications. The great interest in these types of compounds is shown by a large number of publications ranging from purely synthetic and modern physico-chemical studies to biochemically relevant investigations.

This Ph.D thesis is mainly concerned with the synthesis and characterisation of new simple and zeolite encapsulated transition metal (manganese(II), nickel(II) and copper(II)) complexes of quinoxaline based double Schiff base ligands. These ligands are *N*,*N'*-bis(quinoxaline-2-carboxalidene) hydrazine, *N*,*N'*-bis(quinoxaline-2-carboxalidene)-1,2-diaminoethane, *N*,*N'*-bis(quinoxaline-2-carboxalidene)-1,3-diaminopropane, *N*,*N'*-bis(quinoxaline-2-carboxalidene)-1,4-diaminobutane, *N*,*N'*-bis(quinoxaline-2-carboxalidene)-1,2-diaminocyclohexane and *N*,*N'*-bis(quinoxaline-2-carboxalidene)-1,2-diaminobenzene. The Schiff base ligands have been characterised by spectral and single crystal XRD studies. These ligands provide great structural diversity during complexation. Mn(II) and Ni(II) form octahedral complexes with these Schiff bases, whereas Cu(II) forms both octahedral and tetrahedral complexes. Studies on the biological and catalytic activity of the copper(II) complexes are also presented in this thesis.

The thesis is divided into eight chapters. The work embodied in the thesis is mainly concentrated on familiarizing the synthesis, characterisation and applications of simple and encapsulated Schiff base complexes. Chapter 1 of the thesis gives a general introduction to the topic of research carried out. Chapter 2 presents details on the experimental techniques, synthesis and characterisation of Schiff bases. Chapters 3-5 deal with the synthesis and characterisation of Mn(II), Ni(II) and Cu(II) Schiff base complexes, respectively. Studies on the synthesis and characterisation of zeolite encapsulated Cu(II) Schiff base complexes are presented in Chapter 6. Chapter 7 deals with the studies on the catalytic activity of the encapsulated complexes towards cyclohexanol oxidation reaction. Chapter 8 presents the studies on the DNA binding properties and cytotoxicity of the copper(II) Schiff base complexes, which may find application as new anticancer drugs. We hope that the studies presented in the thesis would be useful to those working in the field of catalysis and medicine.

Contents

Chapter | 3 |

SYNTHESIS AND CHARACTERISATION OF MANGANESE(II) SCHIFF BASE COMPLEXES

Chapter | 4 |

SYNTHESIS AND CHARACTERISATION OF NI(II) SCHIFF BASE COMPLEXES

Chapter **5**

SYNTHESIS AND CHARACTERISATION OF CU(II) SCHIFF BASE COMPLEXES..124-189

Chapter **6**

SYNTHESIS AND CHARACTERISATION OF ZEOLITE ENCAPSULATED COPPER COMPLEXES....................................190-216

Chapter 7

STUDIES ON THE CATALYTIC ACTIVITY OF ZEOLITE ENCAPSULATED COPPER COMPLEXES

Chapter 8

BIOLOGICAL STUDIES OF COPPER(II) SCHIFF BASE COMPLEXES

****✿****

Chapter 1

Introduction

Coordination chemistry is undoubtedly most active area of research in inorganic chemistry. This branch of chemistry has now leaped into many areas of science such as analytical chemistry, medicinal chemistry, metallurgy, industrial chemistry and material science. It is mainly the chemistry of metal complexes derived from various types of ligands. A large number of Schiff bases have been synthesised and used as ligands. These ligands have largely played an important role in the development of coordination chemistry [1]. They have also played important roles in biological modeling [2-4], in designing molecular ferromagnets [5,6], in the development of liquid crystals [7,8], in catalysis [9,10] and in medical imaging [11].

Schiff bases are known for their synthetic accessibility, structural diversity and varied denticity. Recently, considerable attention of research activity has been focused on the design and synthesis of multifunctional coordination compounds with interesting structures and potential applications in various fields.

Multidentate Schiff base ligands can bind one, two, or more metal centers involving various coordination modes and allow successful synthesis of homo and/or heteronuclear metal complexes with interesting stereochemistry. Many of such complexes find application as homogeneous or heterogeneous catalysts. Comparative studies of catalytic activity of the transition metal complexes in the free and supported state have attracted a great deal of attention in recent years. The supported transition metal complexes showed high catalytic activities in comparison to the unsupported metal complexes and also provided opportunities for their recovery and recycle from a particular reaction process. This technique of immobilization of catalyst on an inert support increases the catalytic activity, selectivity, efficiency, operational flexibility and stability. The zeolite supported Schiff base complexes, as a result of their particular structure, display enhanced activity and selectivity in a multitude of organic reactions. The chemistry of zeolite encapsulated complexes has been an area of particular interest, because of their high activity, unique size and shape-selective catalytic properties. The zeolite encapsulated Schiff base copper complexes are reported to be catalytically active in oxidation of various organic compounds. As our work is focused on the synthesis, characterisation and application of new Schiff base complexes, the discussion in this chapter is limited to the Schiff bases, their metal complexes and general applications of Schiff base complexes with an emphasis on some catalytic and biological studies.

1.1 SCHIFF BASES

Schiff bases have recently been focused by the coordination chemists as versatile spacers because of their preparative accessibilities and structural varieties [12,13]. They are condensation products of primary amines with carbonyl compounds, and they were first reported by Hugo Schiff in 1864 [14]. These compounds are named after him and contain a carbon nitrogen double bond

with nitrogen atom connected to an aryl or alkyl group. These compounds are variously referred to as imines, azomethines, or anils. The nomenclature for compounds of this type is often variable. In *Chemical Abstracts* these materials are covered under the categories, imines and Schiff bases.

There are several reaction pathways to synthesise Schiff bases. The most common is an acid catalysed condensation reaction of amine and aldehyde or ketone in various solvents under different reaction conditions. The acid-catalyzed reaction is carried out by refluxing the carbonyl compound and amine with an azeotroping agent, if necessary. The formation of a Schiff base is given in scheme 1.1.
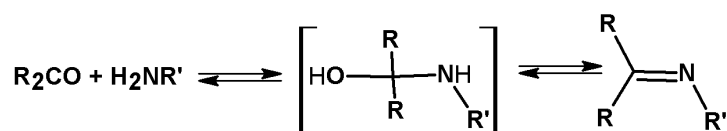
Scheme 1.1: Formation of Schiff base by condensation reaction (R groups may be variously substituted)

Ethanol and methanol, at room temperature or in refluxing conditions, are the solvents used for the preparation of Schiff bases. An attack of nucleophilic nitrogen atom of amine on the carbonyl carbon results in an unstable carbinolamine intermediate. The reaction can reverse to the starting materials, or form a C=N bond by the elimination of hydroxyl group. Many factors like pH of the solution, steric and electronic effects of the carbonyl compound and amine affect this condensation reaction. Fairly high yields of imines can be obtained by using acidic catalysts and removing water from the reaction mixture [15]. The presence of dehydrating agents normally favours the formation of Schiff bases. Magnesium sulphate is commonly employed as a dehydrating agent. The water produced in the reaction can also be removed from the equilibrium using a Dean Stark apparatus for the syntheses conducted in toluene or benzene.

Degradation of the Schiff bases can occur during the purification step. Chromatography of Schiff bases on silica gel might result in the decomposition of the Schiff bases through hydrolysis. In such cases, purification of the Schiff base can be done by crystallization. If the Schiff bases are insoluble in hexane or cyclohexane, they can be purified by stirring the crude reaction mixture in these solvents. A small portion of a more polar solvent can also be added to these solvents to eliminate impurities. In general, Schiff bases are stable solids and could be kept in dry conditions for a longer period without decomposition.

The common structural feature of this compound is the azomethine group, which can be designated structurally as RR′C=NR″, where R, R′ and R″ are alkyl or aryl substituents or hydrogen at the point of attachment to the imino (C=N) carbon or nitrogen. There are two classes of imines based on the R group attached to the azomethine groups: aldimines and ketimines. Aldimines are compounds in which R is alkyl or aryl and R′ is hydrogen; while ketimines are compounds in which both R and R′ are alkyl or aryl. Schiff base ligands derived from ketones are formed less readily when compared to those derived from aldehydes.

Schiff bases of aliphatic aldehydes are relatively unstable and easily polymerizable [16]. In these cases, the imine initially formed undergoes subsequent aldol condensations, which can be avoided by using amines attached with tertiary alkyl group. Steric hindrance makes such aldol condensations difficult to undergo [17]. Tertiary aliphatic and aromatic aldehydes react readily and nearly quantitatively with amines to give the corresponding imines even at room temperature. In the case of aromatic aldehydes, the imines are formed quantitatively even without the removal of the water formed during the reaction [16]. Several studies showed that the presence of a lone pair of electrons in a sp^2 hybridized orbital of nitrogen atom of the azomethine group is of considerable

chemical and biological importance [18-20]. Examples of a few Schiff bases are given in Figure 1.1.

N,N'-bis(pyridin-3-carboxalidene) -1,2-diaminoethane

N,N'-bis(3-nitrobenzylidene)-1,4-diaminobutane

N,N'-bis(3-bromobenzylidene)-1,4-diaminobutane
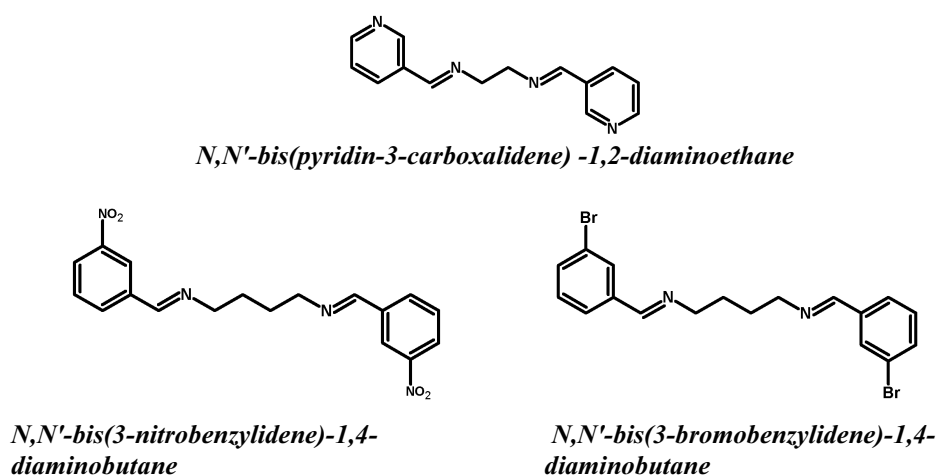
Figure 1.1: Some examples of Schiff bases (Adopted from ref. [21- 23])

The family of Schiff bases derived from diamines and phenolic aldehydes has proved to be the source of versatile ligands for many transition metals. The composition of the products formed in these reactions is determined by several factors, of which the nature of the starting diamine is the most important. All diamines used can be divided into three groups: the most nucleophilic and most flexible (aliphatic ones), nucleophilic and rigid (cycloaliphatic), and slightly nucleophilic and rigid diamines (aromatic ones). Stability of Schiff bases depend upon the strength of C=N bond, the basicity of amino group and steric factors. The spectral (UV-Visible, IR, NMR and Mass spectra) characterisation and single crystal X-ray diffraction techniques are used to determine the structure of Schiff bases and the spectral data of imines depend too much on substituents [24, 25]. The review by Holm, Everett and Chakravorty [26] gives some interesting information on the structure and properties of these types of ligands.

Schiff bases generally possess nitrogen donor atoms. Presence of functional group like –OH or –SH close to the azomethine group assists to form a five or six membered ring (chelate) with the metal ion [27, 28]. Thus the stability of the complex can be increased by chelate effect. Schiff bases formed from salicylaldehyde and o-hydroxy naphthaldehyde meets this requirement. When the aldehyde is a salicylaldehyde derivative and the amine is a diamine derivative, the condensation produces interesting N_2O_2 Schiff base compounds. These types of ligands are called salen ligands. The term salen was originally used to describe the tetradentate Schiff bases derived from salicylaldehyde and ethylenediamine. Now the term salen-type is used in the literature to describe the class of (O, N, N, O) tetradentate bis-Schiff base ligands/double Schiff bases. They are reported to have common features with porphyrins with respect to their electronic structures [29]. Some examples of salen type Schiff bases are given in Figure 1.2.

N,N'-bis(salicylidene)-1,6-diaminohexane

N,N'-bis(salicylidene)-1,2-diaminoethane (salen)

N,N'-bis(salicylidene)-1,2-diaminobenzene
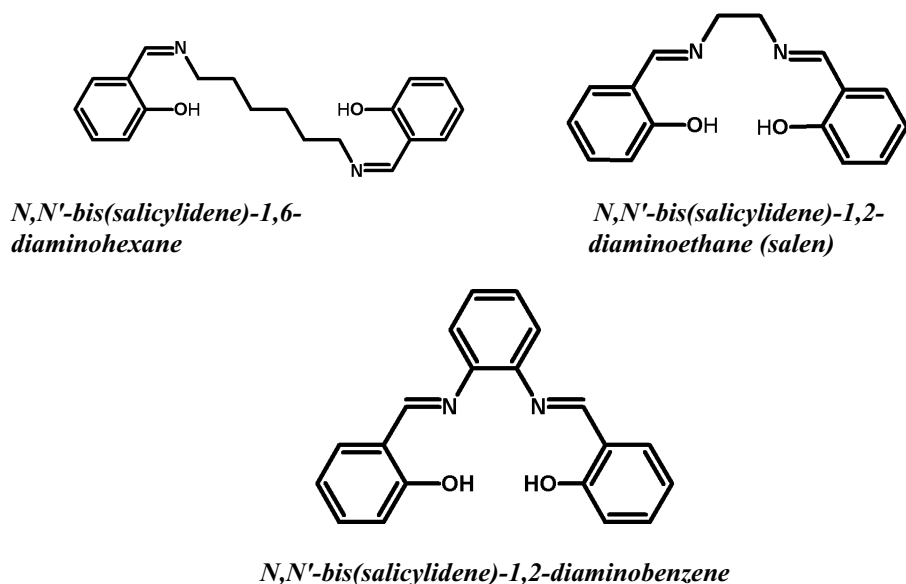
Figure 1.2: Some examples of N_2O_2 Schiff base compounds (Adopted from ref. [30,31])

The use of organic spacers and metal ions to promote the self-assembly of organic-inorganic polymeric coordination frameworks has become a very active and important synthetic strategy recently. Dong *et al.* [32] suggested that there are various factors affecting the formation of the coordination polymers or supramolecular complexes. Among these, the choice of organic ligand is the most important one. Properties of organic spacers, such as coordination activity, length, geometry, and relative orientation of the donor groups, play a very important role in dictating polymer framework topology. These types of organic ligands are given in Figure 1.3.

Figure 1.3: Double Schiff base ligands used in the construction of polymeric metal-organic complexes (Adopted from ref. [32])

Generally, diamine Schiff bases are quite familiar as tetradentate ligands. They are different from monoamine Schiff bases in having two chromophores bridged by a methylene chain in a molecule, and thus the mutual interactions between the chromophores appear to affect their chemical and physical properties. It has been reported that monoamine Schiff bases show strong fluorescence through the proton transfer between the hydroxyl and azomethine groups in the chromophore. Therefore, interesting optical properties derived from the interaction between the two chromophores in the diamine Schiff bases could be expected. One of the examples for this was found with *N,N'*-bis(salicylidene) - 1,4-diaminobutane and its analogues. These compounds show very strong fluorescence in the solid state under ultraviolet irradiation [33]. Their fluorescence intensities are extremely influenced by the length of the bridge between the two chromophores. Kawasaki *et al.* reported [34] the synthesis of

thirteen *N,N'*-bis(α-substituted salicylidene)diamines [Figure 1.4] and examined their absorption, excitation and fluorescence properties in solution with the purpose of obtaining information about the influence of bridge length on their optical properties. The effects of solvent and substituents on the fluorescence intensity were also investigated to obtain fundamental information about the factors responsible for their optical properties. Proton transfer between the hydroxyl and azomethine groups in the Schiff base is dominant and leads to strong fluorescence. Polar solvents tend to give stronger fluorescence than non-polar solvents.
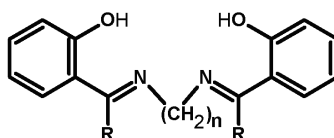
R = H, CH$_3$, C$_2$H$_5$, C$_6$H$_5$; where n is the subscript: n = 2 to 12

Figure 1.4: N,N'-bis(α-substituted salicylidene)diamines (Adopted from ref. [34])

Diamines can form macrocyclic ligands with dicarbonyl compounds [35]. Schiff base macrocycles have generally been prepared *via* the cyclocondensation of the appropriate dicarbonyl and polyamine precursors using metal template reactions [36]. Macrocyclic ligands [37-40] behave as model ligands for natural enzymes, as metal ion selective ligands and as metal chelating agents for medical purposes. They can provide transition metals with unusual ligand environments and consequent novel chemical properties such as stabilization of high and low oxidation states, lessening of ligand lability through the chelating effect and possibility of having several metal atoms in close steric proximity within the same molecule. Macrocyclic ligands with additional donor atoms appended to the ring have generated considerable interest because of their capacity to bind metal ions, the potential to prepare and study their mixed-valance forms, and their ability to

act as models for metalloproteins. A few Schiff base macrocycles are shown in Figure 1.5.
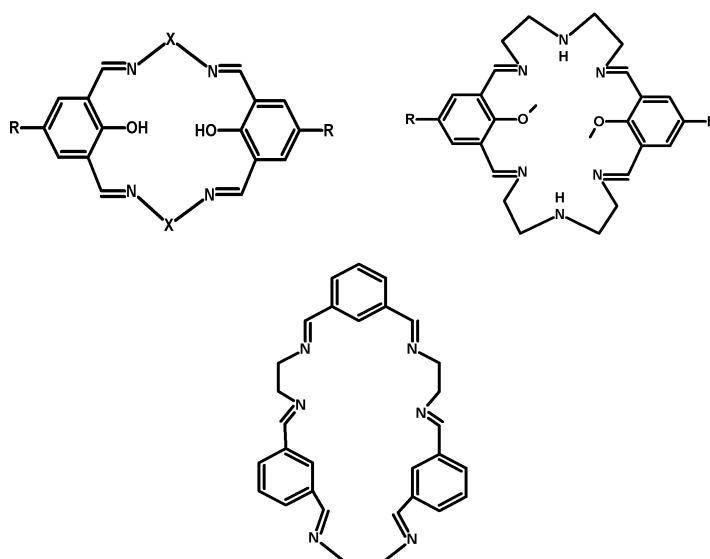
Figure 1.5: Macrocyclic Schiff bases (Adopted from ref. [41])

1.2 SCHIFF BASE COMPLEXES

The chelating Schiff base ligands derived from diamines such as 1,2-ethanediamine, 1,3-propanediamine and 1,4-butanediamine and various carbonyl compounds encompass a highly remarkable class of compounds. The presence of groups like carbonyl or hydroxyl close to the azomethine moiety increases the coordinating effect of the lone pair of electrons thereby increasing the stability of the metal complexes. Thus, functionally substituted Schiff bases bearing additional donor groups represent the most important class of heteropolydentate ligands. Majority of the transition metal complexes reported are those formed with Schiff base ligands. These complexes find a wide range of applications in catalytic, synthetic, analytical, clinical and biochemical areas and in addition they possess considerable physiological activities.

Schiff base transition metal complexes are one of the most adaptable and thoroughly studied systems [42,43]. They are of both stereochemical and magnetochemical interest due to their preparative accessibility, diversity and structural variability [44]. The results of studies on Schiff base complexes provide insight into coordination sphere effects caused by the different ligands employed, such as the influence of the total charge, the steric hindrance, and electronic effects of the ligands on the structures, properties, and the reactivity of the complexes. Various reports about the Schiff base complexes of first transition series metals like, vanadium [45], chromium [46], manganese [47], iron [46], cobalt [48], nickel [49, 50], copper [51, 52] and zinc [53] are available in the literature. However, we limit the discussions to Schiff base complexes of copper(II), manganese(II) and nickel(II) ions, as our work is focused on complexes of these metal ions.

Of the various classes of Schiff base, those derived from salicylaldehyde and primary amines are very popular due to diverse chelating ability [54]. In many catalytic applications Schiff base metal complexes are prepared in situ. Cozzi [47] in his review has outlined five different synthetic routes that are commonly employed for the preparation of Schiff base metal complexes [Figure 1.6]. Route 1 involves the use of metal alkoxides $(M(OR)_n)$, which are sensitive to hydrolysis. The presence of adventitious water can result in the formation of μ-oxo species and therefore traces of water have to be avoided. In route 2, metal amides, $M(NMe_2)_4$ (M = Ti, Zr), are used for the preparation of Schiff base metal complexes of early transition metals. A Schiff base metal complex can be prepared in a clean and effective way using metal alkyl complexes (route 3). Various metal alkyls in the main group of metals $(AlMe_3, GaMe_3,$ and $InMe_3)$ can be used in the preparation of Schiff bases by a direct exchange reaction. Through route 4, many Schiff base metal complexes can be obtained by the treatment of the Schiff base with the corresponding metal acetate under reflux conditions.

Copper, cobalt and nickel Schiff base complexes are prepared using the metal acetates. The synthetic scheme presented in route 5 is quite effective in obtaining salen metal complexes. It consists of a two-step reaction involving the deprotonation of the Schiff bases and a successive reaction with metal halides.
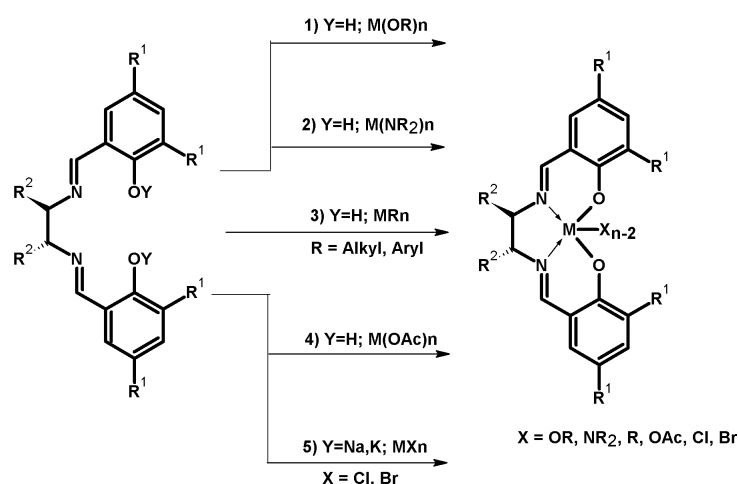
Figure 1.6: Synthetic routes of Schiff base complexes (Adopted from ref. [47])

Nowadays, the research field dealing with Schiff base metal complexes embraces very wide and diversified subjects comprising vast areas of organometallic compounds and various aspects of bioinorganic chemistry [55]. Only a brief discussion on synthesis and characterisation of Schiff base metal complexes is attempted here as numerous literature reviews are available on these aspects [56,57]. A number of metal complexes with multidentate Schiff base ligands have been reported [58,59]. An example for such complex is [N,N′-bis(3,5-di-*tert*-butylsalicylidene)-1,2-cyclohexanediaminomanganese(III)]chloride [Figure 1.7], where the coordination takes place through the N_2O_2 donor set. This well known Schiff base complex is known as Jacobsen's catalyst [60,61]. The Schiff base for this complex was prepared by the condensation reaction between trans-1,2-diaminocyclohexane and 3,5-di-*tert*-butyl-2-hydroxybenzaldehyde.
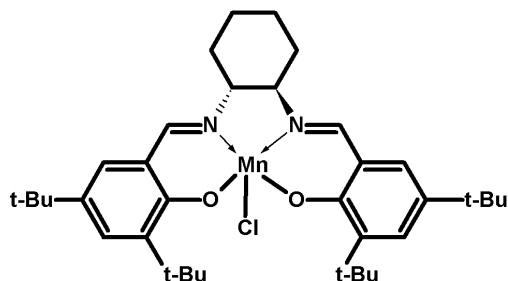
Figure 1.7: Jacobsen's catalyst

The stereochemistries of metal complexes vary according to their coordinated ligands [62-68]. For example, in the case of the complexes of the double Schiff bases derived from aliphatic diamines, [Figure 1.8] as the length of methylene group between the azomethine groups increases from two, the ligand field produced becomes much weaker and lowers the capacity of Ni(II) to bind additional ligands (such as pyridine), which could be confirmed through photophysical investigations. [Ni(salen)] complex does not bind pyridine and maintains four coordinate square planar configuration while [Ni(saltn)] (saltn is N,N′-bis(salicylidene)-1,3-diaminopropane) forms a six coordinate octahedral complex when dissolved in pyridine.

B= $(CH_2)_x$. x = 2, 3, 4, 5
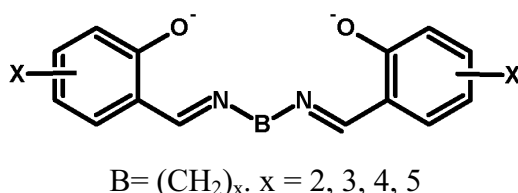
Figure 1.8: Bis(N-alkyl- or bis(N-aryl-salicylideneaminato) Ligand

Tai *et al*. [69] reported the synthesis and spectroscopic properties of Mn(II), Co(II) and Cu(II) complexes with a novel Schiff base ligand derived from 2,2′-bis(p-methoxylphenylamine) and salicylaldehyde. Liu *et al*. [70] synthesised two tetradentate ligands, N,N′-bis[4-(benzeneazo)salicylaldehyde]-o-phenylenediamine and N,N′-bis[4-(benzeneazo)salicylaldehyde]ethylenediamine. These ligands form

complexes with copper(II), nickel(II) and manganese(II) ions. The metal ions are bonded to the Schiff base through the phenolic oxygen and the imino nitrogen as illustrated in Figure 1.9.
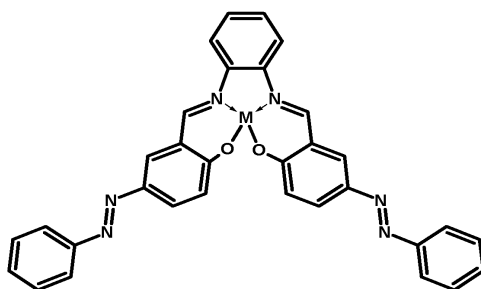
Figure 1.9: Schiff base complex, M=Cu, Ni, or Mn.

Datta *et al*. [71] described the synthesis, characterisation and structural studies of Ni(II) complexes with tetradentate Schiff base ligand. In this complex, the ligand is symmetric since all four nitrogen atoms are identical. The square planar N_4 coordination sphere is slightly distorted as indicated by the bond angles 174.8 (2)° and 171.0 (2)° for N(17)---Ni---N(7) and N(1)---Ni---N(11), respectively. The two aromatic rings in this compound are planar. Therefore the coordination around Ni(II) is rather distorted than planar [Figure 1.10].
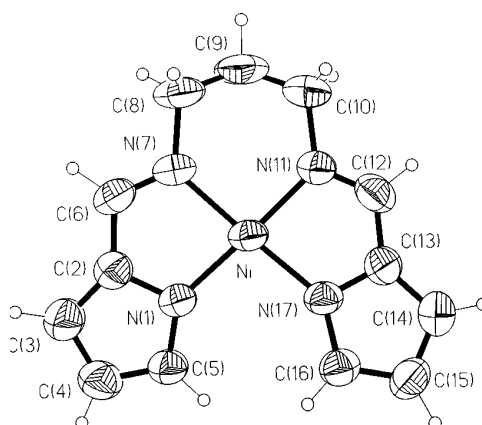
Figure 1.10: ORTEP diagram of [Ni(C₄H₃NCH=N-(CH₂)₃ -N=CHC₄H₃N)]
(Adopted from ref. [71])

A new mononuclear Cu(II) complex, [CuL(ClO$_4$)$_2$], where L is a symmetrical tetradentate di-Schiff base, N,N′-bis(1-pyridin-2-yl-ethylidene)-1,3-diaminopropane, was characterised by single crystal X-ray crystallography [72]. The copper atom assumes a tetragonally distorted octahedral geometry with two perchlorate oxygens coordinated very weakly in the axial positions [Figure 1.11].
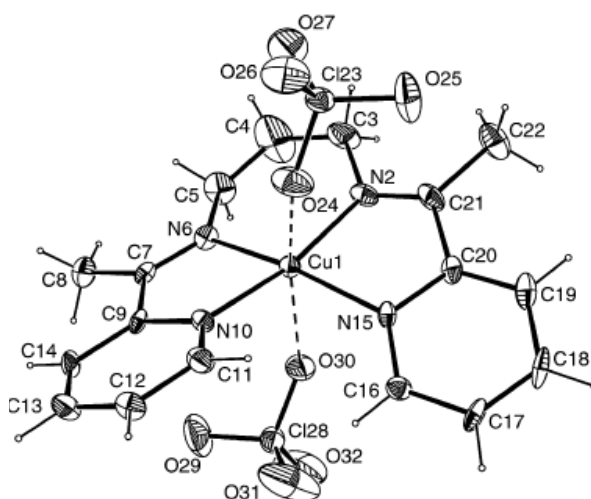
Figure 1.11: ORTEP diagram of [CuL(ClO$_4$)$_2$] (Adopted from ref. [72])

Binuclear transition metal complexes have received much attention [73-75]. The chelating ligands with excess of metal salts may lead to the synthesis of binuclear metal complexes. An example for a binuclear complex is [Cu$_2$(L)$_2$($\mu_{1,1}$-N$_3$)$_2$] [Figure 1.12], where L [L = CH$_3$C(O$^-$)=N-N=CH-C$_5$H$_4$N] is a tridentate ligand [76]. This complex is a centrosymmetric dimer in which the copper centers are five coordinate and are bonded to three coordinating N$_2$O atoms from the ligand L and nitrogen atoms from two bridging azide anions. The structural study reveals square pyramidal coordination geometry for the copper ions. There are reports for the formation of polynuclear complexes with transition metals from double Schiff base ligands [76-78].
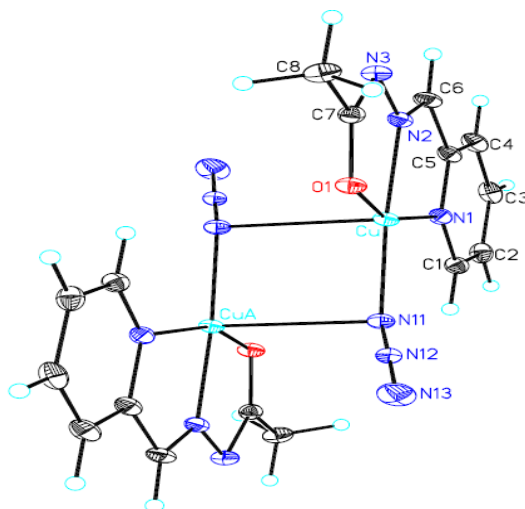
Figure 1.12: ORTEP diagram of [Cu$_2$(L)$_2$($\mu_{1,1}$-N$_3$)$_2$] (Adopted from ref. [76])

Hetero-dinuclear metal complexes with double Schiff bases have been less studied compared to their homo-dinuclear complexes. These complexes are interesting because of the possible magnetic interactions between two different metal ions. Magnetic susceptibility measurements are useful in understanding the spin exchange mechanism in antiferro- or ferromagnetic coupling [79-81]. One such complex (hetero-dinuclear Cu^{II}Mn^{II} complex) is prepared in two steps. Firstly the Schiff base ligand N,N′-bis(2-hydroxy-3-meythoxybenzylidene)-1,3-diaminopropane is interacted with copper acetate in hot methanol to form green crystalline powder of N,N′-bis(2-hydroxy-3-methoxybenzlidene)-1,3-diaminopropane] copper(II) **(a)** [Figure 1.13(a)]. In a second step, manganese acetate dissolved in methanol was added to a solution of **(a)** in dimethylformamide and was heated under reflux for 3 h. The prismatic light green crystals of **(b)** were formed [Figure 1.13(b)].

(a)   (b)
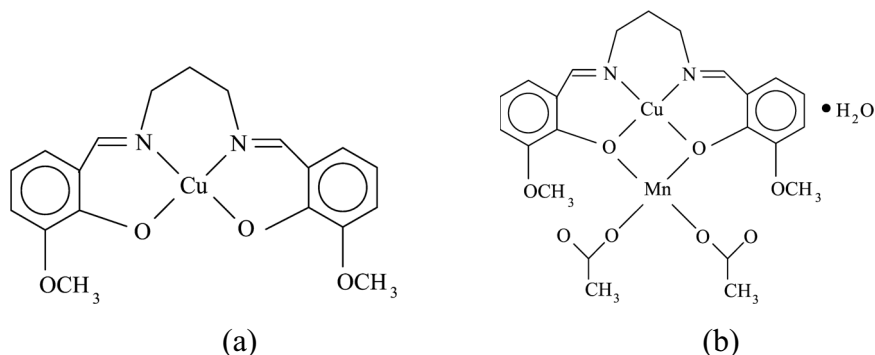
Figure 1.13: Hetero-dinuclear Cu^{II}Mn^{II} complex (Adopted from ref. [81])

Macrocyclic complexes have several applications in fundamental, applied sciences and in the area of coordination chemistry [82-86]. The stability of macrocyclic metal complex depends upon a number of factors, including the number and type of donor atoms present in the ligand, their relative positions within the macrocyclic skeleton and the number and size of the chelate rings formed on complexation. One example is given here from the reports of Temel and Ilhan [86]. They synthesised Cu(II) complexes [Figure 1.14] by template effect by the reaction of 2,6-diaminopyridine and aldehydes and $Cu(ClO_4)_2 \cdot 6H_2O$.
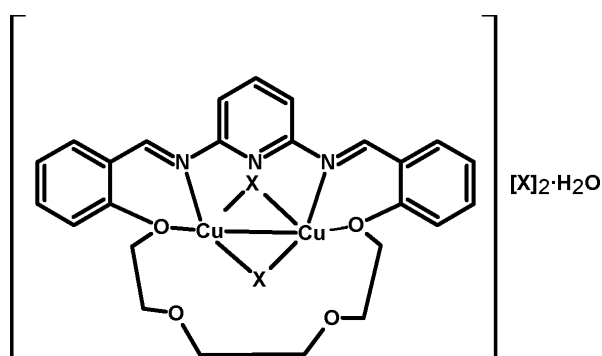
Figure 1.14: Macrocyclic copper(II) complex [Cu$_2$(L^5)(ClO$_4$)$_2$](ClO$_4$)$_2 \cdot$H$_2$O (Adopted from ref. [86])

1.3 QUINOXALINE BASED SCHIFF BASES AND COMPLEXES

The chemistry of heterocyclic compounds is one of the most complex and intriguing branches of organic chemistry. Quinoxalines represent an important class of nitrogen containing heterocycles and have gained increasing attention in recent years due to their different applications in various areas. They are bicyclic, heteroaromatic systems widely distributed in nature. Quinoxalines are also called benzopyrazines, as these compounds contain benzene ring fused with pyrazine ring.

There are numerous synthetic strategies for the preparation of substituted quinoxalines. The most common method relies on the condensation of an aryl 1,2-diamine with 1,2-dicarbonyl compound in refluxing ethanol or acetic acid. Brown reported a well known method for the synthesis of quinoxaline from orthophenylenediamine and 1,2-dicarbonyl compound [87]. There is another method for the synthesis of quinoxaline derivatives, which involves the condensation of 1,2-diamine with 1,2-dicarbonyl compounds in the presence of binary metal oxides supported on Si-MCM- 41 mesoporous molecular sieves [88]. Heravi *et al*. reported Suzuki-Miyaura coupling reaction for the synthesis of 2,3-disubstituted quinoxalines [89]. Synthesis of 3-hydroxyquinoxaline-2-carboxaldehyde involves preparation of 3-hydroxy-2-methylquinoxaline, 3-hydroxy-2-dibromomethylquinoxaline and subsequent conversion of the latter to the aldehyde. The complete procedure for the preparation is reported in a recent article of Arun *et al*. [24].

Quinoxaline derivatives exhibit a broad spectrum of biological activities [90,91] and act as medicinally useful agents [92-95]. It is an integral part of various antibiotics such as echinomycin, levomycin and peptide triostin [96-100]. They are reported to have useful antibacterial, antimicrobial, antidepressant, anticancer, anti-inflammatory, analgesic, antioxidant, tuberculostatic, antimalarial

and anti HIV activities [101-104]. They also find place in the chemical libraries for DNA binding [105,106].

Organic compounds are important for photonic devices because of their non-linear optical properties [107]. In recent years, numerous reports on the photophysical properties of quinoxalines have appeared [108,109] such as fluorescent materials [110], organic light emitting devices [111] and dyes [112]. They have been incorporated in polymers for being used as electron transport materials in multilayer OLEDs [113,114]. Quinoxaline derivatives are also used as analytical reagents for the determination of metal ions [115]. Transition metal complexes with quinoxaline derivatives have also gained attention as catalysts [116].

The properties of quinoxaline based Schiff bases are expected to be quite interesting. The presence of electron withdrawing ring system in any ligand decreases the availability of the lone pair of electrons. Therefore, Schiff bases with an electron withdrawing ring system derived from quinoxaline-2-carboxaldehyde would be weaker than the Schiff bases derived from salicylaldehyde. But the increase in coordination site increases the stability of the complexes by chelate effect. Therefore the electronic environment in the metal complexes of this Schiff base might be different from those derived from salicylaldehyde. A literature search reveals that there are only a few reports about the Schiff base complexes of quinoxaline [117-119]. Most of the reports are from our group [24,116, 120-128].

Quinoxaline compounds show tautomerism if they have a hydroxyl, thiolic or amino group at the ortho position [87]. For example, hydroxyquinoxalines and their derivatives exhibit prototropic amide-iminol tautomerism and most of them exist in the predominant amide form in the solid state [24, 107]. This type of

tautomerism exhibited by a Schiff base, 3-hydroxyquinoxaline-2-carboxalidine-4-aminoantipyrine, is illustrated in Figure 1.15.
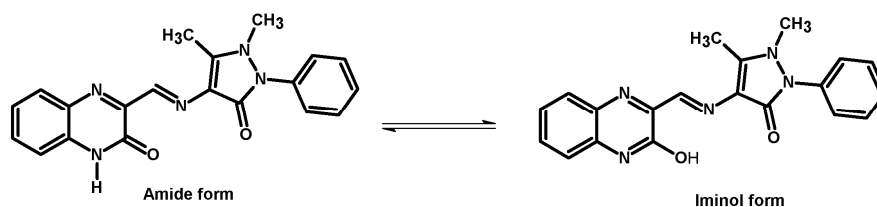
Figure 1.15: Amide-iminol tautomerism in 3-hydroxyquinoxaline-2-carboxalidine-4-aminoantipyrine (Adopted from ref. [121])

In recent years, numerous reports on the photophysical properties of quinoxalines have appeared [24,121]. The Schiff base, *hqcdmn*, synthesised by the condensation of 3-hydroxyquinoxaline-2-carboxaldehyde and 2,3-diaminomaleonitrile [24], exhibits prototropic tautomerism [Figure 1.16]. This Schiff base exhibits positive absorption and fluorescent solvatochromism and large stokes shift. This compound is a suitable candidate for application as fluorescent and charge transport dyes.
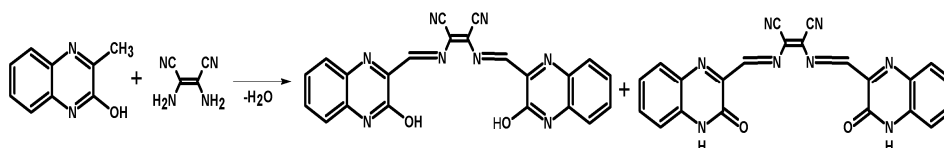
Figure 1.16: Synthesis of *hqcdmn* (Adopted from ref. [24])

The nitrogens in the quinoxaline unit can be an acceptor for hydrogen bonding [129] and may lead to polymeric structures. There are reports about the formation of coordination polymers [32]. Such a type of quinoxaline based ligand, which is responsible for the formation of coordination polymers, is given in Figure 1.17. The special geometry of bisazomethines, including the different relative orientations of N donors and the zigzag conformation of the –RC=N-

N=CR- moiety between the two terminal coordination groups, may result in coordination polymers with novel network patterns.
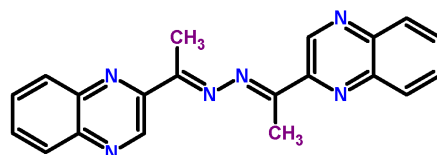
Figure 1.17: Bipyrazine ligand used in the construction of polymeric metal-organic complexes (Adopted from ref. [32])

By careful control of the synthetic conditions employed, a few crystal structures of quinoxaline based Schiff bases have been reported. One example for the crystal structure of Schiff base derived from quinoxaline-2-carboxaldehyde is N-[(E)-quinoxalin-2-ylmethylidene]-1H-indazol-5-amine [122]. This compound is non-planar due to the twisting of rings with respect to azomethine group. In the crystal structure, molecules are held together by π–π stacking interactions and N—H···N intermolecular hydrogen bonding.

A novel Schiff base, quinoxaline-2-carboxalidene-2-aminophenol, is formed by the condensation of quinoxaline-2-carboxaldehyde with 2-aminophenol. Complexes of mangenese(II), nickel(II) and copper(II) ions with this schiff base were reported [120]. The crystal structure of a mononuclear cobalt(II) complex [CoL$_2$]·H$_2$O, given in Figure 1.18, where L is quinoxaline-2-carboxalidine-2-amino-5-methylphenol, was recently reported [123]. The Schiff base was obtained by the condensation of quinoxaline-2-carboxaldehyde and 2-amino-5-methylphenol. The crystallographic study shows that the cobalt(II) coordination sphere is distorted octahedrally with a cis arrangement of N$_4$O$_2$ donor set of two tridentate NNO Schiff bases. A Ni(II) complex of the same ligand, [NiL$_2$]·H$_2$O, with structure similar to that of the cobalt(II) complex, has been reported [125].
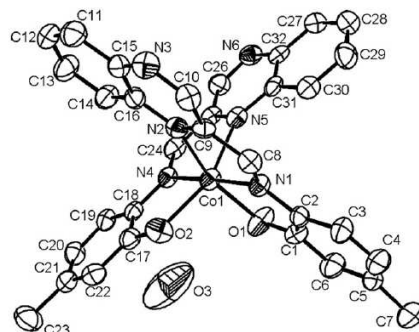
Figure 1.18: ORTEP diagram of [CoL$_2$]·H$_2$O (Adopted from ref. [123])

1.4 APPLICATIONS OF SCHIFF BASES AND COMPLEXES

Schiff base complexes [130,131] of various transition metals have been investigated due to their coordinating capability and their applications in various fields. Oxygen and nitrogen donor Schiff bases (salen type) are of particular interest because of their ability to form transition metal complexes with unusual configurations, structural lability, and sensitivity to molecular environments [132,133]. Schiff base complexes have proven effective in constructing supramolecular architectures such as coordination polymers and helical assemblies [134-136]. They have been found to be associated with biological activities [137,138], such as, antibacterial, antiviral, and antimalarial action [139-141]. The Schiff base complexes also exhibit catalytic activity [142] and act as homogeneous and heterogeneous catalysts in various reactions [127,116]. The Schiff base complexes can also serve as efficient models for the metal containing sites in metalloproteins and enzymes [142,143]. There are Schiff base complexes, which show interesting photochromic properties [144] and magnetic properties [145]. Salicylaldimine based ligands are of considerable interest due to their potential applications in the development of photonic devices [146,147].

1.4.1 Biological applications

Schiff base complexes are becoming increasingly important as biochemical, analytical and antimicrobial reagents [148-150]. It is found that some drugs have greater activity when administered as metal complexes than as free organic compounds. The Schiff base complexes derived from 4-hydroxysalicylaldehyde and amines have strong anticancer activity, e.g., against Ehrlich Ascites Carcinoma (EAC) [151,152]. The discussion in this part is limited to DNA cleavage and cytotoxicity studies of metal complexes.

The clinical success of cisplatin as anticancer agent constitutes the most important contribution to the use of metals in medicine. The main cellular target for platinum drugs is genomic DNA. Major antitumor activity results from intrastrand crosslinks and the formation of DNA kinks [153]. For this reason, considerable efforts are still ongoing to find more effective DNA targeting drugs. Metal complexes are known to interact with DNA and such complexes are called as chemical nucleases. Natural nucleases cleave the phosphate diester backbone of DNA by hydrolysis, while chemical nucleases cleave DNA by oxidatively degrading the deoxyribose moiety or by hydrolysis of the phosphate ester. Chemical nucleases present some advantages over conventional enzymatic nucleases in that they are smaller in size and thus can reach more sterically hindered regions of DNA. The most efficient chemical nucleases contain redox-active Cu and/or Fe, or the redox-inactive Zn in their active sites [154]. Among these transition metal complexes, copper complexes with a nitrogen donor heterocyclic ligand play an important role due to their structural diversity and are used to improve nuclease activity. Many reports are available for the DNA cleavage by using Schiff base complexes [155-160].

Kou *et al*. have synthesised and characterised five binuclear copper(II) complexes with Schiff base ligand N,N′-bis(3,5-*tert*-butylsalicylidene-2-

hydroxy)-1,3-propanediamine [159]. This complex can effectively promote cleavage of plasmid DNA without addition of external agents and in the presence of hydrogen peroxide at pH = 7.2 and 37 $^{\circ}$C.

Three new Schiff bases derived from 2-oxoquinoline-3-carbaldehyde and their Cu(II) complexes are reported to exhibit good binding activity with CT-DNA [160]. The binding mode is intercalative. Among the three copper complexes, the most active compound is given in Figure 1.19. The cytotoxicity studies of the three Cu(II) complexes were conducted in vitro and the biological assays suggest that the Cu(II) complexes exhibit higher activity than corresponding ligands against HeLa and HL-60 cells.
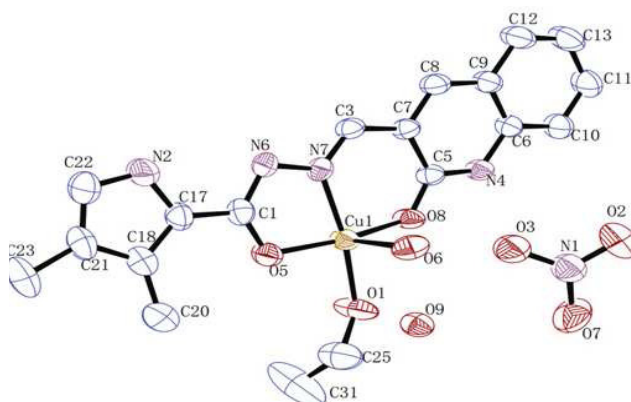
Figure 1.19: Copper Schiff base complex of 2-oxoquinoline-3-carbaldehyde (Adopted from ref. [160])

Many more Schiff base complexes are also claimed for cytotoxic activities [154,158,160]. The cytotoxic properties of the ligands [Figure 1.20] and their Cu(II) complexes were evaluated on the following human cancer cell lines: prostate cancer PC-3 cells, breast cancer MCF-7 cells, A2780 human ovarian carcinoma cells and the respective cisplatin resistant cell line (A2780cisR). The ligands and their complexes have shown a similar cytotoxicity activity against

A2780 and A2780cisR cell lines, with resistance factors (RF) factors spanning between 0.89 and 1.40 and much lower than the RF of 8.9 presented by cisplatin.
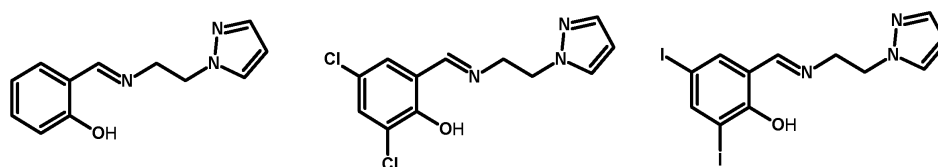
Figure 1.20: Schiff base ligands responsible for cytotoxicity (Adopted from ref. [154])

1.4.2 Catalytic applications

Catalysts have played a vital role in organic transformations as they have wide range of applications in chemical industries and have major impact on the quality of human life as well as on economic progress. Complexes of the salen ligand and its derivatives have been known since 1869 [161] and they are known to act as good catalysts in many organic reactions. Some of the chiral Schiff base complexes were specifically used in catalytic asymmetric synthesis.

A great effort has been devoted to the research and development of new catalysts for the industrially important oxidation of organic substrates. Epoxidation is one of the fundamental reactions in industrial organic synthesis. Epoxides are highly reactive compounds, which can be converted to various products of great importance. Manganese(III) salen complexes have been the subject of intensive investigations over the past years, as they act as excellent catalysts for the chiral and achiral epoxidation of alkenes [162,163]. The manganese(III) complexes derived from nonracemic trans-1,2-diaminocyclohexane were first studied in the 1960s [164-166] and they have been widely used especially in catalytic asymmetric epoxidation of non-functionalised olefins [167-169]. The best active catalyst known for an alkene epoxidation is Jacobsen's

catalyst [149] whereas the most selective catalysts are those developed by Katsuki [170].

Lee *et al*. [171] studied the development of Schiff base complexes of Mn(III) as the catalyst for olefin oxygenation to alcohols in the presence of NaBH$_4$. By screening various Mn(III) complexes, it was found that dimethyl substituted complex analogue is the most active catalyst for this oxidation.
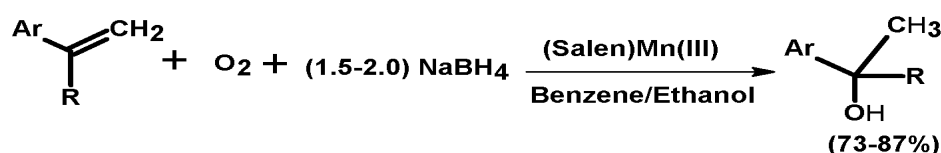
Figure 1.21: Oxidative conversion of olefins to the alcohols (Adopted from ref. [171])

Aziridines and their ring opened products are valuable intermediates in organic synthesis. With the emergence of Cr(III) complexes of salen as useful catalysts for the enantioselective ring opening of epoxides with TMSN$_3$ [172-174]. A series of chiral salen complexes were screened for catalysis for the model ring opening reaction of cyclopentene derived aziridine with TMSN$_3$ [Figure 1.22]. The complexes of Zn, Ni, Fe, Cu, and Co with more sterically demanding substituents were found to have higher enantioselectivity [175].
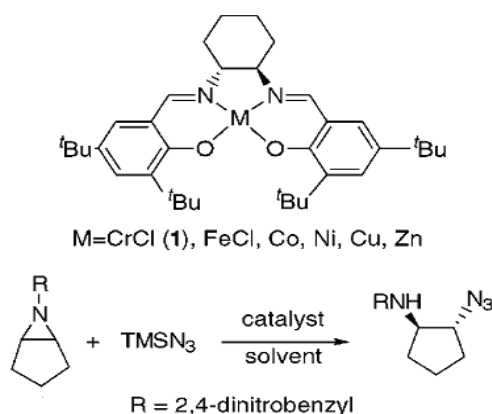
Figure 1.22: Ring opening reaction (Adopted from ref. [175])

Liquid phase hydroxylation of phenol catalyzed by the Schiff base complexes using H_2O_2 as an oxidant has been studied in acetonitrile [125]. The catalysts used for the oxidation reaction of phenol is manganese(II), iron(III) and copper(II) complexes of quinoxaline-2-carboxalidine-2-amino-5-methylphenol. The products obtained for hydroxylation of phenol is catechol and hydroquinone [Figure 1.23]. The nickel(II) and zinc(II) complexes of the same ligand, which are coordinatively saturated octahedral complexes, are not active. Thus the activity can be correlated with geometry of the complex.
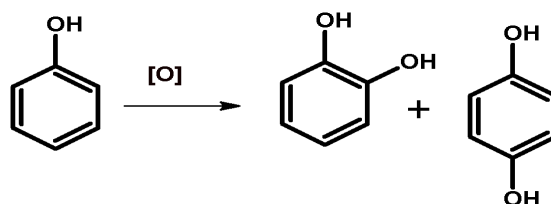
Figure 1.23: Oxidation of phenol

Hydrogenation of aromatic compounds to aliphatic cyclic products is an important reaction with potential applications in chemical industry [176,177]. Various metal based catalysts including that of nickel have been extensively used for the partial and complete reduction of benzene [Figure 1.24] [178-182]. Arun *et al.* reported octahedral complexes with general molecular formula $[M^{II}(L)(Cl)(H_2O)_2] \cdot H_2O$, where M is Ni or Ru and L = 3-hydroxyquinoxaline-2-carboxalidene-4-aminoantipyrine [116]. The nickel complex is more selective for cyclohexene and this selectivity increases with increase in the benzene concentration. These complexes were shown to be efficient catalysts for the reduction of benzene. Compared to the nickel complex catalyst, the ruthenium complex gives a higher conversion with a turnover frequency of 5372 h^{-1} under identical experimental conditions. The ruthenium catalyst is more selective towards cyclohexane, while the nickel catalyst is more selective for cyclohexene. At 80 $^\circ$C the nickel complex gives a conversion with a turnover frequency of 1718 h^{-1}.
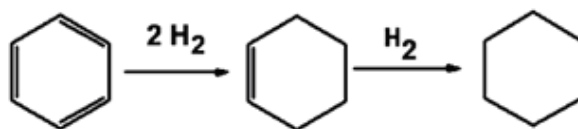
Figure 1.24: Hydrogenation reaction

Homogeneous catalysts have higher selectivity and act under mild experimental conditions in various reactions; however, they have problems of separation and recovery from reaction products. Hence current research activities are aimed at anchoring such metal complex catalysts on suitable supports. This technique of immobilization of catalyst on an inert support increases the catalytic activity, selectivity, efficiency, operational flexibility and stability. The zeolite supported Schiff base complexes, as a result of their particular structure, display enhanced activity and selectivity in a multitude of organic reactions. The chemistry of zeolite encapsulated complexes has been an area of particular interest, because of their high activity, unique size and shape-selective catalytic properties.

1.5 THE ZEOLITE ENCAPSULATED COMPLEXES

The term "molecular sieve" was introduced by Mc Bain [183] in 1932 to define porous solid materials that act as sieves at a molecular level. Molecular sieves are of generally two types: zeolite for (metallo)aluminosilicates and zeotype for analogous molecular sieves. Zeolites are aluminosilicate members of the family of microporous solids and considered as "philosopher's stone" of modern chemistry [184]. Chemically they are constructed of SiO_4 and AlO_4 containing alkali and/or alkaline earth cations tetrahedra linked through oxygen bridges. The Si:Al ratio in these vary from 1:1 to ∞:1 and the zeolites consist of a regular pore system with diameters in the range of 4-13 Å [185,186]. The different values of Si (tetravalent) and Al (trivalent) produce an overall negative

charge for each incorporated aluminum atom. Thus, chemical composition of zeolites is $(Si^{IV}\text{-O-}Al^{III}\text{-O-}Si^{IV})^{-} H^{+}$ or M^{+}. They have negatively charged framework and is hydrophilic in nature. Since these negative charges are compensated by exchangeable cations, metal ions can be introduced by direct ion exchange. Usually, these negative charges are balanced by alkali and/or alkaline earth cations [187]. The sodalite units, shown in the Figure 1.25, are basic building blocks for A, X and Y type molecular sieves.
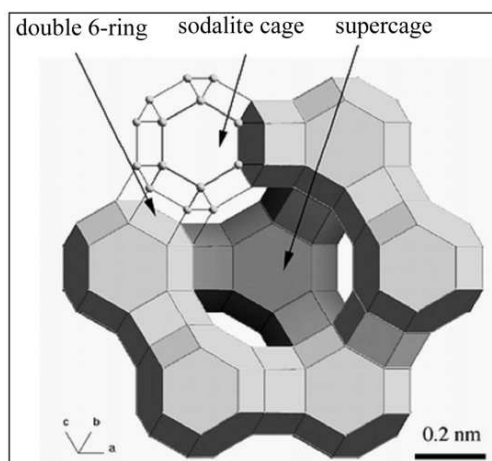
Figure 1.25: The structure of zeolite Y.

The sodalite cages enclose a supercage or α cage with diameter 13 Å and a cage mouth opening of 8 Å. Because of these large spatially accessible pores, the X and Y type zeolites are suitable candidates for encapsulating transition metal complexes. The encapsulation of transition metal complexes into the framework sites of zeolite ("host materials") might combine some characteristics of the support (like pore diameter, cavity size and electrostatic potential) with the electronic and stereochemical properties of the complex. The framework atoms which are catalytically active, also improve the steric constraints on the complex causing it to distort and thereby changing its stability and reactivity. The

dimerisation of the complexes which lead to its deactivation are also strongly retarded by encapsulation. Hence, the catalytic efficiency of zeolite encapsulated metal complexes (ZEMC) is much higher than that of the neat complexes.

For encapsulating a metal complex within the cage of a zeolite, the zeolite must possess an optimum cage size. The encapsulation of transition metal complexes was first described by Klier and Ralek in 1968 [188]. Such encapsulated complexes are generally referred to as "ship-in-a-bottle complexes". The various strategies for the preparation of the zeolite encapsulated complexes with sufficient examples have been presented in the paper of Balkus and Gabrielov [189]. There are three main approaches for encapsulating the complexes: the zeolite synthesis (ZS), the flexible ligand (FL) and ship-in-a-bottle methods. In the ZS method, transition metal complexes, which are stable under the conditions of zeolite synthesis (high pH and elevated temperature), are included in the synthesis mixture. The resulting zeolite encapsulates the transition metal complex in its voids. In the FL method, a flexible ligand is able to diffuse freely through the zeolite pores. The metal complexes physically entrapped in the cavities of the zeolites on the basis of their size, are also referred to as 'ship-in-a-bottle' complexes.

To ensure encapsulation, FTIR, UV-Vis spectroscopy, powder X-ray diffraction patterns (XRD), scanning electron microscopic studies (SEM) and BET (Brunauer-Emmett-Teller) technique can be applied. Comparative studies of the EPR spectra of the zeolite encapsulated and their simple complexes revealed interesting results. Bennur *et al*. reported the structural aspects of the encapsulated complexes of copper and manganese [190]. The EPR spectroscopy distinguishes the encapsulated complexes from the "neat" and surface adsorbed metal complexes. The EPR spectra differentiate complexes in such a way that neat one will show broad spectrum and encapsulated will exhibit a well resolved hyperfine spectra.

Neat complexes show broad spectrum corresponding to nearest neighbour spin-spin interactions.

Csicsery [191] defined the three well known categories of shape selectivity for the zeolites: (1) Reactant selectivity: only molecules that are able to enter zeolite channels react. (2) Product selectivity: only molecules that are able to leave zeolite channels are found in the product mixture. (3) Restricted transition state selectivity: reaction occurs when the required transition state can be formed in the zeolite cavities. Shape selectivity has been mostly studied in reversible, acid catalyzed reactions.

Transition metal complexes encapsulated in the pores and void spaces of zeolite and zeolite type materials have been receiving special attention as inorganic mimics of enzymes [192]. According to Herron [193] and Mitchell [194], zeolite encapsulated complexes can be considered as inorganic analogues of enzymes. There are a numerous reports about the encapsulated complexes of Schiff bases. Among them most studied one is the encapsulated salen complexes [195-197]. Zeolite encapsulated chiral metal complexes are used as heterogeneous catalysts for asymmetric oxidations [198]. The zeozymes possess dual advantages of the heterogeneous catalysts as well as homogeneous catalysts.

Intrinsic catalytic activity of zeolite encapsulated metal acetate, phthalocyanine and Schiff base complexes was enhanced significantly in the selective oxidation of aliphatic and aromatic hydrocarbons, hydroxylation of phenols, epoxidation of olefins, oxyhalogenation of aromatic compounds and decomposition of hydrogen peroxide and *tert*-butylhydroperoxide [199,200]. Zeolite encapsulated metal complexes (heterogeneous catalysts) exhibit higher selectivity and conversion percentage than that of the homogeneous catalysts. The enhanced catalytic activity of the zeolite encapsulated copper salens in the oxidation of phenol/paraxylene and the decomposition of H_2O_2/TBHP probably

arises due to the changes in the molecular and electronic structure of the complexes on encapsulation.

The double Schiff base complexes of copper and manganese encapsulated in zeolite NaX were reported by Jacob *et al*. [201]. Zeolite Y encapsulated Co(II), Ni(II) and Cu(II) complexes have been synthesised using the flexible ligand method. Well-defined inclusion and distribution of complexes in the zeolite matrix could be understood through physico-chemical and IR spectral characterisation. Tentative assignments are made for the geometry of complexes on the basis of magnetic moment, UV-Vis and EPR data [202].

The heterogeneous oxidation catalysis of alcohols with an environmentally suitable oxidant is useful in both the academic and industrial fields. The ability of the zeolite encapsulated complexes to bind oxygen reversibly has encouraged the scientists to explore the possibility of using them as efficient oxygen carriers. Interestingly, the majority of reactions catalyzed by zeolite encapsulated complexes are oxidation reactions. The Schiff base transition metal complexes are attractive oxidation catalysts because of their cheap, easy synthesis and their chemical and thermal stability. Oxidation of alcohols to the corresponding carbonyl compounds is one of the important reactions in the organic chemistry both at the laboratory and industry. The product of oxyfunctionalization of alcohols to aldehydes and ketones are important precursors or intermediates in the synthesis of many drugs, vitamins and fragrances [203,204]. A number of methods are known for alcohol oxidation [205], however, the development of newer methods and methodologies is gaining much attention currently due to the significance of this reaction.

The zeolite encapsulated Schiff base copper complexes are reported to be catalytically active in oxidation of various organic compounds. Niasari showed that some zeolite Y encapsulated complexes of Mn(II), catalyse the oxygen

transfer from TBHP to cyclohexene and concluded that such simple systems mimic the behavior of cytochrome P-450 type oxidation systems [206]. They have also shown that copper complexes encapsulated within nanocavity of zeolite-Y coupled with TBHP, as oxidant is a very active catalyst for the oxidation of cyclohexanol [207]. The high conversion percentage of about 88.6 with 100% selectivity toward the formation of cyclohexanone, which is the precursor of caprolactam, was observed. Zeolite encapsulated octahydro-Schiff base copper(II) complex was found to be more active than the corresponding cobalt(II), manganese(II) and nickel(II) complexes for cyclohexane oxidation. The catalytic properties of the complexes are influenced by their geometry and by the steric environment of the active sites [208]. Zeolite encapsulated copper(II) salen complex was found to be active in the oxidation of cyclohexanol [209]. It has also been claimed that zeolite encapsulated [Cu(salen)] catalyses the oxidation of cyclohexanol to cyclohexanone, [210] the epoxidation of norbornene and the hydroxylation of 1-naphthol [211], all under mild conditions

Selective oxidation [212] of various olefins on the basis of their size was achieved by the use of Mn(salen) complexes in zeolite Y. Bridged bis(2-pyridinecarboxamide) derived manganese complexes in NaY zeolites were used as catalysts for the epoxidation of olefins with H_2O_2 and *t*-BuOH [213]. Adipic acid is obtained as the oxidation product of cyclohexene with hydrogen peroxide by manganese diimine catalysts in faujasite zeolites [214].

The complex [Cu(sal-ambmz)Cl] has been encapsulated in the super cages of zeolite-Y. The Schiff base (Hsal-ambmz) used for the synthesis is derived from salicylaldehyde and 2-aminomethylbenzimidazole in refluxing methanol. The integrity of encapsulation was confirmed by spectroscopic, chemical and thermal analysis. This encapsulated complex is found active for the oxidation of phenol and styrene with good conversion. A maximum of 43.9% of phenol

oxidation was observed with this catalyst and it is more selective (73.9%) towards the formation of catechol. But oxidation of styrene gives four different products. The expected product styrene oxide was found only in small yield, and the percentage of benzaldehyde was relatively high [215].

Oxovanadium(IV), copper(II) and nickel(II) complexes of Schiff base derived from salicylaldehyde and *o*-aminobenzyl alcohol have been encapsulated in the nano-pores of zeolite-Y by flexible ligand method and characterised. These encapsulated complexes act as the catalyst for the oxidation of styrene, cyclohexane and methyl phenyl sulfide. In the presence of *tert*-butylhydroperoxide all catalysts gave styrene oxide in major yield. The oxidation products of cyclohexane are cyclohexanone and cyclohexanol. Conversion of methyl phenyl sulfide has been achieved with vanadium catalyst using H_2O_2 as oxidant, where selectivity of sulfoxide was 96.9%. Other encapsulated complexes were inactive towards the oxidation of methyl phenyl sulfide [216].

The complexes of Mn(II), Co(II), Ni(II) and Cu(II) with tetradentate Schiff base ligand was entrapped in the nanocavity of zeolite-Y by a two step process in the liquid phase: (i) adsorption of [bis(salicylaldiminato)metal(II)] in the supercages of the zeolite, and (ii) in situ Schiff condensation of the metal(II) precursor complex with oxaloyldihydrazone. The complexes of Co(II), Ni(II) and Cu(II) were suggested to have square planar geometry while the Mn(II) complex have tetrahedral geometry. These host-guest nanocomposite materials (HGNM) were characterised by several techniques. It was found that zeolite copper(II) complexes are good catalysts for the partial oxidation of cyclohexane with hydrogen peroxide, whereas the complexes of Mn(II), Co(II) and Ni(II) are weakly active [217].

1.6 SCOPE OF THE PRESENT STUDY

Quinoxaline derivatives serve as integral part of various antibiotics, antibacterial, anti-inflammatory, analgesic, tuberculostatic and antimalarial agents. They also have good DNA binding, catalytic and photophysical properties. Thus there is a continuing interest in synthesising quinoxaline based compounds suitable for such applications. In view of these, our group has mainly focused on the Schiff bases derived from quinoxaline-2-carboxaldehyde instead of salicylaldehydes, especially on the synthesis of double Schiff bases derived from quinoxaline-2-carboxaldehyde. The ligational aspects of quinoxaline based Schiff bases are important, as quinoxaline ring nitrogen is also capable of coordination. Therefore N_4 coordination (two from azomethines and two from quinoxaline ring) is expected to occur in their complexes. Furthermore the stability of the complexes would be increased by chelate effect. Therefore the electronic environment in the metal complexes of these Schiff bases might be different from those derived from salicylaldehyde. It was therefore thought worthwhile to synthesise the Schiff bases derived from quinoxaline-2-carboxaldehyde and study their coordination behaviour.

The ligands chosen for the present study are the following:

1. *N,N′*-bis(quinoxaline-2-carboxalidene)hydrazine (*qch*)
2. *N,N′*-bis(quinoxaline-2-carboxalidene)-1,2-diaminoethane (*qce*)
3. *N,N′*-bis(quinoxaline-2-carboxalidene)-1,3-diaminopropane (*qcp*)
4. *N,N′*-bis(quinoxaline-2-carboxalidene)-1,4-diaminobutane (*qcb*)
5. *N,N′*-bis(quinoxaline-2-carboxalidene)-1,2-diaminocyclohexane (*qcc*)
6. *N,N′*-bis(quinoxaline-2-carboxalidene)-1,2-diaminobenzene (*qco*)

The objectives of the work are as follows:

- To design the Schiff bases as neutral tetradentate ligands by selecting diamines and hydrazine hydrate.
- To characterise these double Schiff bases by spectroscopic and single crystal XRD studies.
- To synthesise and characterise the transition metal complexes of the above Schiff bases.
- To synthesise and characterise the zeolite encapsulated copper complexes of these Schiff bases.
- To study the catalytic activities of the encapsulated complexes.
- To study the biological activities, such as cytotoxicity and DNA binding, of copper(II) Schiff base complexes.

Manganese(II), nickel(II) and copper(II) complexes of these Schiff bases have been synthesised and characterised. Among these complexes, copper complexes were screened for biological activity studies. The zeolite encapsulated copper complexes were synthesised and characterised. These complexes were screened for their catalytic activity in oxidation of cyclohexanol.

REFERENCES

1. R. H. Holm, *J. Am. Chem. Soc.*, 82 (**1960**) 5632.

2. E. C. Niederhoffer, J. H. Timmons, J. H. Timmons, A. E. Martell, *Chem. Rev.*, 84 (**1984**) 137.

3. C. O. Rodriguez de Barbarin, N. A. Bailey, D. E. Fenton, Q.-Y. He, *J. Chem. Soc.*, *Dalton Trans.*, (**1997**) 161.

4. E. J. Larson, V. L. Pecoraro, *J. Am. Chem. Soc.*, 113 (**1991**) 3810.

5. H. J. Choi, J. J. Sokol, J. R. Long, *Inorg. Chem.*, 43 (**2004**) 1606.

6. R. E. P. Winpenny, *Chem. Soc. Rev.*, 27 (**1998**) 447.

7. R. W. Date, E. F. Iglesias, K. E. Rowe, J. M. Elliott, D. W. Bruce, *Dalton Trans.*, (**2003**) 1914.

8. E. Terazzi, S. Torelli, G. Bernardinelli, J.-P. Rivera, J.-M. Bénech, C. Bourgogne, B. Donnio, D. Guillon, D. Imbert, J.-C. G. Bünzli, A. Pinto, D. Jeannerat, C. Piguet, *J. Am. Chem. Soc.*, 127 (**2005**) 888.

9. E. Tsuchida, K. Oyaizu, *Coord. Chem. Rev.*, 237 (**2003**) 213.

10. A. R. Silva, K. Wilson, J. H. Clark, C. Freire, *Stud. Surf. Sci. Catal.*, 158 (**2005**) 1525.

11. M. E. Marmion, S. R. Woulfe, W. L. Newmann, G. Pilcher, D. L. Nosco, *Nucl. Med. Biol.*, 23 (**1996**) 567.

12. N. S. Venkataramanan, G. Kuppuraj, S. Rajagopal, *Coord. Chem. Rev.*, 249 (**2005**) 1249.

13. A. Ray, S. Banerjee, R. J. Butcher, C. Desplanches, S. Mitra, *Polyhedron*, 27 (**2008**) 2409.

14. H. Schiff, *Ann.*, 131 (**1864**) 118.

15. Hp. Fischer, C. A. Grob, E. Renk, *Helv. Chim. Acta*, 42 (**1959**) 872.

16. Z. Li, K. R. Conser, E. N. Jacobsen, *J. Am. Chem. Soc.*, 115 (**1993**) 5326.

17. R. W. Layer, *The chemistry of Imines*, (**1962**) 489.

18. Y.-Y. Yu, H.-D. Xian, J.-F. Liu, G.-L. Zhao, *Molecules*, 14 (**2009**) 1747.

19. S. Adsule, V. Barve, D. Chen, F. Ahmed, Q. P. Dou, S. Padhye, F. H. Sarkar, *J. Med. Chem.*, 49 (**2006**) 7242.

20. X.-H. Bu, M. L. Tong, Y.-B. Xie, J.-R. Li, H.-C. Chang, S. Kitagawa, J. Ribas, *Inorg. Chem.*, 44 (**2005**) 9837.

21. M. Sarkar, K. Biradha, *Cryst. Eng. Comm.*, 6 (**2004**) 310.

22. M. H. Habibi, K. Barati, M. Zendehdel, R. W. Harrington, W. Clegg, *Analyt. Sci.*, 23 (**2007**) x61.

23. H.-K. Fun, H. Kargar, R. Kia, *Acta Cryst.*, E64 (**2008**) o1894.

24. V. Arun, P. P. Robinson, S. Manju, P. Leeju, G. Varsha, V. Digna, K. K. M. Yusuff, *Dyes and Pigments*, 82 (**2009**) 268.

25. M. H. Habibi, M. Montazerozohori, A. Lalegani, R. W. Harrington, W. Clegg, *J. Fluorine Chem.*, 127 (**2006**) 769.

26. R. H. Holm, G. W. Evertt, A. Chakravorty, *Prog. Inorg. Chem.*, 7 (**1966**) 83.

27. C. G. Zhang, D. Wu, C.-X. Zhao, J. Sun, X.-F. Kong, *Transition Met. Chem.*, 24 (**1999**) 718.

28. E. Tas, M. Aslanoglu, M. Ulusoy, M. Guler, *Polish. J. Chem.*, 78 (**2004**) 903.

29. R. M. Wang, X. D. Li, Y. F. He, *Chinese Chem. Lett.*, 17 (**2006**) 265.

30. J. Zhao, B. Zhao, J. Liu, W. Xu, Z. Wang, *Spectrochim. Acta Part A*, 57 (**2001**) 149.

31. D. Chatterjee, A. Mitra, *J. Coord. Chem.*, 57 (**2004**) 175.

32. Y.-B. Dong, H.-Q. Zhang, J.-P. Ma, R.-Q. Huang, *Crystal Growth & Design*, 5 (**2005**) 1857.

33. T. Kawasaki, T. Kamata, H. Ushijima, S. Murata, F. Mizukami, Y. Fujii, Y. Usui, *Mol. Cryst. Liq. Cryst.*, 286 (**1996**) 257.

34. T. Kawasaki, T. Kamata, H. Ushijima, M. Kanakubo, S. Murata, F. Mizukami, Y. Fujii, Y. Usui , *J. Chem. Soc., Perkin Trans.*, 2 (**1999**) 193.

35. N. E. Borisova, M. D. Reshetova, Y. A. Ustynyuk, *Chem. Rev.*, 107 (**2007**) 46.

36. A. Panda, S. C. Menon, H. B. Singh, C. P. Morley, R. Bachman, T. M. Cocker, R. J. Butcher, *Eur. J. Inorg. Chem.*, (**2005**) 1114.

37. W. Radecka- Paryzek, V. Patroniak, J. Lisowski, *Coord. Chem. Rev.*, 249 (**2005**) 2156.

38. S. R. Collinson, D. E. Fenton, *Coord. Chem. Rev.*, 148 (**1996**) 19.

39. U. Beckmann, S. Brooker, *Coord. Chem. Rev.*, 245 (**2003**) 17.

40. S. Brooker, *Coord. Chem. Rev.*, 222 (**2001**) 33.

41. M. Sarkar, K. Biradha, *Cryst. Eng. Comm.*, 6 (**2004**) 310.

42. D. Pucci, A. Bellusci, A. Crispini, M. Ghedini, M. La Deda, *Inorg. Chim. Acta*, 357 (**2004**) 495.

43. C. Biswas, M. G. B. Drew, A. Figuerola, S. Gómez-Coca, E. Ruiz, V. Tangoulis, A. Ghosh, *Inorg. Chim. Acta*, 363 (**2010**) 846.

44. A. D. Garnovski, A. L. Nivorozkhin, V. I. Minkin, *Coord. Chem. Rev.*, 126 (**1993**) 1.

45. W. Plass, *Coord. Chem. Rev.*, 237 (**2003**) 205.

46. G. Kumar, D. Kumar, S. Devi, A. Kumar, R. Johari, *E-Journal of Chemistry*, 7 (**2010**) 813.

47. P. G. Cozzi, *Chem. Soc. Rev.*, 33 (**2004**) 410.

48. J.-N. Liu, B.-W. Wu, B. Zhang, Y.-C. Liu, *Turk J. Chem.*, 30 (**2006**) 41.

49. I. I. Ebralidze, G. Leitus, L. J.W. Shimon, R. Neumann, *Inorg. Chim. Acta*, 362 (**2009**) 4760.

50. P. Mukherjee, M. G. B. Drew, V. Tangoulis, M. Estrader, C. Diaz, A. Ghosh, *Polyhedron*, 28 (**2009**) 2989.

51. S. Thakurta, C. Rizzoli, R. J. Butcher, C. J. Gómez-García, E. Garribba, S. Mitra, *Inorg. Chim. Acta*, 363 (**2010**) 1395.

52. P. Talukder, S. Shit, A. Sasmal, S. R. Batten, B. Moubaraki, K. S. Murray, S. Mitra, *Polyhedron*, 30 (**2011**) 1767.

53. R. Rajavel, M. S. Vadivu, C. Anitha, *E-Journal of Chemistry*, 5 (**2008**) 620.

54. C. Maxim, T. D. Pasatoiu, V. C. Kravtsov, S. Shova, C. A. Muryn, R. E. P. Winpenny, F. Tuna, M. Andruh, *Inorg. Chim. Acta*, 361 (**2008**) 3903.

55. R. C. Maurya, A. Pandey, J. Chaurasia, H. Martin, *J. Mol. Struct.*, 798 (**2006**) 89.

56. J. Chakraborty, S. Thakurta, B. Samanta, A. Ray,G. Pilet, S. R. Batten, P. Jensen, S. Mitra, *Polyhedron*, 26 (**2007**) 5139.

57.   Y. Sunatsuki, Y. Motoda, N. Matsumoto, *Coord. Chem. Rev.*, 226 (**2002**) 199.

58.   A. Mustapha, K. Busch, M. Patykiewicz, A. Apedaile, J. Reglinski, A. R. Kennedy, T. J. Prior, *Polyhedron*, 27 (**2008**) 868.

59.   P. M. Alex, K. K. Aravindakshan, *E-Journal of Chemistry*, 6 (**2009**) 449.

60.   E. N. Jacobsen. In: I. Ojima, *Catalytic Asymmetric Synthesis*, Weinheim, (**1993**) 159 Ch. 4.2.

61.   E. N. Jacobsen In: E.W. Abel, F. G. A. Stone, G. Wilkinson, *Comprehensive Organometallic Chemistry II*, Pergamon, New York, 12 (**1996**) 1097.

62.   S. Yamada, *Coord. Chem. Rev.*, 190-192 (**1999**) 537.

63.   M. A. Ali, A. H. Mirza, F. H. Bujang, M. H. S. A. Hamid, P. V. Bernhardt, *Polyhedron*, 25 (**2006**) 3245.

64.   T. Akitsu, Y. Einaga, *Polyhedron*, 24 (**2005**) 1869.

65.   M. Habib, T. K. Karmakar, G. Aromı, J. Ribas-Arino, H.-K. Fun, S. Chantrapromma, S. K. Chandra, *Inorg. Chem.*, 47 (**2008**) 4109.

66.   I. C. Santos, M. Vilas-Boas, M. F. M. Piedade, C. Freire, M. T. Duarte, B. de Castro, *Polyhedron*, 19 (**2000**) 655.

67.   S. Naskar, S. Naskar, R. J. Butcher, S. K. Chattopadhyay, *Inorg. Chim. Acta*, 363 (**2010**) 404.

68.   A. Burkhardt, H. Gorls, W. Plass, *Carbohydrate Research*, 343 (**2008**) 1266.

69.   X. Tai, X. Yin, Q. Chen, M. Tan, *Molecules*, 8 (**2003**) 439.

70.   J.-N. Liu, B.-W. Wu, B. Zhang, Y.-C. Liu, *Turk J. Chem*, 30 (**2006**) 41.

71.   A. Datta, N. K. Karan, S. Mitra, V. Gramlich, *Journal of Chemical Crystallography*, 33 (**2003**) 579.

72   S. Chattopadhyay, M. G. B. Drew, A. Ghosh, *Inorg. Chim. Acta*, 359 (**2006**) 4519.

73. S. Sarkar, A. Mondal, M. Salah El Fallah, J. Ribas, D. Chopra, H. Stoeckli-Evans, K. K. Rajak, *Polyhedron*, 25 (**2006**) 25.

74. B. Geeta, K. Shravankumar, P. Muralidhar Reddy, E. Ravikrishna, M. Sarangapani, K. Krishna Reddy, V. Ravinder, *Spectrochim. Acta Part A*, 77 (**2010**) 911.

75. D. Plaul, D. Geibig, H. Gorls, W. Plass, *Polyhedron*, 28 (**2009**) 1982.

76. M. G. B. Drew, R. N. Prasad, R. P. Sharma, *Acta Crystallogr.,* C41 (**1985**) 1755.

77 C. Arıcı, F. Ercan, R. Kurtaran, O. Atakol, *Acta Crystallogr.*, C57 (**2001**) 812.

78. H. H. Yua, J. M. Lo, B. H. Chen, T. H. Lu, *Acta Crystallogr.*, C53 (**1997**) 1012.

79. O. Kahn. *Struct. Bonding*, 68 (**1987**) 89.

80. O. Kahn, *Molecular Magnetism*, New York (**1993**).

81. Y. Elerman, A. Elmali, C. T. Zeyrek, I. Svoboda, H. Fuess, *Z. Naturforsch.*, 58b (**2003**) 271.

82. H. Okawa, H. Furutachi, D. E. Fenton, *Coord. Chem. Rev.*, 174 (**1998**) 51.

83. L. F. Lindoy, *The Chemistry of Macrocyclic Ligand Complexes*, Cambridge University, Cambridge, UK, (**1989**).

84. A. Martell, J. Penitka, D. Kong, *Coord. Chem. Rev.*, 55 (**2001**) 216.

85. V. Amendola, L. Fabbrizzi, C. Mangano, P. Pallavicini, A. Poggi, A. Taglietti, *Coord. Chem. Rev.*, 219-221 (**2001**) 821.

86. H. Temel, S. Ilhan, *Spectrochim. Acta Part A*, 69 (**2008**) 896.

87. D. J. Brown, *Quinoxalines, Supplement II, The chemistry of heterocyclic compounds*, John Wiley and Sons, Hoboken, New Jersey 61 (**2004**).

88. S. Ajaikumar, A. Pandurangan, *Appl. Catal. A: Gen.*, 357 (**2009**) 184.

89. M. M. Heravi, K. Bakhtiari, M. H. Tehrani, N. M. Javadi, H. A. Oskooie, *Arkivoc*, 16 (**2006**) 16.

90. A. Carta, S. Piras, G. Loriga, G. Paglietti Chemistry, *Mini-Rev Med. Chem.*, 6 (**2006**) 1179.

91. X. Li, K.-H. Yang, W.-L. Li, W.-F. Xu, *Drugs Future*, 31 (**2006**) 979.

92. M. M. Badran, K. A. M. Abouzid, M. H. M. Hussein, *Arch. Pharm. Res.*, 26 (**2003**) 107.

93. L. E. Seitz, W. J. Suling, R. C. Reynolds, *J. Med. Chem.*, 45 (**2002**) 5604.

94. S. A. El-Hawash, N. S. Habib, N. H. Fanaki, *Pharmazie*, 54 (**1999**) 808.

95. H.-L. Gao, K.-C. Huang, E. Y. Yamasaki, K.-K. Cham, L. Chohan, P. Corona, G. Vitale, M. Loriga, G. Paglietti, M. P. Costi, *Il Farmaco*, 53 (**1998**) 480.

96. C. Bailly, S. Echepare, F. Gago, M. J. Waring, *Anti Cancer Drug Des.*, 15 (**1999**) 291.

97. D. V. Jarikote, W. Li, T. Jiang, L. A. Eriksson, *Bioorg. Med. Chem.*, 19 (**2011**) 826.

98. K. Sato, O. Shiratori, K. Katagiri, S. Antibiotic, *Ser. A.*, 20 (**1967**) 270.

99. A. Dell, D. H. William, H. R. Morris, G. A. Smith, J. Feeney, G. C. K. Roberts, *J. Am. Chem. Soc.*, 97 (**1975**) 2497.

100. Y. Tadashi, K. Yasuo, K. Ken, *Progr. Antimicrob. Anticancer Chemother.*, *Proc. Int. Congr. Chemother.*, 2 (**1969**) 1160.

101. V. S. Kulkarni, M. D. Lele, B. B. Gavitre, M. D. Patil, K. R. Bobe, D. T. Gaikwad, *International Journal of Drug Formulation & Research*, 1 (**2010**) 134.

102. O. S. Moustafa, *Journal of the Chinese Chemical Society*, 50 (**2003**) 1205.

103. A. K. Patidar, M. Jeyakandan, A. K. Mobiya, G. Selvam, *International Journal of PharmTech Research*, 3 (**2011**) 386.

104. J. Guillon, E. Mouray, S. Moreau, C. Mullié, I. Forfar, V. Desplat, S. Belisle-Fabre, N. Pinaud, F. Ravanello, A. Le-Naour, J.-M. Léger, G.

Gosmann, C. Jarry, G. Déléris, P. Sonnet, P. Grellier, *Eur. J. M. Chem.*, 46 (**2011**) 2310.

105.   C. A. Mitsopoulou, C. E. Dagas, C. Makedonas, *J. Inorg. Biochem.,* 102 (**2008**) 77.

106.   H. Amiri, N. Nekhotiaeva, J.-S. Sun, C.-H. Nguyen, D. S. Grierson, L. Good, R. Zain, *J. Mol. Biol.*, 351 (**2005**) 776.

107.   W. Blau, *Physics in Technology*, 18 (**1987**) 250.

108.   M. F. Cain, S. C. Reynolds, B. J. Anderson, D. S. Glueck, J. A. Golen, C. E. Moore, A. L. Rheingold, *Inorg. Chim. Acta*, 369 (**2011**) 55.

109.   J.-H. Kim, J. Y. Jaung, *Dyes and Pigments*, 77 (**2008**) 474.

110.   B. B. Çarbas, A. Kivrak, M. Zora, A. M. Önal, *Reactive & Functional Polymers*, 71 (**2011**) 579.

111.   Y. Ha, J.-H. Seo, Y. K. Kim, *Synthetic Metals*, 158 (**2008**) 548.

112.   J.-W. Jang, H. Park, M.-K. Shin, H. H. Kang, D.-H. Oha, S. O. Jung, S.-K. Kwon, Y.-H. Kim, *Dyes and Pigments*, 88 (**2011**) 44.

113.   T. Yamamoto, K. Sugiyama, T. Kushida, T. Inoue, T. Kanbara, *J. Am. Chem. Soc.*, 118 (**1996**) 3930.

114.   T. Fukuda, T. Kanbara, T. Yamamoto, K. IshikawA, H. Takezoe, A. Fukuda, *Applied Physics Letters*, 68 (**1996**) 2346.

115.   A. S. Amina, A. L. Saberb, T. Y. Mohammed, *Spectrochim. Acta Part A*, 73 (**2009**) 195.

116.   V. Arun, N. Sridevi, P. P. Robinson, S. Manju, K. K. M. Yusuff, *J. Mol. Catal. A: Chem.*, 304 (**2009**) 191.

117.   G. W. Inman, J. A. Barnes, W. E. Hatfield, *Inorg. Chem.*, 11 (**1972**) 764.

118.   R. Balamurugan, M. Palaniandavar, H. Stoeckli-Evans, M. Neuburger, *Inorg. Chim. Acta*, 359 (**2006**) 1103.

119.   P. K. Sasmal, A. K. Patra, M. Nethaji, A. R. Chakravarty, *Inorg. Chem.*, 46 (**2007**) 11112.

120. S. Mayadevi, K. K. M. Yusuff, *Synth. React. Inorg. Met.-Org. Chem.*, 27 (**1997**) 319.

121. V. Arun, S. Mathew, P. P. Robinson, M. Jose, V. P. N. Nampoori, K. K. M. Yusuff, *Dyes and Pigments*, 87 (**2010**) 149.

122. P. Leeju, V. Arun, M. Sebastian, G. Varsha, D. Varghese, K. K. M. Yusuff, *Acta Cryst.* E65 (**2009**) o1981.

123. M. Sebastian, V. Arun, P. P. Robinson, P. Leeju, D. Varghese, G. Varsha, K. K. M. Yusuff, *J. Coord. Chem.*, 63 (**2009**) 307.

124. S. Mayadevi, P. G. Prasad, K. K. M. Yusuff, *Synth. React. Inorg. Met.-Org. Chem.*, 33 (**2003**) 481.

125. M. Sebastian, V. Arun, P. P. Robinson, A. A. Varghese, R. Abraham, E. Suresh, K. K. M. Yusuff, *Polyhedron*, 29 (**2010**) 3014.

126. R. Sreekala, K. K. M. Yusuff, *Reaction Kinetics & Catalysis Letters*, 48 (**1992**) 575.

127. P. S. Chittilappilly, N. Sridevi, K. K. M. Yusuff, *J. Mol. Catal. A: Chem.*, 286 (**2008**) 92.

128. S. Mayadevi, N. Sridevi, K. K. M. Yusuff, *Indian J. Chem.*, 37A (**1998**) 413.

129. A. Kadzewski, M. Gdaniec. Acta Cryst., E62 (**2006**) o3498.

130. M. R. Bermejo, A. M. Gonzalez-Noya, V. Abad, M. I. Fernandez, M. Maneiro, R. Pedrido, M. Vazquez, *Eur. J. Inorg. Chem.*, (**2004**) 3696.

131. H. Z. Kou, Z. H. Ni, B. C. Zhou, R. J. Wang, *Inorg. Chem. Comm.*, 7 (**2004**) 1150.

132. A. D. Garnovskii, I. S. Vasilchenko, D. A. Garnovskii, B. I. Kharisov, *J. Coord. Chem.*, 62 (**2009**) 151.

133. N. Raman, S. J. Raja, A. Sakthivel, *J. Coord. Chem.*, 62 (**2009**) 691.

134. M. S. Ibrahim, S. E. H. Etaiw, *Synth. React. Inorg. Met.-Org. Chem.*, 34 (**2004**) 629.

135. A. Lalehzari, J. Desper, C. J. Levy, *Inorg. Chem.*, 47 (**2008**) 1120.

136. P. A. Vigato, S. Tamburini. *Coord. Chem. Rev.*, 248 (**2004**) 1717.

137. S. Ren, R. Wang, K. Komatsu, P. Bonaz-Krause, Y. Zyrianov, C. E. McKenna, C. Csipke, Z. A. Tokes, E. J. Lien, *J. Med. Chem.*, 45 (**2002**) 410.

138. N. Raman, A. Kulandaisamy, C. Thangaraja, *Transition Met. Chem.*, 28 (**2003**) 29.

139. M. S. Refat, I. M. El-Deen, Z. M. Anwer, S. El-Ghol. *J. Coord. Chem.*, 62 (**2009**) 1709.

140. M. Amanullah, S. K. Sadozai, W. Rehman, Z. Hassan, A. Rauf, M. Iqbal, *African Journal of Biotechnology*, 10 (**2011**) 209.

141. J. Ziegler, T. Schuerle, L. Pasierb, C. Kelly, A. Elamin, K. A. Cole, D. W. Wright, *Inorg. Chem.*, 39 (**2000**) 3731.

142. E. N. Jacobsen, W. Zhang, A. R. Muci, J. R. Ecker, L. Deng, *J. Am. Chem. Soc.*, 113 (**1991**) 7063.

143. P. Espinet, M. A.Esteruelas, L. A. Oro, J. L. Serrano, E. Sola, *Coord. Chem. Rev.*, 117 (**1992**) 215.

144. M. Z. Zgierski, A. Grabowska, *J. Chem. Phys.*, 113 (**2000**) 7845.

145. X. He, C. Z. Lu, C. D. Wu, *J. Coord. Chem.*, 59 (**2006**) 977.

146. M. Jalali-Heravi, A. A. Khandar, I. Sheikshoaie, *Spectrochim. Acta Part A*, 56 (**2000**) 1575.

147. I. Sheikhshoaie, W. M. F. Fabian, *Dyes and Pigments*, 70 (**2006**) 91.

148. I. Yilmaz, A. Cukurovali, *Transition Met. Chem.*, 28 (**2003**) 399.

149. A. Golcu, M. Tumer, H. Demirelli, R. A. Wheatley, *Inorg. Chim. Acta*, 358 (**2005**) 1785.

150. N. A. Illan-Cabeza, F. Hueso-Urena, M. N. Moreno-Carretero, J. Martınez-Martos, M. J. Ramırez-Exposito, *J. Inorg. Biochem.*, 102 (**2008**) 647.

151. W. Zishen, L. Zhiping, Y. Zhenhuan, *Transition Met. Chem.*, 18 (**1993**) 291.

152. A. Golcu, M. Tumer, H. Demirelli, R. A. Wheatley, *Inorg. Chim. Acta*, 358 (**2005**) 1785.

153. S. Roy, P. U. Maheswari, M. Lutz, A. L. Spek, H. D. Dulk, S. Barends, G. V. Wezel, F. Hartl, J. Reedijk, *Dalton Trans.*, (**2009**) 10846.

154. S. Gama, F. Mendes, F. Marques, I. C. Santos, M. F. Carvalho, I. Correia, J. C. Pessoa, I. Santos, A. Paulo, *J. Inorg. Biochem.*, 105 (**2011**) 637.

155. Q. Jiang, N. Xiao, P. F. Shi, Y. G. Zhu, Z. J. Gou, *Coord. Chem.Rev.*, 251 (**2007**) 1951.

156. M. N. Patel, P. A. Dosi, B. S. Bhatt, V. R. Thakkar, *Spectrochim. Acta Part A*, 78 (**2011**) 763.

157. S. A. Ross, M. Pitie, B. Meunier, *Eur. J. Inorg. Chem.*, 3 (**1999**) 557.

158. C.-Y. Shi, E.-J. Gao, S. Mab, M.-L. Wang, Q.-T. Liu, *Bioorg. Medicinal Chem. Lett.*, 20 (**2010**) 7250.

159. Y. Kou, J. Tian, D. Li, W. Gu, X. Liu, S. Yan, D. Liao, P. Cheng, *Dalton Trans.*, (**2009**) 2374.

160. Z.-C. Liu, B.-D. Wang, B. Li, Q. Wang, Z.-Y. Yang, T.-R. Li, Y. Li, *Eur. J. Med. Chem.*, 45 (**2010**) 5353.

161. H. Schiff, *Ann. Suppl.*, 150 (**1869**) 193.

162. E. N. Jacobsen, W. Zhang, *J. Org. Chem.*, 56 (**1991**) 2296.

163. W. Zhang, J. L. Loebach, S. R. Wilson, E. N. Jacobsen, *J. Am.Chem. Soc.*, 112 (**1990**) 2801.

164. H. A. Staab, F. Voegtle, *Chem. Ber.*, 98 (**1965**) 2691.

165. R. S. Downing, F. L. Urbach, *J. Am. Chem. Soc.*, 91 (**1969**) 5977.

166. M. Calligaris, G. Nardin, L. Randaccio, *Coord. Chem. Rev.*, 7 (**1972**) 385.

167. E. N. Jacobsen, A. Pfaltz, H. Yamamoto, *Comprehensive Asymmetric Catalysis*, Springer, New York, Chapter 18.2., 2 (**1999**) 649.

168.   I. Ojima, *Catalytic Asymmetric Synthesis*, 2nded., Wiley/VCH, New York, Chapter 6 (**2000**) 229.

169.   E. M. Mc Garrigle, D. G. Gilheany, *Chem. Rev.*, 105 (**2005**) 1563.

170.   T. Katsuki, *Coord. Chem. Rev.*, 140 (**1995**) 189.

171.   N. H. Lee, J. C. Byun, J. S. Baik, C.-H. Han, S.-B. Han, *Bull. Korean Chem. Soc.*, 23 (**2002**) 1365.

172.   L. E. Martinez, J. L. Leighton, D. H. Carsten, E. N. Jacobsen, *J. Am. Chem. Soc.*, 117 (**1995**) 5897.

173.   J. F. Larrow, S. E. Schaus, E. N. Jacobsen, *J. Am. Chem. Soc.*, 118 (**1996**) 7420.

174.   S. E. Schaus, J. F. Larrow, E. N. Jacobsen, *J. Org. Chem.*, 62 (**1997**) 4197.

175.   Z. Li, M. Fernandez, E. N. Jacobsen, *Org. Lett.*, 1 (**1999**) 1611.

176.   C. Morin, D. Simon, P. Sautet, *Surf. Sci.*, 600 (**2006**) 1339.

177.   J. A.Widegren, R.G. Finke, *J. Mol. Catal. A: Chem.*, 191 (**2003**) 187.

178.   J. Wang, Y. Wang, S. Xie, M. Qiao, H. Li, K. Fan, *Appl. Catal. A: Gen.*, 272 (**2004**) 29.

179.   P. J. Baricelli, L. Izaguirre, J. Lopez, E. Lujano, F. Lopez-Linares, *J. Mol. Catal. A: Chem.*, 208 (**2004**) 67.

180.   B. Chen, U. Dingerdissen, J. G. E. Krauter, H. G. J. Lansink Rotgerink, K. Mobus, D. J. Ostgard, P. Panster, T. H. Riermeier, S. Seebald, T. Tacke, H. Trauthwein, *Appl. Catal. A: Gen.,* 280 (**2005**) 17.

181.   P. G. Savva, K. Goundani, J. Vakros, K. Bourikas, Ch. Fountzoula, D. Vattis, A.Lycourghiotis, Ch. Kordulis, *Appl. Catal. B: Environ.*, 79 (**2008**) 199.

182.   S. Lu, W. W. Lonergan, J. P. Bosco, S. Wang, Y. Zhu, Y. Xie, J. G. Chen, *J. Catalysis*, 259 (**2008**) 260.

183.   J. W. Mc Bain, *The Sorption of Gases and Vapours by Solids*, Rutledge and Sons, London, (**1932**).

184. H. M. Leicester, The Historical Background of Chemistry, Dover, New York, (**1971**).

185. M. Salavati-Niasari, F. Mohandes, *Advances in Diverse Industrial Applications of Nanocomposites From Zeolite to Host-Guest Nanocomposite Materials*, 341.

186. J. Weitkamp, *Solid State Ionics*, 131 (**2000**) 175.

187. V. J. Inglezakis, *J. Colloid Interface Sci.*, 281 (**2005**) 68.

188. K. Klier, M. Ralek, *J. Phys. Chem. Solids*, 29 (**1968**) 951.

189. K. J. Balkus Jr, A. G. Gabrielov, *J. Inclusion Phenom. Mol. Recognit. Chem.*, 21 (**1995**) 159.

190. T. H. Bennur, D. Srinivas, P. Ratnasamy, *Micropor. Mesopor. Mater*, 48 (**2001**) 111.

191. S. M. Csicsery, *Zeolites*, 4 (**1984**) 202.

192. D. E. DeVos, J. L. Meinershagen, T. Bein, *Angew. Chem. Int. Ed. Engl.*, 35 (**1996**) 2211.

193. N. Herron, *Chemtech*, (**1989**) 542.

194. P. C. H. Mitchell, *Chem. Ind.*, (**1991**) 308.

195. F. Bedioui, L. Roue, J. Devynck, K. J. Balkus, *Stud. Surf. Sci. Catal.*, 84 (**1994**) 917.

196. K. J. Balkus, A. A. Welch, B. E. Gnade, *Zeolites*, 10 (**1990**) 722.

197. S. Kowalak, R. C. Weiss, K. J. Balkus Jr., *J. Chem. Soc. Chem. Commun.*, (**1991**) 57.

198. V. Schurig, F. Betschinger, *Chem. Rev.*, 92 (**1992**) 873.

199. R. Raja, P. Ratnasamy, *J. Catalysis*, 170 (**1997**) 244.

200. R. Raja, P. Ratnasamy, *Catal. Lett.*, 48 (**1997**) 1.

201. C. R. Jacob, S. P. Varkey, P. Ratnasamy, *Micropor. Mesopor. Mater*, 22 (**1998**) 465.

202. K. O. Xavier, J. Chacko, K. K. M. Yusuff, *Appl.Catal. A: Gen.*, 258 (**2004**) 251.

203. R. A. Sheldon, J. K. Kochi, *Metal-Catalyzed Oxidation of Organic Compounds*, Academic Press, New York, (**1981**).

204. M. Hudlicky, *Oxidations in Organic Chemistry*, ACS Monograph 186; American Chemical Society: Washington, DC, (**1990**).

205. R. A. Sheldon, I. W. C. E. Arends, A. Dijkman, *Catal. Today*, 57 (**2000**) 157.

206. M. Salavati-Niasari, F. Farzaneh, M. Ghandi, *J. Mol. Catal. A: Chem.*, 175 (**2001**) 105.

207. M. Salavati-Niasari, E. Zamani, M. R. Ganjali, P. Norouzi, *J. Mol. Catal. A: Chem*, 261 (**2007**) 196.

208. M. Salavati-Niasari, Z. Salimi, M. Bazarganipour, F. Davar, *Inorg. Chim. Acta*, 362 (**2009**) 3715.

209. R. Chandra, A. Murugkar, S. Padhye, S. A. Pardhy, *Indian J. Chem.*, 35A (**1996**) 1.

210. C. Ratnasamy, A. Murugkar, S. Padhye, *Indian J. Chem.*, 36A (**1996**) 1.

211. S. Koner, *J. Chem. Soc. Chem. Commun.*, (**1998**) 593.

212. C. Bowers, P. K. Dutta, *J. Catalysis*, 122 (**1990**) 271.

213. P. P. Knops Gerrits, C. A. Treijillo, B. Z. Zhan, P. A. Jacobs, *Stud. Surf. Sci. Catal.*, 108 (**1997**) 445.

214. P. P. Knops Gerrits, F. T. Starzyk, P. A. Jacobs, *Stud. Surf. Sci. Catal.*, 84 (**1994**) 1411.

215. M. R. Maurya, A. K. Chandrakar, S. Chand, *J. Mol. Catal. A: Chem*, 263 (**2007**) 227.

216. M. R. Maurya, A. K. Chandrakar, S. Chand, *J. Mol. Catal. A: Chem*, 274 (**2007**) 192.

217. M. Salavati-Niasari, A. Sobhani, *J. Mol. Catal. A: Chem*, 285 (**2008**) 58.

****✿****

Experimental techniques, synthesis and characterisation of Schiff bases

2.1 INTRODUCTION

This chapter deals with the reagents used and various analytical and physico-chemical techniques employed in the characterisation, biological and catalytic activity studies. Details regarding the synthesis and characterisation including single crystal X-ray studies of the Schiff bases are also given in this chapter.

2.2 REAGENTS

The diamines used for the synthesis of Schiff bases are: 1,3-diaminopropane, 1,4-diaminobutane and 1,2-diaminocyclohexane and these were purchased from Sigma Aldrich Chemicals Private Limited, Bangalore. 1,2-Diaminoethane (Merck), orthophenylenediamine (Lobachemie), hydrazine

hydrate (Qualigens), D-glucose (S.D Fine Chem Limited), sodium sulphate (Merck), glacial acetic acid, sodium bicarbonate (Sisco Research Laboratories Limited) and diethyl ether (Lobachemie) were the other chemicals used for the synthesis and characterisation studies.

The following metal salts were used for the synthesis of Schiff base complexes: manganese(II) chloride tetrahydrate (Merck), nickel(II) perchlorate hexahydrate (Merck), copper(II) acetate tetrahydrate (Merck), copper(II) chloride dihydrate (Merck), copper(II) nitrate trihydrate (Merck) and copper(II) perchlorate hexahydrate (Merck).

Synthetic Y type zeolites were obtained from Zeoanalyst, Netherlands. Hydrogen peroxide (30% w/v, Merck), *tert*-butylhydroperoxide (Sigma Aldrich Chemicals Private Limited, Bangalore) and cyclohexanol (Qualigens) were used for the catalytic activity studies. Gas cylinders containing oxygen, nitrogen or hydrogen (Sterling gases, Cochin) were also used for the catalytic activity studies.

Phosphate buffered saline (PBS), Dalton's Lymphoma Ascites (DLA) cells, pUC18 DNA (GeNei, Bangalore), trypan blue, agarose gel, tris-acetate-EDTA buffer and ethydium bromide (Sigma Aldrich Chemicals Private Limited, Bangalore) were used for biological activity studies. All other reagents were of analytical reagent grade and the solvents employed were of 99% purity.

2.3 CHARACTERISATION TECHNIQUES

Different techniques were used to elucidate the bonding, structure and stereochemistry of the Schiff bases and the complexes prepared. The characterisation techniques used for the characterisation of synthesised compounds were elemental analysis, AAS, FTIR, UV-Visible, NMR and EPR spectral studies, molar conductance measurements, magnetic susceptibility measurements, single crystal XRD analysis, powder XRD analysis, thermogravimetric (TG) analysis, surface

area and pore volume analysis, scanning electron micrographs (SEM), gas chromatography (GC), trypan blue exclusion technique and gel electrophoresis. The characterisation techniques adopted are discussed below:

2.3.1 Elemental analysis

Micro analysis for carbon, hydrogen and nitrogen in the synthesised ligands and complexes were carried out on an Elementar model Vario EL III at Sophisticated Analytical Instrument Facility (SAIF), Sophisticated Test and Instrumentation centre (STIC), Kochi, Kerala.

2.3.2 Estimation of metal ions

The organic part of the complexes was completely eliminated before the estimation of metal ions. The following procedure was used for the estimation of metal ions present in the complexes [1]. A known weight of the complex (~ 0.3 g) was treated with concentrated sulphuric acid (5 mL) followed by concentrated nitric acid (20 mL). After the reaction was subsided, perchloric acid (5 mL, 60 %) was added. This mixture was kept aside until the colour of the solution changes to that of the metal salt. The clear solution thus obtained was evaporated to dryness on a water bath. After cooling, concentrated nitric acid (15 mL) was added and solution was evaporated to dryness on a water bath. The residue was dissolved in demineralised water and this solution was used for the estimation of metals. The estimation of metals was carried out on a Thermo Electron Corporation, M Series Atomic Absorption Spectrophotometer (AAS).

In the case of zeolite encapsulated copper complexes, the sample was accurately weighed (c g) and transferred to a beaker. Concentrated sulphuric acid (~40-50 mL) was added until the solution just fumed. It was then diluted with 200 mL water after cooling and filtered through an ashless filter paper. The residue was dried at 1000 °C in a platinum crucible, cooled and weighed (a g).

Then hydrofluoric acid (10 mL) was added to remove all the silica, which is removed as SiF_4 and the remaining solid, was finally ignited to 1000 °C (*b* g). From this the percentage of silica (SiO_2) was calculated using the equation.

$$\% \ SiO_2 = \frac{(a - b)}{c} \times 100$$

The residue in the platinum crucible was then fused with potassium persulphate until a clear melt was obtained. The melt was dissolved in demineralised water and filtered, and the filtrate was combined with earlier filtrate. This solution was used for the estimation of metals.

2.3.3 Estimation of chloride

Chlorine present in the complexes was converted into soluble sodium chloride by the peroxide fusion. A mixture of the complex (0.2 g), sodium carbonate (3 g) and sodium peroxide (2 g) was fused in a nickel crucible for nearly two hours. After this, it was treated with concentrated nitric acid. Chloride ion was then volumetrically estimated by Volhard's method [2], by precipitating it as silver chloride by the addition of a known volume of standard silver nitrate solution. The excess silver nitrate was titrated against standard ammonium thiocyanate solution using ferric alum as indicator.

2.3.4 Conductance measurements

The molar conductance values of the complexes were measured using a Systronic conductivity bridge type 305. The solvent used for the conductance measurement of the complexes under investigation was methanol. The molarity of the solution for this measurement was 10^{-3} M.

2.3.5 Electronic spectra

Electronic spectra of the ligands and its complexes in solution phase were recorded in the region 200-1100 nm on a Thermoelectron Nicolet evolution 300 UV-Vis spectrophotometer. Diffuse reflectance spectra of the zeolite encapsulated copper complexes were recorded at room temperature in a Jasco V 570 UV-Vis spectrophotometer in the wavelength range 200-900 nm. Absorbance spectra were obtained from the reflectance spectra by means of Kubelka–Munk transformations.

2.3.6 Infrared spectra

Room temperature FTIR spectra of the ligands, their simple and encapsulated complexes were recorded as KBr pellets with a JASCO FTIR 4100 spectrophotometer in the 4000-400 cm^{-1} range.

2.3.7 NMR spectra

^{1}H NMR spectra were recorded in CDCl$_3$ on a Bruker AVAVCE III 400 MHz-NMR spectrometer using TMS as the internal standard at the SAIF, Sophisticated Test and Instrumentation Center (STIC), Kochi, Kerala.

2.3.8 EPR spectra

X-band EPR spectra of the complexes were recorded in the solid state at RT, in the solid state at LNT and in DMF at LNT using Varian E-112 X/Q band spectrophotometer using tetracyanoethylene (TCNE) as standard at the SAIF, IIT, Mumbai, India.

2.3.9 Magnetic susceptibility measurements

The magnetic susceptibility measurements were done on a Magway MSB Mk 1 magnetic susceptibility balance, which works in the principle of Gouy balance. The Gouy tube was standardized using Hg[Co(NCS)$_4$] as recommended

by Figgis and Nyholm [3]. The most widely adopted method for determining magnetic moment of a complex is the Gouy method in which the weight difference experienced by a given amount of substance in the presence and absence of magnetic field is measured. The solid sample is tightly packed into weighed sample tube with a suitable length (*l*) and noted the sample weight (*m*). Then the packed sample tube was placed into tube guide of the balance and noted the reading (*R*). The mass susceptibility, χ_g, was calculated using the following equation.

$$\chi_g = \frac{C_{Bal} * l * (R - R_0)}{10^9 * m}$$

l = the sample length (cm)

m = the sample mass (g)

R = the reading for the tube plus sample

R_0 = the empty tube reading

C_{Bal} = the balance calibration constant

Then molar susceptibility, $\chi_m = \chi_g \times$ *molecular formula of the complex*. The molar susceptibility was corrected with diamagnetic contribution. The effective magnetic moment, μ_{eff}, was then calculated using the following expression: $\mu_{eff} = 2.83(X_A T)^{1/2}$ where X_A is the corrected molar susceptibility and T is the absolute temperature.

2.3.10 Thermogravimetric analysis

As the synthesised complexes contain varying number of water molecules, TG study was mainly carried out to know the number of coordinated or lattice water molecules. TG-DTA-DTG analyses of the complexes were carried out

under nitrogen at a heating rate of 10 ºC min^{-1} using a Perkin Elmer Pyres Diamond TG/DTA analyzer.

2.3.11 Single crystal XRD

Single crystal XRD analysis was performed with a BRUKER SMART APEX CCD X-ray diffractometer at University of Hyderabad and at CSMCRI Gujarat using Graphite monochromated Mo $K\alpha$ radiation ($\lambda = 0.71073$ Å, φ and ω scans). The data was reduced using SAINTPLUS [4] and a multiscan absorption correction using SADABS was performed [5]. The structure was solved using SHELXS-97 and full matrix least squares refinement against F^2 was carried out using SHELXL-97 in anisotropic approximation for non-hydrogen atoms [6]. All hydrogen atoms were assigned on the basis of geometrical considerations and were allowed to ride upon the respective carbon atoms.

2.3.12 Powder XRD analysis

The parent zeolite and the zeolite encapsulated complexes were analysed by powder X-ray diffraction for comparing their crystallinities. The X-ray diffractometer used in the present investigation is Rigaka D-Max C at the SAIF, Sophisticated Test and Instrumentation Center (STIC), Kochi, Kerala. Measurements were done with a stationary X-ray source, Ni filtered Cu$K\alpha$ radiation ($\lambda = 1.5404$ Å) and a movable detector which scans the intensity of the diffracted radiation as a function of the angle *2θ* between the incident and diffracted beams.

2.3.13 SEM

The morphology of the zeolite encapsulated complexes was examined by scanning electron microscope (JEOL model JSM-6390LV) at the SAIF, Sophisticated Test and Instrumentation Centre (STIC), Kochi, Kerala.

2.3.14 Surface area analysis

Surface area of the encapsulated complexes was measured by multipoint BET method using a Micromeritics Gemini 2360 surface area analyzer. Nitrogen gas was used as the adsorbate at liquid nitrogen temperature.

2.3.15 Gas chromatography

The catalytic activity studies were performed with a Chemito 8510 Gas chromatograph. The instrumentation consists of a tank of carrier gas, an injection port for introducing the sample, the column and a detector. The various components in the reaction mixture were separated using an OV-17 or carbowax column. The peaks appearing on the recorder are characteristic of the components present in the reaction mixture and its area corresponds to the amount of the component present in the mixture.

2.3.16 Trypan blue exclusion method

In vitro cytotoxicity of the complexes was studied on Dalton Lymphoma Ascites (DLA) cells by trypan blue exclusion method. The dye exclusion test is used to determine the number of viable cells present in a cell suspension. It is based on the principle that live cells possess intact cell membranes that exclude dye, like trypan blue, eosin or propidium, whereas dead cells do not. The number of dead cells was counted using a haemocytometer. This experiment was done at Amala Cancer Research Center, Thrissur, Kerala.

2.3.17 Gel electrophoresis

Gel electrophoresis is usually performed for analytical purposes. It is most commonly used for the separation of biological macromolecules such as DNA, RNA or protein. Electrophoresis refers to the movement of a charged particle in an electrical field. This method enables the sorting of molecules based on size

and charge. In gel electrophoresis a gel is used as an anticonvective medium and or sieving medium. Gels suppress the thermal convection caused by application of the electric field, and can also act as a sieving medium retarding the passage of molecules. The molecules being sorted are dispensed into a well in the gel material. The gel is placed in an electrophoresis chamber, which is then connected to a power source. When the electric current is applied, the larger molecules move more slowly through the gel, while the smaller molecules move faster. The different sized molecules form distinct bands on the gel. After the electrophoresis is complete, the molecules in the gel can be stained to make them visible. Ethydium bromide, silver, or coomassie brilliant blue dye may be used for this process. This can be viewed under UV transilluminator (Bio-Rad UV Transilluminator 2000) and photographed. Depending on the number of different molecules, each lane shows separation of the components from the original mixture as one or more distinct bands, one band per component. Incomplete separation of the components can lead to overlapping bands, or to indistinguishable smears representing multiple unresolved components. The distance a band travels is approximately inversely proportional to the logarithm of the size of the molecule. This experiment was carried out at Department of Biotechnology, Cochin University of Science and Technology, Kochi, Kerala.

2.4 SYNTHESIS AND CHARACTERISATION OF SCHIFF BASES

2.4.1 Synthesis of quinoxaline-2-carboxaldehyde

The aldehyde selected for the synthesis of Schiff bases was quinoxaline-2-carboxaldehyde. The following procedure was adopted to synthesise quinoxaline-2-carboxaldehyde [7,8]. Refluxing D-glucose (36 g, 0.2 mol) with orthophenylene diamine (21.6 g, 0.2 mol) in the presence of hydrazine hydrate (5 mL, 0.1 mol) and glacial acetic acid (6 mL), on a boiling water bath under carbon dioxide atmosphere (provided by the addition of a pinch of sodium carbonate) for 5 hours

gave the compound, 2(D-arabinotetrahydroxybutyl)quinoxaline. This product was purified by recrystallisation from hot water. The recrystallised 2-(D-arabinotetrahydroxybutyl)quinoxaline (5 g, 0.02 mol) was dissolved in water (300 mL) containing glacial acetic acid (10 mL) and sodium metaperiodate (13 g, 0.06 mol) and was kept at room temperature (28 ± 2 °C) with controlled stirring for 16 hours. It was then filtered and the filtrate was neutralized with sodium bicarbonate. The neutral solution was extracted with ether. The ether extract was dried with anhydrous sodium sulphate. It was then filtered and evaporated to dryness. The resulting residue was recrystallised from petroleum ether to give pure quinoxaline-2-carboxaldehyde [Figure 2.1] (60% yield, m.p. 107 °C).
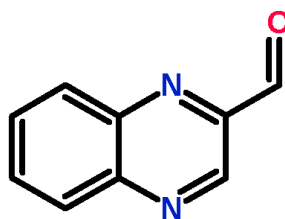
Figure 2.1: Structure of quinoxaline-2-carboxaldehyde

2.4.2 Synthesis of Schiff bases

The Schiff bases derived from quinoxaline-2-carboxaldehyde and diamines constitute one of the important ligand systems [9,10]. In the present investigation, the Schiff bases were formed by the condensation reaction of quinoxaline-2-carboxaldehyde with hydrazine hydrate, 1,2-diaminoethane, 1,3-diaminopropane, 1,4-diaminobutane, 1,2-diaminocyclohexane or 1,2-diaminobenzene to obtain the following Schiff bases:
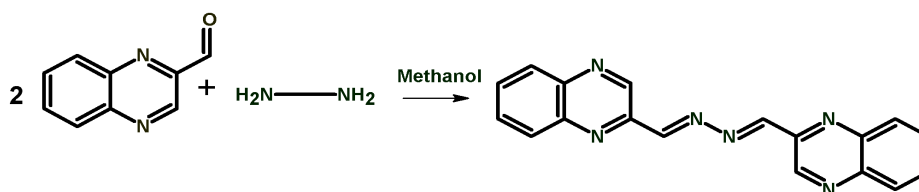
1. *N,N′*-bis(quinoxaline-2-carboxalidene)hydrazine (*qch*)
2. *N,N′*-bis(quinoxaline-2-carboxalidene)-1,2-diaminoethane (*qce*)
3. *N,N′*-bis(quinoxaline-2-carboxalidene)-1,3-diaminopropane (*qcp*)

4.   *N,N'*-bis(quinoxaline-2-carboxalidene)-1,4-diaminobutane (*qcb*)

5.   *N,N'*-bis(quinoxaline-2-carboxalidene)-1,2-diaminocyclohexane (*qcc*)

6.   *N,N'*-bis(quinoxaline-2-carboxalidene)-1,2-diaminobenzene (*qco*)

The prepared six Schiff bases were found to be neutral ligands and their structure was confirmed by various analytical and physico-chemical techniques. Very few reports are available on the crystal structures of the Schiff bases derived from quinoxaline-2-carboxaldehyde. Therefore efforts were made to obtain the single crystals of these ligands and the crystals obtained were characterised by single crystal X-ray diffraction methods.

2.4.2.1 *Synthesis of N,N'-bis(quinoxaline-2-carboxalidene)hydrazine (qch)*

To a hot solution of qunioxaline-2-carboxaldehyde (0.3163 g, 2 mmol; in 50 mL methanol), a hot solution of hydrazine hydrate (0.05 mL, 1 mmol; in 25 mL methanol) was slowly added with constant stirring. The resulting solution on cooling gave the yellow Schiff base, *qch* (Scheme 2.1), which was filtered off, washed with cold methanol and dried over anhydrous calcium chloride. (60% yield, m.p. 252 °C)
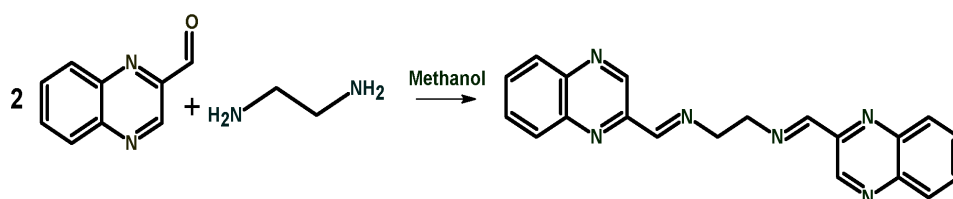

Scheme 2.1: *Preparation of qch*

2.4.2.2 *Synthesis of N,N'-bis(quinoxaline-2-carboxalidene)-1,2-diaminoethane (qce)*

A hot solution of 1,2-diaminoethane (0.1 mL, 1 mmol; in 25 mL methanol) was slowly added to a hot solution of qunioxaline-2-carboxaldehyde (0.3163 g, 2 mmol; in 50 mL methanol). The resulting solution on cooling yielded the Schiff
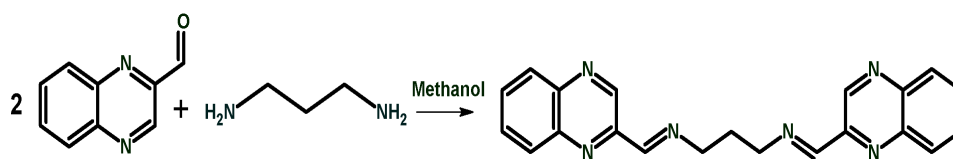
base, *qce* (Scheme 2.2). The Schiff base was filtered off, washed with cold methanol and dried over anhydrous calcium chloride. Light yellow single crystals of the *qce* were obtained from a solution of dichloromethane by slow evaporation [11]. (60% yield, m.p. 191 °C)

Scheme 2.2: *Preparation of qce*

2.4.2.3 Synthesis of N,N'-bis(quinoxaline-2-carboxalidene)-1,3-diaminopropane (*qcp*)

A hot solution of 1,3-diaminopropane (0.08 mL, 1 mmol; in 25 mL methanol) was slowly added to a hot solution of qunioxaline-2-carboxaldehyde (0.3163 g, 2 mmol; in 50 mL methanol). The solution obtained after mixing was cooled and formed the Schiff base, *qcp*, (Scheme 2.3) separated out was filtered off, washed with cold methanol and dried over anhydrous calcium chloride. Colourless single crystals of *qcp* suitable for X-ray diffraction were grown by slow evaporation from a mixture of solution containing dichloromethane and toluene in 1:1 ratio [12]. (75% yield, m.p. 158 °C)

Scheme 2.3: *Preparation of qcp*

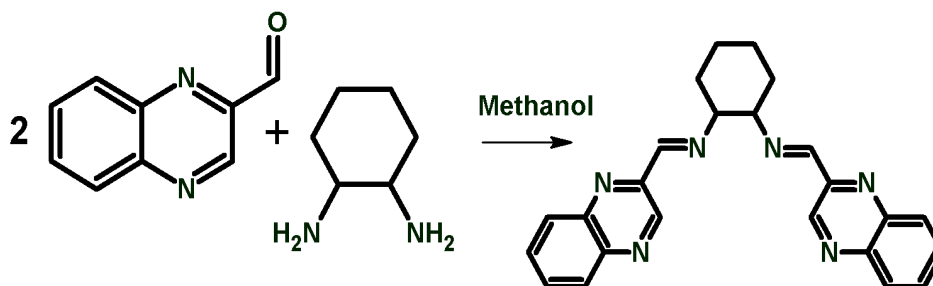**2.4.2.4 *Synthesis of N,N'-bis(quinoxaline-2-carboxalidene)-1,4-diaminobutane (qcb)***

A hot solution of 1,4-diaminobutane (0.1 mL, 1 mmol; in 25 mL methanol) was slowly added to a hot solution of qunioxaline-2-carboxaldehyde (0.3163 g, 2 mmol; in 50 mL methanol). The resulting solution on cooling yielded the Schiff base, *qcb* (Scheme 2.4). The precipitated Schiff base was filtered off, washed with cold methanol and dried over anhydrous calcium chloride. Colourless single crystals of *qcb* suitable for X-ray diffraction were grown by slow evaporation from a mixture of solution containing dichloromethane and toluene in 1:1 ratio [12]. (75% yield, m.p. 153 °C)
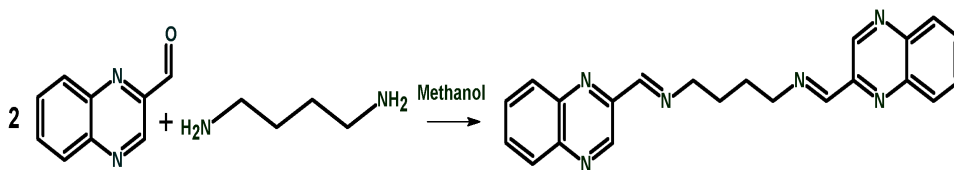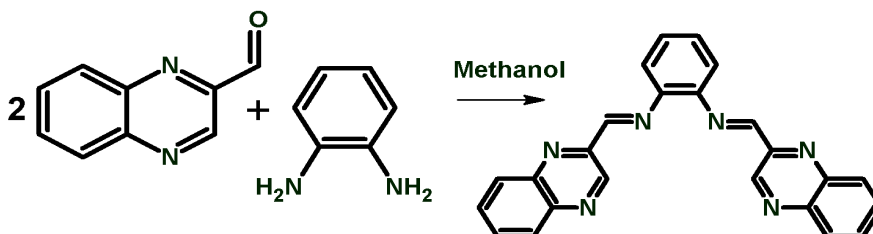

Scheme 2.4: *Preparation of qcb*

2.4.2.5 *Synthesis of N,N'-bis(quinoxaline-2-carboxalidene)-1,2-diaminocyclohexane (qcc)*

A mixture of quinoxaline-2-carboxaldehyde (0.3163 g, 2 mmol; in 50 mL methanol) and 1,2-diaminocyclohexane (0.1 mL, 1 mmol in 25 mL methanol) were refluxed for three hour. After that, the resulting solution was cooled in a refrigerator. The Schiff base, *qcc*, (Scheme 2.5) was precipitated within half an hour. The precipitate was filtered and recrystallised from methanol. The recrystallised product was dried in a desiccator over anhydrous calcium chloride. Colourless single crystals of *qcc* suitable for X-ray diffraction were grown by slow evaporation from a solution of dichloromethane and toluene in a 1:1 ratio. (85% yield, m.p.170 °C)

Scheme 2.5: *Preparation of qcc*

2.4.2.6 Synthesis of N,N'-bis(quinoxaline-2-carboxylidene)-1,2-diaminobenzene (qco)

A mixture of quinoxaline-2-carboxaldehyde (0.3163 g, 2 mmol; in 50 mL methanol) and orthophenylenediamine (0.1 g, 1 mmol; in 25 mL methanol) were refluxed for three hour. After that, the solution was cooled in a refrigerator. A yellow Schiff base, *qco,* (Scheme 2.6) formed was filtered and recrystallised from methanol. The recrystallised product was dried in a desiccator over anhydrous calcium chloride. (90% yield, m.p. 175 °C)

Scheme 2.6: *Preparation of qco*

2.4.3 Characterisation of the Schiff bases

The synthesised Schiff bases, *qch*, *qce*, *qcp*, *qcb*, *qcc* and *qco*, were characterised by elemental analysis, electronic spectra, infrared spectra, ^{1}H NMR spectra and single crystal XRD studies.

2.4.3.1 Elemental analysis

The analytical data of the Schiff base are in good agreement with the expected molecular formula and are given in Table 2.1.

Table 2.1: Analytical data of Schiff bases

| Schiff base	Empirical formula	Colour	Formula weight	Carbon (%)	Hydrogen (%)	Nitrogen (%)
qch	$C_{18}H_{12}N_6$	Yellow	312	69.27 (69.22)	3.70 (3.87)	27.02 (26.91)
qce	$C_{20}H_{16}N_6$	Colourless	340	70.70 (70.57)	4.30 (4.74)	24.40 (24.69)
qcp	$C_{21}H_{18}N_6$	Colourless	354	70.86 (71.17)	5.42 (5.12)	23.59 (23.71)
qcb	$C_{22}H_{20}N_6$	Colourless	368	71.12 (71.72)	5.95 (5.47)	22.95 (22.81)
qcc	$C_{24}H_{22}N_6$	Colourless	394	72.92 (73.07)	5.50 (5.62)	21.22 (21.30)
qco	$C_{24}H_{16}N_6$	Yellow	388	73.81 (74.21)	4.12 (4.15)	21.36 (21.64)

∗Calculated values in parentheses

2.4.3.2 Electronic spectra

The electronic spectroscopic investigations of Schiff bases were carried out in methanol solution (1×10^{-5} M) in the range 200-900 nm. The absorption maxima of Schiff bases are listed in the Table 2.2. The UV-Visible spectra of these are shown in Figure 2.2. The spectra of Schiff bases exhibit three major bands. These bands may be due to either $\pi \rightarrow \pi^*$ or $n \rightarrow \pi^*$ transitions of both quinoxaline and azomethine systems. The Schiff base *qch* shows two bands, which can be assigned to $\pi \rightarrow \pi^*$ type transitions of the heterocyclic quinoxaline ring or azomethine of the Schiff bases. Other Schiff bases exhibit bands of both $\pi \rightarrow \pi^*$ and $n \rightarrow \pi^*$ transitions. The $n \rightarrow \pi^*$ transition (less intense) may be due to the nonbonding electrons present on the transition of the C=N group in quinoxaline ring or in the azomethine group [9, 15].

Table 2.2: UV-Visible spectral data of Schiff bases

Schiff base	λ_{max} (nm)	λ_{max} (cm^{-1})
qch	230	43480
	271	36900
	343	29150
qce	202	49504
	245	40810
	316	31640
qcp	216	46290
	243	41150
	320	31250
qcb	207	48300
	245	40810
	318	31440
qcc	204	49020
	245	40810
	320	31250
qco	239	41840
	265	37730
	359	27850
	433	23094
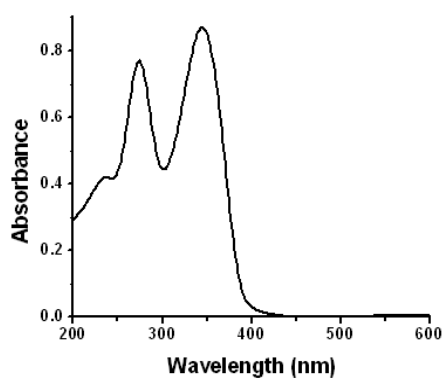
UV-Vis spectrum of qch

UV-Vis spectrum of qce

UV-Vis spectrum of qcp

UV-Vis spectrum of qcb

UV-Vis spectrum of qcc
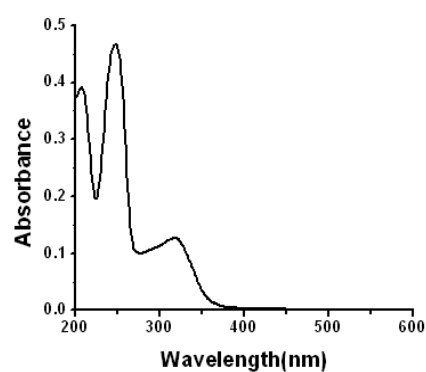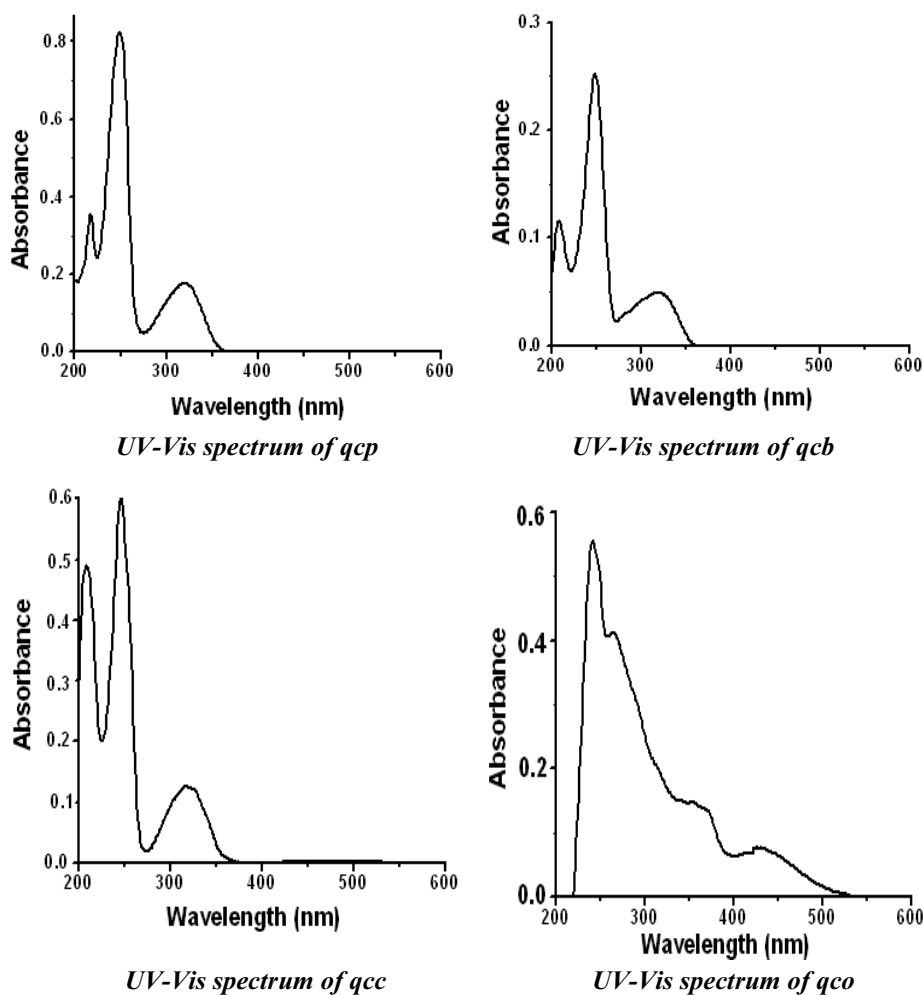

UV-Vis spectrum of qco

Figure 2.2: Electronic spectra of Schiff bases

2.4.3.3 Infrared spectra

The most significant IR spectral bands are given in Table 2.3. Examination of the $-NH_2$, $-CH=O$, and $-C=N-$ regions of the infrared spectra provided valuable structural information related to the structure of the Schiff bases. The absence of the characteristic stretching frequency of C=O of the aromatic

aldehyde and $-NH_2$ groups of diamine, indicates that the condensation was complete. Although all the free ligands, *qch, qce, qcp, qcb, qcc* and *qco*, contain different types of C=N bonds (two from each quinoxaline ring and two from the azomethine linkage), the IR bands due to them are not well resolved in the infrared spectra of the ligand. These ligands show [Figure 2.3] a very strong absorption band in 1610-1640 cm^{-1} range, which is characteristic of the azomethine ν(C=N) group [10,13]. The peaks that appear in the range 1550-1580 cm^{-1} in the range could be due to the ν(C=N) stretches of the quinoxaline ring [9]. The bands in the range 3050-2980 cm^{-1} could be assigned to the C-H stretching of aromatic and methylene groups, respectively. The medium intensity bands observed in the range 1220-923 cm^{-1} may be due to the in-plane bending of the aromatic C-H, and those at 900-700 cm^{-1} range may be due to the out of plane bending vibration of the aromatic C-H.

Table 2.3: IR spectral data of Schiff bases (ν in cm^{-1})

Schiff base	ν(C=N) (Azomethine)	ν(C=N) (Quinoxaline)	ν (C-H) (Aromatic)
qch	1622	1568	3048
qce	1639	1555	3047
qcp	1636	1573	3053
qcb	1640	1555	3056
qcc	1640	1556	3062
qco	1610	1568	3062

FTIR spectrum of qch

FTIR spectrum of qce

FTIR spectrum of qcp

FTIR spectrum of qcb

FTIR spectrum of qcc
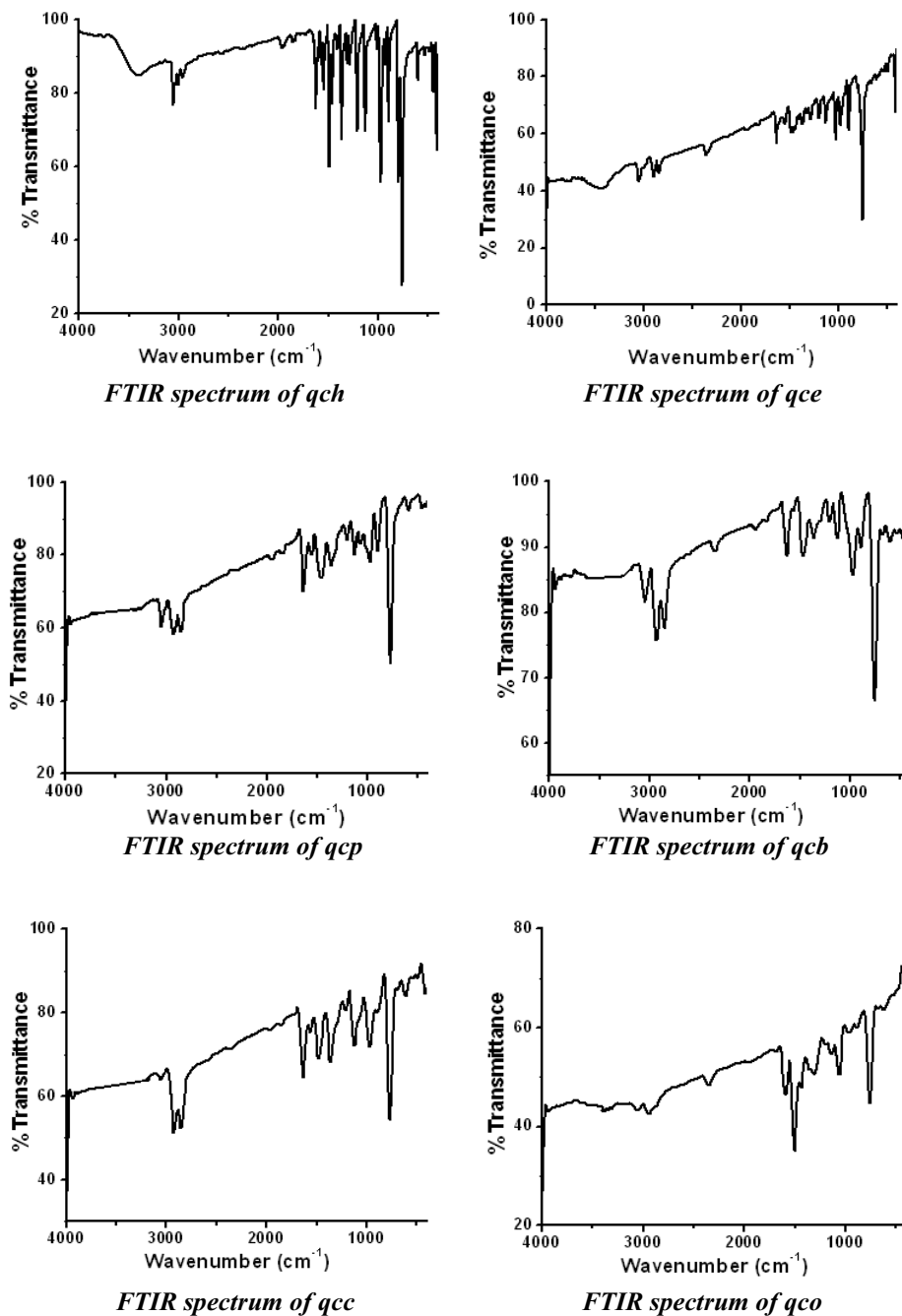
FTIR spectrum of qco

Figure 2.3: FTIR spectra of Schiff bases
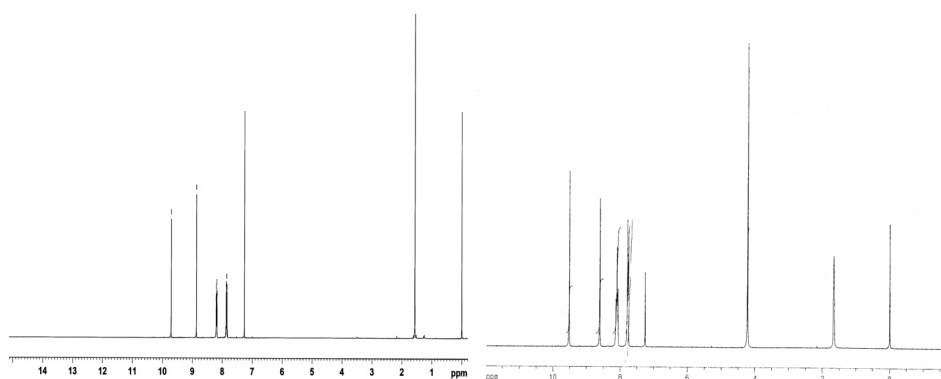
2.4.3.4 ^{1}H NMR spectra

The proton NMR spectra of the ligands in CDCl$_3$ were recorded using tetramethylsilane (TMS) as the internal standard. The NMR spectra of Schiff bases are shown in Figure 2.4 and the spectral data are summarised in Table 2.4.

Table 2.4: ^{1}H NMR spectral data of Schiff bases

Schiff base	Chemical shift δ (ppm)	Assignment
qch	9.70, 8.90	(s, 2H, CH azomethine)
	7.80-8.20	(m, 8H, aromatic protons)
qce	9.70, 8.90	(s, 2H, CH azomethine)
	7.80-8.20	(m, 8H, aromatic protons)
	4.20	(s, 4H aliphatic protons)
qcp	9.70, 8.90	(s, 2H, CH azomethine)
	7.80-8.20	(m, 8H, aromatic protons)
	2.26-2.32	(m, 2H aliphatic protons)
	4.25	(s, 4H aliphatic protons)
qcb	9.70, 8.90	(s, 2H, CH azomethine)
	7.80-8.20	(m, 8H, aromatic protons)
	1.92-1.95	(m, 4H aliphatic protons)
	3.84-3.87	(t, 4H aliphatic protons)
qcc	9.70, 8.90	(s, 2H, CH azomethine)
	7.80-8.20	(m, 8H, aromatic protons)
	1.80-1.90	(m, 8H aliphatic protons)
	3.67-3.69	(t, 2H aliphatic protons)
qco	9.70, 8.90	(s, 2H, CH azomethine)
	7.80-8.20	(m, 8H, aromatic protons)

The NMR spectra of all Schiff bases show signal at ~1.6 ppm, which is due to water present in CDCl$_3$. The signals due to the CHCl$_3$ and TMS are present in the spectra at ~7.2 ppm and at 0 ppm, respectively. The azomethine protons

appear as a singlet at ~ 9.7 and 8.9 ppm and all the eight aromatic protons appear as a multiplet in the range 7.80-8.20 ppm. In addition to this, there are aliphatic protons present as a bridge between the azomethine groups in the case of Schiff bases, *qce*, *qcp* and *qcb*. Usually the aliphatic protons are found at 2-3 ppm [14,15]. Four aliphatic protons are present in *qce* (-CH$_2$-CH$_2$-) and it appears as a singlet at 4.2 ppm. This value is found to be higher than that expected for usual aliphatic protons, which might be due to the presence of an adjacent imine group. There are six aliphatic protons (-CH$_2$-CH$_2$-CH$_2$-) in *qcp*, of which the two protons of the central carbon atom appear as a multiplet in the region 2.26-2.32 ppm and the other four protons adjacent to imine groups appear as a singlet at higher chemical shift value 4.25 ppm. In the case of *qcb* (-CH$_2$-CH$_2$-CH$_2$-CH$_2$-), the central four protons appear as a multiplet at 1.92-1.95 ppm and the other protons nearer to imine group appear as a triplet in the range 3.84-3.87 ppm. Cyclohexane acts as a bridge between two azomethine groups in *qcc*. In this case eight protons in the ring appear as a multiplet in the range 1.8-1.9 ppm. The two protons connected to the imino group appear as a triplet in the region 3.67-3.69 ppm. The spectrum obtained for *qco* was not good and the splitting could not be resolved.

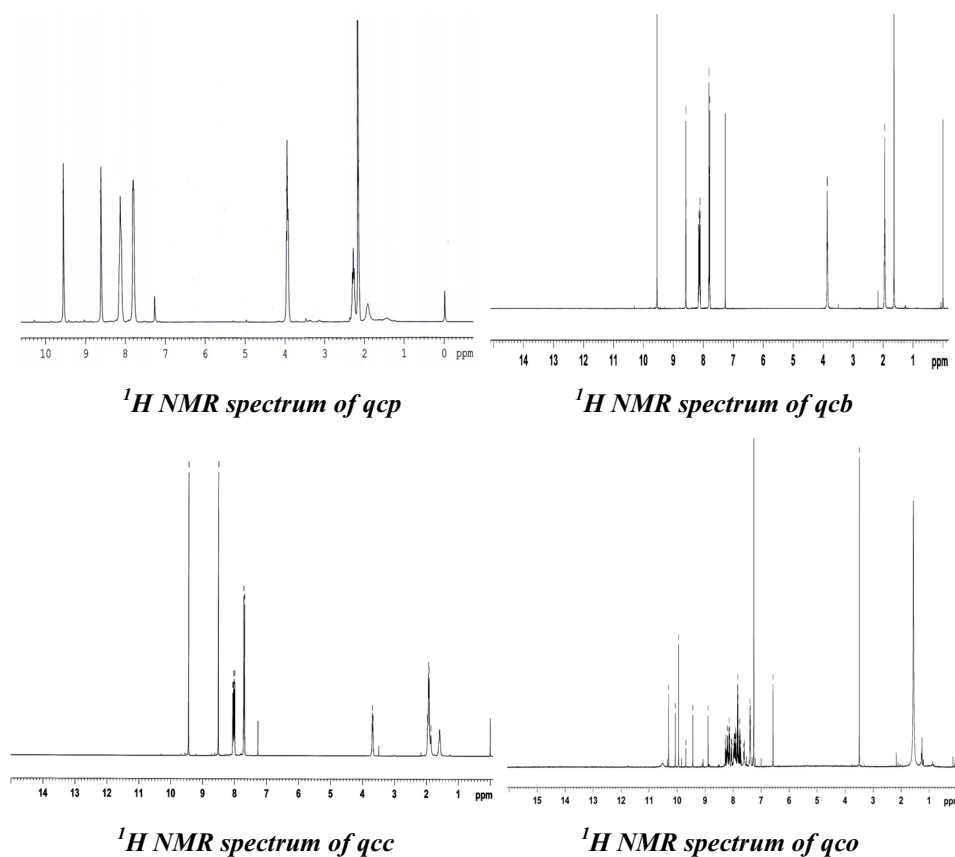*¹H NMR spectrum of qch*   *¹H NMR spectrum of qce*

^{1}H NMR spectrum of qcp

^{1}H NMR spectrum of qcb

^{1}H NMR spectrum of qcc

^{1}H NMR spectrum of qco

Figure 2.4: ^{1}H NMR spectra of Schiff bases

2.4.3.5 Crystal structure analysis

2.4.3.5.1 *Crystal structure analysis of N,N'-bis(quinoxaline-2-carboxalidene)-1,2-diaminoethane (qce)*

The single crystals suitable for XRD were obtained by the slow evaporation of solution of *qce* in dichloromethane [11]. The compound crystallises in triclinic crystal system with the space group *P-1*. Summary of the crystallographic data and refinement parameters is given in Table 2.5.

Table 2.5: Crystallographic and refinement details of *qce*

Empirical formula	$C_{20}H_{16}N_6$	a (Å)	6.888 (2)
Formula weight	340.39	b (Å)	7.381 (3)
Crystal size (mm)	0.40 x 0.24 x 0.18	c (Å)	9.638 (4)
		α (°)	101.674 (6)
Crystal system	Triclinic	β (°)	96.233 (6)
Space group	*P-1*	γ (°)	116.046 (5)
Z	1	V (Å³)	420.1(3)
μ (mm⁻¹)	0.085	Mo $K\alpha$ radiation λ = 0.71073 Å	

Data collection	**Refinement**
Brucker SMART APEX CCD area detector diffractometer	Refinement on F^2
φ and ω scans	$R[F^2 > 2\sigma(F^2)] = 0.0714$
Absorption correction: empirical	$wR(F^2) = 0.1584$
T_{min} = 0.9668 $\quad$ T_{max} = 0.9848	S = 1.268
3956 measured reflections	1465 reflections
1465 independent reflections	118 parameters
1239 reflections with $I > 2\sigma(I)$	All H atoms parameters refined
R_{int} = 0.0252	Δp_{max} = 0.131 e Å⁻³
	Δp_{min} = -0.212 e Å⁻³

The molecular structure of the compound was solved at 298 K. Figure 2.5 gives the ORTEP diagram of the compound with atomic labeling scheme. The important interatomic distances and angles are listed in Table 2.6. In the *qce*, $C_{20}H_{16}N_6$, the central C—C bond lies on a crystallographic inversion centre. The quinoxalidine ring is nearly planar, with a maximum deviation of 0.021 (2) Å

from the mean plane. The crystal structure is stabilised by intermolecular C—H…N interactions, leading to the formation of a layer-like structure, which extends along the *a* axis [Figure 2.6].
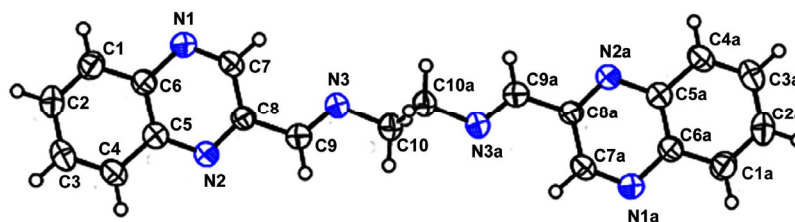

Figure 2.5: ORTEP diagram of *qce* with atomic labeling scheme with 50% probability ellipsoids

Table 2.6: Selected bond lengths (Å) and angles (°).

N(1)-C(7)	1.298 (3)
N(1)-C(6)	1.373 (3)
N(2)-C(8)	1.315 (3)
N(2)-C(5)	1.369 (3)
N(3)-C(9)	1.260 (3)
N(3)-C(10)	1.455 (3)
C(8)-C(9)	1.472 (3)
C(10)-C(10)#1	1.512 (5)
C(8)-N(2)-C(5)	116.2 (2)
C(9)-N(3)-C(10)	117.9 (2)
N(3)-C(9)-C(8)	121.5 (2)
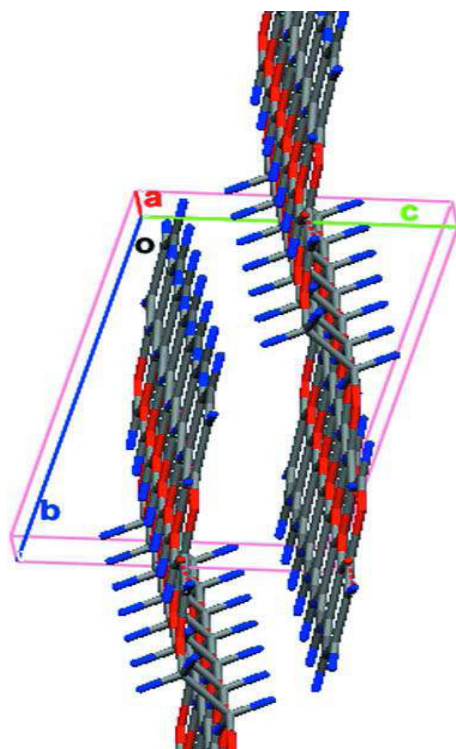
Figure 2.6: Pairs of C-H…N interactions lead to a layer like structure along the *a* axis

2.4.3.5.2 *Crystal structure analysis of N,N'-bis(quinoxaline-2-carboxalidene)-1,3-diaminopropane (qcp)*

Colourless single crystals of *qcp* suitable for X-ray diffraction were grown by slow evaporation from a solution in dichloromethane and toluene (1:1 v/v) [12]. The compound crystallises in monoclinic crystal system with the space group *C2/c*. Summary of the crystallographic data and refinement parameters is given in Table 2.7.

Table 2.7: Crystallographic and refinement details of *qcp*

Empirical formula	$C_{21}H_{18}N_6$	*a* (Å)	10.371 (2)
Formula weight	354.41	*b* (Å)	9.180 (2)
Crystal size (mm)	0.45 x 0.35 x 0.12	*c* (Å)	19.084 (4)
Crystal system	Monoclinic	β (°)	90.209 (4)
Space group	*C2/c*	V (Å^3)	1817.0 (7)
Z	4	Mo $K\alpha$ radiation	
μ (mm^{-1})	0.08	λ = 0.71073 Å	
Data collection		**Refinement**	
Brucker SMART APEX CCD area detector diffractometer		Refinement on F^2	
φ and ω scans		R[F^2 > 2σ(F^2)] = 0.076	
Absorption correction: empirical		wR(F^2) = 0.169	
T_{min} = 0.964 T_{max} = 0.990		S = 1.18	
5277 measured reflections		2086 reflections	
2086 independent reflections		159 parameters	
1695 reflections with *I* > *2σ(I)*		All H atoms parameters refined	
R$_{int}$ = 0.023		$\triangle p_{max}$ = 0.23 e Å $^{-3}$	
		$\triangle p_{min}$ = -0.17 e Å $^{-3}$	

Table 2.8: Selected bond lengths (Å) and angles (°).

N1-C1	1.303 (3)	N2-C8-C1	122.0 (2)
N1-C2	1.373 (3)	N2-C8-C7	116.5 (2)
N2-C8	1.315 (3)	N3-C9-C8	122.3 (2)
N2-C7	1.366 (3)	N3-C10-C11	110.3 (2)
N3-C9	1.256 (3)	C10-C11-C10	112.3 (3)
N3-C10	1.459 (3)		
C11-C10	1.514 (3)		

In *qcp*, [Figure 2.7] one half of the molecule is related to the other half by a twofold axis passing through atom C11. The value of the N3—C10—C11—C10A torsion angle [180.0 (2)°] implies a trans alignment of the quinoxaline ring systems with respect to the azomethine C=N bond (*i.e.* C9—N3) [16]. The quinoxaline systems are nearly planar, with a maximum deviation of 0.0021 Å from the mean plane. The dihedral angle between the two quinoxaline ring systems is 87.97 (3)°. The crystal structure cohesion is reinforced by π-π stacking interactions, forming a zigzag pattern along the *c* axis, with a mean Cg1---Cg1(-x+1/2, -y+3/2, -z+1) distance of 3.784 (14) Å (Cg1 is the centroid of the six membered ring that includes atoms C2–C7) [Figure 2.8]. The perpendicular distance between the rings is 3.4737 (8) Å. The important bond lengths and angles are given in Table 2.8.
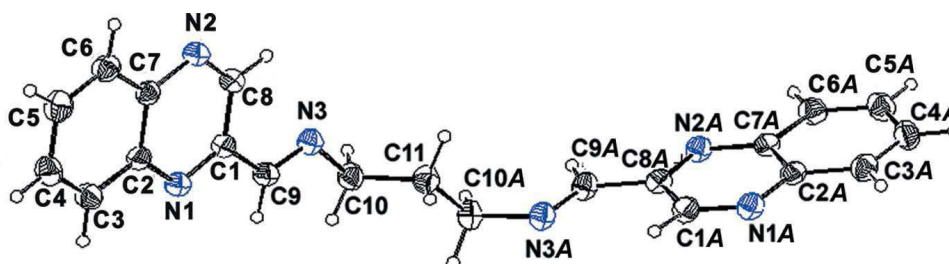
Figure 2.7: ORTEP diagram of *qcp* with atomic labeling scheme with 50% probability ellipsoids
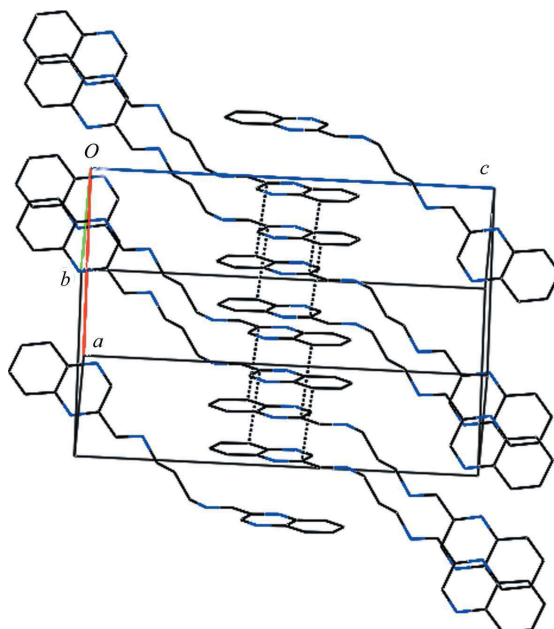
Figure 2.8: π-π stacking interactions of *qcp* forming chains, H atoms have been omitted for clarity

2.4.3.5.3 *Crystal structure analysis of N,N'-bis(quinoxaline-2-carboxalidene)-1,4-diaminobutane (qcb)*

Colourless single crystals of *qcb* suitable for X-ray diffraction were grown by slow evaporation from a solution in dichloromethane and toluene (1:1 v/v) [12]. The compound crystallises in monoclinic crystal system with the space group *C2/c*. Summary of the crystallographic data and refinement parameters is given in Table 2.9.

For *qcb* [Figure 2.9], the central C—C bond lies on a crystallographic inversion centre and the two halves of the molecule are in a trans orientation. The quinoxalidene ring systems and the C=N imine bonds are coplanar, as indicated by the C10—N3—C9—C8 torsion angle [-179.2 (2)°]. The central N3—C10—C11—C11A fragment is planar [177.3 (3)°]. The quinoxaline systems are nearly

planar, with a maximum deviation of 0.0022 Å from the mean plane. The selected bond lengths and angles are listed in Table 2.10. The crystal structure of this compound is also stabilised by π-π stacking interactions, along the *b* axis, with a mean centroid–centroid distance of 4.243 (18) Å [Figure 2.10]. The perpendicular distance between adjacent rings is 3.165 Å.

Table 2.9: Crystallographic and refinement details of *qcb*

Empirical formula	$C_{22}H_{20}N_6$	*a* (Å)	4.4819 (12)
Formula weight	368.44	*b* (Å)	5.3333 (14)
Crystal size (mm)	0.75 x 0.35 x 0.14	*c* (Å)	39.456 (10)
Crystal system	Monoclinic	β (°)	92.266 (4)
Space group	*P2₁/c*	V (Å³)	942.4 (4)
Z	2	Mo *Kα* radiation	
μ (mm⁻¹)	0.08	λ = 0.71073 Å	

Data collection		**Refinement**	
Brucker SMART APEX CCD area detector diffractometer		Refinement on F^2	
φ and ω scans		R[$F^2 > 2\sigma(F^2)$] = 0.071	
Absorption correction: empirical		wR(F^2) = 0.186	
T_{min} = 0.942	T_{max} = 0.989	S = 1.14	
5220 measured reflections		2132 reflections	
2132 independent reflections		167 parameters	
1748 reflections with *I > 2σ(I)*		All H atoms parameters refined	
R$_{int}$ = 0.020		$\Delta \rho_{max}$ = 0.21 e Å⁻³	
		$\Delta \rho_{min}$ = -0.17 e Å⁻³	

Table 2.10: **Selected bond lengths (Å) and angles (°).**

N(2)-C(7)	1.302 (3)	N(1)-C(1)-C(8)	123.9 (2)
N(1)-C(8)	1.373 (3)	N(2)-C(7)-C(6)	116.9 (2)
N(2)-C(6)	1.313 (3)	C(7)-C(8)-C(9)	121.6 (2)
N(1)-C(1)	1.369 (3)	N(3)-C(9)-C(8)	121.8 (2)
N(3)-C(9)	1.255 (3)	N(3)-C(10)-C(11)	110.8(2)
N(3)-C(10)	1.463 (3)	C(10)-C(11)-C(11)A	113.1(3)
C(8)-C(9)	1.476 (3)		
C(10)-C(11)	1.509 (4)		
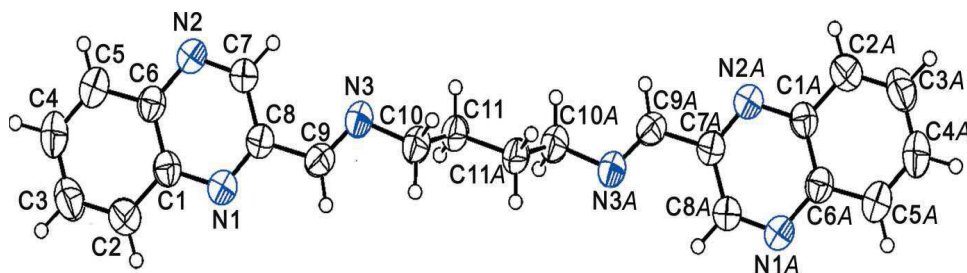
Figure 2.9: ORTEP diagram of *qcb* with atomic labeling scheme with 50% probability ellipsoids
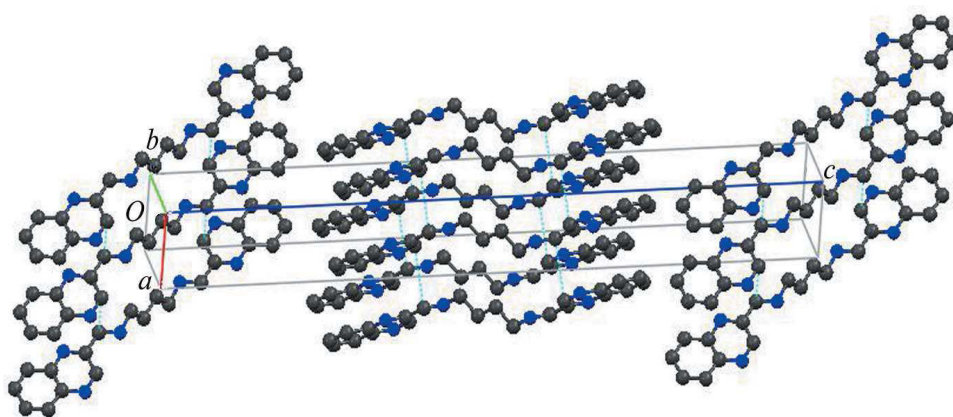
Figure 2.10: π-π stacking interactions of *qcb*, forming chains in the [010] direction. H atoms have been omitted for clarity.

2.4.3.5.4 *Crystal structure analysis of N,N'-bis(quinoxaline-2-carboxylidene)-1,2-diaminocyclohexane (qcc)*

Colourless single crystals of *qcc* suitable for X-ray diffraction were grown by slow evaporation from a solution in methanol. The compound [Figure 2.11] crystallises in triclinic crystal system with the space group *P-1*. Summary of the crystallographic data and refinement parameters is given in Table 2.11. The important interatomic distances and angles are listed in Table 2.12. In the *qcc*, $C_{24}H_{22}N_6$, the central C—C bond of cyclohexanediamine lies on a crystallographic inversion centre. The quinoxalidine ring is nearly planar. The crystal structure is stabilised by intermolecular C—H…N interactions. The packing diagram is given in the Figure 2.12.

Table 2.11: Crystallographic and refinement details of *qcc*

Empirical formula	$C_{24}H_{22}N_6$	a (Å)	10.407 (2)
Formula weight	394.47	b (Å)	10.656 (2)
Crystal size (mm)	0.75 x 0.35 x 0.14	c (Å)	11.857 (2)
Crystal system	Triclinic	α (°)	112.53 (2)
Space group	*P-1*	β (°)	100.386 (17)
Z	3	γ (°)	108.946 (19)
μ (mm^{-1})	0.075	V (Å^3)	1076.6 (4)
Mo $K\alpha$ radiation		λ = 0.71073 Å	
Data collection		**Refinement**	
Brucker SMART APEX CCD area detector diffractometer		Refinement on F^2	
φ and ω scans		R[F^2 > 2σ(F^2)] = 0.045	
Absorption correction: empirical		wR(F^2) = 0.127	
T_{min} = 0.942 T_{max} = 0.989		S = 0.775	
8025 measured reflections		2413 reflections	
4907 independent reflections		271 parameters	
2413 reflections with $I > 2\sigma(I)$		All H atoms parameters refined	
R$_{int}$ = 0.020		$\Delta\rho_{max}$ = 0.12 e Å^{-3}	
		$\Delta\rho_{min}$ = -0.16 e Å^{-3}	

Table 2.12: **Selected bond lengths (Å) and angles (°).**

N1-C7	1.3179 (17)		
N1-C5	1.363 (2)	C9-N3-C10	118.24 (13)
N2-C8	1.305 (2)		
N2-C6	1.3704 (19)	C16-N4-C15	117.60 (13)
N3-C9	1.2580 (17)		
N3-C10	1.4640 (2)	N4-C15-C10	109.84 (12)
N4-C16	1.2588 (19)		
N4-C15	1.4684 (19)	N3-C10-C15	108.75 (12)
N3-C9	1.2580 (17)		
N3-C10	1.4640 (2)	N3-C9-C7	122.29 (14)
N4-C16	1.2588 (19)		
N4-C15	1.4684 (19)	N4-C16-C17	122.01 (14)
N5-C18	1.3060 (2)		
N5-C19	1.3770 (2)		
N6-C17	1.3140 (18)		
N6-C24	1.3684 (19)		
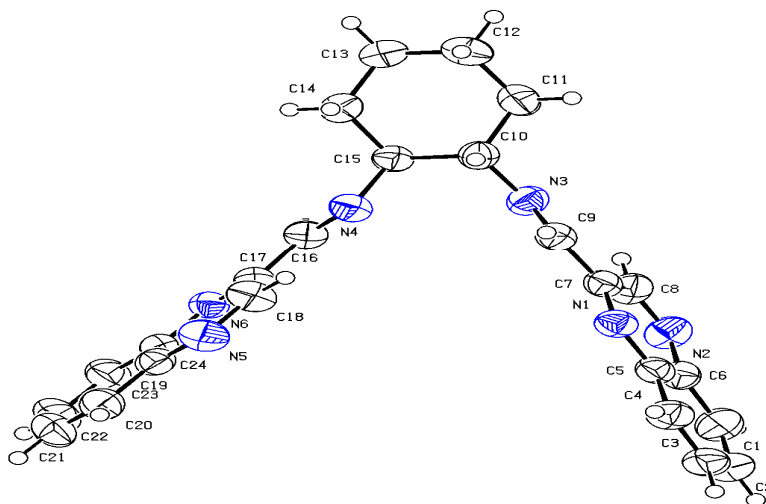
Figure 2.11: ORTEP diagram of *qcc* with atomic labeling scheme with 50% probability ellipsoids
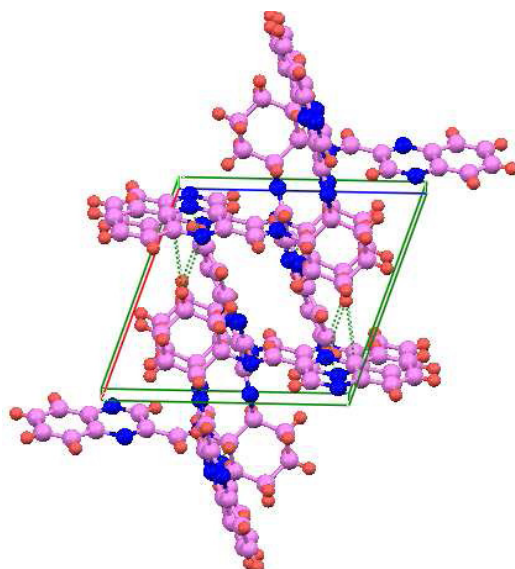
Figure 2.12: Packing diagram of *qcc*, showing weak intermolecular H-bonding interactions along the *b* axis.

2.5 CONCLUSIONS

This chapter deals with the details on various experimental and characterisation techniques employed in the present study. The synthesis and characterisation of the six Schiff bases, *N,N'*-bis(quinoxaline-2-carboxalidene)hydrazine (*qch*), *N,N'*-bis(quinoxaline-2-carboxalidene)-1,2-diaminoethane (*qce*), *N,N'*-bis(quinoxaline-2-carboxalidene)-1,3-diaminopropane (*qcp*), *N,N'*-bis(quinoxaline-2-carboxalidene)-1,4-diaminobutane (*qcb*), *N,N'*-bis(quinoxaline-2-carboxalidene)-1,2-diaminocyclohexane (*qcc*) and *N,N'*-bis(quinoxaline-2-carboxalidene)-1,2-diaminobenzene (*qco*) are also described in detail. The Schiff bases are formed *via* the condensation of quinoxaline-2-carboxaldehyde with hydrazine hydrate, 1,2-diaminoethane, 1,3-diaminopropane, 1,4-diaminobutane, 1,2-diaminocyclohexane or orthophenylenediamine. The structure of these Schiff bases has been confirmed with the help of spectroscopic techniques such as FTIR, UV-

visible, NMR. Among the six Schiff bases, we got single crystals of four Schiff bases (*qce*, *qcp*, *qcb* and *qcc*) and these crystals were studied by single crystal XRD technique. These Schiff bases crystallise in triclinic (*qce, qcc*) and monoclinic (*qcp, qcb*) crystal systems. These ligands are considered to act as neutral bidentate/tetradentate ligands.

REFERENCES

1. S. Mayadevi, Ph.D thesis, *Studies on some new transition metal complexes of the Schiff bases derived from quinoxaline-2-carboxaldehyde*, Cochin University of Science and Technology, (**1997**).

2. A. T. Stuart, *J. Am. Chem. Soc.*, 33 (**1911**) 1344.

3. B. N. Figgis, R. S. Nyholm, *J. Chem. Soc.*, (**1958**) 4190.

4. Bruker, SAINT-Plus, Bruker AXS, Inc., Madison, Wisconsion, USA, (**2003**).

5. G. M. Sheldrick, SADABS, *Program for Empirical Absorption Correction*, University of Gottingen, Germany, (**1996**).

6. G. M. Sheldrick, SHELX-97, Program for Crystal Structure Analysis, University of Gottingen, Germany, (**1997**).

7. H. Ohle, M. Hielscher, *Chem. Ber.*, 74 (**1941**) 13.

8. C. L. Leese, H. N. Rydon, *J. Chem. Soc.*, (**1955**) 303.

9. V. Arun, P. P. Robinson, S. Manju, P. Leeju, G. Varsha, V. Digna, K. K. M. Yusuff, *Dyes and Pigments*, 82 (**2009**) 268.

10. P. S. Chittilappilly, N. Sridevi, K. K. M. Yusuff, *J. Mol. Catal. A: Chem.*, 286 (**2008**) 92.

11. D. Varghese, V. Arun, M. Sebastian, P. Leeju, G. Varsha, K. K. M. Yusuff, *Acta Cryst.*, E65 (**2009**) o435.

12. D. Varghese, V. Arun, P. P. Robinson, M. Sebastian, P. Leeju, G. Varsha, K. K. M. Yusuff, *Acta Cryst.*, C65 (**2009**) o612.

13. Y. J. Seok, K. S. Yang, S. T. Kim, W. K. Huh, S. O. Kang, *J. Carbohydr. Chem.*, 15 (**1996**) 1085.

14. P. S. Kalsi, *Spectroscopy of organic compounds*, 6th Ed., New Age International (P) Ltd., Publishers, (**2004**).

15. D. L. Pavia, G. M. Lampman, G. S. Kriz, J. R. Vyvyan, *Spectroscopy*, (**2008**).

16. M. H. Habibi, M. Montazerozohori, A. Lalegani, R. W. Harrington, W. Clegg, *J. Fluorine Chem.*, 127 (**2006**) 769.

****᠅****

Synthesis and characterisation of manganese(II) Schiff base complexes

Contents

3.1 Introduction
3.2 Experimental
3.3 Results and discussion
3.4 Conclusions
References

3.1 INTRODUCTION

The coordination chemistry of manganese(II) has attracted considerable interest due to the crucial role played by the metal in redox and non-redox proteins. Studies involving the synthesis and characterisation of manganese complexes are useful towards the understanding of the structure and reactivity of manganese sites in biological systems [1-3]. These complexes provide structural support for metalloproteins such as pyruvate carboxylase [4], arginase [5], ribonuclease hydrolases [6] and concanavalin A [7]. Furthermore, this metal ion plays an important role in the metabolism of biological systems such as superoxide dismutase [8], manganese peroxidase [9] and manganese(II) dioxygenase [10].

Many manganese complexes with double Schiff base ligands have been reported in recent years [11-13]. Manganese complexes of Schiff bases are known to be involved in the catalytic epoxidation of olefins and other substrates and in the design of artificial metalloproteins [14,15]. Furthermore, tetradentate

Schiff base complexes of manganese(III) act as catalyst in the oxidation of organic substrates [13,16,17].

Manganese(II) ion has a high spin d^5 electronic configuration, which gives no crystal field stabilisation energies for any coordination geometries. Therefore various coordination geometries are expected for manganese(II) complexes. However, surprisingly, most manganese(II) complexes take an octahedral geometry and only few examples are known to take other coordination geometries [18]. Coordination numbers exceeding six are uncommon for manganese(II) ion. This metal ion prefers a limited number of coordination geometries, which minimize ligand-ligand repulsions. But, a novel eight coordinate Mn(II) Schiff base complex of N,N′-bis(2-pyridylmethylene)-1,3-diaminopropan-2-ol has been reported [19]. This complex has a distorted square antiprism geometry.

Studies of high oxidation state complexes are of special importance because of their potential uses as oxidizing agents, catalysts and electro catalysts, for the oxidation of compounds such as alcohols, esters, and water. A large number of manganese complexes involving different ligand environments have been structurally characterized and their electron transfer properties have been studied extensively; however, there remains a wider scope to study the chemistry of Mn^{II}, Mn^{III} and Mn^{IV} oxidation states [20]. This is especially relevant in the context of modeling the active sites of biological systems. A report has also demonstrated the synthesis of manganese(IV) complexes from manganese(III) precursors [21].

Perusal of the literature reveal that manganese(II) complexes of Schiff bases, *qch*, *qce*, *qcp*, *qcb*, *qcc* and *qco*, have not yet been reported. Further more these complexes are expected to exhibit electronic properties different from those of the salen and the Schiff base complexes derived from benzaldehyde. In this

chapter we describe the synthesis, and characterisation of six new manganese(II) Schiff base complexes.

3.2 EXPERIMENTAL

3.2.1 Materials

The details of materials used for the syntheses of Schiff base ligands are given in Chapter 2. The metal salt used is manganese(II) chloride tetrahydrate ($MnCl_2 \cdot 4H_2O$).

3.2.2 Synthesis of Schiff base ligands

Details of the synthesis and characterisation of Schiff base ligands, *qch*, *qce*, *qcp, qcb*, *qcc* and *qco*, are presented in chapter 2.

3.2.3 Synthesis of complexes

Schiff base complexes of Mn(II) (**1-6**) were synthesised using the following procedure. A solution of $MnCl_2 \cdot 4H_2O$ (0.9895 g, 5 mmol) in 25 mL methanol was mixed with the Schiff base ligand (5 mmol), *qch, qce, qcp, qcb, qcc* or *qco*, in 60 mL methanol/chloroform. The resulting yellow coloured solution was then refluxed on an electric heating mantle at 50 °C for three hours. The reaction mixture was then filtered and the solvent was evaporated to obtain a light brown precipitate. The complex was washed with cold methanol. The products were dried over anhydrous calcium chloride in a desiccator. (~ 75% yield)

3.3 RESULTS AND DISCUSSION

The light brown coloured complexes were prepared from the interaction of the ligands, *qch, qce, qcp, qcb, qcc* or *qco*, with manganese(II) chloride in the ratio 1:1. The prepared complexes are non-hygroscopic and air stable. The complexes are soluble in common organic solvents such as methanol, ethanol,

benzene, tetrahydrofuran, dichloromethane, DMF and DMSO. However, our attempts to isolate single crystals suitable for X-ray crystal structure determination were not successful.

3.3.1 Elemental analysis

The analytical data for the complexes are given in Table 3.1. The data agree with the suggested molecular formula of the complexes.

Table 3.1: Analytical data of the manganese(II) Schiff base complexes

Complex	Empirical formula	Formula weight	Carbon (%)	Hydrogen (%)	Nitrogen (%)	Mn (%)	Cl (%)
1	$C_{36}H_{28}Cl_2MnN_{12}O_2$	786	54.67 (54.97)	3.19 (3.59)	21.42 (21.37)	6.83 (6.98)	8.83 (9.02)
2	$C_{20}H_{18}Cl_2MnN_6O$	484	49.16 (49.61)	3.67 (3.75)	17.03 (17.36)	11.21 (11.35)	14.21 (14.64)
3	$C_{21}H_{22}Cl_2MnN_6O_2$	516	48.32 (48.85)	4.23 (4.30)	16.27 (16.28)	10.73 (10.64)	13.44 (13.73)
4	$C_{22}H_{24}Cl_2MnN_6O_2$	530	49.69 (49.83)	4.43 (4.56)	15.54 (15.85)	10.09 (10.36)	13.09 (13.37)
5	$C_{24}H_{27}Cl_2MnN_6O_2$	557	51.32 (51.71)	4.62 (4.71)	15.16 (15.11)	9.46 (9.87)	12.66 (12.74)
6	$C_{24}H_{18}Cl_2MnN_6O$	532	54.21 (54.15)	3.15 (3.41)	15.64 (15.79)	10.44 (10.32)	13.53 (13.32)

* Calculated values in parentheses

3.3.2 Molar conductivity measurements

In general the molar conductance data for complexes in methanol have been suggested in the following range (ohm^{-1} cm^2 mole^{-1}): for 1:1 electrolytes 80-115; for 2:1 electrolytes 160-220 and for 3:1 electrolytes 290-350 [22]. The

conductance measurements of our complexes are given in Table 3.2. Among these Mn(II) complexes, complexes **2** and **5** are 1:1 electrolytes; complexes **3** and **4** are 2:1 electrolytes and other complexes are consistent with their non-electrolyte nature. The conclusions arrived from molar conductance measurements agree with the molecular formulae arrived from the analytical data.

Table 3.2: Molar conductance data of the manganese(II) Schiff base complexes.

Complex	Molar conductance (ohm^{-1} cm^2 mole^{-1})
1	55
2	113
3	185
4	175
5	95
6	64

3.3.3 Thermal analysis

Thermal analysis of the Mn(II) complexes were carried out under nitrogen atmosphere at a heating rate of 10 °C min^{-1} from 50 °C to 1000 °C. The thermograms of these complexes are represented in Figure 3.1. With TG/DTG analysis it is often possible to check whether there is coordinated or lattice water in the complexes [23]. From the TG/DTG plots, all the complexes are found to be thermally stable and exhibit multistage decomposition pattern. A thermal study was carried out to obtain the nature and number of water molecules present in

these complexes. The molecular formulae of all the Mn(II) complexes deduced from elemental analysis indicate the presence of lattice/coordinated water. The hydrated water molecules associated with complex formation are found outside the coordination sphere. The dehydration of this type of water molecules takes place at the temperature below 140 °C. On the other hand the coordinated water molecules are eliminated in the range 140-300 °C [24].

Thermal analysis data of Mn(II) complexes are given in Table 3.3. Complex **1** shows an initial weight loss of 4% in the temperature range 50-135 °C. This weight loss might be due to the removal of the two lattice water molecule. Thermal analysis for the complex **2** shows a first weight loss of about 4% in the temperature range 140 to 180 °C, which can be attributed to the removal of a coordinated water molecule. For the complex **3**, the initial weight loss of 7% in the range 140-250 °C is due to the removal of two coordinated water molecules. TG plot of **4** shows a several stages of decomposition and the initial weight loss is about 7% in the range 140-235 °C, which might be due to the removal of two coordinated water molecules. Complex **5** shows multistage decomposition in the TG plot and the initial weight loss (60-130 °C) is found to be 3% due to the removal of one lattice water molecule. This also shows another 3% weight loss in the range 140-220 °C, due to the removal of one coordinated water molecule. The complex **6** decomposes in the range 60-90 °C and 3% weight loss in this region is due to the removal of one lattice water molecule. The decomposition patterns of complexes are in good agreement with the suggested formulae.

Table 3.3: Thermal analysis data of manganese(II) Schiff base complexes

Complex	Temperature Range (°C)	% Loss	Fragment lost	Nature of water molecule
1	50-135	4	$2H_2O$	Lattice water
2	140-180	4	H_2O	Coordinated water
3	140-250	7	$2H_2O$	Coordinated water
4	140-235	7	$2H_2O$	Coordinated water
5	60-130	3	H_2O	Lattice water
	140-220	3	H_2O	Coordinated water
6	60-90	3	H_2O	Lattice water
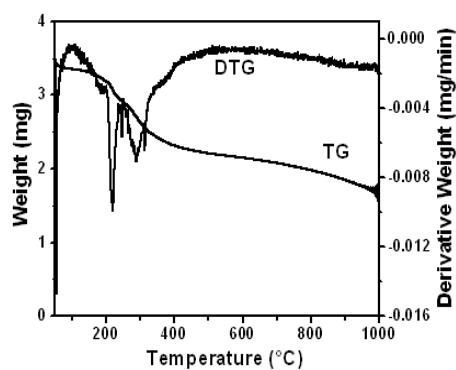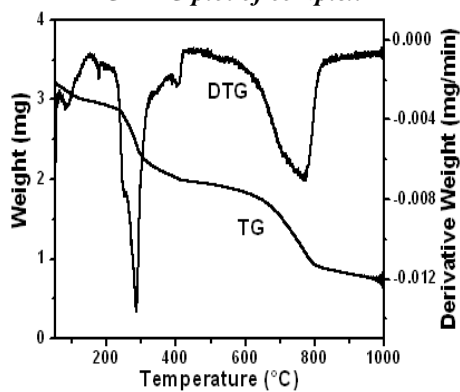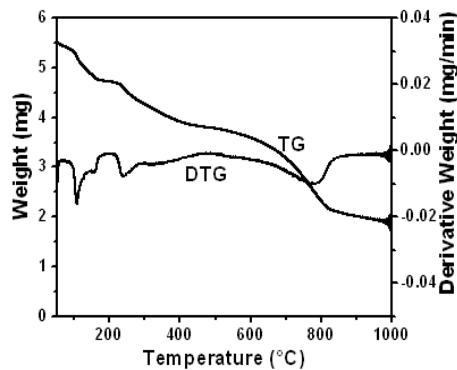
TG-DTG plot of complex 1

TG-DTG plot of complex 2

TG-DTG plot of complex 3
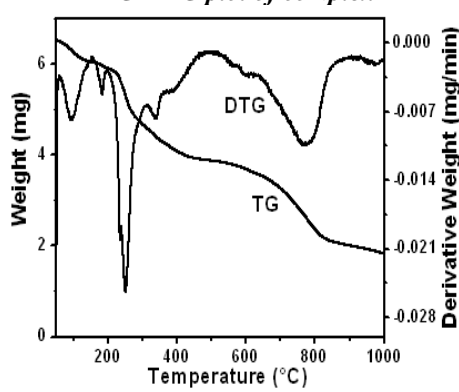
TG-DTG plot of complex 4
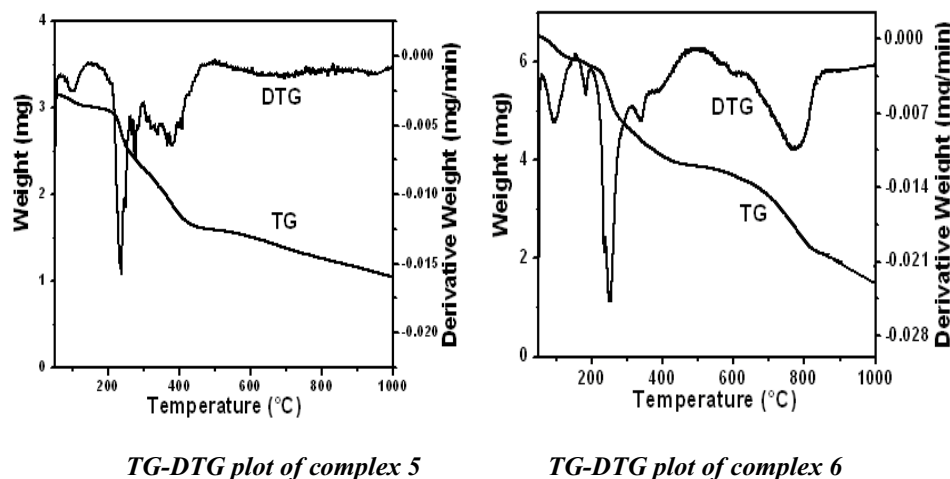
TG-DTG plot of complex 5   *TG-DTG plot of complex 6*

Figure 3.1: TG-DTG plots of Mn(II) Schiff base complexes

Based on the analytical, molar conductance and TG data, the following molecular formulae have been assigned for the complexes: $[Mn(qch)_2Cl_2]\cdot2H_2O$ for **1**; $[Mn(qce)Cl(H_2O)]Cl$ for **2**; $[Mn(qcp)(H_2O)_2]Cl_2$ for **3**; $[Mn(qcb)(H_2O)_2]Cl_2$ for **4**; $[Mn(qcc)Cl(H_2O)]Cl\cdot H_2O$ for **5** and $[Mn(qco)Cl_2]\cdot H_2O$ for **6**.

3.3.4 Magnetic susceptibility measurements

Room temperature magnetic moments, μ_{eff}, of these complexes were found to be in the range 5.71–6.10 B.M. Values obtained are shown in Table 3.4. These values are in agreement with the spin only value of 5.92 B.M. In all cases the results are close to 5.9 B.M., as expected for typical high spin manganese(II) complexes. Further the values indicate little or no antiferromagnetic interaction.

Table 3.4: Magnetic moment values of the manganese(II) Schiff base complexes.

Complex	Magnetic moment (B.M.)
[Mn(qch)$_2$Cl$_2$]·2H$_2$O **1**	5.76
[Mn(qce)Cl(H$_2$O)]Cl **2**	5.94
[Mn(qcp)(H$_2$O)$_2$]Cl$_2$ **3**	5.93
[Mn(qcb)(H$_2$O)$_2$]Cl$_2$ **4**	6.01
[Mn(qcc)Cl(H$_2$O)]Cl·H$_2$O **5**	5.95
[Mn(qco)Cl$_2$]·H$_2$O **6**	5.74

3.3.5 Infrared spectra

The IR spectra of the Mn(II) complexes are presented in Figure 3.2. The spectra of free ligands are given in chapter 2. The most significant vibrational bands of the free ligands and those of the manganese(II) complexes are given in Table 3.5. These data are useful for determining the mode of coordination of the ligands.

The ν(C=N) of azomethine and that of quinoxaline in spectra of the Schiff base ligands and their complexes appear as a group of bands in the region 1550-1640 cm^{-1}. The azomethine stretching frequencies (1610-1640 cm^{-1}) of the free ligands were found to be shifted to lower frequency on complexation (for **1**, **2**, **3**, **4, 5** and **6**) indicating the participation of the azomethine nitrogen in chelation. The quinoxaline C=N stretching frequency (1550-1580 cm^{-1}) is also shifted on complexation indicating that these nitrogen atoms are also involved in the coordination with manganese(II) ions. The ν(C=N) of quinoxaline undergoes a small shift on complexation; such small shifts have been reported when ring nitrogens are involved in coordination to the metal [26,27]. The appearance of a

broad absorption band (due to ν(OH)) centered around 3408, 3429, 3373, 3441, 3361 and 3449 cm^{-1} for the complexes, **1**, **2**, **3**, **4**, **5** and **6**, respectively indicate the presence of lattice/coordinated water [28]. These bands are absent in the free ligands. There is another weak band in the region 700-850 cm^{-1}, which can be attributed to the Mn-OH$_2$ rocking mode. The Mn-OH$_2$ wagging mode was also observed in the 600-700 cm^{-1} region as a band of medium intensity. Conclusive evidence of the bonding of the Schiff base ligands to manganese(II) is also shown by the appearance of new bands in the region 500-400 cm^{-1} in the spectra of the complexes due to ν(Mn-O) and ν(Mn-N) stretching vibrations [Table 3.5] [27]. The Mn-Cl stretching bands may appear in the far IR regions of 300-200 cm^{-1} [29]; however, the spectra could not be recorded in this range.

Table 3.5: FTIR spectral bands for the manganese(II) Schiff base complexes.

(ν in cm^{-1})

Complex	ν(C=N)a*	ν(C=N)q*	ν(OH)	ν(Mn-N)	ν(Mn-O)
qch [Mn(qch)$_2$Cl$_2$]·2H$_2$O **1**	1622 1611	1568 1563	 3408	 409	 -
qce [Mn(qce)Cl(H$_2$O)]Cl **2**	1639 1628	1555 1551	 3429	 424	 592
qcp [Mn(qcp)(H$_2$O)$_2$]Cl$_2$ **3**	1636 1628	1573 1568	 3373	 411	 531
qcb [Mn(qcb)(H$_2$O)$_2$]Cl$_2$ **4**	1640 1626	1555 1550	 3441	 491	 532
qcc [Mn(qcc)Cl(H$_2$O)]Cl·H$_2$O **5**	1640 1632	1556 1551	 3361	 418	 518
qco [Mn(qco)Cl$_2$]·H$_2$O **6**	1610 1601	1568 1563	 3449	 424	 -

* a (C=N) of azomethine group; q (C=N) of quinoxaline ring; ν(OH) of coordinated/lattice water molecule
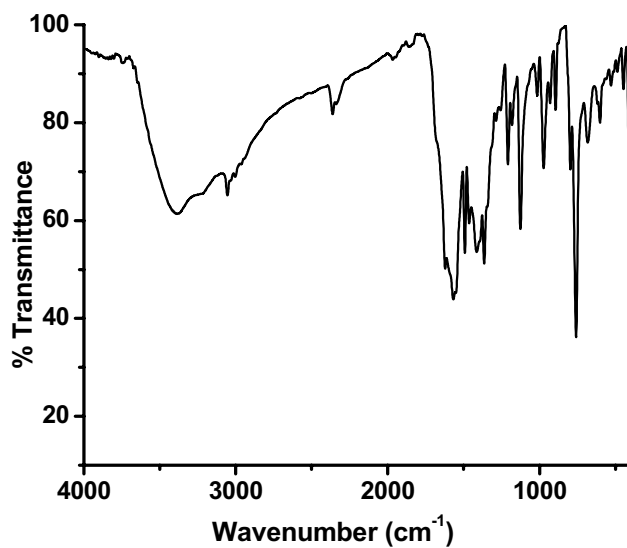
IR spectrum of [Mn(qch)$_2$Cl$_2$]·2H$_2$O
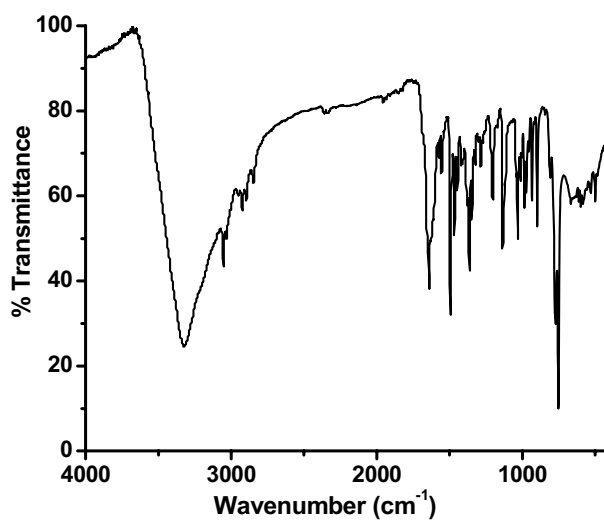
IR spectrum of [Mn(qce)Cl(H$_2$O)]Cl
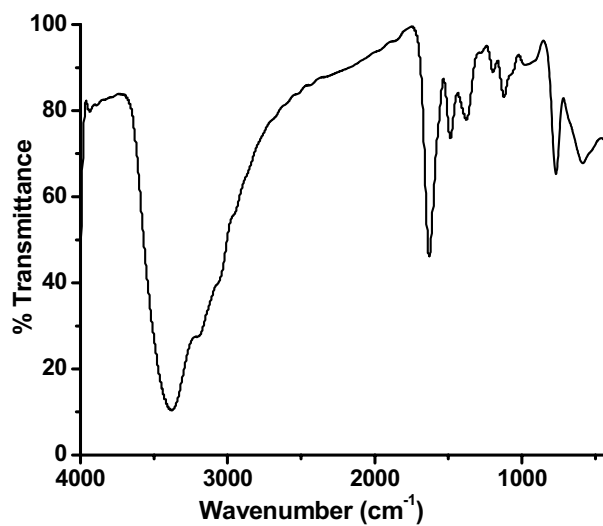
IR spectrum of [Mn(qcp)(H₂O)₂]Cl₂
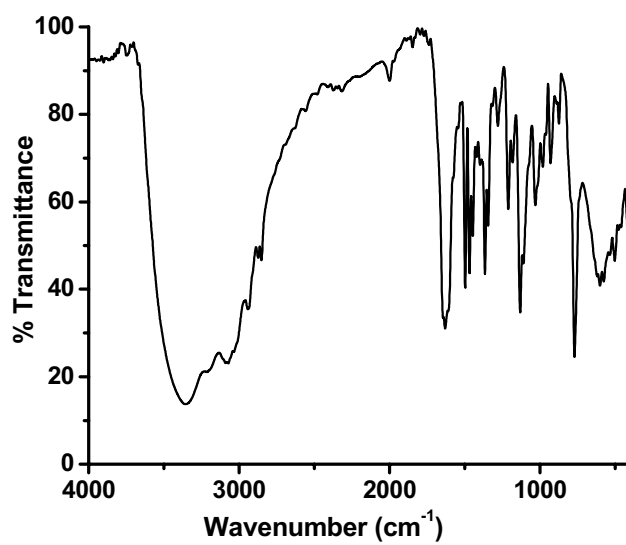
IR spectrum of [Mn(qcb)(H₂O)₂]Cl₂
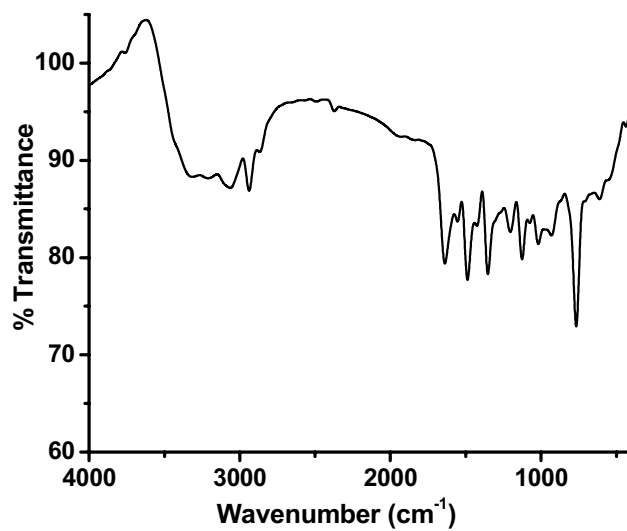
IR spectrum of [Mn(qcc)Cl(H₂O)]Cl·H₂O
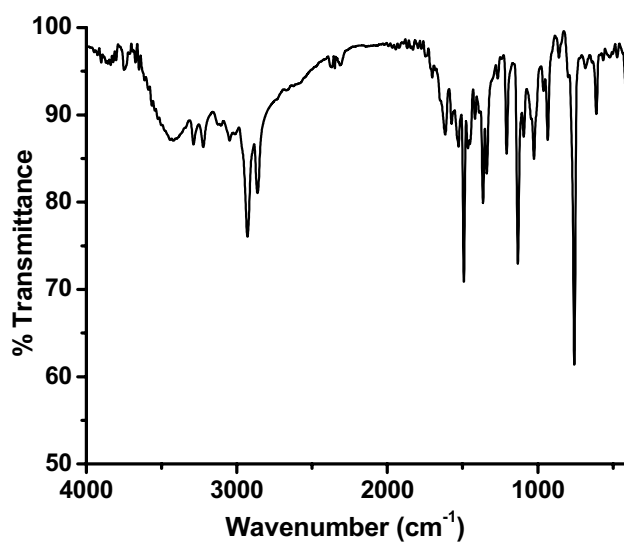
IR spectrum of [Mn(qco)Cl₂]·H₂O

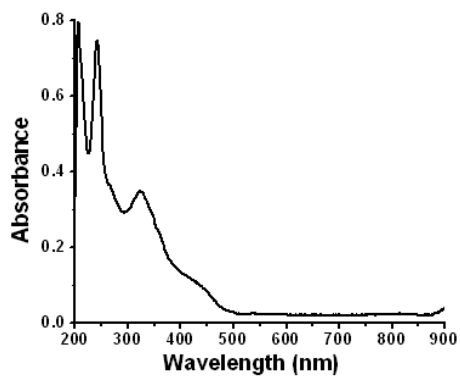**Figure 3.2: IR spectra of manganese(II) Schiff base complexes**

3.3.6 Electronic spectra

The electronic spectra of the free ligands show absorption bands in the UV–Vis region (200-400 nm), due to the $\pi \to \pi^*$ and $n \to \pi^*$ transitions [Figures are given in chapter 2]. The significant electronic absorption bands in the spectra of the Mn(II) complexes in methanol solution (10^{-4} M) are presented in Table 3.6. The spectra of the Mn(II) complexes [Figure 3.3] exhibit some variations in the position and intensity of the characteristic bands for free ligands, as well as new weak, characteristic absorptions in the visible region. Manganese(II) high spin complexes are very weakly coloured due to spin forbidden d-d transition. It is very difficult to identify the d-d bands of a manganese(II) complex as these bands are not very well defined and submerged in the tail of the strong intraligand transitions or charge transfer bands. The bands in the region 200-400 nm can be attributed to intraligand transitions and these bands were seen to be modified by complexation. The broad bands of low intensity observed in the UV-Vis range can be assigned to the spin forbidden d-d transition or charge-transfer d-π^* transitions [30]. The Mn(II) complexes, **1**, **4**, **5** and **6** exhibit new bands over 400 nm and can be attributed to the d-d or d-π^* transitions. In the spectra of the complexes, the d–d transitions were not very well defined and were observed as shoulder bands.

Mn(II) has d^5 high spin configuration with a ^6S ground term. Crystal field of any symmetry cannot split it. These complexes have light brown colour. Usually high spin Mn(II) complexes rarely show d-d transitions, as they are spin and laporte forbidden. However, the complexes show low intensity peaks around 25,000 cm^{-1} corresponding to the $^6A_{1g}$ (F) $\to$ $^4T_{2g}$ (G) transitions, as has been reported for Mn(II) octahedral complexes [Table 3.6] [31,32].

Table 3.6: Electronic spectral assignments for manganese(II) Schiff base complexes

| Complex | Absorption Maxima | | log ε | Band |
	nm	cm^{-1}	L mol^{-1} cm^{-1}	Assignment
[Mn(qch)$_2$Cl$_2$]·2H$_2$O **1**	205	48780	3.90	$\pi \rightarrow \pi^*$
	241	41490	3.86	$\pi \rightarrow \pi^*$
	270	37040	2.70	$\pi \rightarrow \pi^*$
	323	30960	2.30	$\pi \rightarrow \pi^*$
	444	22520	1.48	$^6A_1 \rightarrow {}^4T_{2g}$
	536	18660	0.95	$^6A_1 \rightarrow {}^4T_{1g}$
[Mn(qce)Cl(H$_2$O)]Cl **2**	207	48310	3.84	$\pi \rightarrow \pi^*$
	241	41490	3.97	$\pi \rightarrow \pi^*$
	317	31540	3.39	$\pi \rightarrow \pi^*$
	357	28010	2.84	$\pi \rightarrow \pi^*$
[Mn(qcp)(H$_2$O)$_2$]Cl$_2$ **3**	207	48310	3.85	$\pi \rightarrow \pi^*$
	238	42020	3.72	$\pi \rightarrow \pi^*$
	317	31540	3.46	$\pi \rightarrow \pi^*$
[Mn(qcb)(H$_2$O)$_2$]Cl$_2$ **4**	242	41320	3.82	$\pi \rightarrow \pi^*$
	321	31150	3.27	$\pi \rightarrow \pi^*$
	462	21640	1.40	$n \rightarrow \pi^*$
	530	18870	0.99	$^6A_1 \rightarrow {}^4T_{2g}$
	720	13890	0.95	$^6A_1 \rightarrow {}^4T_{1g}$
[Mn(qcc)Cl(H$_2$O)]Cl·H$_2$O **5**	207	48310	3.95	$\pi \rightarrow \pi^*$
	242	41320	3.89	$\pi \rightarrow \pi^*$
	317	31540	3.33	$\pi \rightarrow \pi^*$
	403	24810	1.43	$^6A_1 \rightarrow {}^4T_{2g}$
[Mn(qco)Cl$_2$]·H$_2$O **6**	273	36630	3.98	$\pi \rightarrow \pi^*$
	312	32050	3.09	$\pi \rightarrow \pi^*$
	374	26740	3.59	$\pi \rightarrow \pi^*$
	460	21740	3.60	CT

UV-Vis spectrum of [Mn(qch)₂Cl₂]·2H₂O
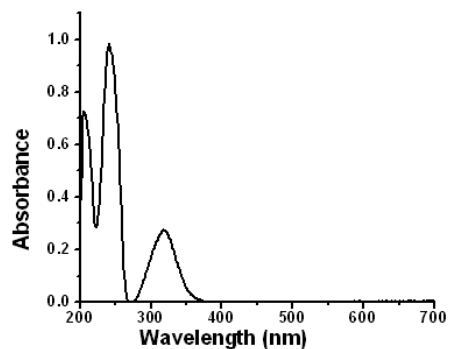
UV-Vis spectrum of [Mn(qce)Cl(H₂O)]Cl
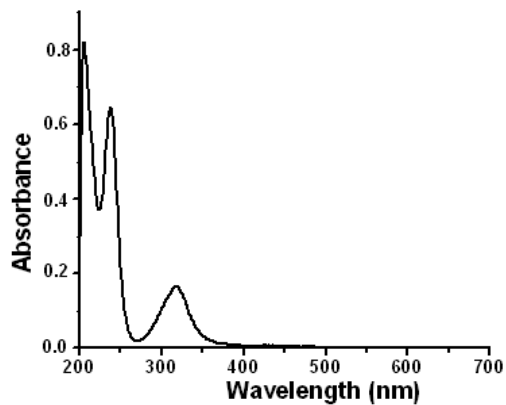
UV-Vis spectrum of [Mn(qcp)(H₂O)₂]Cl₂
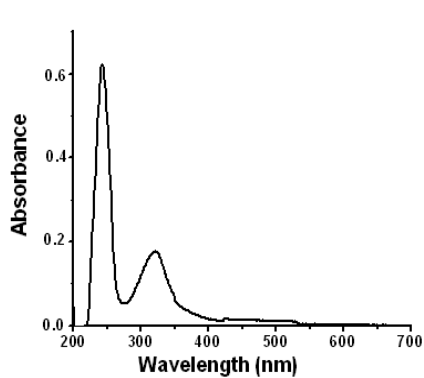
UV-Vis spectrum of [Mn(qcb)(H₂O)₂]Cl₂
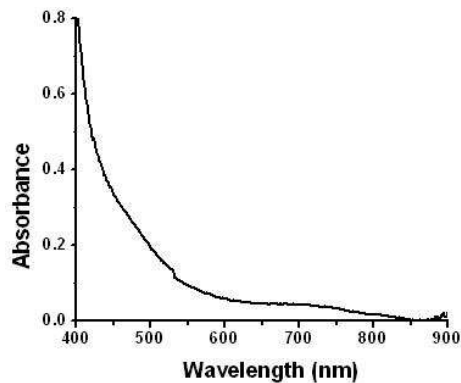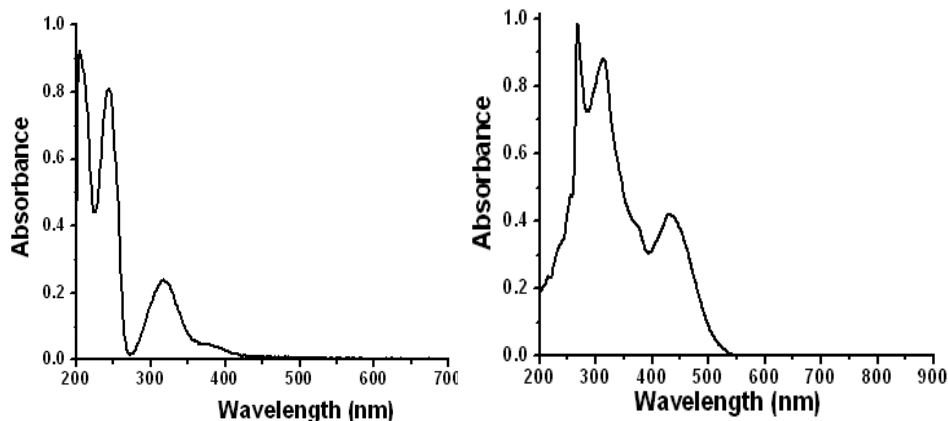
UV-Vis spectrum of [Mn(qcc)Cl(H₂O)]Cl·H₂O   *UV-Vis spectrum of [Mn(qco)Cl₂]·H₂O*

Figure 3.3: Electronic spectra of manganese(II) Schiff base complexes

3.3.7 EPR spectra

The X-band EPR spectra of Mn(II) complexes were recorded in DMF solution at 77 K. The EPR spectra of these complexes are shown in Figure 3.4 and the spin Hamiltonian parameters are given in the Table 3.7. The spin Hamiltonian for Mn(II) may be described as

$$\hat{H} = g\beta HS + D[Sz^2 - S(S+1)/3] + E(Sx^2 - Sy^2)$$

Where H is the magnetic field vector, g is the spectroscopic splitting factor, β is the Bohr magneton, D is the axial zero field splitting term, E is the rhombic field splitting parameter and S is the electron spin vector [33]. If D and E are very small compared to *gβHS,* six EPR transitions are expected. The EPR of the mononuclear complexes of manganese(II) should exhibit six hyperfine lines [34]. The EPR spectrum of the frozen solution (in DMF) for the complexes under study shows six lines [Figure 3.4] arising due to hyperfine interaction between the unpaired electrons of the Mn(II) ions (I=5/2). The broadening of the spectra in DMF solution was due to spin relaxation.

Table 3.7: EPR spectral parameters of manganese(II) Schiff base complexes

Complex	g	A*
[Mn(qch)$_2$Cl$_2$]·2H$_2$O 1	2.029	93
[Mn(qce)Cl(H$_2$O)]Cl 2	2.015	88
[Mn(qcp)(H$_2$O)$_2$]Cl$_2$ 3	2.026	93
[Mn(qcb)(H$_2$O)$_2$]Cl$_2$ 4	2.015	92
[Mn(qcc)Cl(H$_2$O)]Cl·H$_2$O 5	2.026	91
[Mn(qco)Cl$_2$]·H$_2$O 6	2.028	92

*The '*A*' values are expressed in units of cm^{-1} multiplied by a factor of 10^{-4}.
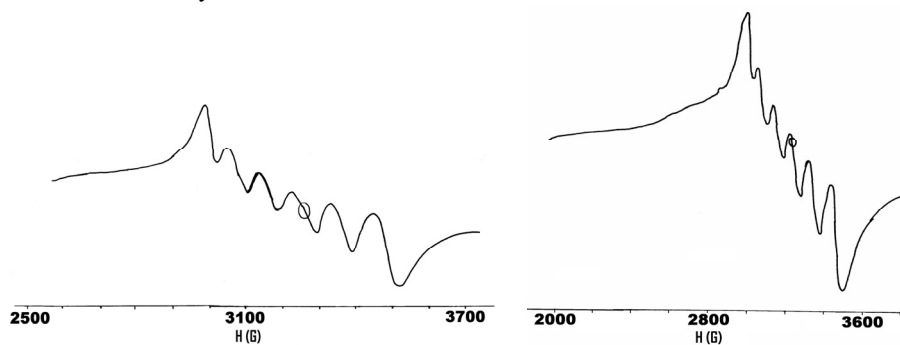
EPR spectrum of [Mn(qch)$_2$Cl$_2$]·2H$_2$O

EPR spectrum of [Mn(qce)Cl(H$_2$O)]Cl
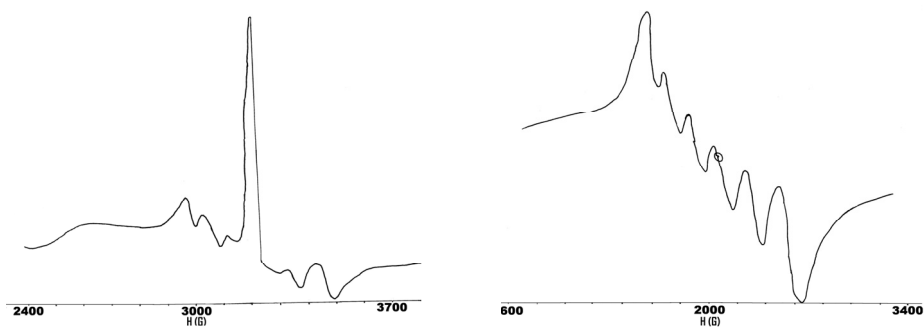
EPR spectrum of [Mn(qcp)(H$_2$O)$_2$]Cl$_2$

EPR spectrum of [Mn(qcb)(H$_2$O)$_2$]Cl$_2$

EPR spectrum of [Mn(qcc)Cl(H₂O)]Cl·H₂O *EPR spectrum of [Mn(qco)Cl₂]·H₂O*
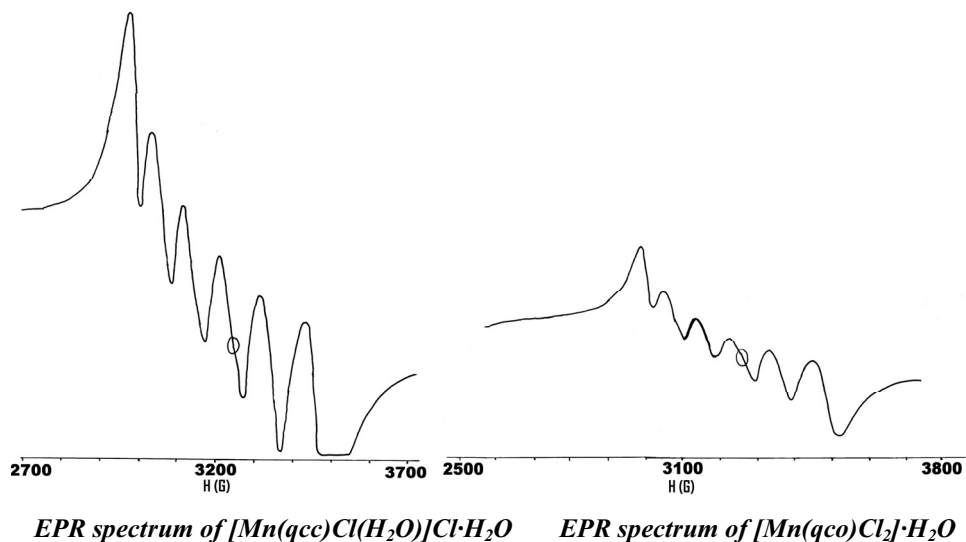
Figure 3.4: EPR spectra of manganese(II) Schiff base complexes

3.4 CONCLUSIONS

This chapter describes the synthesis and characterisation of six new Mn(II) Schiff base complexes. The molecular formula arrived for the complexes are as follows: [Mn(qch)$_2$Cl$_2$]·2H$_2$O, [Mn(qce)Cl(H$_2$O)]Cl, [Mn(qcp)(H$_2$O)$_2$]Cl$_2$, [Mn(qcb)(H$_2$O)$_2$]Cl$_2$, [Mn(qcc)Cl(H$_2$O)]Cl·H$_2$O and [Mn(qco)Cl$_2$]·H$_2$O. The magnetic moment, thermal analysis, IR, electronic and EPR spectral data of these complexes suggest that the complexes have octahedral geometry. The Schiff bases coordinate through azomethine nitrogens and quinoxaline ring nitrogens. Thus, the *qch* acts as neutral bidentate ligand and other Schiff bases (*qce*, *qcp*, qcb, qcc and qco) can act as tetradentate ligand in their complexes. Based on the analytical and physico-chemical data we have proposed the following structures for the Mn(II) Schiff base complexes (solvated water molecules are omitted in the figures).
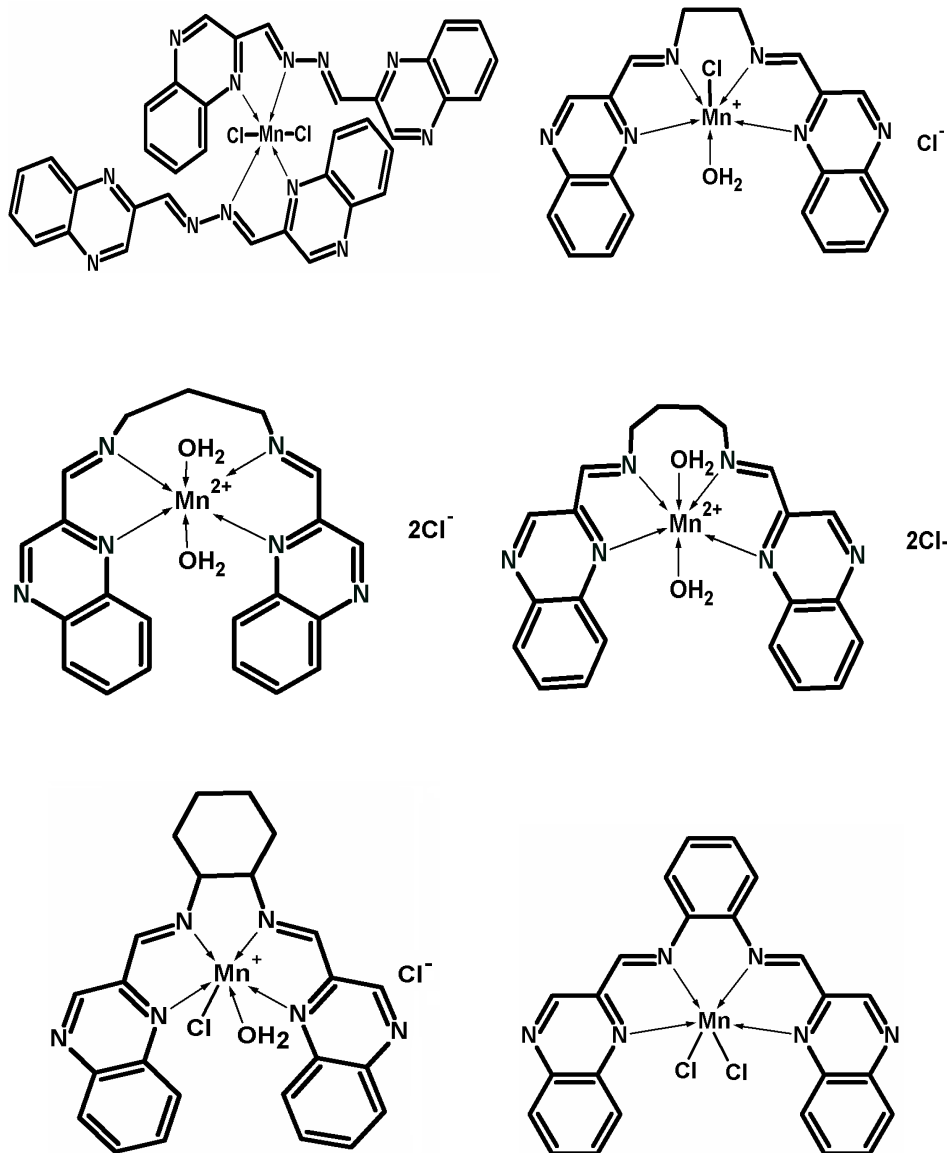
REFERENCES

1. S. Kumar, D. N. Dhar, P. N. Saxena, *Journal of Scientific and Industrial Research,* 68 (**2009**) 181.

2. L. Que, Jr., A. E. True, *Prog. Inorg. Chem.*, 38 (**1990**) 97.

3. J. B. Vincent, G. Christou, *Adv. Inorg. Chem.*, 33 (**1989**) 197.

4. G. C. Dismukes, *Chem. Rev.*, 96 (**1996**) 2909.

5. S. V. Khangulov, P. J. Pessiki, V. V. Barynin, D. E. Ash, G. C. Dismukes, *Biochemistry*, 34 (**1995**) 2015.

6. D. Wilcox, *Chem. Rev.*, 96 (**1996**) 2435.

7. A. Deacon, T. Gleichmann, A. J. Kalb, H. Price, J. Raftery, G. Bradbrook, J. Yariv, J. R. Helliwell, *J. Chem. Soc., Faraday Trans.*, 93 (**1997**) 4305.

8. C. Bull, E. C. Neiderhofer, T. Yoshida, J. A. Fee, *J. Am. Chem.Soc.*, 113 (**1991**) 4069.

9. A. Khindaria, D. P. Barr, S. D. Aust, *Biochemistry*, 34 (**1995**) 7773.

10. A. K. Whiting, Y. R. Boldt, M. P. Hendrich, L. P. Wackett, L. Que, *Biochemistry*, 35 (**1996**) 160.

11. P. M. Alex, K. K. Aravindakshan, *E-Journal of Chemistry*, 6 (**2009**) 449.

12. V. S. Thampidas, T. Radhakrishnan, R. D. Pike, *Acta Cryst.*, E64 (**2008**) m150.

13. S. Majumder, S. Hazra, S. Dutta, P. Biswas, S. Mohanta, *Polyhedron*, 28 (**2009**) 2473.

14. L. J. Simandi, T. M. Simandi, Z. May, G. Besenyei, *Coord. Chem. Rev.*, 245 (**2003**) 85.

15. J. R. Carey, S. K. Ma, T. D. Pfister, D. K. Garner, H. K. Kim, J. A. Abramite, Z. Wang, Z. Guo, Y. Lu, *J. Am. Chem. Soc.*, 126 (**2004**) 10812.

16. F. A. Cotton, G. Wilkinson, C. A. Murillo, M. Bochmann, *Advanced Inorganic Chemistry*, 6th Edn. Wiley: New York, (**1999**) 762.

17. D. Das, C. P. J. Cheng, *Chem. Soc. Dalton Trans.*, 7 (**2000**) 1081.

18. F. A. Cotton, G. Wilkinson, *Advanced Inorganic chemistry*, Wiley Interscience, (**1988**) 697.

19. M. Mikuriya,Y. Hatano, E. Asato, *Bull. Chem. Soc. Jpn.*, 70 (**1997**) 2495.

20. S. Biswas, K. Mitra, S. K. Chattopadhyay, B. Adhikary, *Transition Met. Chem.*, 30 (**2005**) 393.

21. E. J. Larson, V. L. Pecoraro, *J. Am. Chem. Soc.*, 113 (**1991**) 3810.

22. W. J. Geary, *Coord. Chem. Rev.*, 7 (**1971**) 81.

23. S. A. Sallam, *Transition Met. Chem.*, 30 (**2005**) 341.

24. G. G. Mohamed. *Spectrochimica Acta Part A: Molecular and Biomolecular Spectroscopy*, 64 (**2006**) 188.

25. T. M. Marykutty, N. T. Madhu, P. K. Radhakrishnan, *Synth. React. Inorg. Met.-Org. Chem.*, 31 (**2001**) 1239.

26. V. Arun, P. P. Robinson, S. Manju, P. Leeju, G. Varsha, V. Digna, K. K. M. Yusuff, *Dyes and Pigments*, 82 (**2009**) 268.

27. M. Sebastian, V. Arun, P. P. Robinson, A. A. Varghese, R. Abraham, E. Suresh, K. K. M. Yusuff, *Polyhedron*, 29 (**2010**) 3014.

28. K. Nakamoto, *Coordination Compounds. In Infrared and Raman Spectra of Inorganic and Coordination Compounds*, 4th Ed.; John Wiley and Sons, Inc.: New York, (**1986**).

29. W. E. Estes, J. R. Wasson, J. W. Hall, W. E. Hatfield. *Inorg. Chem.*, 17 (**1978**) 3657.

30. S. Chandra, U. Kumar. *Spectrochim. Acta Part A*, 61 (**2005**) 219.

31. A. B. P. Lever, *Electronic Spectra of Ions. In Inorganic Electronic Spectroscopy*, 2nd Ed.; Elsevier: Amsterdam, (**1984**) 449.

32. V. Philip, V. Suni, M. R. P. Kurup, M. Nethaji, *Spectrochim. Acta Part A*, 64 (**2006**) 171.

33. D. J. E. Ingram, *Spectroscopy at Radio and Microwave frequencies*, 2nd ed., Butterworth, London, (**1967**).

34. M. J. Baldwin, J. W. Kampf, M. L. Kirk, V. Pecoraro, *Inorg. Chem.*, 34 (**1995**) 5252.

****✿****

Chapter 4

Synthesis and characterisation of nickel(II) Schiff base complexes

4.1 INTRODUCTION

Chemistry of metal complexes of multidentate Schiff base ligands is quite interesting due to their ability to bind with one, two or more metal centers [1-5]. The chemistry of nickel complexes with multidentate Schiff base ligands has attracted particular attention, as this metal is able to exhibit several oxidation states in the complexes [3,6]. Such complexes with different oxidation states have a strong role in bioinorganic chemistry and may provide the basis of models for active sites of biological systems [7,8]. These complexes can also act as potential catalysts [9-11].

Nickel(II) complexes with tetradentate N_2O_2 Schiff base ligands derived from salicylaldehyde can act as hydrogenation catalysts both homogeneously and heterogeneously in the cages of zeolites X and Y [12-14]. Kureshy *et al*. have reported the catalytic activity of the nickel(II) Schiff base complexes of N,N′-bis(2-

hydroxyphenyl)ethylenediimine and N,N′-(2-hydroxyphenyl)acetylaldimine-N-(2-hydroxyphenyl)acetamide, in the epoxidation of olefins such as cyclohexene, 1-hexene, cis- and trans- stilbenes, indene with sodium hypochloride [15].

Studies on the interactions of DNA with transition metal complexes are helpful for rational drug design, as well as for the development of sensitive chemical probes for DNA. The nickel(II) complexes are reported to interact with calf-thymus DNA [16]. DNA binding studies of the cationic Ni(II) complex of the 5-triethyl ammonium methyl salicylideneorthophenylenediimine ligand shows that the metal complex strongly interacts with DNA [17]. Many biological activities of Ni(II) Schiff base complexes have been reported in the literature [18]. Further more depending upon the electronic and steric factors of the Schiff base ligands, Ni(II) form four-, five- and six- coordinate complexes [19-21].

In view of the interesting properties of nickel(II) Schiff base complexes, we have synthesised and characterised some new nickel(II) complexes of the Schiff bases derived from quinoxaline-2-carboxaldehyde. Details regarding these studies are presented in this chapter.

4.2 EXPERIMENTAL

4.2.1 Materials

The details of materials used for the synthesis of Schiff base ligands are given in chapter 2. The metal salt used for the synthesis of the Ni(II) Schiff base complexes is nickel(II) perchlorate hexahydrate ($Ni(ClO_4)_2 \cdot 6H_2O$).

4.2.2 Synthesis of complexes

The complexes were synthesised as follows: A solution of nickel(II) perchlorate hexahydrate (5 mmol, 1.828 g) in 30 mL methanol was added to the solution of the Schiff base, *qch, qce, qcp, qcb, qcc* or *qco*, (5 mmol) in 50 mL

methanol/chloroform. The solution was refluxed for three hours. The resulting solution was filtered hot and kept at room temperature. The precipitate was formed on slow evaporation of the solvent. The product was washed with cold methanol before drying over phosphorous pentoxide in a desiccator. Perchlorate salts/complexes are potentially explosive and it should be handled carefully.

4.3 RESULTS AND DISCUSSION

The interaction between the divalent nickel ion and the Schiff base, *qch, qce, qcp, qcb, qcc* or *qco*, in a 1:1 ratio leads to the formation of the complexes. The complexes formed are of fairly good stability and are found to be coloured. These complexes are readily soluble in common organic solvents. However, our attempts to grow single crystals suitable for X-ray crystal structure determination were not met with success. Due to their explosive nature, these complexes were not subjected to thermal analysis. Therefore, the nature of the water molecules present in the complexes could be ascertained only from the IR spectra.

4.3.1 Elemental analysis

The analytical data of the Ni(II) Schiff base complexes are presented in Table 4.1. The data clearly agree with the suggested molecular formula of these complexes. The data further suggest that all these complexes are mononuclear.

Table 4.1: Analytical data of the nickel(II) Schiff base complexes

Complex	Empirical formula	Formula weight	Colour	Carbon (%)	Hydrogen (%)	Nitrogen (%)	Nickel (%)
1	$C_{36}H_{26}Cl_2NiN_{12}O_9$	900	Black	48.47 (48.03)	2.79 (2.91)	18.42 (18.67)	6.73 (6.52)
2	$C_{20}H_{18}Cl_2NiN_6O_9$	615	Violet	39.43 (39.00)	2.77 (2.95)	13.56 (13.64)	9.65 (9.53)
3	$C_{21}H_{22}Cl_2NiN_6O_{10}$	648	Black	38.65 (38.92)	3.43 (3.42)	12.87 (12.97)	9.14 (9.06)
4	$C_{22}H_{24}Cl_2NiN_6O_{10}$	662	Black	39.69 (39.91)	3.33 (3.65)	12.64 (12.69)	8.79 (8.87)
5	$C_{24}H_{24}Cl_2NiN_6O_9$	670	Brown	43.42 (43.02)	3.52 (3.61)	12.36 (12.54)	8.46 (8.76)
6	$C_{24}H_{18}Cl_2NiN_6O_9$	664	Black	43.61 (43.41)	2.85 (2.73)	12.64 (12.66)	8.44 (8.84)

* Calculated values in parentheses

4.3.2 Molar conductivity and magnetic susceptibility measurements

The molar conductivity values are given in Table 4.2 for the nickel(II) Schiff base complexes in methanol (10^{-3} M). The nature of electrolyte type was arrived by comparing the observed molar conductivity values to those reported for various salts at similar concentrations and for various complex ions [22]. Molar conductivity measurement (80-115 $ohm^{-1}cm^2mole^{-1}$) of complexes, **1**, **2** and **6**, indicate that the complexes behave as univalent electrolytes in solution. Furthermore the conductance data suggest that complex **4** is 2:1 electrolyte, and complexes **3** and **5** are non-electrolytes in methanol.

The magnetic moment value of the complexes is found to be in the range 2.8-3.2 B.M [Table 4.2] at 298 K. These values are in accordance with the values expected for the d^8 complexes in octahedral environment [23,24].

Table 4.2: Magnetic moment values and molar conductance data of the nickel(II) Schiff base complexes.

Complex	Magnetic moment (B.M.)	Molar conductance (ohm^{-1} cm^2 mole^{-1})
1	3.01	85
2	3.15	106
3	2.86	31
4	2.97	175
5	3.21	37
6	3.15	91

Based on the analytical and molar conductance data, the following molecular formulae have been assigned for the complexes: $[Ni(qch)_2(ClO_4)H_2O]$ ClO_4 for **1**; $[Ni(qce)ClO_4(H_2O)]ClO_4$ for **2**; $[Ni(qcp)(ClO_4)_2]\cdot 2H_2O$ for **3**; $[Ni(qcb)(H_2O)_2](ClO_4)_2$ for **4**; $[Ni(qcc)(ClO_4)_2]\cdot H_2O$ for **5** and $[Ni(qco)(ClO_4)$ $H_2O]ClO_4$ for **6**.

4.3.3 Infrared spectra

The main IR bands of the complexes were compared with those of the free ligands. Table 4.3 lists the most important IR spectral bands of the nickel(II) complexes and their corresponding ligands. The spectra [Figure 4.1] show typical bands of Schiff bases. A strong peak observed in the region 1610-1640 cm^{-1} is characteristic of azomethine (ν(C=N)) group present in the ligands. On comparing with the spectra of ligands, it could be seen that, ν(C=N) bands in these complexes are shifted to lower energy regions. These shifts are due to the involvement of the nitrogen donor atoms of azomethine (C=N) in coordination to the nickel(II) ions [25]. The band due to the C=N stretching of quinoxaline ring (1550-1580 cm^{-1}) undergoes a shift on complexation suggesting the involvement of ring nitrogen in bonding [26,27]. There is a broad band in the range 3400-3300 cm^{-1} which is due to ν(OH) indicating the presence of water of hydration or coordinated water [28]. These bands were absent in the spectra of free Schiff bases, *qch, qce, qcp, qcb, qcc* and *qco*. Thus, the structure of these complexes

contain water molecules, which was also indicated by the analytical data of Ni(II) complexes. The observed bands concerning the perchlorate (ClO_4^-) anion are also given in Table 4.3. The complex **4** shows a broad unsplit band at 1094 cm^{-1} corresponding to the $v_3(ClO_4^-)$ and an unsplit strong band at 627 cm^{-1} assignable to $v_4(ClO_4^-)$. This along with the absence of a band corresponding to $v_1(ClO_4^-)$ at 920 cm^{-1} indicates the presence of an ionic perchlorate group [29]. The perchlorate vibrations are observed in the 1160-1080 cm^{-1} range, for the complexes, **1**, **2**, **3**, **5** and **6**, suggesting monodentate coordination of perchlorate. But the molar conductivity studies indicate that complexes **1**, **2** and **6** are 1:1 electrolytes. Therefore, these complexes have an uncoordinated perchlorate group along with a coordinated one.

Table 4.3: FTIR spectral bands for the nickel(II) Schiff base complexes.(v in cm^{-1})

Complex	$v(C=N)a$	$v(C=N)q$	$v(OH)$	$v(Ni-N)$	$v(Ni-O)$	$v(ClO_4)$
qch [Ni(qch)₂(ClO₄)H₂O]ClO₄ **1**	1622 1613	1568 1564	3366	407	530	1144 1094 970 623
qce [Ni(qce)(ClO₄)H₂O]ClO₄ **2**	1639 1628	1555 1550	3326	413	548	1114 1095 939 623
qcp [Ni(qcp)(ClO₄)₂]·2H₂O **3**	1636 1630	1573 1569	3312	420	530	1141 1085 968 621
qcb [Ni(qcb)(H₂O)₂](ClO₄)₂ **4**	1640 1631	1555 1551	3326	417	505	1094 627
qcc [Ni(qcc)(ClO₄)₂]·H₂O **5**	1640 1628	1556 1550	3408	429	533	1140 1083 960 625
qco [Ni(qco)(ClO₄)H₂O]ClO₄ **6**	1610 1601	1568 1561	3353	411	532	1154 1094 620

a C=N of azomethine group; q C=N of quinoxaline ring; v(OH) of coordinated/lattice water molecule.
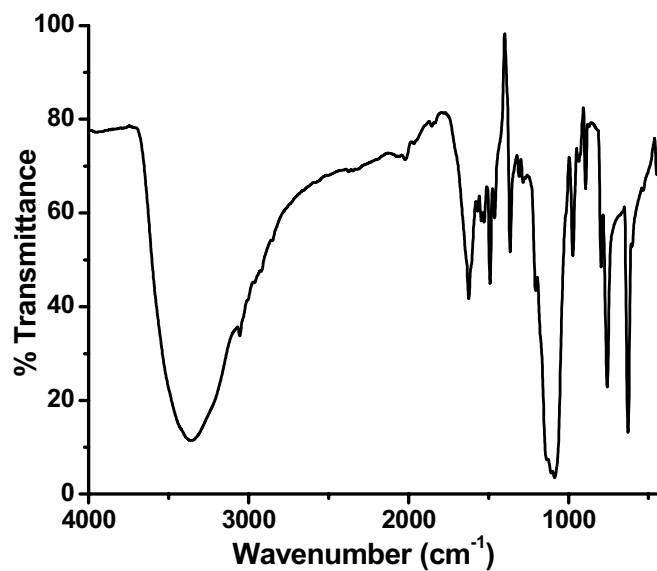
IR spectrum of [Ni(qch)$_2$(ClO$_4$)H$_2$O]ClO$_4$
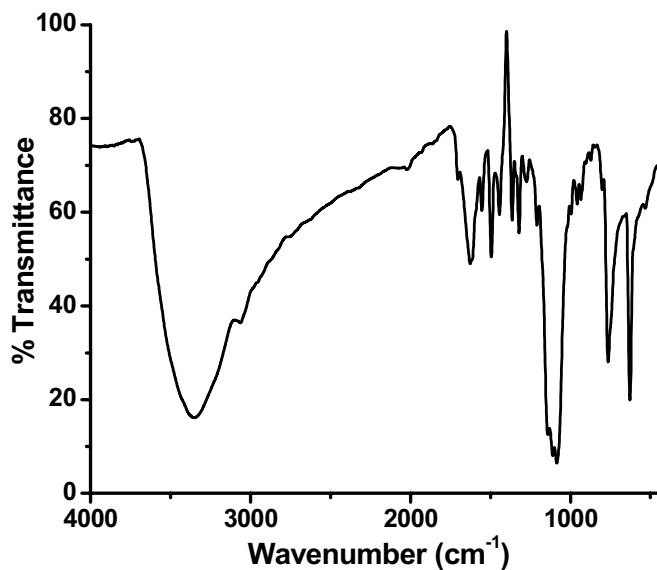
IR spectrum of [Ni(qce)(ClO$_4$)H$_2$O]ClO$_4$
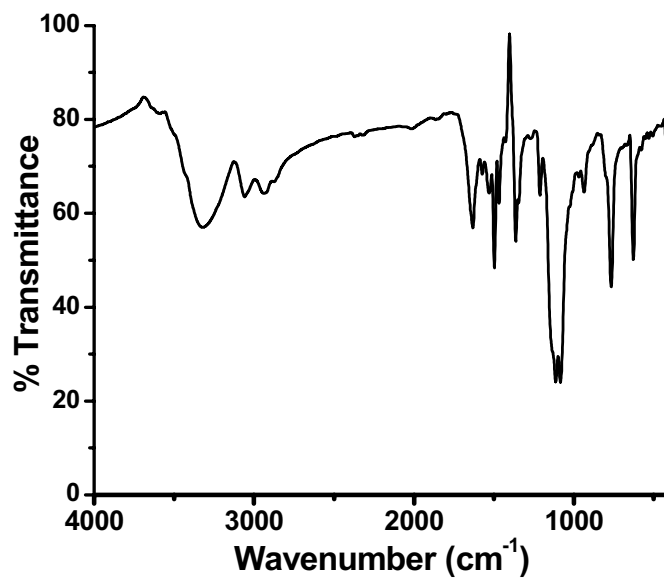
IR spectrum of [Ni(qcp)(ClO$_4$)$_2$]·2H$_2$O
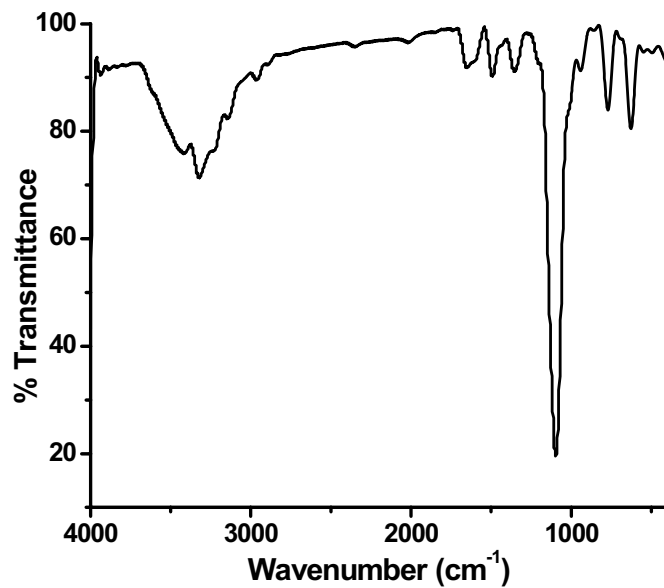
IR spectrum of [Ni(qcb)(H$_2$O)$_2$](ClO$_4$)$_2$
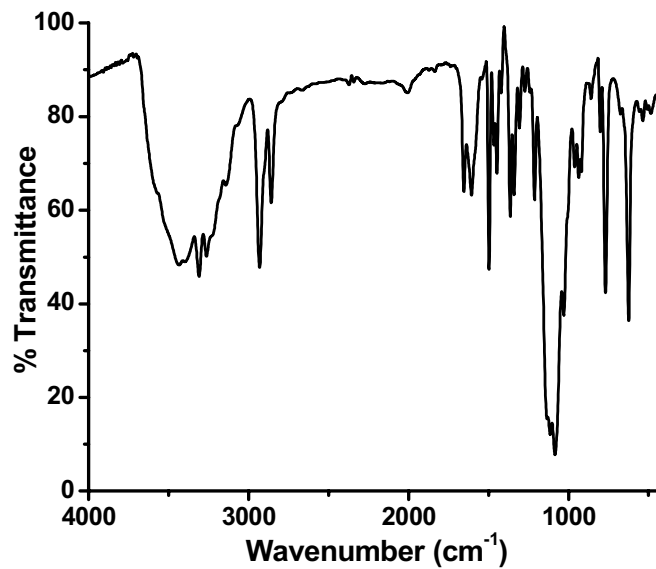
IR spectrum of [Ni(qcc)(ClO$_4$)$_2$]·H$_2$O
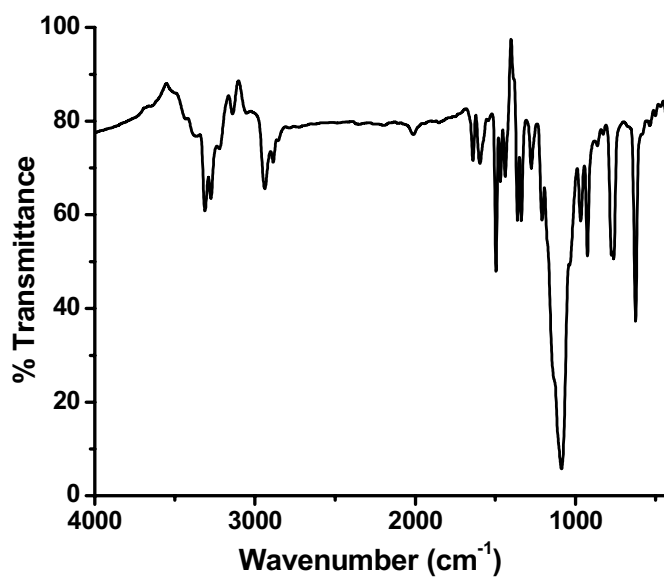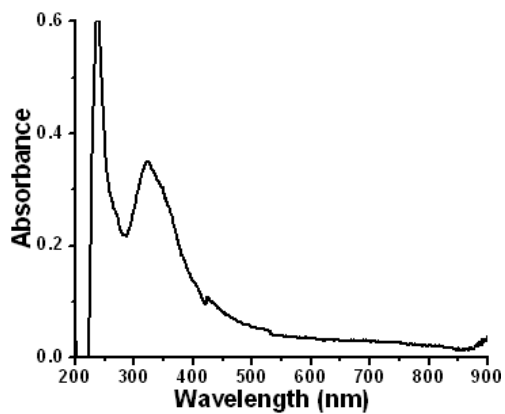

IR spectrum of [Ni(qco)(ClO$_4$)H$_2$O]ClO$_4$

Figure 4.1: FTIR spectra of nickel(II) Schiff base complexes

4.3.4 Electronic spectra

The electronic spectra of nickel(II) complexes were recorded in methanol (10^{-4} M) in the region of 200-1100nm (50,000-8000 cm^{-1}) and the spectral data are given in Table 4.4. The bands in the 200-400 nm region of the spectra [Figure 4.2] almost coincide with the bands observed for the free ligands. In addition to these, the bands are also present in the 400-900 nm region of the spectra of these complexes. The spectra of most of the ligands show two bands in the region 200-300 nm (30,000-50,000 cm^{-1}), due to $\pi \rightarrow \pi^*$ and $n \rightarrow \pi^*$ transitions. Among these $\pi \rightarrow \pi^*$ transitions are not altered to a greater extent on complexation. The three spin allowed transitions, $^3A_{2g}$ to $^3T_{2g}$ (F), $^3A_{2g}$ to $^3T_{1g}$ (F) and $^3A_{2g}$ to $^3T_{1g}$ (P), generally fall within the ranges 7000-13,000 cm^{-1}, 11,000-20,000 cm^{-1} and 19,000-27,000 cm^{-1} respectively for regular octahedral systems [30]. The d-d transitions observed for the complexes lie within these ranges [Table 4.4] and are in good agreement with those reported for an octahedral geometry around the Ni(II) ion. Based on the electronic spectral data and magnetic moment values (2.8-3.2 B.M.) an octahedral structure can be assigned for these complexes.

**Table 4.4: Electronic spectral assignments for nickel(II) complexes**

Complex	Absorption Maxima		log ε	Band Assignment
	nm	cm^{-1}	L mol^{-1} cm^{-1}	
[Ni(qch)$_2$(ClO$_4$)H$_2$O]ClO$_4$ **1**	238	42020	3.77	$\pi \rightarrow \pi^*$
	323	30960	3.10	$\pi \rightarrow \pi^*$
	424	23580	0.99	$^3A_{2g} \rightarrow {}^3T_{1g}$ (P)
	533	18760	0.83	$^3A_{2g} \rightarrow {}^3T_{1g}$ (F)
	705	14180	0.75	$^3A_{2g} \rightarrow {}^3T_{1g}$ (F)
[Ni(qce)(ClO$_4$)H$_2$O]ClO$_4$ **2**	219	45660	3.85	$\pi \rightarrow \pi^*$
	238	42020	4.23	$\pi \rightarrow \pi^*$
	323	30960	3.45	$\pi \rightarrow \pi^*$
	525	19050	1.10	$^3A_{2g} \rightarrow {}^3T_{1g}$ (F)
	846	11820	0.94	$^3A_{2g} \rightarrow {}^3T_{2g}$ (F)
[Ni(qcp)(ClO$_4$)$_2$]·2H$_2$O **3**	238	40820	3.87	$\pi \rightarrow \pi^*$
	257	38910	3.95	$\pi \rightarrow \pi^*$
	332	30120	3.57	$\pi \rightarrow \pi^*$
	420	23810	1.13	$^3A_{2g} \rightarrow {}^3T_{1g}$ (P)
	533	18760	1.08	$^3A_{2g} \rightarrow {}^3T_{1g}$ (F)
	705	14180	0.85	$^3A_{2g} \rightarrow {}^3T_{1g}$ (F)
[Ni(qcb)(H$_2$O)$_2$](ClO$_4$)$_2$ **4**	245	41320	3.76	$\pi \rightarrow \pi^*$
	325	30770	3.24	$\pi \rightarrow \pi^*$
	477	20960	1.08	$^3A_{2g} \rightarrow {}^3T_{1g}$ (P)
	777	12870	0.98	$^3A_{2g} \rightarrow {}^3T_{2g}$ (F)
[Ni(qcc)(ClO$_4$)$_2$]·H$_2$O **5**	236	41370	3.47	$\pi \rightarrow \pi^*$
	255	39220	3.85	$\pi \rightarrow \pi^*$
	350	28570	3.34	$\pi \rightarrow \pi^*$
	475	21050	0.92	$^3A_{2g} \rightarrow {}^3T_{1g}$ (P)
[Ni(qco)(ClO$_4$)H$_2$O]ClO$_4$ **6**	207	48310	3.83	$\pi \rightarrow \pi^*$
	241	41490	3.79	$\pi \rightarrow \pi^*$
	295	33900	3.41	$\pi \rightarrow \pi^*$
	317	31540	3.44	$\pi \rightarrow \pi^*$
	361	27700	3.60	$\pi \rightarrow \pi^*$
	725	13790	0.75	$^3A_{2g} \rightarrow {}^3T_{1g}$ (F)

UV-Vis spectrum of [Ni(qch)₂(ClO₄)H₂O]ClO₄
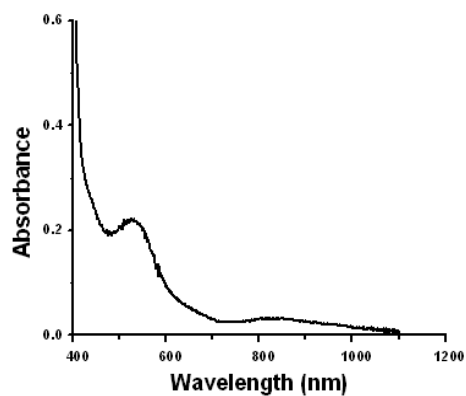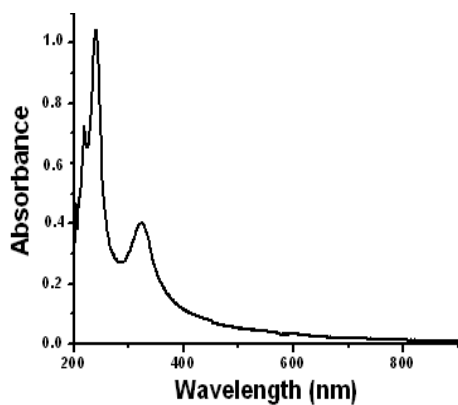
UV-Vis spectrum of [Ni(qce)(ClO₄)H₂O]ClO₄
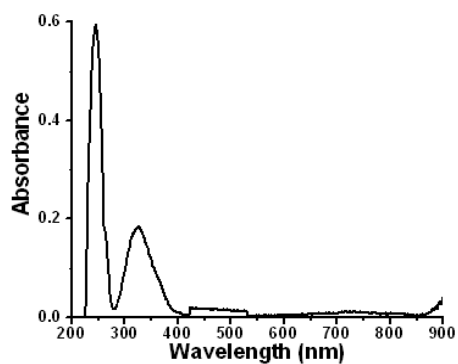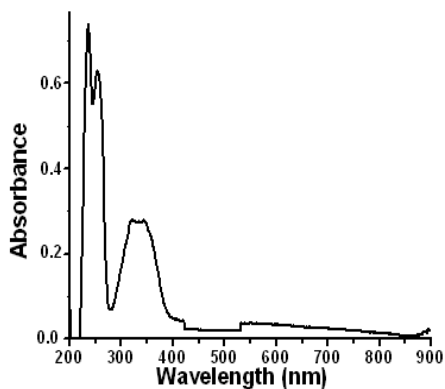
UV-Vis spectrum of [Ni(qcp)(ClO₄)₂]·2H₂O   *UV-Vis spectrum of [Ni(qcb)(H₂O)₂](ClO₄)₂*

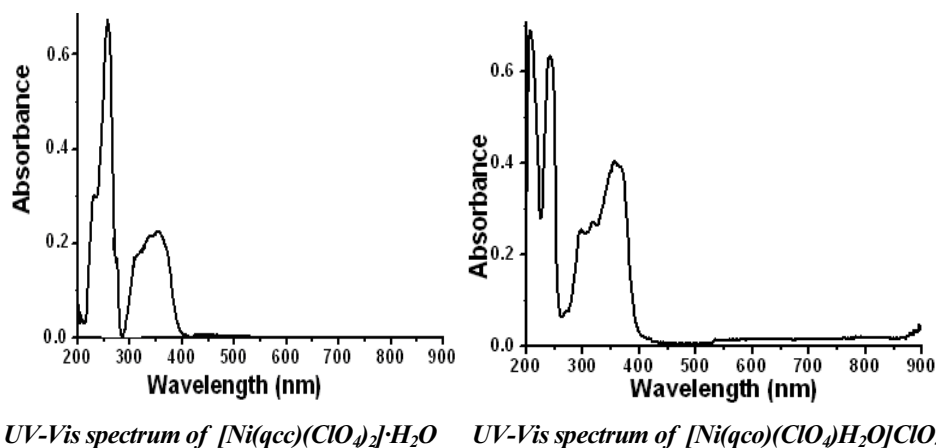*UV-Vis spectrum of [Ni(qcc)(ClO₄)₂]·H₂O*   *UV-Vis spectrum of [Ni(qco)(ClO₄)H₂O]ClO₄*

Figure 4.2: Electronic spectra of nickel(II) Schiff base complexes

4.4 CONCLUSIONS

This chapter describes the synthesis and characterisation of six new Ni(II) complexes of Schiff bases, *qch, qce, qcp, qcb, qcc* and *qco*. The molecular formula for the complexes derived from the analytical and molar conductance measurements are; [Ni(qch)₂(ClO₄)H₂O]ClO₄, [Ni(qce)(ClO₄)H₂O]ClO₄, [Ni (qcp) (ClO₄)₂]·2H₂O, [Ni(qcb)(H₂O)₂](ClO₄)₂, [Ni(qcc)(ClO₄)₂]·H₂O and [Ni(qco) (ClO₄)H₂O]ClO₄. The magnetic moment values and electronic spectra confirm that the complexes have octahedral geometry. The Schiff base, *qch*, acts as neutral bidentate ligand and the Schiff bases, *qce, qcp, qcb, qcc* and *qco*, act as tetradentate ligand in the complexes. Based on the analytical and physico-chemical data we have proposed the following structures for the Ni(II) Schiff base complexes.
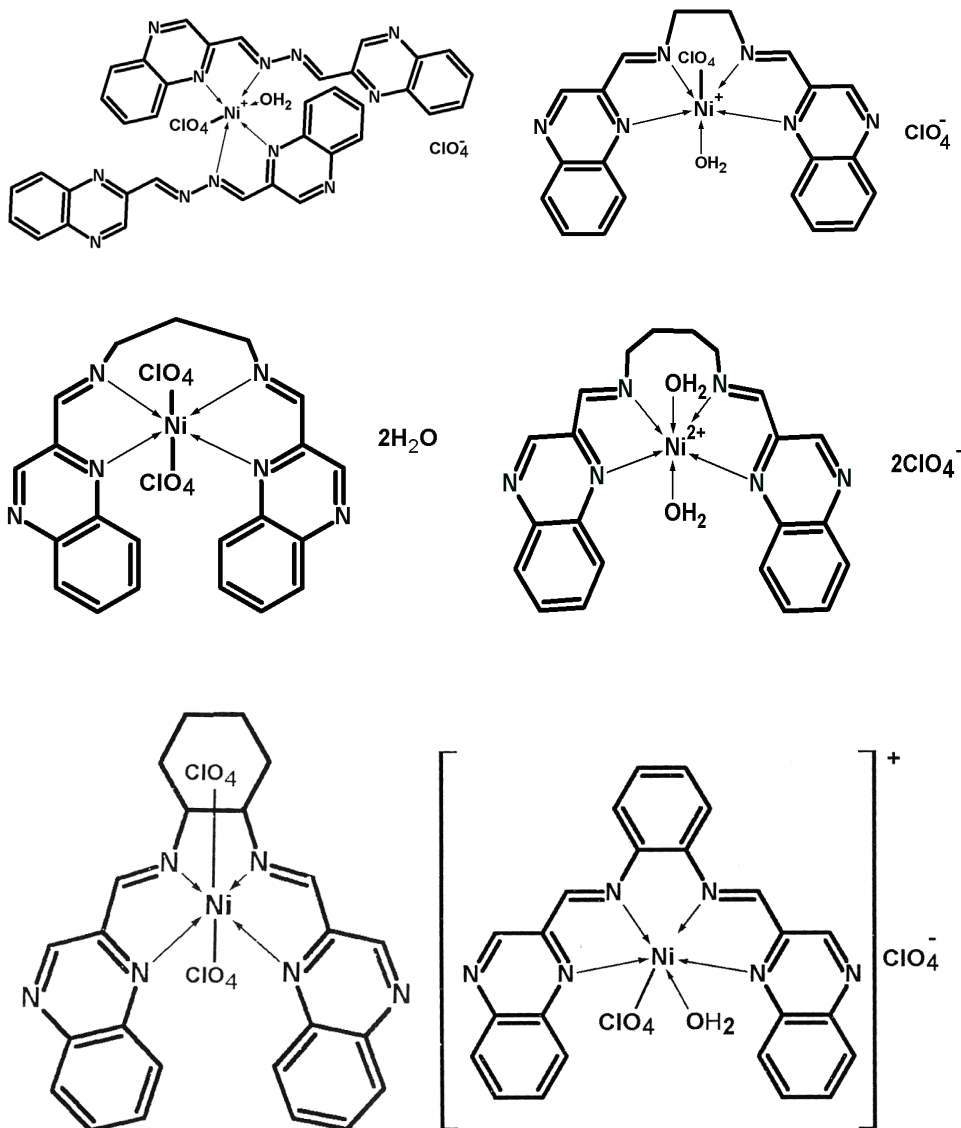
REFERENCES

1. P. Zanello, S. Tamburim, P. A. Vigato, G. A. Mazzocchin, *Coord. Chem. Rev.,* 77 (**1987**) 165.

2. W. D. Carlisle, D. E. Fenton, P. B. Roberts, U. Casellato, P. A. Vigato, R. Graziani, *Transition Met. Chem.,* 11 (**1986**) 292.

3. A. Mustapha, P. Duckmanton, J. Reglinski, A. R. Kennedy, *Polyhedron*, 29 (**2010**) 2590.

4. T. Aono, H. Wada, Y.-I. Aratake, N. Matsumoto, H. Okawa, Y.Matstuda, *J. Chem. Soc., Dalton Trans.*, (**1996**) 25.

5. M. D. Timken, W. A. Marrit, D. N. Hendrickson, R. R. Gagne, E. Sinn, *Inorg. Chem.*, 24 (**1985**) 4202.

6. I. C. Santos, M. Vilas-Boas, M. F. M. Piedade, C. Freire, M. T. Duarte, B. de Castro, *Polyhedron*, 19 (**2000**) 655.

7. J. R. Lancaster, *The Bioinorganic Chemistry of Nickel*, VCH, New York, (**1988**).

8. A. Prakash, M. P. Gangwar, K. K. Singh, *Journal of Developmental Biology and Tissue Engineering*, 3 (**2011**) 13.

9. K. C. Gupta, A. Kumar Sutar, *Coord. Chem. Rev.*, 252 (**2008**) 1420.

10. K. C. Gupta, A. K. Sutar, *J. Mol. Catal. A: Chem*, 272 (**2007**) 64.

11. D. Chatterjee, S. Mukherjee, A. Mitra, *J. Mol. Catal. A: Chem*, 154 (**2000**) 5.

12. D. Chatterjee, H. C. Bajaj, A. Das, K. Bhatt, *J. Mol. Catal.,* 92 (**1994**) L235.

13. H. Meyer zu Altenschildesche, R. Nesper, *Stud. Surf. Sci. Catal.*, 98 (**1995**) 120.

14. S. Kowalak, R. C. Weiss, K. J. Balkus, *J. Chem. Soc. Chem. Commun.*, (**1991**) 57.

15. R. I. Kureshy, N. H. Khan, S. H. R. Abdi, S. T. Patel, P. K. Iyer, R. V. Jasra, *J. Catalysis*, 209 (**2002**) 99.

16. Z.-H. Xu, F.-J. Chen, P.-X. Xi, X.-H. Liu, Z.-Z. Zeng, *Journal of Photochemistry and Photobiology A: Chemistry*, 196 (**2008**) 77.

17. G. Barone, N. Gambino, A. Ruggirello, A. Silvestri, A. Terenzi, V. T. Liveri, *J. Inorg. Biochem.*, 103 (**2009**) 731.

18. R. Akkasali, N. Patil, S. D. Angadi, *Rasayan J. Chem.*, 2 (**2009**) 81.

19. S. Yamada, E. Ohno, Y. Kuge, A. Takeuchi, K. Yamanouci, K. Iwasaki, *Coord. Chem. Rev.*, 3 (**1968**) 247.

20. K. Yamanouci, S. Yamada, *Bull. Chem. Soc. Jpn.*, 49 (**1976**) 163.

21. D. Pucci, A. Bellusci, A. Crispini, M. Ghedini, M. La Deda, *Inorg. Chim. Acta*, 357 (**2004**) 495.

22. W. J. Geary. *Coord. Chem. Rev.*, 7 (**1971**) 81.

23. F. A. Cotton, G. Wilkinson, C. A. Murillo, M. Bochmann, *Advanced Inorganic Chemistry*, sixth ed., Wiley, NewYork, (**1999**).

24. S. Buffagni, L. M. Vallarino, J. V. Quagliaxo, *Inorg. Chem.*, 3 (**1964**) 480.

25. S. Mayadevi, K. K. M. Yusuff, *Synth. React. Inorg. Met-Org. Chem.*, 27 (**1997**) 319.

26. M. Sebastian, V. Arun, P. P. Robinson, A. A. Varghese, R. Abraham, E. Suresh, K. K. M. Yusuff , *Polyhedron*, 29 (**2010**) 3014.

27. M. Sebastian, V. Arun, P. P. Robinson, P. Leeju, D. Varghese, G. Varsha, K. K. M. Yusuff, *J. Coord. Chem.*, 63 (**2009**) 307.

28. A. A. El-Sherif, T. M. A. Eldebss, *Spectrochim. Acta Part A*, 79 (**2011**) 1803.

29. M. R. Bermejo, M. Fondo, A. Garcia-Deibe, M. Rey, J. Sanmartin, A. Sousa, M. Watkinson, *Polyhedron,* 15 (**1996**) 4185.

30. A. B. P. Lever, *Electronic Spectra of the Ions. In Inorganic Electronic Spectroscopy*, 2nd Ed., Elsevier: Amsterdam, (**1984**) 507.

****✿****

Synthesis and characterisation of copper(II) Schiff base complexes

5.1 INTRODUCTION

A large number of Schiff bases and their complexes have been studied because of their ability to reversibly bind oxygen [1], act as catalysts [2] and exhibit photochromic properties [3,4]. The high affinity for the chelation of the Schiff bases towards the transition metal ions, especially copper ions, is utilised in preparing their complexes. The chemistry of copper complexes is of interest owing to their importance in biological and industrial processes [5,6]. The copper complexes derived from Schiff bases were found to be extremely efficient catalysts in both homogeneous [7] and heterogeneous [2] conditions.

Complexes of copper show various geometries. Among them most common are tetrahedral, square planar, square pyramidal, trigonal bipyramidal and octahedral. Unlike the other first row transition metal ions, copper complexes show distortions [8]. For example, the hexa coordinated Cu(II) ion with d^9 configuration prefers distorted octahedral geometry, which is a direct consequence of Jahn–Teller effect [9]. Thus, octahedral complexes usually exist with a set of four strongly and two weakly coordinating ligands.

The study of mononuclear copper complexes has been stimulated by a desire to 'mimic' the active sites of metalloproteins such as the enzyme galactose oxidase [10] and nitrite reductase [11]. One of the current interests in the coordination chemistry is synthesis of high-nuclearity transition metal complexes [12,13]. These complexes are studied as models for the multimetal active sites of metal-storage proteins [14,15], and as single molecule magnets (SMMs) [16,17]. Dinuclear copper complexes attract attention as models of active centers of copper containing enzymes (tyrosinase, haemocyanin, haemerythrin, cytochrome *c* oxidase, *etc*.) and as potential components of homogeneous catalytic systems [7,18]. They have also been investigated frequently, because of the interest in new inorganic materials showing molecular ferro- or antiferromagnetic interactions [19-22].

In the present chapter, we report the synthesis and characterisation of twenty four copper(II) Schiff base complexes. Single crystal XRD analyses of some of the prepared complexes were carried out. The ligands used here are the tetradentate symmetrical di-Schiff base ligands, *qch, qce, qcp, qcb, qcc* and *qco*. Details of the synthesis and characterisation of these ligands are described in chapter 2.

5.2 EXPERIMENTAL

5.2.1 Materials

The materials used for the preparation of Schiff bases, *qch, qce, qcp, qcb, qcc* and *qco*, are given in chapter 2. The copper(II) complexes were prepared from four copper salts, $Cu(OAc)_2 \cdot 4H_2O$, $CuCl_2 \cdot 2H_2O$, $Cu(NO_3)_2 \cdot 3H_2O$ and $Cu(ClO_4)_2 \cdot 6H_2O$.

5.2.2 Synthesis of complexes

The complexes **1-6** was prepared by adding a solution of Cu(OAc)$_2$·4H$_2$O (0.908 g, 5 mmol, in 30 mL methanol) to a solution of the Schiff base, *qch*, *qce*, *qcp*, *qcb*, *qcc* or *qco*, (5 mmol, in 50 mL methanol/chloroform) and refluxing for 3 h. The resulting solution was allowed to evaporate at room temperature. The complexes separated were collected and washed with cold methanol. The product was dried over anhydrous calcium chloride in a desiccator (~ 80% yield).

The complexes **7-12** was prepared by adding a solution of CuCl$_2$·2H$_2$O (0.8524 g, 5 mmol, in 25 mL methanol) to a hot 50 mL methanol/chloroform solution of the Schiff bases, *qch*, *qce*, *qcp*, *qcb*, *qcc* or *qco*, (5 mmol). This solution was refluxed for 3 h. After this, the resulting solution was allowed to evaporate at room temperature to give complex, which was collected and washed with cold methanol. The product was dried over anhydrous calcium chloride in a desiccator (~ 70% yield).

The complexes **13-18** were prepared by the following method. Methanol solution (30 mL) of Cu(NO$_3$)$_2$·3H$_2$O (1.208 g , 5 mmol) was mixed with hot solution of the Schiff bases, *qch*, *qce*, *qcp*, *qcb*, *qcc* or *qco*, (5 mmol, in 50 mL methanol/chloroform) and refluxed for 3 h. The resulting solution was allowed to evaporate at room temperature to give complex, which were collected and washed with cold methanol. The product was dried over anhydrous calcium chloride in a desiccator (~ 70% yield).

The complexes **19-24** was prepared by adding a solution of Cu(ClO$_4$)$_2$·6H$_2$O (1.852 g, 5 mmol, in 25 mL methanol) to a hot solution of the Schiff bases, *qch*, *qce*, *qcp*, *qcb*, *qcc* or *qco*, (5 mmol, in 50 mL methanol/chloroform) was added and refluxed for 3 h. The resulting solution was allowed to evaporate at room temperature to give product, which were collected and washed with cold methanol. The product was dried over anhydrous calcium chloride in a desiccator (~ 75% yield).

However, our attempts to isolate single crystals suitable for X-ray crystal structure determination were not successful for most of the complexes. We got a single crystal of a complex derived from the reaction of $Cu(NO_3)_2 \cdot 3H_2O$ and *qce* in methanol. We have carried out the single crystal X-ray analysis of this complex and the results of the analysis are presented in section 5.3.8.

5.3 RESULTS AND DISCUSSION

Facile condensation of quinoxaline-2-carboxaldehyde and compounds, like, hydrazine hydrate, 1,2-diaminoethane, 1,3-diaminopropane, 1,4-diaminobutane, cyclohexanediamine and orthophenylenediamine, in a 2:1 molar ratio lead to the formation of neutral N_4 tetradentate Schiff base ligands, denoted as *qch, qce, qcp, qcb, qcc* and *qco*. Reaction of these with copper salts, $Cu(OAc)_2 \cdot 4H_2O/ CuCl_2 \cdot 2H_2O/Cu(NO_3)_2 \cdot 3H_2O/Cu(ClO_4)_2 \cdot 6H_2O$, in methanol yield a variety of copper complexes. In the case of the reaction between $CuCl_2 \cdot 2H_2O$ and *qce* in methanol, a black coloured complex was separated. On keeping the filtrate after separation of the complex blue crystals were obtained. The blue crystals on single crystal XRD analysis was found to be dichloro(ethylenediamine)copper(II), which was reported in 1986 by Harvey and Lock [23]. This study indicate that excess Schiff base part gets decomposed and form ethylenediamine, which results in the formation of the complex dichloro(ethylenediamine)copper(II). The copper complexes are coloured, non-hygroscopic and found to be air stable. The complexes are soluble in common organic solvents such as methanol, ethanol, benzene, tetrahydrofuran, dichloromethane, DMF and DMSO. Due to the explosive nature, perchlorate complexes were not subjected to thermal analysis. Therefore, the nature of the water molecules present in these complexes could be ascertained only from the IR spectra.

5.3.1 Elemental analysis

The elemental analysis data of the complexes are given in Table 5.1. The analytical data suggest that most of the complexes are mononuclear except the complexes of *qce*, which is binuclear. The data also show that metal to ligand ratio for the complexes of *qce*, *qcp*, *qcb*, *qcc* and *qco* is 1:1 and that for the complexes of *qch* is 1:2.

Table 5.1: Analytical data of the copper(II) Schiff base complexes

Complex	Molecular formula	Formula weight	Colour	Carbon (%)	Hydrogen (%)	Nitrogen (%)	Cu (%)
1	$C_{40}H_{34}CuN_{12}O_6$	842	Black	57.57 (57.04)	4.19 (4.07)	20.12 (19.95)	7.63 (7.54)
2	$C_{48}H_{46}Cu_2N_{12}O_9$	1062	Black	54.56 (54.28)	4.67 (4.37)	15.63 (15.83)	11.81 (11.97)
3	$C_{25}H_{28}CuN_6O_6$	572	Black	52.32 (52.49)	4.73 (4.93)	14.87 (14.69)	11.43 (11.11)
4	$C_{26}H_{32}CuN_6O_7$	604	Black	51.60 (51.69)	5.43 (5.34)	13.64 (13.91)	10.54 (10.52)
5	$C_{28}H_{34}CuN_6O_7$	630	Brown	53.32 (53.37)	5.22 (5.44)	13.16 (13.34)	10.16 (10.08)
6	$C_{28}H_{24}CuN_6O_5$	588	Brown	57.11 (57.19)	4.45 (4.11)	14.34 (14.29)	10.64 (10.81)
7	$C_{36}H_{28}Cl_2CuN_{12}O_2$	795	Black	54.55 (54.38)	3.49 (3.55)	21.52 (21.14)	8.53 (8.92)
8	$C_{40}H_{34}Cl_4Cu_2N_{12}O$	967	Black	49.66 (49.65)	3.67 (3.54)	17.73 (17.37)	14.28 (14.65)
9	$C_{21}H_{24}Cl_2CuN_6O_3$	542	Dark green	46.22 (46.46)	4.77 (4.46)	15.35 (15.48)	13.48 (13.06)
10	$C_{22}H_{22}Cl_2CuN_6O$	520	Dark green	50.62 (50.73)	4.53 (4.26)	16.54 (16.13)	13.43 (13.61)
11	$C_{24}H_{22}Cl_2CuN_6O$	528	Black	54.32 (54.50)	4.22 (4.19)	15.67 (15.89)	13.29 (13.41)
12	$C_{24}H_{18}Cl_2CuN_6O_3$	540	Brown	53.31 (53.29)	3.45 (3.35)	15.34 (15.54)	11.36 (11.75)
13	$C_{36}H_{26}CuN_{14}O_7$	830	Black	52.48 (52.08)	3.29 (3.16)	23.52 (23.62)	7.53 (7.65)

Complex	Molecular formula	Formula weight	Colour	Carbon (%)	Hydrogen (%)	Nitrogen (%)	Cu (%)
14	$C_{40}H_{52}Cu_2N_{14}O_{17}$	1128	Violet	42.46 (42.59)	4.69 (4.65)	17.53 (17.38)	11.48 (11.27)
15	$C_{21}H_{20}CuN_8O_7$	559	Black	45.52 (45.04)	3.47 (3.60)	20.35 (20.01)	11.55 (11.35)
16	$C_{22}H_{22}CuN_8O_7$	574	Green	46.22 (46.03)	3.43 (3.86)	19.50 (19.52)	11.13 (11.07)
17	$C_{24}H_{26}CuN_8O_8$	618	Black	48. 43 (48.64)	4.46 (4.24)	18.23 (18.13)	10.21 (10.28)
18	$C_{24}H_{20}CuN_8O_8$	612	Black	4.43 (47.10)	3.56 (3.29)	18.43 (18.31)	10.44 (10.38)
19	$C_{36}H_{28}Cl_2CuN_{12}O_{10}$	923	Black	46.78 (46.84)	3.18 (3.06)	18.42 (18.21)	6.54 (6.88)
20	$C_{40}H_{34}Cl_4Cu_2N_{12}O_{17}$	1223	Violet	39.46 (39.26)	2.69 (2.80)	13.45 (13.74)	10.48 (10.39)
21	$C_{21}H_{22}Cl_2CuN_6O_{10}$	652	Green	38.42 (38.63)	3.47 (3.40)	12.65 (12.87)	9.66 (9.73)
22	$C_{22}H_{22}Cl_2CuN_6O_9$	648	Black	40.56 (40.72)	3.48 (3.42)	12.70 (12.95)	9.63 (9.79)
23	$C_{24}H_{26}Cl_2CuN_6O_{10}$	692	Green	41. 54 (41.60)	3.67 (3.78)	12.53 (12.13)	9.44 (9.17)
24	$C_{24}H_{22}Cl_2CuN_6O_{11}$	704	Brown	40.68 (40.89)	3.36 (3.15)	11.73 (11.92)	9.39 (9.01)

* Calculated values in parentheses

5.3.2 Molar conductivity measurements

The molar conductivity values of the complexes (10^{-3} M) are given in Table 5.2. Generally, the conductance values of complexes in methanol are found in the range, 80-115 $ohm^{-1}cm^2mol^{-1}$ for 1:1 electrolyte, 160-220 $ohm^{-1}cm^2mol^{-1}$ for 2:1 electrolyte, 290-350 for 3:1 electrolyte and higher values for 4:1 electrolytes. The very low molar conductance values (less than 60 $ohm^{-1}cm^2 mol^{-1}$) observed for **1-7**, **11**, **12**, **18**, **19** and **24**, indicate non-electrolytic nature of these complexes [24]. The conductance data for complexes **9**, **10**, **13**, **15**, **16** and **22** suggest them to be 1:1 electrolytes and the data for the complexes **17**, **21** and **23** agree with that for

the 2:1 electrolytes. The complexes **8**, **14** and **20** show higher conductance values than those of other complexes and these are considered as 4:1 electrolytes.

Table 5.2: Molar conductance data of the copper(II) Schiff base complexes.

Complex	Molar conductance $(ohm^{-1}\ cm^2\ mole^{-1})$
1	29
2	23
3	26
4	41
5	30
6	9
7	55
8	386
9	100
10	113
11	36
12	14
13	83
14	405
15	117
16	137
17	182
18	54
19	54
20	394
21	168
22	117
23	171
24	35

5.3.3 Thermal analysis

The analytical data suggest most of these complexes contain water molecules. We have to find out whether these water molecules are coordinated or not. For these, thermal analysis of copper(II) complexes were conducted. TG-DTG plots of the complexes are given in Figures 5.1-5.3. The properties of coordinatively saturated transition metal complexes can be profoundly influenced by their environment. The coordinated water is stable and volatilised above 140 ºC. The removal of lattice water usually occurs below 140 ºC [Tables 5.3-5.5]. TG results show good agreement with the molecular formula arrived from the analytical data. The weight loss observed for the complexes, **1-6**, **7**, **8**, **12** and **18**, is found to be below 140 ºC. TG-DTG analysis of complex **14** shows several peaks of weight loss below 200 ºC; the weight loss in this case corresponds to 9 H_2O molecules. In these complexes the water molecules are present as lattice water. From the TG data of complexes, **10**, **13**, **15**, **16** and **17**, the weight loss of complexes starts from 140 °C which indicates that these contain coordinated water only. The complex **9** has both lattice and coordinated water, as the weight loss occurs in two stages: 50-135 and 140-190 °C. Complex **11** have no weight loss below 200 °C and contain no water molecules. All the copper(II) complexes are found to be thermally stable and exhibit multistage decomposition pattern

Table 5.3: Thermal analysis data of copper(II) acetate complexes

Complex	Temperature Range (°C)	% Loss	Fragment lost	Nature of water molecule
1	60-135	4.1	$2H_2O$	Lattice water
2	50-120	1.9	H_2O	Lattice water
3	60-130	6.1	$2H_2O$	Lattice water
4	75-140	7.9	$3H_2O$	Lattice water
5	50-140	8.0	$3H_2O$	Lattice water
6	50-140	3.2	H_2O	Lattice water
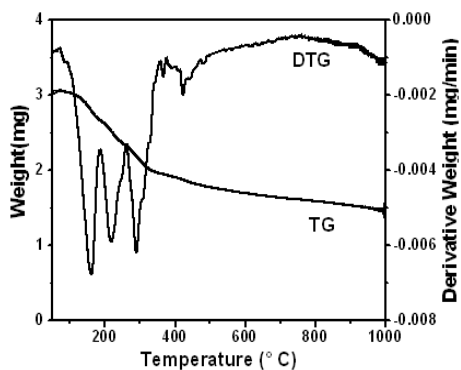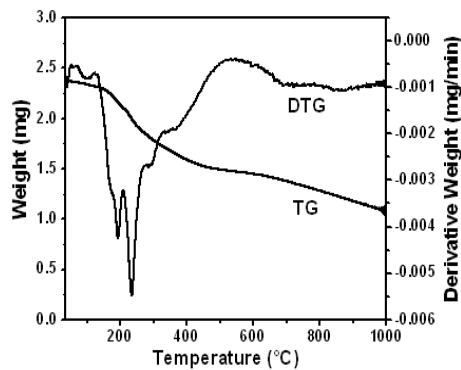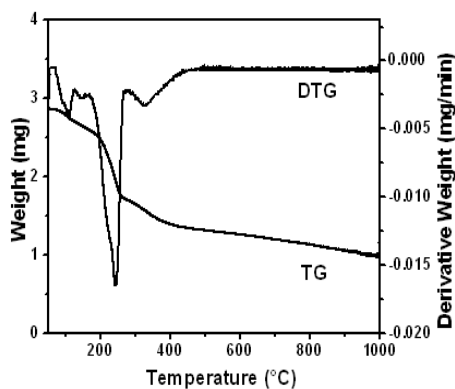
TG-DTG plot of complex 1

TG-DTG plot of complex 2

TG-DTG plot of complex 3
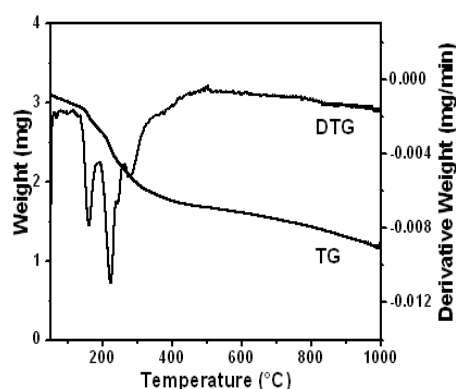
TG-DTG plot of complex 4
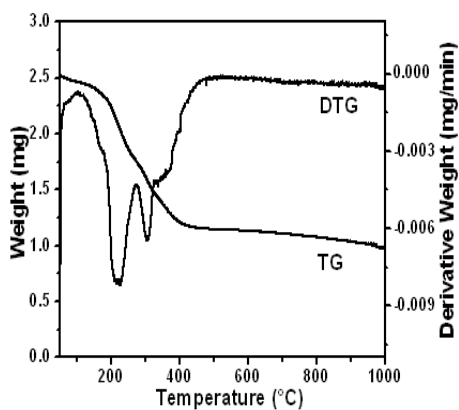
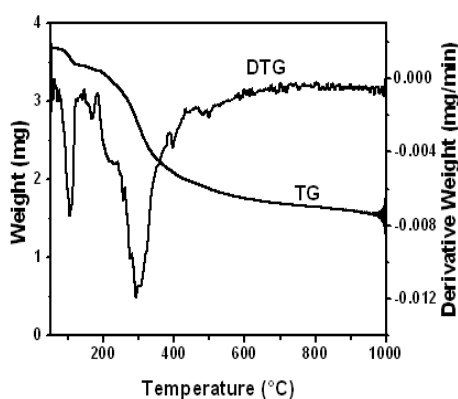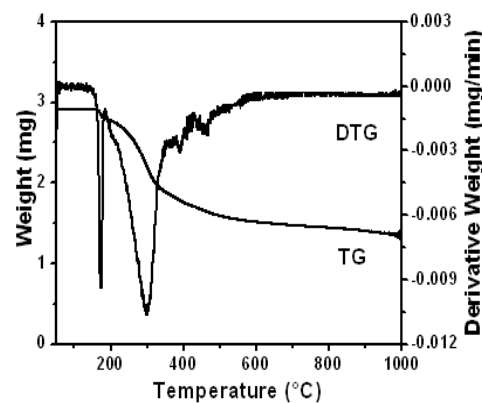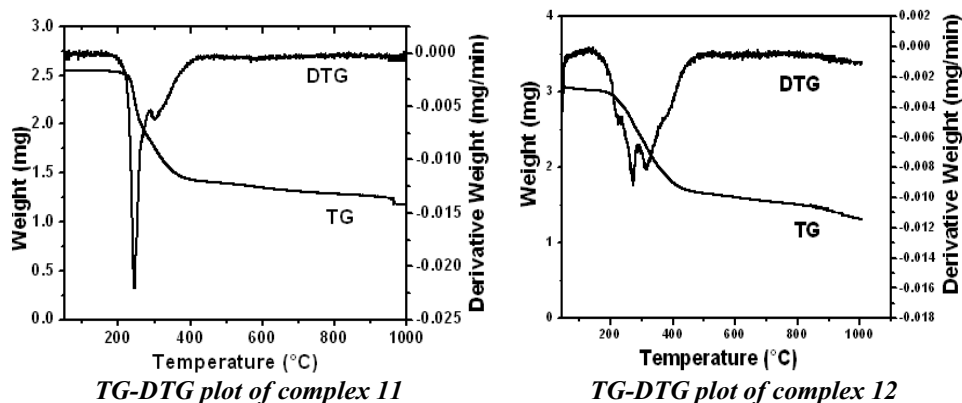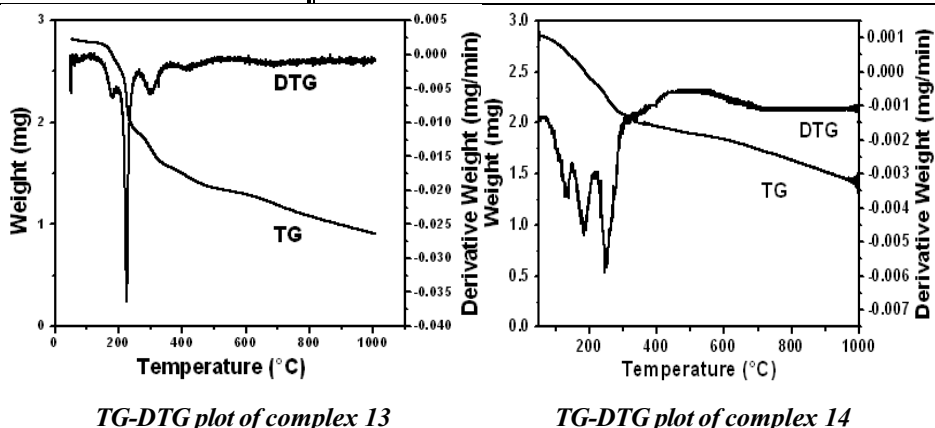*TG-DTG plot of complex 5*
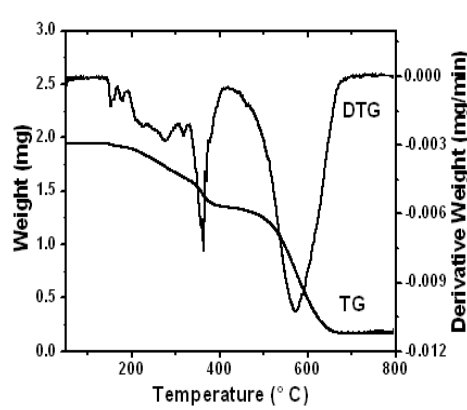
TG-DTG plot of complex 6

Figure 5.1: TG-DTG plots of copper(II) acetate complexes

Table 5.4: Thermal analysis data of copper(II) chloride complexes

Complex	Temperature Range (°C)	% Loss	Fragment lost	Nature of water molecule
7	50-140	3.9	$2H_2O$	Lattice water
8	50-140	2.1	H_2O	Lattice water
9	50-135	7.0	$2H_2O$	Lattice water
	140-190	3.4	H_2O	Coordinated water
10	140-190	4.2	H_2O	Coordinated water
11	-	-	-	-
12	50-140	3.0	H_2O	Lattice water
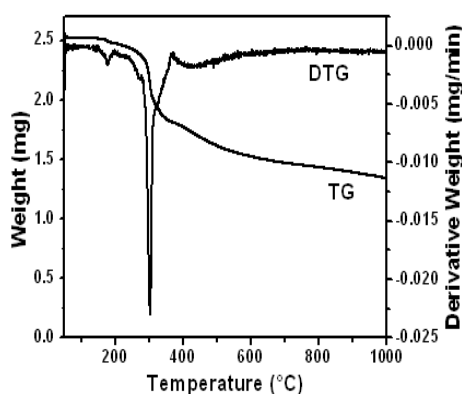
TG-DTG plot of complex 7
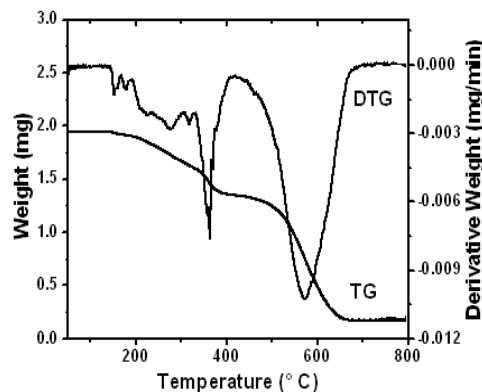
TG-DTG plot of complex 8

TG-DTG plot of complex 9

TG-DTG plot of complex 10

TG-DTG plot of complex 11

TG-DTG plot of complex 12

Figure 5.2: TG-DTG plots of copper(II) chloride complexes

Table 5.5: Thermal analysis data of copper(II) nitrate complexes

Complex	Temperature Range (°C)	% Loss	Fragment lost	Nature of water molecule
13	140-160	2.2	H_2O	Coordinated water
14	50-185	14.3	$9H_2O$	Lattice water
15	180-220	3.2	H_2O	Coordinated water
16	140-170	3.2	H_2O	Coordinated water
17	140-200	5.8	$2H_2O$	Coordinated water
18	50-140	5.2	$2H_2O$	Lattice water

TG-DTG plot of complex 13

TG-DTG plot of complex 14

TG-DTG plot of complex 15

TG-DTG plot of complex 16

TG-DTG plot of complex 17

TG-DTG plot of complex 18
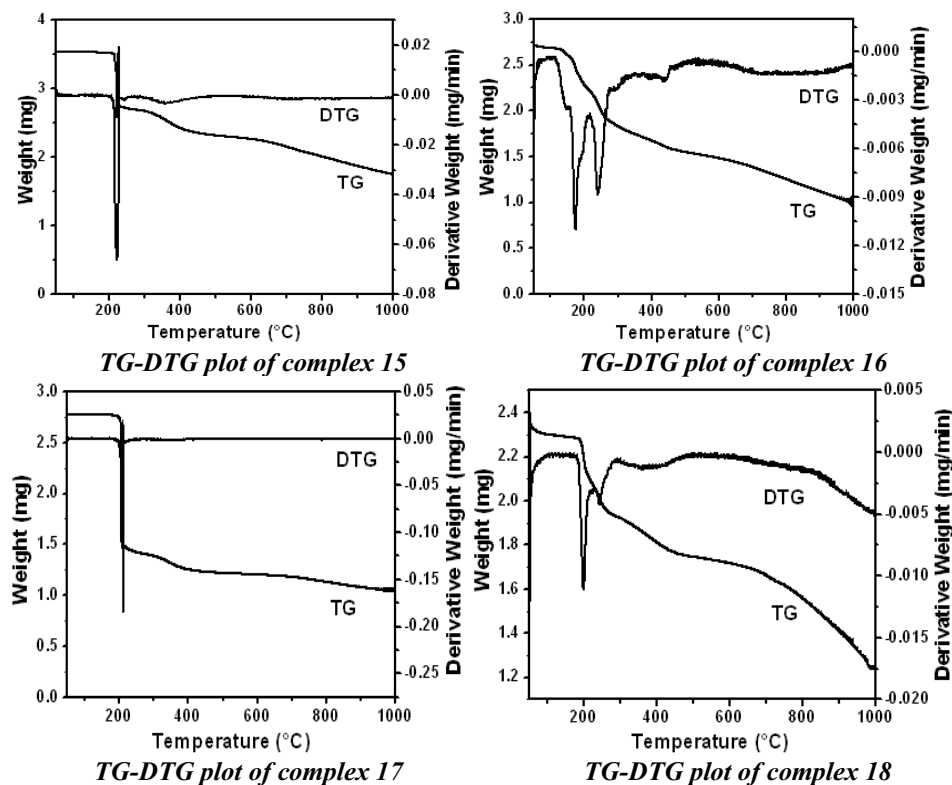
Figure 5.3: TG-DTG plots of copper(II) nitrate complexes

Based on the elemental analysis, molar conductance and TG data suggest that the molecular formula of these copper(II) complexes as: $[Cu(qch)_2(OAc)_2]\cdot 2H_2O$ (**1**), $[Cu_2(qce)_2(OAc)_4]\cdot H_2O$ (**2**), $[Cu(qcp)(OAc)_2]\cdot 2H_2O$ (**3**), $[Cu(qcb)(OAc)_2]\cdot 3H_2O$ (**4**), $[Cu(qcc)(OAc)_2]\cdot 3H_2O$ (**5**), $[Cu(qco)(OAc)_2]\cdot H_2O$ (**6**), $[Cu(qch)Cl_2]\cdot 2H_2O$ (**7**), $[Cu_2(qce)_2]Cl_4\cdot H_2O$ (**8**), $[Cu(qcp)ClH_2O]Cl\cdot 2H_2O$ (**9**), $[Cu(qcb)$ $Cl(H_2O)]Cl$ (**10**), $[Cu(qcc)Cl_2]$ (**11**), $[Cu(qco)Cl_2]\cdot H_2O$ (**12**), $[Cu(qch)NO_3(H_2O)]$ NO_3 (**13**), $[Cu_2(qce)_2](NO_3)_2(OH)_2\cdot 9H_2O$ (**14**), $[Cu(qcp)NO_3(H_2O)]NO_3$ (**15**), $[Cu(qcb)NO_3H_2O]NO_3$ (**16**), $[Cu(qcc)(H_2O)_2](NO_3)_2$ (**17**), $[Cu(qco)$ $(NO_3)_2]\cdot 2H_2O$ (**18**), $[Cu(qch)(ClO_4)_2]\cdot 2H_2O$ (**19**), $[Cu_2(qce)_2](ClO_4)_4\cdot H_2O$ (**20**), $[Cu(qcp)(H_2O)_2](ClO_4)_2$ (**21**), $[Cu(qcb)ClO_4(H_2O)]ClO_4$ (**22**), $[Cu(qcc)(H_2O)_2]$ $(ClO_4)_2$ (**23**), $[Cu(qco)(ClO_4)_2]\cdot 3H_2O$ (**24**).

5.3.4 Magnetic susceptibility measurements

Effective magnetic moments were calculated by the equation $\mu_{\text{eff}} = 2.828(\chi_A T)^{1/2}$, where χ_A is the magnetic susceptibility per copper. Room temperature magnetic susceptibility measurements (Gouy method, powdered sample) show that all the complexes have magnetic moments close to 1.73 B.M. as expected for discrete magnetically non-coupled copper(II) ion [25]. Magnetic moments of the copper complexes under investigation fall in the 1.60-1.92 B.M. range [Table 5.6], and lie within the range reported for tetrahedral and tetragonally distorted octahedral structures [26-28]. Complexes of *qce* exhibit magnetic moments less than 1.70 B.M., which are less than the spin only value (1.73 B.M.). Low magnetic value can be expected for complexes having antiferromagnetic effect, with spin-orbital coupling in the ground state for spin doublet species [26], or with dimeric or polymeric structures. The lower magnetic moment values for the complexes of *qce* might be due to the dimeric nature of these complexes. In such cases, antiferromagnetic interaction between the Cu(II) centers might occur.

Table 5.6: Magnetic moment values of the copper(II) Schiff base complexes.

Complex	Magnetic moment (B.M.)
[Cu(qch)$_2$(OAc)$_2$]·2H$_2$O **1**	1.90
[Cu$_2$(qce)$_2$(OAc)$_4$]·H$_2$O **2**	1.70
[Cu (qcp)(OAc)$_2$]·2H$_2$O **3**	1.91
[Cu(qcb)(OAc)$_2$]·3H$_2$O **4**	1.92
[Cu(qcc)(OAc)$_2$]·3H$_2$O **5**	1.90
[Cu(qco)(OAc)$_2$]·H$_2$O **6**	1.89
[Cu(qch)Cl$_2$]·2H$_2$O **7**	1.92

Complex	Magnetic moment (B.M.)
[Cu$_2$(qce)$_2$]Cl$_4$·H$_2$O **8**	1.69
[Cu(qcp)ClH$_2$O]Cl·2H$_2$O **9**	1. 90
[Cu(qcb)Cl(H$_2$O)]Cl **10**	1.91
[Cu(qcc)Cl$_2$] **11**	1.85
[Cu(qco)Cl$_2$]·H$_2$O **12**	1.89
[Cu(qch)NO$_3$(H$_2$O)]NO$_3$ **13**	1.91
[Cu$_2$(qce)$_2$](NO$_3$)$_2$(OH)$_2$·9H$_2$O **14**	1.64
[Cu(qcp)NO$_3$(H$_2$O)]NO$_3$ **15**	1.89
[Cu(qcb)NO$_3$H$_2$O]NO$_3$ **16**	1.85
[Cu(qcc)(H$_2$O)$_2$](NO$_3$)$_2$ **17**	1.91
[Cu(qco)(NO$_3$)$_2$]·2H$_2$O **18**	1.86
[Cu(qch)(ClO$_4$)$_2$]·2H$_2$O **19**	1.85
[Cu$_2$(qce)$_2$](ClO$_4$)$_4$·H$_2$O **20**	1.70
[Cu(qcp)(H$_2$O)$_2$](ClO$_4$)$_2$ **21**	1.92
[Cu(qcb)ClO$_4$(H$_2$O)]ClO$_4$ **22**	1.90
[Cu(qcc)(H$_2$O)$_2$](ClO$_4$)$_2$ **23**	1.87
Cu(qco)(ClO$_4$)$_2$]·3H$_2$O **24**	1.91

5.3.5 Infrared spectra

IR spectral data of the Schiff bases and their copper(II) complexes are given in Tables 5.7-5.10. The IR spectra of these complexes are shown in Figures 5.4-5.7. The details of IR spectra of ligands are given in chapter 2. On coordination of the Schiff base ligand, the C=N stretching frequency are slightly displaced to lower frequencies indicating a decrease in the C=N bond order due to the coordinate bond of the metal with the azomethine nitrogen lone pair [29]. The ν(C=N) band of the quinoxaline ring which appears in the region 1550-1580 cm^{-1} in the ligand undergoes a shift in the spectra of all the complexes indicating the involvement of ring nitrogen atom in coordination to the metal [30]. These results suggest that the Schiff base ligands act as tetradentate (N_4) ligands. The presence of broad band is seen in the spectra of all the complexes in the 3300-3500 cm^{-1} region, which is associated with the coordinated or solvent water molecules [29]. IR bands observed in the complexes at ~800 cm^{-1}, ~640 cm^{-1}, ~410 cm^{-1} could be assigned to γH_2O, ωH_2O and νH_2O stretching frequencies respectively of coordinated water molecules. In all complexes, weak bands at ~3000 cm^{-1} in both complexes could be assigned to aromatic C-H stretching of quinoxaline ring. The presence of multiple bands in the 2500-2935 cm^{-1} region in the ligand and its complexes with slight shifts suggests the presence of the CH_2 group of alkyl part in the ligand and its complexes. The bands due to Cu-O and Cu-N stretching occur at ~525 and ~406 cm^{-1} respectively, in the spectra of all the complexes. These bands are not present in the spectra of the free ligand.

5.3.5.1 *Nature of acetate*

In the copper(II) complexes **1-6**, derived from copper acetate, presence of acetate group is noticed. The IR data of these complexes is given in the Table 5.7. The ν_{asym}(COO$^-$) and ν_{sym}(COO$^-$) stretching frequencies of free acetate ions

are observed at 1560 and 1461 cm^{-1}, respectively. For the coordinate acetate ion, the ν_{asym}(COO$^-$) stretching occurs in the range 1650-1500 cm^{-1} and the ν_{sym}(COO$^-$) stretching is seen above 1400 cm^{-1} [29]. In the case of unidentate coordination of acetate group, ν(C=O) is higher than ν_{asym}(COO$^-$) and ν(C-O) is lower than ν_{asym}(COO$^-$) and the energy of separation between ν_{asym}(COO$^-$) and ν_{sym}(COO$^-$) is usually greater than 144 cm^{-1}. The opposite trend is observed in the case of bidentate coordination of acetate, the separation between the two ν(C-O) is smaller than that of free ion. In the case of bridging acetate group, the two ν(C-O) are close to the free ion values. The present copper(II) complexes show infrared absorption frequency bands [Figure 5.4] corresponding to ν_{asym}(COO$^-$) and ν_{sym}(COO$^-$) at 1600-1621 and 1430-1465 cm^{-1}, respectively. As the separation is greater than 144 cm^{-1}, both the acetate groups might be acting as monodentate ligand.

5.3.5.2 *Nature of chloride*

The copper(II) complexes **7-12**, contain chloride ion. The IR bands corresponding to Cu-Cl can be seen only below 400 cm^{-1}. As we could not record the spectra in the far IR region, this band could not be identified. However, the conductance studies indicate that in the complexes, **7**, **11** and **12**, the chloride ions are coordinated. In the case of complexes **9** and **10**, one of the chloride ions is coordinated and the other is not. The chloride ions are not coordinated in complex **8**. Their IR spectra are given in Figure 5.5 and data are given in Table 5.8.

5.3.5.3 *Nature of nitrate*

Free NO$_3^-$ ion belongs to a high symmetry point group D$_{3h}$. On coordination of a nitrate ion to a metal, either as a monodentate or as a bidentate, the local symmetry of the nitrate ion is lowered from D$_{3h}$ to C$_{2v}$. Only three

infrared bands are expected for ionic nitrate (ν_1, ν_2 and ν_4 in D_{3h} symmetry). For the coordinated nitrate, six infrared bands (ν_1 to ν_6) in C_{2v} symmetry are expected [29]. On coordination of NO_3^- ion to a metal as a monodentate, there is flow of electron density from the coordinated oxygen to the metal. As a result, the double bond character of N-O (bonded) will decrease with concomitant increase in the double bond character of the other two N-O bonds due to mesomeric electron release from the two oxygens. The separation between the two highest frequency bands ν_1 and ν_4 of the coordinated nitrate group is used to distinguish the different mode of bonding of nitrate ion to a metal often. It is usually greater (> 180 cm^{-1}) for bidentate nitrates relative to that for monodentate nitrate (< 130 cm^{-1}) groups. The uncoordinated nitrate group shows bands near ~ ν_1 (1050 cm^{-1}), ν_2 (830 cm^{-1}), ν_3 (1350 cm^{-1}) and ν_4 (715 cm^{-1}). Usually the nitrate complexes show sharp bands at ~1380 cm^{-1}, which corresponds to the $\nu(NO)_{asy}$ of free nitrate ion. The bands at ~1480 and 1380 cm^{-1} are the two split bands ν_4 and ν_1, respectively, of the coordinated nitrate ion. For the complexes, **13**, **15**, **16** and **18**, the magnitude of $\Delta\nu = (\nu_4 - \nu_1) \approx 100$ cm^{-1} shows the monodentate coordination of the nitrate ion. The bands observed in the region 1480-1350 cm^{-1} [Table 5.9], prove the presence of coordinated nitrate groups in that complexes. The band at 1385 cm^{-1} for the complexes, **14** and **17** indicates an uncoordinated nitrate group. For the complexes, **13**, **15** and **16**, both these type of bands are seen suggesting that nitrate group exist in the complexes as both coordinated and free form [Figure 5.6]. These results are in good agreement with the molar conductivity measurement studies, which show that the complexes, **13**, **15** and **16**, behave as 1:1 electrolytes. The conductance data of **14** and **17** suggest that two nitrate ions are not coordinated to the copper(II) ion. Monodentate coordination of the nitrate ions for **18** is in agreement with non electrolytic nature of the complexes.

5.3.5.4 *Nature of perchlorate*

Free ClO_4^- ion belongs to a high symmetry point group T_d. The tetrahedral symmetry of the free ion, ClO_4^- is reduced to C_{3v} on unidentate coordination of the ion to a metal. The symmetry is further lowered to C_{2v} if the anion binds to a metal as bidentate, either as a chelate or as a bridging ligand. The uncoordinated ClO_4^- ion shows two sharp bands at 1100 (v_3) and 620 (v_4) cm^{-1} [29]. Generally, the monodentate coordinated perchlorate ion show four bands at ~ 920 (v_1), 480 (v_2), 1158, 1030 (v_3), and 605, 620, 648 (v_4) cm^{-1}. The present complexes show IR bands characteristics of both the ionic and unidentately coordinated perchlorate groups [Figure 5.7]. The v_3 mode at 1095, 1093 and 1086 cm^{-1} for **20**, **21** and **23** respectively is somewhat broadened, but the v_4 band at 620 cm^{-1} is devoid of any splitting and are consistent with the IR active normal modes for T_d symmetry suggesting that these anions are not coordinated to the copper ions as substantiated by the results of molar conductivity measurements.

The spectra of complex **22** shows bands at around 1138, 1113, 1086, 936, 620 cm^{-1} , suggesting the coexistence of both ionic and unidentately coordinated perchlorate groups in these complexes. This result is in agreement with the conductance data and suggests that one of the perchlorate group is coordinated. Complexes **19** and **24** show bands around 1106, 1079, 937, 633 cm^{-1}, suggesting the monodentate coordination of perchlorate ions to copper ion.
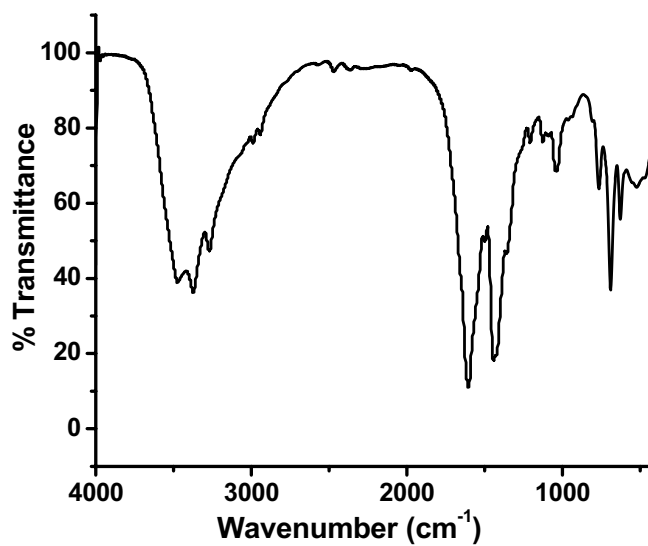
Table 5.7: FTIR spectral data for the copper(II) acetate complexes.
(ν in cm^{-1})

Complex	ν(C=N)a	ν(C=N)q	ν(OH)	ν(Cu-N)	ν(Cu-O)	ν(COO$^-$)$_a$ & ν(COO$^-$)$_s$
qch [Cu(qch)$_2$(OAc)$_2$]·2H$_2$O **1**	1622 1605	1568 1564	3429	418	525	1605 1452
qce [Cu$_2$(qce)$_2$(OAc)$_4$]·H$_2$O **2**	1639 1604	1555 1551	3463	464	521	1604 1436
qcp [Cu (qcp)(OAc)$_2$]·2H$_2$O **3**	1636 1606	1573 1570	3469	413	530	1606 1445
qcb [Cu(qcb)(OAc)$_2$]·3H$_2$O **4**	1640 1621	1555 1550	3408	417	521	1621 1459
qcc [Cu(qcc)(OAc)$_2$]·3H$_2$O **5**	1640 1631	1556 1553	3381	410	509	1601 1465
qco [Cu(qco)(OAc)$_2$]·H$_2$O **6**	1610 1607	1568 1562	3448	417	518	1607 1445

a C=N of azomethine group; q C=N of quinoxaline ring; ν(OH) of coordinated/lattice water molecule, ν(COO$^-$)$_a$ asymmetric stretching of acetate group & ν(COO$^-$)$_s$ symmetric stretching of acetate group.
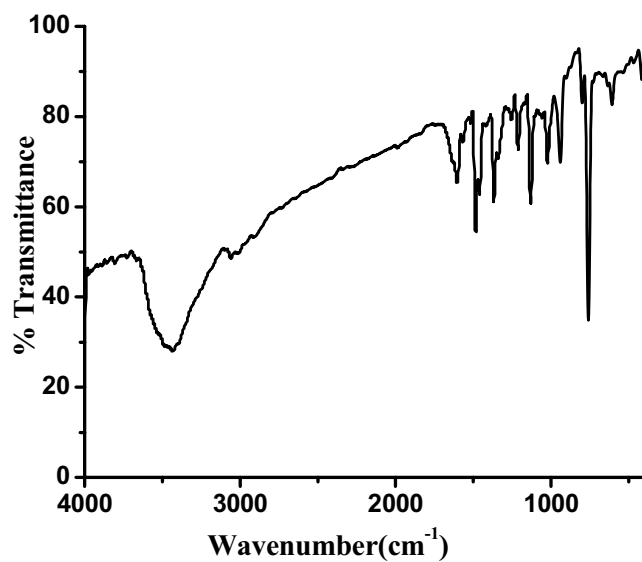
IR spectrum of [Cu(qch)₂(OAc)₂]·2H₂O

IR spectrum of [Cu₂(qce)₂(OAc)₄]·H₂O
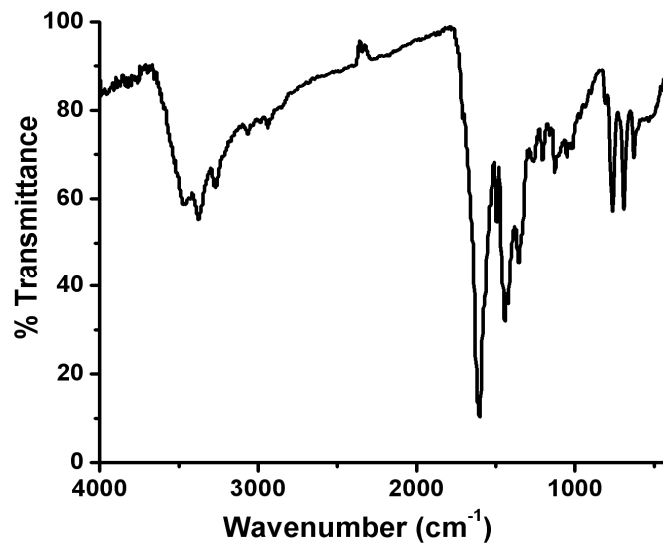
IR spectrum of [Cu(qcp)(OAc)$_2$]·2H$_2$O
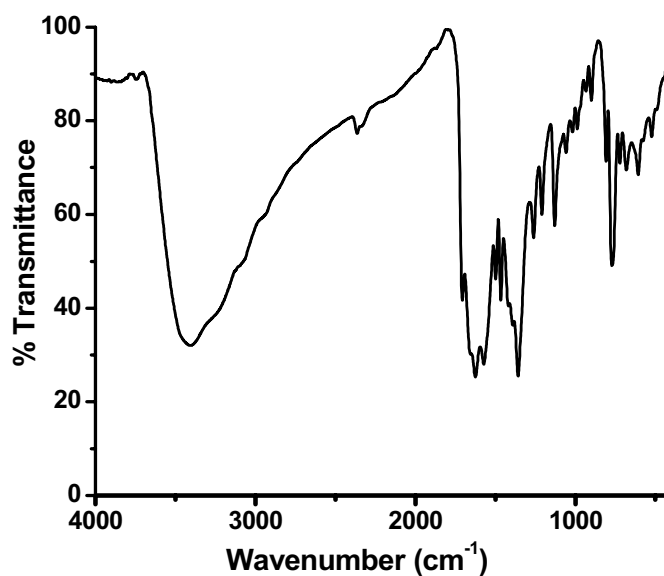
IR spectrum of [Cu(qcb)(OAc)$_2$]·3H$_2$O
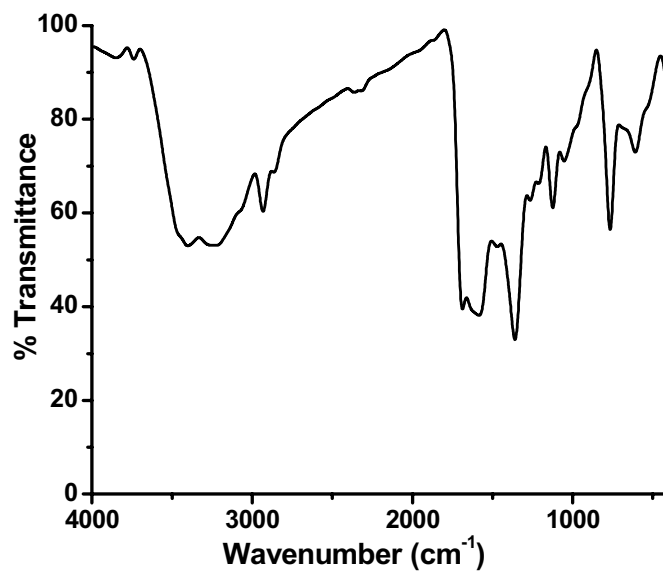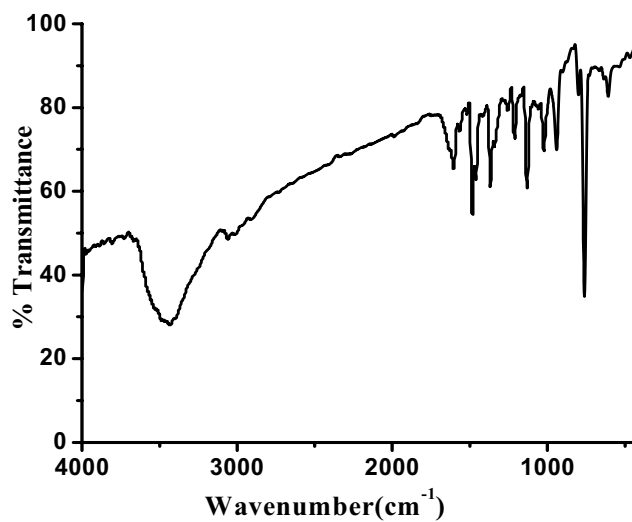
IR spectrum of [Cu(qcc)(OAc)₂]·3H₂O
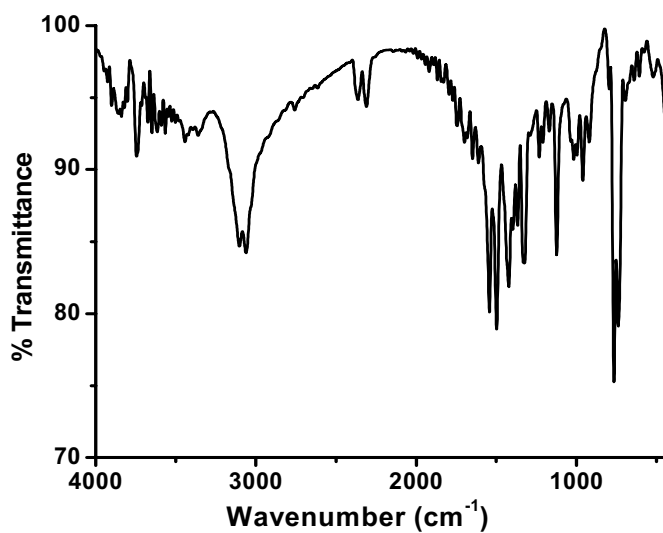
IR spectrum of [Cu(qco)(OAc)₂]·H₂O

Figure 5.4: IR spectra of Cu(II) acetate complexes

Table 5.8: FTIR spectral data for the copper(II) chloride complexes. (ν in cm^{-1})

Complex	ν(C=N)a	ν(C=N)q	ν(OH)	ν(Cu-N)	ν(Cu-O)
qch [Cu(qch)Cl₂]·2H₂O **7**	1622 1603	1568 1564	 3435	 413	 -
qce [Cu₂(qce)₂]Cl₄·H₂O **8**	1639 1632	1555 1552	 3429	 423	 -
qcp [Cu(qcp)ClH₂O]Cl·2H₂O **9**	1636 1629	1573 1569	 3463	 420	 530
qcb [Cu(qcb)Cl(H₂O)]Cl **10**	1640 1634	1555 1550	 3435	 493	 527
qcc [Cu(qcc)Cl₂] **11**	1640 1632	1556 1552	 -	 424	 -
qco [Cu(qco)Cl₂]·H₂O **12**	1610 1606	1568 1561	 3422	 416	 -

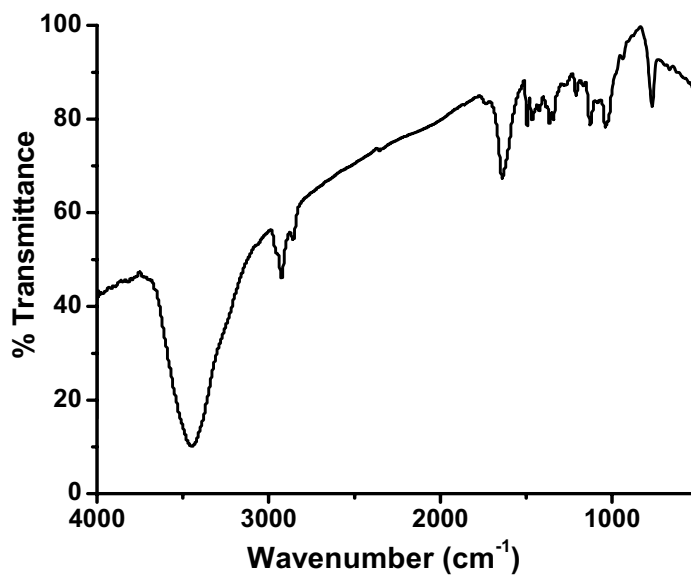a C=N of azomethine group; q C=N of quinoxaline ring; ν(OH) of coordinated/lattice water molecule
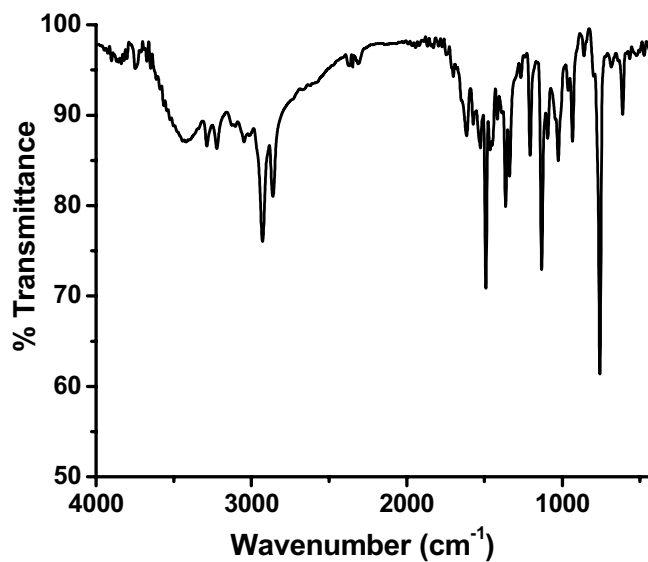

IR spectrum of [Cu(qch)Cl₂]·2H₂O
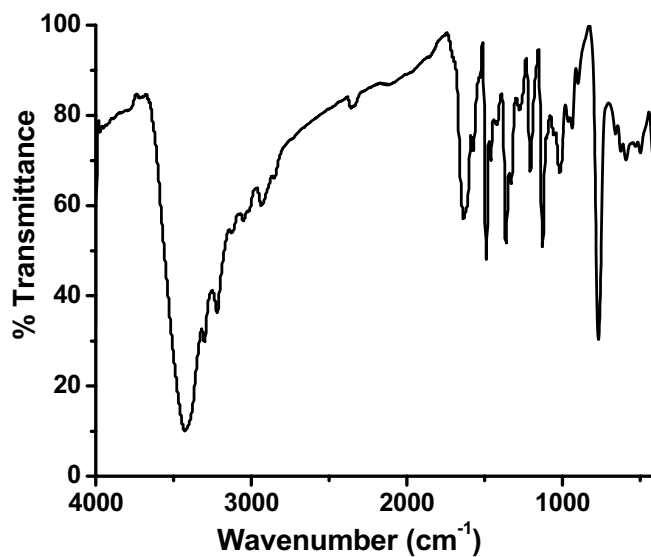
IR spectrum of [Cu$_2$(qce)$_2$]Cl$_4$·H$_2$O
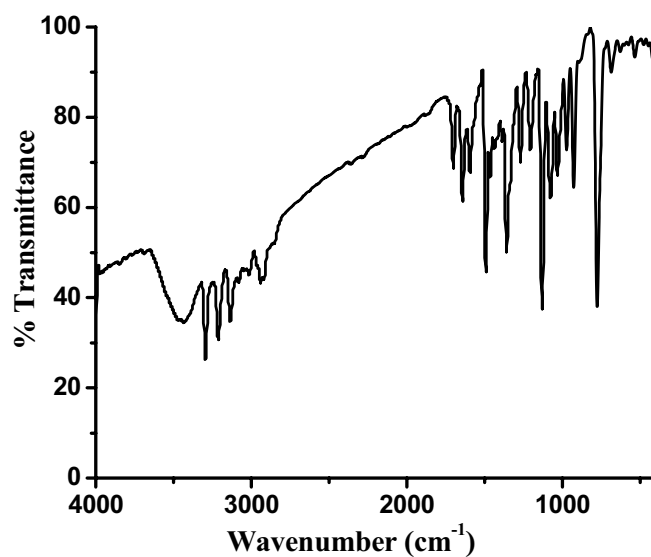
IR spectrum of [Cu(qcp)ClH$_2$O]Cl·2H$_2$O

IR spectrum of [Cu(qcb)Cl(H₂O)]Cl

IR spectrum of [Cu(qcc)Cl₂]

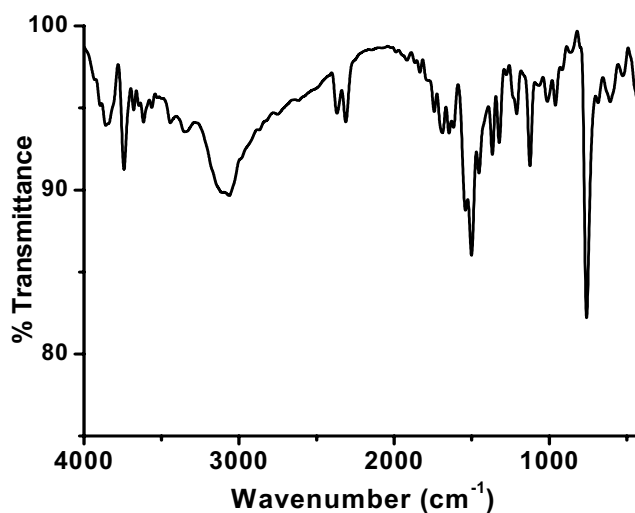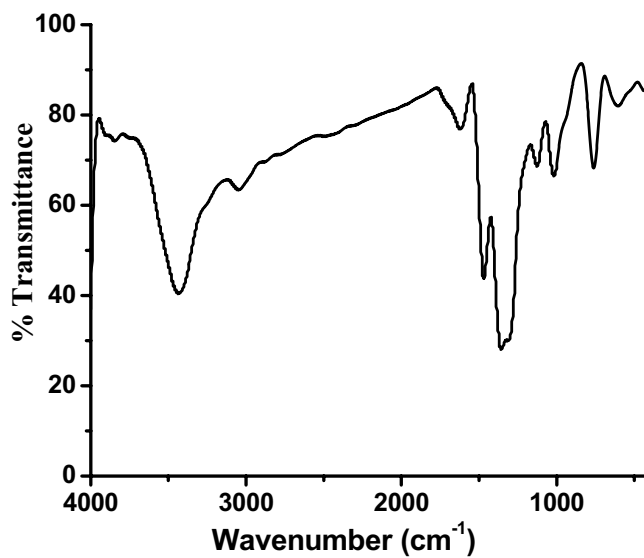*IR spectrum of [Cu(qco)Cl₂]·H₂O*
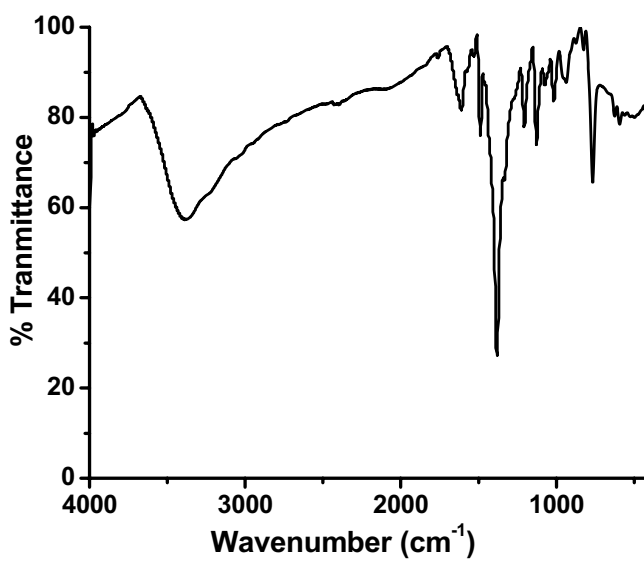
Figure 5.5: IR spectra of copper(II) chloride complexes

Table 5.9: FTIR spectral data for the copper(II) nitrate complexes. (ν in cm^{-1})

| Complex	ν(C=N)a	ν(C=N)q	ν(OH)	ν(Cu-N)	ν(Cu-O)	ν_1(NO$_3^-$) & ν_4(NO$_3^-$)
qch [Cu(qch)NO₃(H₂O)]NO₃ 13	1622 1615	1568 1564	3442	431	571	1470 1357
qce [Cu₂(qce)₂](NO₃)₂(OH)₂·9H₂O 14	1639 1618	1555 1550	3395	418	-	1385
qcp [Cu(qcp)NO₃(H₂O)]NO₃ 15	1636 1628	1573 1571	3361	417	524	1473 1364
qcb [Cu(qcb)NO₃H₂O]NO₃ 16	1640 1634	1555 1550	3385	423	505	1473 1375
qcc [Cu(qcc)(H₂O)₂](NO₃)₂ 17	1640 1625	1556 1552	3475	444	524	1385
qco [Cu(qco)(NO₃)₂]·2H₂O 18	1610 1638	1568 1562	3408	404	524	1477 1369

a C=N of azomethine group; q C=N of quinoxaline ring; ν(OH) of coordinated/lattice water molecule
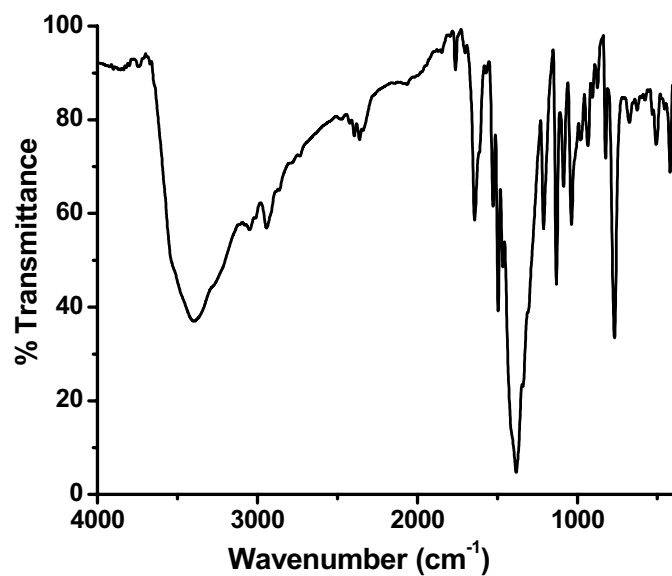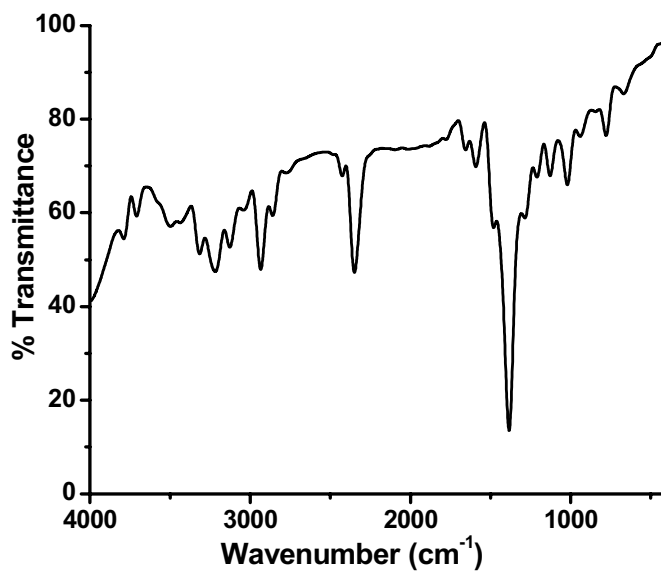
IR spectrum of [Cu(qch)NO₃(H₂O)]NO₃
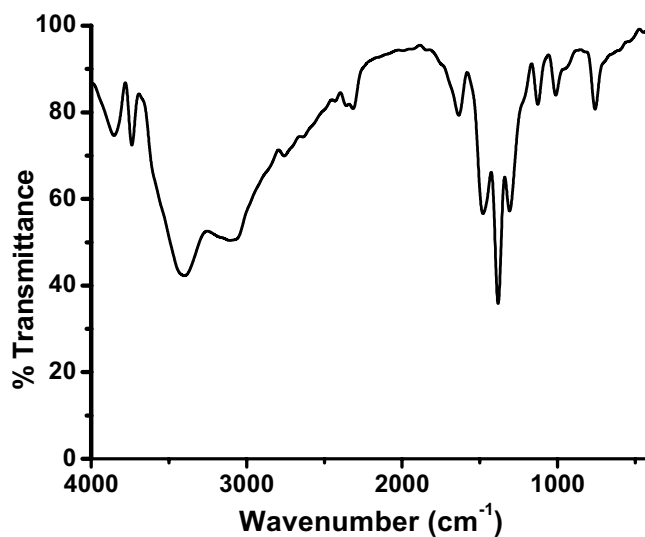

IR spectrum of [Cu₂(qce)₂](NO₃)₂(OH)₂·9H₂O
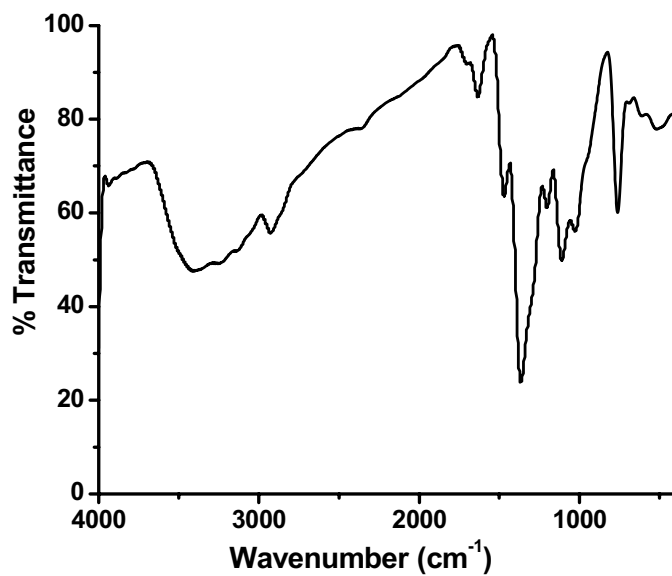
IR spectrum of [Cu(qcp)NO₃(H₂O)]NO₃

IR spectrum of [Cu(qcb)NO₃H₂O]NO₃

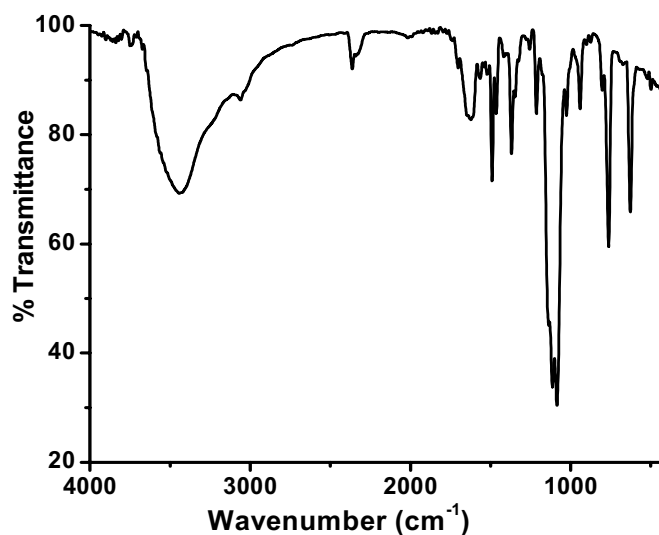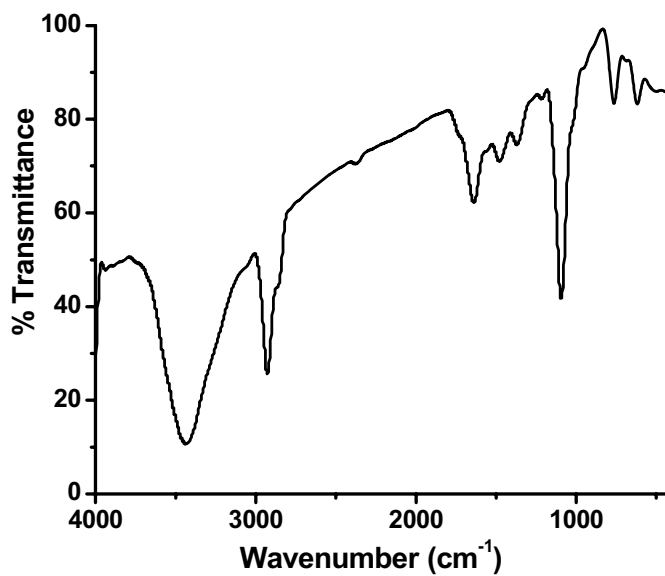*IR spectrum of [Cu(qcc)(H₂O)₂](NO₃)₂*

IR spectrum of [Cu(qco)(NO₃)₂]·2H₂O

Figure 5.6: IR spectra of copper(II) nitrate complexes

Table 5.10: FTIR spectral data for the copper(II) perchlorate complexes. (v in cm^{-1})

Complex	v(C=N)a	v(C=N)q	v(OH)	v(Cu-N)	v(Cu-O)	v(ClO$_4$)
qch [Cu(qch)(ClO$_4$)$_2$]·2H$_2$O 19	1622 1616	1568 1564	3435	423	503	1144,1114, 1087, 936, 626
qce [Cu$_2$(qce)$_2$](ClO$_4$)$_4$·H$_2$O 20	1639 1634	1555 1552	3435	436	-	1095, 620
qcp [Cu(qcp)(H$_2$O)$_2$](ClO$_4$)$_2$ 21	1636 1630	1573 1570	3427	444	518	1093, 620
qcb [Cu(qcb)ClO$_4$(H$_2$O)]ClO$_4$ 22	1640 1634	1555 1550	3470	423	545	1138, 1113 1086, 936, 620
qcc [Cu(qcc)(H$_2$O)$_2$](ClO$_4$)$_2$ 23	1640 1630	1556 1553	3339	417	532	1086 620
qco [Cu(qco)(ClO$_4$)$_2$]·3H$_2$O 24	1610 1601	1568 1564	3448	416	520	1138, 1114,1084, 939,620

a C=N of azomethine group; q C=N of quinoxaline ring; v(OH) of coordinated/lattice water molecule

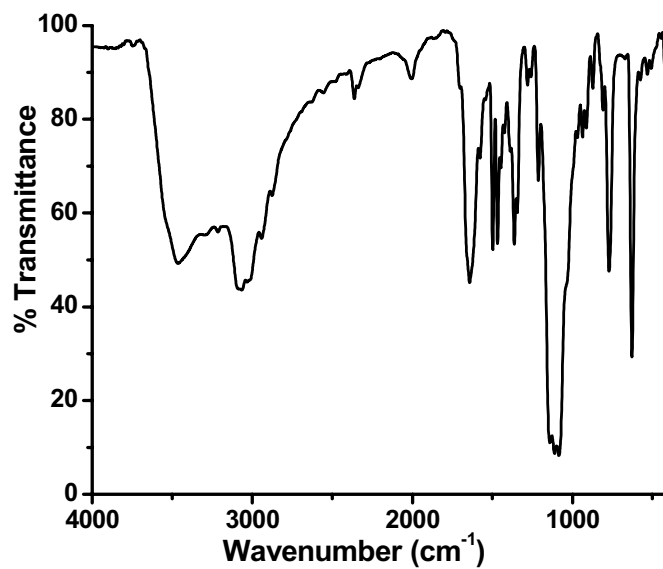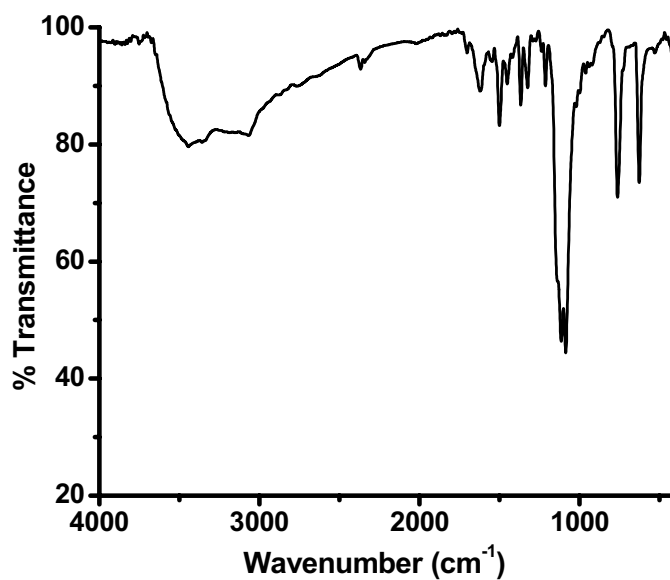
***IR spectrum* of [Cu(qch)(ClO$_4$)$_2$]·2H$_2$O**

IR spectrum of $[Cu_2(qce)_2](ClO_4)_4 \cdot H_2O$
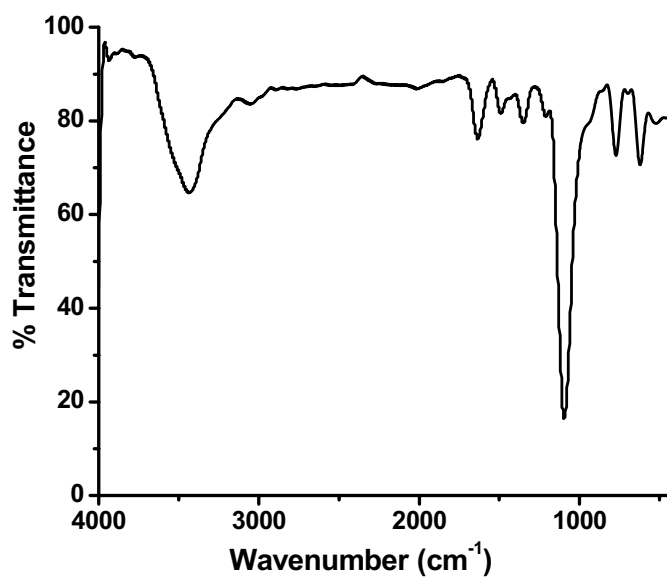
IR spectrum of *$[Cu(qcp)(H_2O)_2](ClO_4)_2$*

IR spectrum of [Cu(qcb)ClO₄(H₂O)]ClO₄

IR spectrum of *[Cu(qcc)(H₂O)₂](ClO₄)₂*
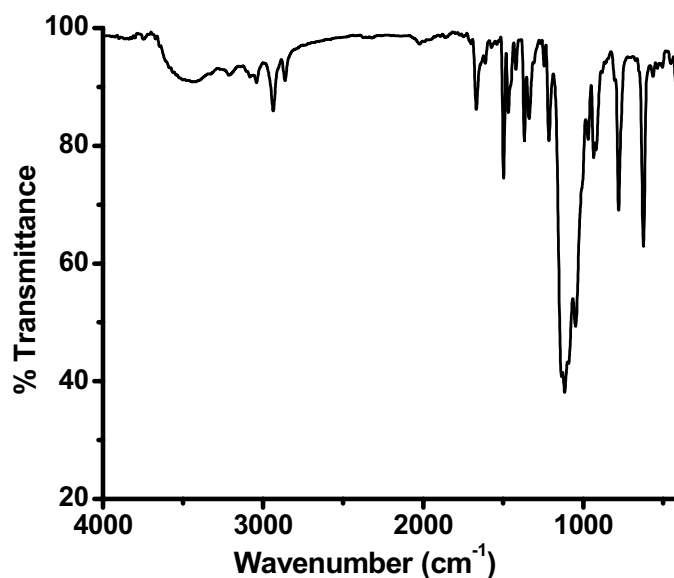
IR spectrum of [Cu(qco)(ClO₄)₂]·3H₂O

Figure 5.7: IR spectra of copper(II) perchlorate complexes

5.3.6 Electronic spectra

Electronic spectra of these complexes, **1-24**, were recorded in methanol in the range 50,000-10,000 cm^{-1} [Table 5.11-5.14]. Additional details concerning electronic structure and reactivity for the complex may be seen from the electronic absorption spectra in Figure 5.9-5.12. The spectra of the ligands (discussed in chapter 2) show the bands at higher energies around ~ 41,000 cm^{-1} are associated with the quinoxaline and azomethine $\pi \rightarrow \pi^*$ transitions. The electronic spectra of the complexes were observed as three main transitions. The absorption maxima of the metal chelate bear close resemblance with those of the free ligands, which indicates that no structural alteration of the ligand occurred during complexation. The spectra of the complexes also show moderate intense

bands at 30,000-35,000 cm^{-1}, attributable to nitrogen centered ligand to metal charge transfer (LMCT) transitions from the coordinated unsaturated ligand to the metal ion [31]. The bands at higher energies around ~30,000 cm^{-1} are associated with the azomethine/quinoxaline n→π* transitions. On complexation these bands are shifted to lower wavelength, suggesting coordination of azomethine/ quinoxaline nitrogen with copper [32]. This suggests that ligand is coordinated to copper ion.

According to Lever [33], since the ground state in an octahedral field is the Jahn-Teller unstable ^2E_g, regular octahedral copper(II) complexes can not exist. The t_{2g}---e_g separation in a regular octahedral copper(II) complex varies from about 13,000 cm^{-1} (for CuO$_6$) to about 18,000 cm^{-1} (for CuN$_6$). In the case distorted complexes, several absorption bands may be expected in these regions, corresponding to transitions from components of t_{2g} to $d_{x^2-y^2}$. In general there will be a marked tetragonal splitting of the e_g level such that d_{z^2} lies below $d_{x^2-y^2}$ (6000-15,000 cm^{-1}) and will give rise to absorption at those energies. In general the greater the tetragonality, e_g, the longer the axial bond, the greater will be the energy of the d_{z^2} --- $d_{x^2-y^2}$ transition. The usually broad visible band envelope will contain d_{xy}--- $d_{x^2-y^2}$, and d_{xz}, d_{yz} --- $d_{x^2-y^2}$ (the latter perhaps split into two transitions). Indeed as the axial bond lengthens, the d_{xy}--- $d_{x^2-y^2}$, and d_{xz}, d_{yz} --- $d_{x^2-y^2}$ transitions shift to the blue because of a synergic effect. The order of energy levels of octahedral complexes is $d_{x^2-y^2}$> d_{z^2} > d_{xy} > $d_{yz, =}$ $d_{xz,}$ [Figure 5.8].
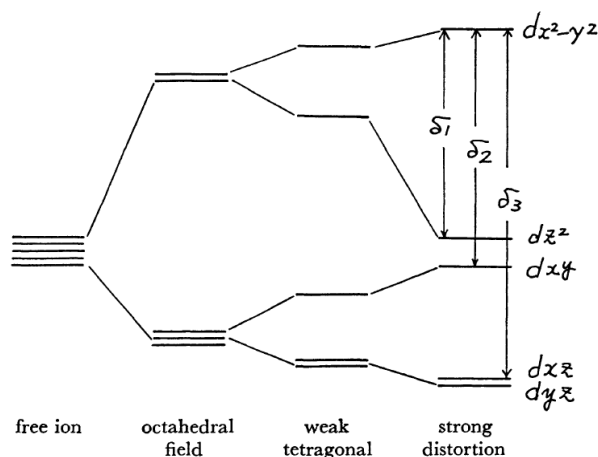
Figure 5.8: Splitting of d-orbitals

The electronic spectrum of the copper(II) complexes (**1-7, 9-13, 15-19, 21-24**) in methanol (10^{-3} M) showed d-d bands in the regions 20,000-13,000 cm^{-1} which can be assigned to $^2T_{2g} \rightarrow {}^2E_g$ transition of an octahedral geometry. Though in cases where the ^2E_g and $^2T_{2g}$ states of the octahedral Cu(II) ion (d^9) split under the influence of the tetragonal distortion the three transitions $^2B_{1g} \rightarrow {}^2E_g$, $^2B_{1g} \rightarrow {}^2B_{2g}$, and $^2B_{1g} \rightarrow {}^2A_{1g}$ are expected [33], their very close energies could have made them appear in the form of one broad band envelope. Our results [Tables 5.11-5.14] are in good agreement with those reported for a distorted octahedral geometry around Cu(II) ion [33]. The spectra of copper(II) complexes exhibit broad d-d absorption bands in the region 13,000-20,000 cm^{-1} [Figure 5.9-5.12] indicative of a distorted octahedral system with weak apical coordination of solvent/anion molecules. The magnetic and electronic data point to distorted octahedral environments for Cu(II) ions in complexes (**1-7, 9-13, 15-19, 21-24**).

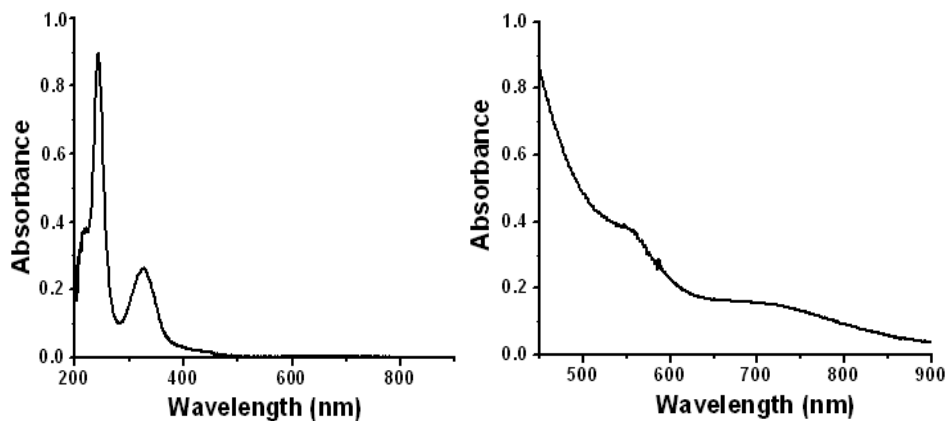**Table 5.11: Electronic spectral assignments for the copper(II) complexes**

| Complex | Absorption Maxima (cm^{-1}) | | log ε | Band |
	nm	cm^{-1}	L mol^{-1} cm^{-1}	Assignment
[Cu(qch)$_2$(OAc)$_2$]·2H$_2$O **1**	208	48070	2.98	π→π*
	244	40980	2.73	π→π*
	324	30860	2.22	π→π*
	547	18280	0.30	^{2}T$_{2g}$→ ^{2}E$_g$
[Cu$_2$(qce)$_2$(OAc)$_4$]·H$_2$O **2**	214	46730	2.59	π→π*
	244	40980	2.95	π→π*
	326	30670	2.46	π→π*
	462	18870	1.68	^{2}T$_{2g}$→ ^{2}E$_g$
	553	18080	1.32	^{2}T$_{2g}$→ ^{2}E$_g$
	726	13770	0.94	^{2}T$_{2g}$→ ^{2}E$_g$
[Cu (qcp)(OAc)$_2$]·2H$_2$O **3**	215	46510	2.11	π→π*
	242	41320	2.13	π→π*
	323	30960	1.55	n→π*
	482	20750	0.89	^{2}T$_{2g}$→ ^{2}E$_g$
[Cu(qcb)(OAc)$_2$]·3H$_2$O **4**	242	41320	2.98	π→π*
	324	30860	2.62	π→π*
	408	24510	2.00	π→π*
	544	18380	1.36	^{2}T$_{2g}$→ ^{2}E$_g$
	711	14060	0.95	^{2}T$_{2g}$→ ^{2}E$_g$
[Cu(qcc)(OAc)$_2$]·3H$_2$O **5**	217	46080	2.71	π→π*
	242	41320	2.91	π→π*
	324	30860	2.34	π→π*
	550	18180	0.84	^{2}T$_{2g}$→ ^{2}E$_g$
[Cu(qco)(OAc)$_2$]·H$_2$O **6**	210	47620	3.06	π→π*
	245	40820	2.96	π→π*
	304	32890	2.59	π→π*
	360	27780	2.72	π→π*
	417	23980	0.78	^{2}T$_{2g}$→ ^{2}E$_g$

A regular tetrahedral copper(II) complex (in the absence of spin orbit splitting) should yield a single transition (^2E---$^2T_2$) at relatively low energy [33]. However tetrahedral copper(II) complexes are almost invariably distorted. Since a four coordinate square planar coordination complex is strongly favoured for the d^9 configuration, the usual distortion is a flattening of the tetrahedron along a two-fold axis. This will result in a structure of D_{2d} symmetry which would retain the degeneracy of d_{xz}, d_{yz} and lead to three possible transitions, namely from the ground state $^2B_2$ to ^2E, $^2B_1$ and $^2A_1$. Commonly four transitions are observed due to further distortion to D_2 or C_s, and/or due to the splitting of the *e* level in D_{2d} by spin orbit coupling. There are reports for tetrahedral complexes, which show four transitions below 10,000 cm^{-1}. The electronic spectra of the complexes (**8**, **14** and **20**) consist of d-d bands in the (~) 18,000-11,000 cm^{-1} range, with a log ε 1.30-0.90 L mol^{-1} cm^{-1}, and a broad absorption. This is indicating the tetrahedral geometry around copper. From the magnetic susceptibility measurements, it was found that these complexes have magnetic moments in the range 1.6-1.7 B.M. These values are lower than those for the tetrahedral complexes, which might be due to the presence of two copper(II) ions in the complexes.
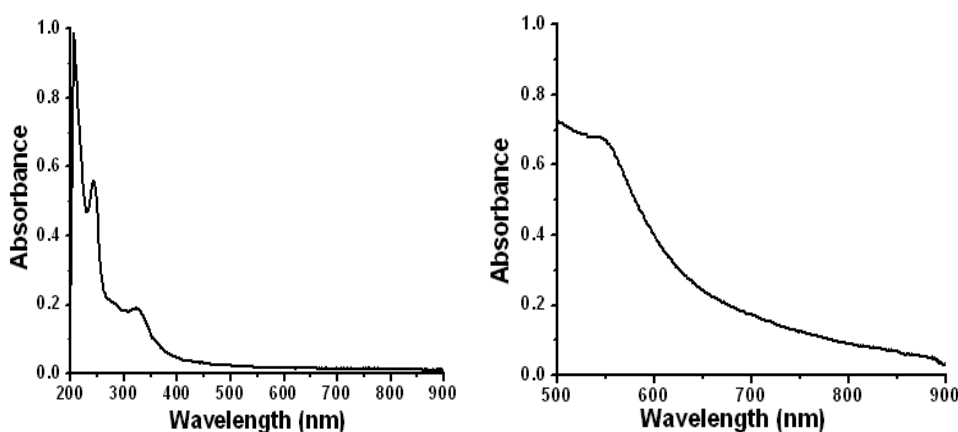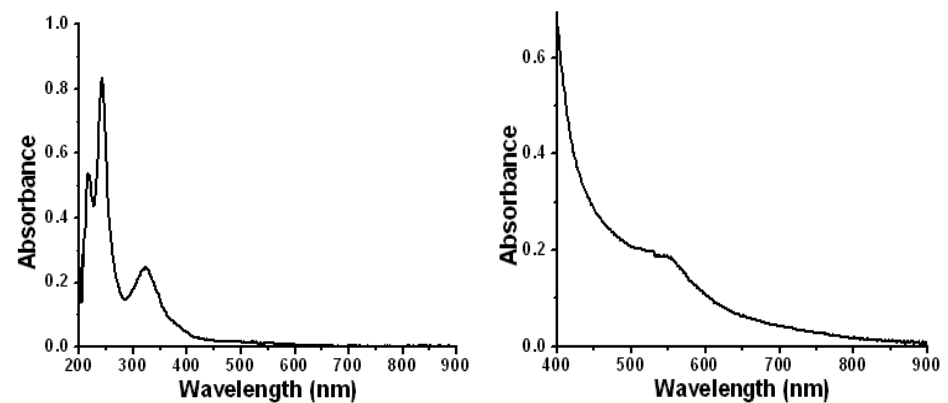

UV-Vis spectrum of [Cu(qch)$_2$(OAc)$_2$]·2H$_2$O
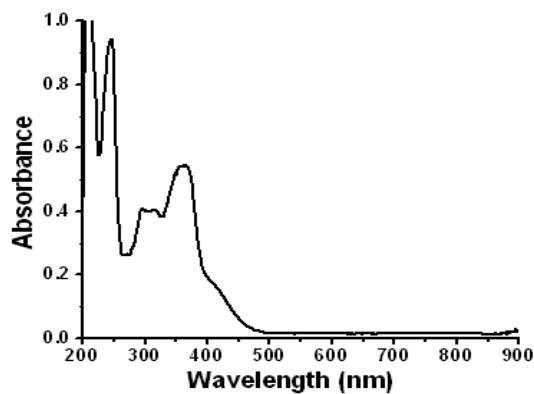
UV-Vis spectrum of [Cu₂(qce)₂(OAc)₄]·H₂O
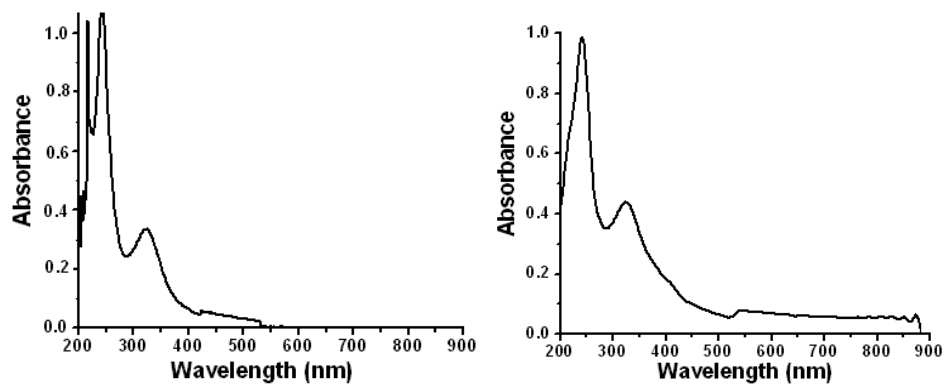
UV-Vis spectrum of [Cu(qcp)(OAc)₂]·2H₂O   *UV-Vis spectrum of [Cu(qcb)(OAc)₂]·3H₂O*
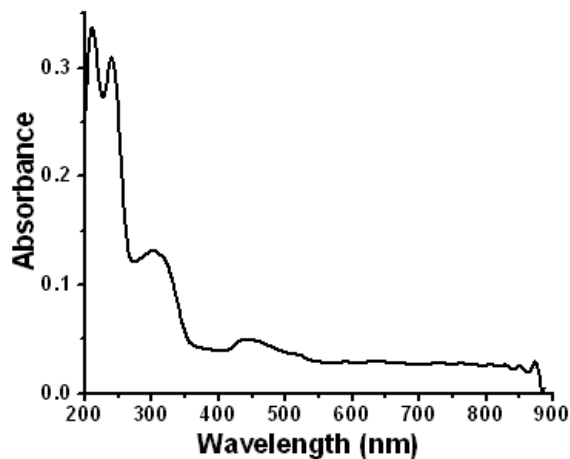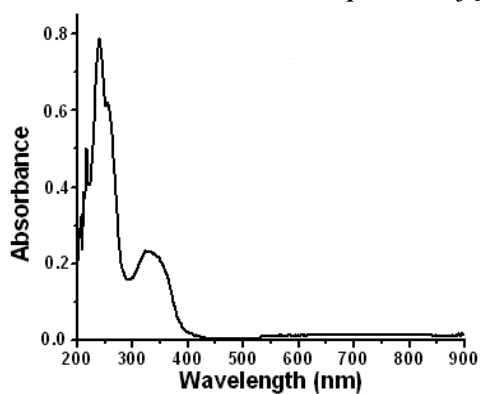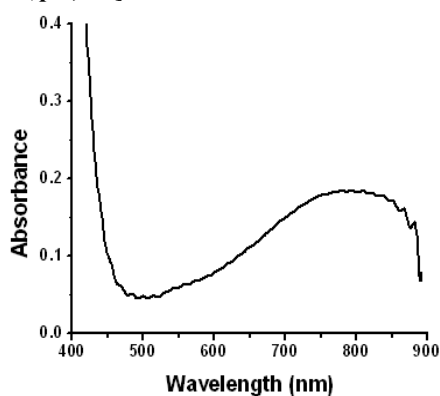
UV-Vis spectrum of [Cu(qcc)(OAc)₂]·3H₂O

UV-Vis spectrum of [Cu(qco)(OAc)₂]·H₂O

Figure 5.9: Electronic spectra of the copper(II) acetate complexes

Table 5.12: Electronic spectral assignments for the copper(II) chloride complexes

Complex	Absorption Maxima (cm^{-1})		log ε L mol^{-1} cm^{-1}	Band Assignment
	nm	cm^{-1}		
[Cu(qch)Cl₂]·2H₂O **7**	212	47170	2.52	$\pi \rightarrow \pi^*$
	244	41670	2.48	$\pi \rightarrow \pi^*$
	310	32260	2.05	$\pi \rightarrow \pi^*$
	442	22620	1.30	$^2T_{2g} \rightarrow {}^2E_g$
	519	19270	0.99	$^2T_{2g} \rightarrow {}^2E_g$
	716	13970	0.90	$^2T_{2g} \rightarrow {}^2E_g$
[Cu₂(qce)₂]Cl₄·H₂O **8**	216	46300	2.71	$\pi \rightarrow \pi^*$
	240	41670	2.85	$\pi \rightarrow \pi^*$
	254	39370	2.80	$\pi \rightarrow \pi^*$
	333	30030	2.52	$n \rightarrow \pi^*$
	810	12340	1.12	$^2B_2 \rightarrow {}^2E$
[Cu(qcp)ClH₂O]Cl·2H₂O **9**	236	42370	2.87	$\pi \rightarrow \pi^*$
	257	38910	2.97	$\pi \rightarrow \pi^*$
	346	28900	2.53	$n \rightarrow \pi^*$
	514	19460	0.99	$^2T_{2g} \rightarrow {}^2E_g$
	762	13120	1.20	$^2T_{2g} \rightarrow {}^2E_g$
[Cu(qcb)Cl(H₂O)]Cl **10**	219	45660	2.45	$\pi \rightarrow \pi^*$
	256	39060	2.73	$\pi \rightarrow \pi^*$
	343	29150	2.32	$\pi \rightarrow \pi^*$
	487	20530	0.94	$^2T_{2g} \rightarrow {}^2E_g$
	752	13300	1.06	$^2T_{2g} \rightarrow {}^2E_g$

Complex	Absorption Maxima (cm^{-1})		log ε L mol^{-1} cm^{-1}	Band Assignment
	nm	cm^{-1}		
[Cu(qcc)Cl$_2$] **11**	236	42370	2.72	$\pi \rightarrow \pi^*$
	320	31250	1.99	$\pi \rightarrow \pi^*$
	527	18970	1.22	$^2T_{2g} \rightarrow {}^2E_g$
	665	15030	0.94	$^2T_{2g} \rightarrow {}^2E_g$
[Cu(qco)Cl$_2$]·H$_2$O **12**	210	47620	2.45	$\pi \rightarrow \pi^*$
	248	47620	2.47	$\pi \rightarrow \pi^*$
	300	33330	2.02	$\pi \rightarrow \pi^*$
	360	27780	2.38	$\pi \rightarrow \pi^*$
	461	21690	0.90	$^2T_{2g} \rightarrow {}^2E_g$
	803	12450	0.78	$^2T_{2g} \rightarrow {}^2E_g$

UV-Vis spectrum of [Cu(qch)Cl$_2$]·2H$_2$O

UV-Vis spectrum of [Cu$_2$(qce)$_2$]Cl$_4$·H$_2$O

UV-Vis spectrum of *[Cu(qcp)ClH₂O]Cl·2H₂O*

UV-Vis spectrum of *[Cu(qcb)Cl(H₂O)]Cl*
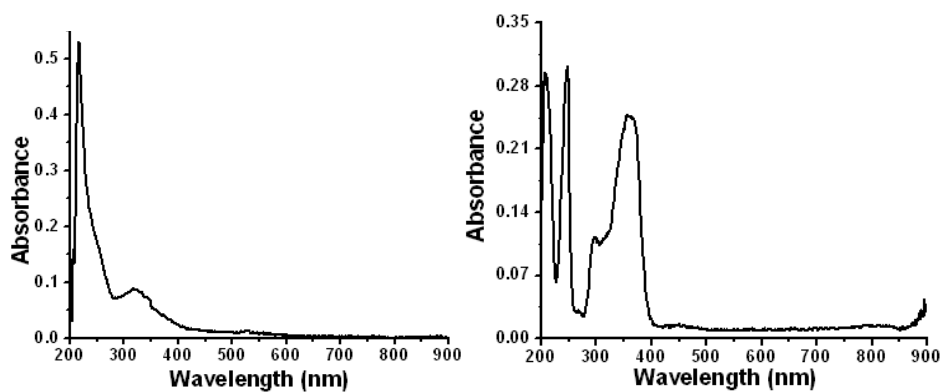
UV-Vis spectrum of [Cu(qcc)Cl₂]   *UV-Vis spectrum of [Cu(qco)Cl₂]·H₂O*
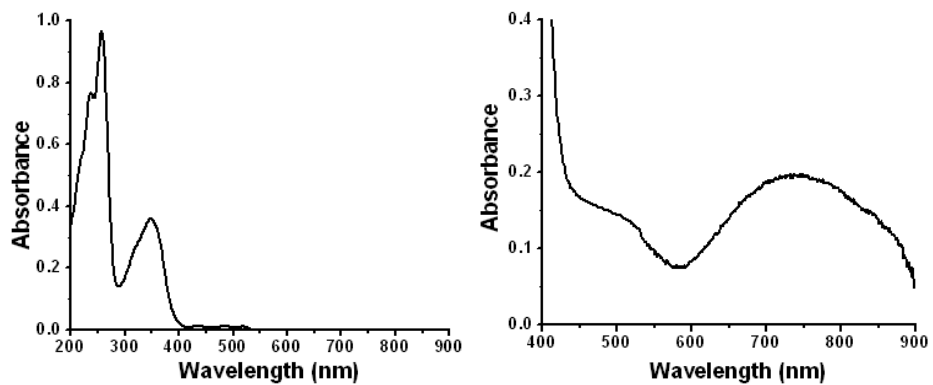
Figure 5.10: Electronic spectra of the copper(II) chloride complexes

Table 5.13: Electronic spectral assignments for the copper(II) nitrate complexes
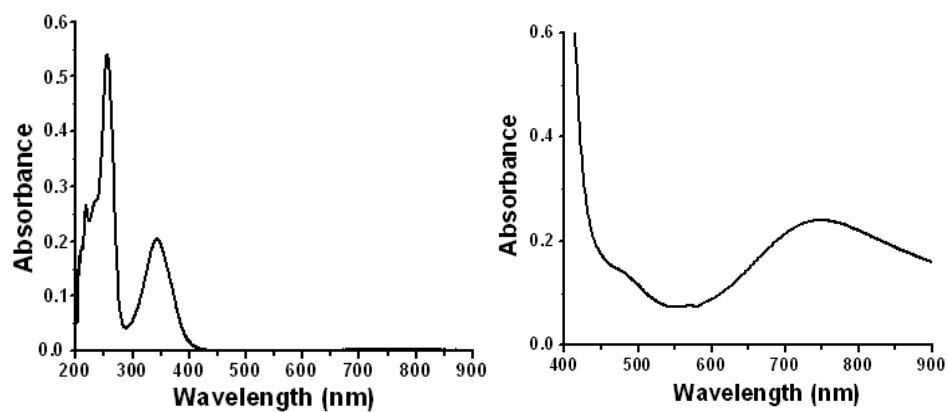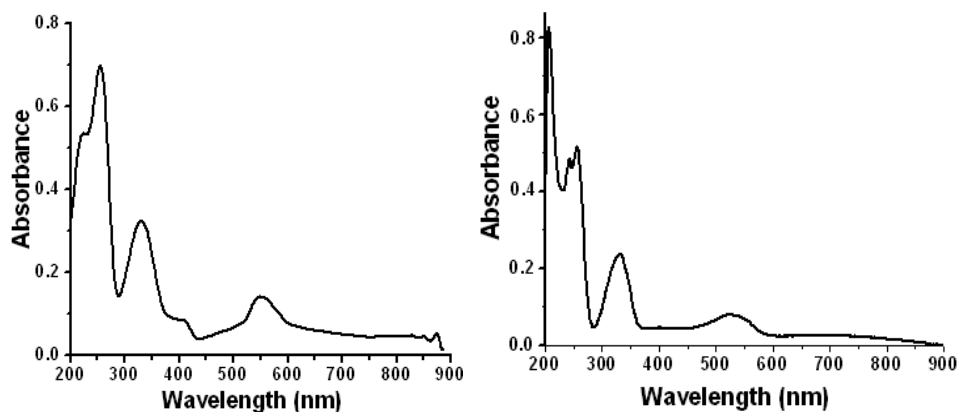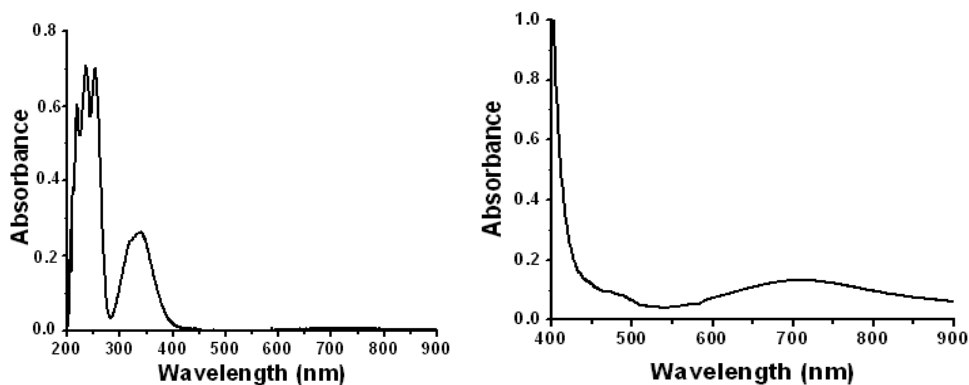
Complex	Absorption Maxima (cm^{-1})		log ε L mol^{-1} cm^{-1}	Band Assignment
	nm	cm^{-1}		
[Cu(qch)NO$_3$(H$_2$O)]NO$_3$ **13**	205	48780	2.88	$\pi \rightarrow \pi^*$
	244	41320	2.72	$\pi \rightarrow \pi^*$
	273	36630	2.57	$\pi \rightarrow \pi^*$
	328	30490	2.26	$\pi \rightarrow \pi^*$
	453	22070	1.09	$^2T_{2g} \rightarrow {}^2E_g$
	595	16810	0.99	$^2T_{2g} \rightarrow {}^2E_g$
[Cu$_2$(qce)$_2$](NO$_3$)$_2$(OH)$_2$·9H$_2$O **14**	223	44840	2.71	$\pi \rightarrow \pi^*$
	254	39370	2.83	$\pi \rightarrow \pi^*$
	330	30300	2.49	$\pi \rightarrow \pi^*$
	408	24510	1.05	$n \rightarrow \pi^*$
	550	18180	1.32	$^2B_2 \rightarrow {}^2E$
	870	11490	1.04	$^2B_2 \rightarrow {}^2E$
[Cu(qcp)NO$_3$(H$_2$O)]NO$_3$ **15**	205	42370	2.90	$\pi \rightarrow \pi^*$
	258	38910	2.68	$\pi \rightarrow \pi^*$
	330	30300	2.72	$\pi \rightarrow \pi^*$
	536	18660	1.05	$^2T_{2g} \rightarrow {}^2E_g$
	729	13720	0.73	$^2T_{2g} \rightarrow {}^2E_g$
[Cu(qcb)NO$_3$H$_2$O]NO$_3$ **16**	218	45870	2.98	$\pi \rightarrow \pi^*$
	235	42550	2.62	$\pi \rightarrow \pi^*$
	254	39370	2.00	$\pi \rightarrow \pi^*$
	338	29590	1.36	$n \rightarrow \pi^*$
	486	20580	0.95	$^2T_{2g} \rightarrow {}^2E_g$
	714	14000	0.99	$^2T_{2g} \rightarrow {}^2E_g$
[Cu(qcc)(H$_2$O)$_2$](NO$_3$)$_2$ **17**	220	45450	2.97	$\pi \rightarrow \pi^*$
	256	39060	2.99	$\pi \rightarrow \pi^*$
	346	28900	2.52	$\pi \rightarrow \pi^*$
	478	20920	0.84	$^2T_{2g} \rightarrow {}^2E_g$
	550	18180	1.04	$^2T_{2g} \rightarrow {}^2E_g$
	688	14530	0.98	$^2T_{2g} \rightarrow {}^2E_g$
[Cu(qco)(NO$_3$)$_2$]·2H$_2$O **18**	218	45870	2.65	$\pi \rightarrow \pi^*$
	261	38310	2.78	$\pi \rightarrow \pi^*$
	350	28570	2.36	$\pi \rightarrow \pi^*$
	490	20410	0.78	$^2T_{2g} \rightarrow {}^2E_g$
	700	14280	1.12	$^2T_{2g} \rightarrow {}^2E_g$
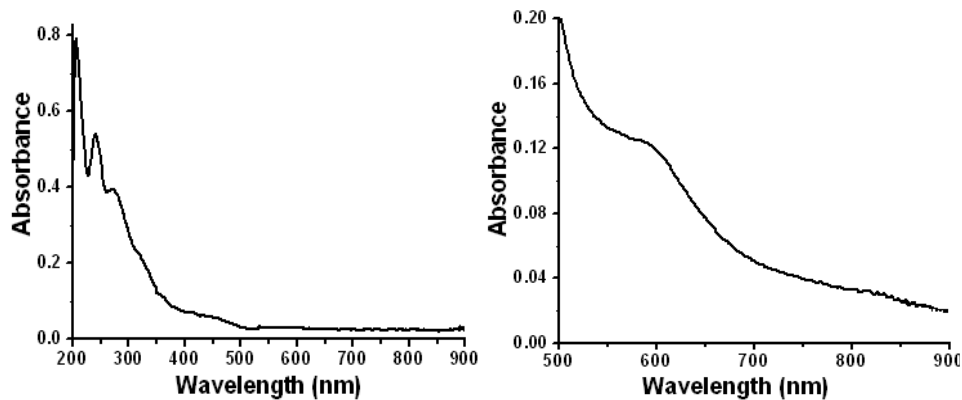
UV-Vis spectrum of [Cu(qch)NO₃(H₂O)]NO₃

UV-Vis spectrum of [Cu₂(qce)₂](NO₃)₂(OH)₂·9H₂O   **UV-Vis spectrum of [Cu(qcp)NO₃(H₂O)]NO₃**

UV-Vis spectrum of [Cu(qcb)NO₃H₂O]NO₃
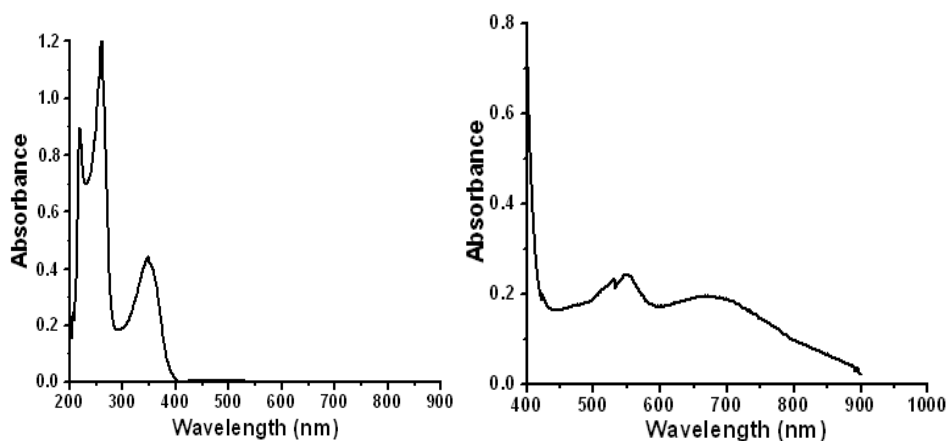
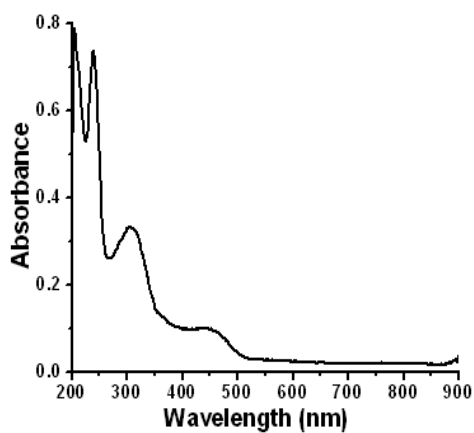*UV-Vis spectrum of [Cu(qcc)(H$_2$O)$_2$](NO$_3$)$_2$*
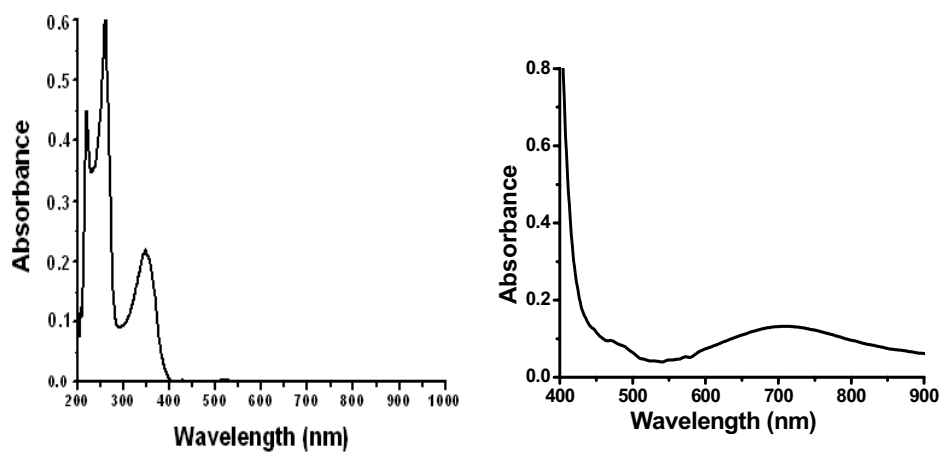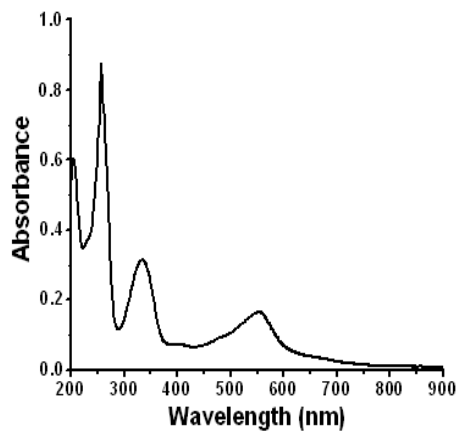

UV-Vis spectrum of [Cu(qco)(NO$_3$)$_2$]·2H$_2$O

Figure 5.11: Electronic spectra of the copper(II) nitrate complexes

Table 5.14: Electronic spectral assignments for the copper(II) perchlorate complexes

Complex	Absorption Maxima (cm^{-1})		log ε L mol^{-1} cm^{-1}	Band Assignment
	nm	cm^{-1}		
[Cu(qch)(ClO$_4$)$_2$]·2H$_2$O **19**	204	49020	2.89	$\pi \rightarrow \pi^*$
	238	42020	2.86	$\pi \rightarrow \pi^*$
	306	32680	2.49	$n \rightarrow \pi^*$
	450	22220	1.90	$n \rightarrow \pi^*$
	716	13960	0.94	$^2T_{2g} \rightarrow {}^2E_g$
[Cu$_2$(qce)$_2$](ClO$_4$)$_4$·H$_2$O **20**	204	49020	2.78	$\pi \rightarrow \pi^*$
	254	39370	2.92	$\pi \rightarrow \pi^*$
	334	29940	2.41	$\pi \rightarrow \pi^*$
	407	24570	0.95	$n \rightarrow \pi^*$
	557	17950	1.10	$^2B_2 \rightarrow {}^2E$
[Cu(qcp)(H$_2$O)$_2$](ClO$_4$)$_2$ **21**	234	42730	2.77	$\pi \rightarrow \pi^*$
	324	30860	2.27	$\pi \rightarrow \pi^*$
	480	20830	0.95	$n \rightarrow \pi^*$
	521	19190	1.39	$^2T_{2g} \rightarrow {}^2E_g$
	723	13830	1.07	$^2T_{2g} \rightarrow {}^2E_g$
[Cu(qcb)ClO$_4$(H$_2$O)]ClO$_4$ **22**	238	42070	3.03	$\pi \rightarrow \pi^*$
	324	30860	2.51	$\pi \rightarrow \pi^*$
	486	20830	1.19	$^2T_{2g} \rightarrow {}^2E_g$
	560	17850	0.30	$^2T_{2g} \rightarrow {}^2E_g$
	720	13880	0.99	$^2T_{2g} \rightarrow {}^2E_g$
[Cu(qcc)(H$_2$O)$_2$](ClO$_4$)$_2$ **23**	215	46510	2.73	$\pi \rightarrow \pi^*$
	254	39370	2.42	$\pi \rightarrow \pi^*$
	320	31250	1.97	$\pi \rightarrow \pi^*$
	484	20660	1.12	$^2T_{2g} \rightarrow {}^2E_g$
	552	18120	1.20	$^2T_{2g} \rightarrow {}^2E_g$
	691	14470	0.99	$^2T_{2g} \rightarrow {}^2E_g$
[Cu(qco)(ClO$_4$)$_2$]·3H$_2$O **24**	207	48310	2.44	$\pi \rightarrow \pi^*$
	249	40160	2.41	$\pi \rightarrow \pi^*$
	367	27250	2.35	$\pi \rightarrow \pi^*$
	430	23250	0.85	$^2T_{2g} \rightarrow {}^2E_g$
	530	18870	0.78	$^2T_{2g} \rightarrow {}^2E_g$
	733	13640	0.30	$^2T_{2g} \rightarrow {}^2E_g$

UV-Vis spectrum of [Cu(qch)(ClO₄)₂]·2H₂O

UV-Vis spectrum of [Cu₂(qce)₂](ClO₄)₄·H₂O
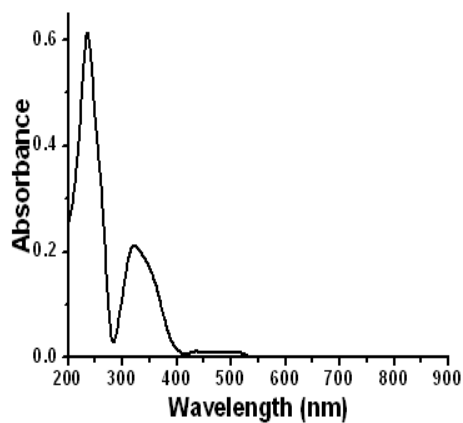
UV-Vis spectrum of [Cu(qcp)(H₂O)₂](ClO₄)₂
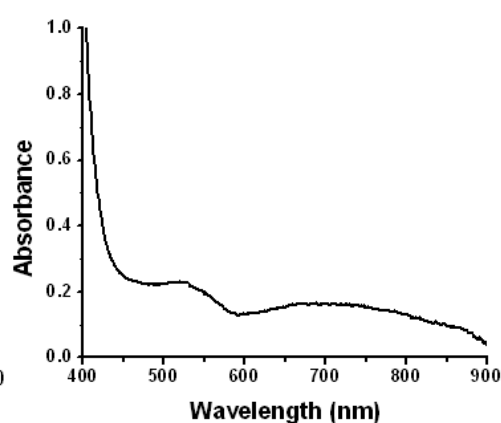
UV-Vis spectrum of [Cu(qcb)ClO₄(H₂O)]ClO₄
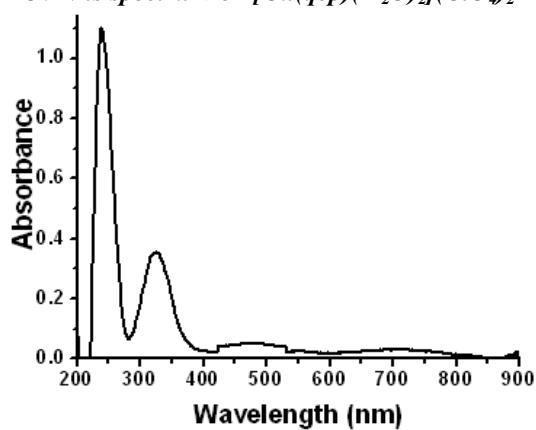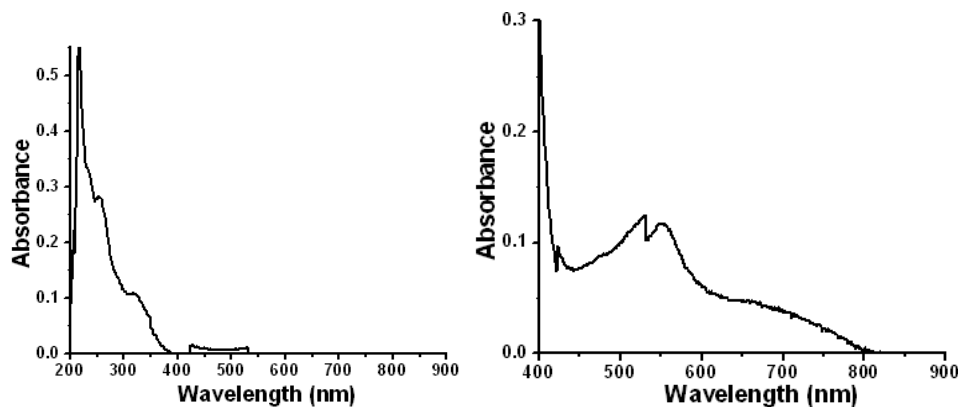
UV-Vis spectrum of [Cu(qcc)(H₂O)₂](ClO₄)₂
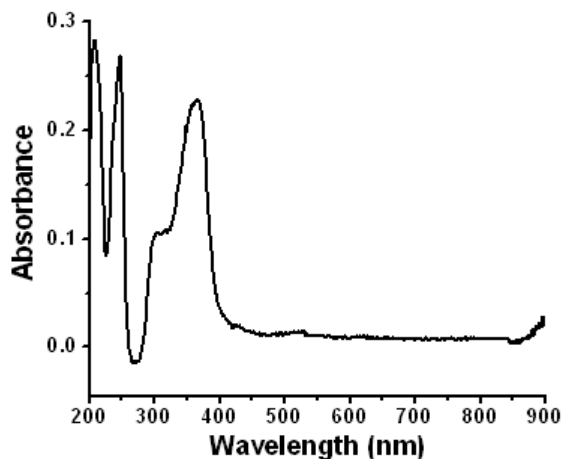
UV-Vis spectrum of [Cu(qco)(ClO₄)₂]·3H₂O

Figure 5.12: Electronic spectra of the copper(II) perchlorate complexes

5.3.7 EPR spectra

The X-band EPR spectrum of Cu(II) complexes in DMSO at 77K shows well resolved hyperfine splitting which are listed in Tables 5.15-5.18. These complexes showed EPR spectra (anisotropic signal) with four line hyperfine structure due to copper (I=3/2) [Figures 5.13-5.16]. The magnetic susceptibility values (lie in the range 1.73-1.92 B.M.) for the complexes, **1-7**, **9-13**, **15-19** and

21-24, indicate that the complex is mononuclear. The absence of a half field signal also rules out any Cu-Cu interaction. The resolution of the spectra did not improve upon cooling to 77 K and no super hyperfine interactions were observed [35,36]. EPR spectral data indicates the following:

❖ The copper(II) complexes have nearly equal *g*-values.

❖ Among the copper complexes, the copper complexes of *qch* ligand have high *g* values. This ligand is different from the rest, as it is derived from the hydrazine hydrate.

❖ Most of the complexes exhibit axial spectra.

❖ The ordering of *g*-values: $g_\parallel > g_\perp > g_e$, suggests that the $d_{x^2-y^2}$ ground state is occupied by an unpaired electron.

❖ A rhombic type EPR spectrum with three g-values, $g_1 \neq g_2 \neq g_3$, is obtained for complexes **9**, **13**, **14**, **15** and **19**.

❖ The ESR parameters of the present complexes (**1-7**, **9-13**, **15-19** and **21-24**) coincide with related systems and suggest that these have octahedral geometry [37].

Table 5.15: EPR Spectral data of the copper(II) acetate complexes

Complex	$g_\parallel$	$g_\perp$	$A_\parallel$ *
$[Cu(qch)_2(OAc)_2]\cdot2H_2O$ **1**	2.30	2.09	120
$[Cu_2(qce)_2(OAc)_4]\cdot H_2O$ **2**	2.29	2.07	130
$[Cu(qcp)(OAc)_2]\cdot2H_2O$ **3**	2.27	2.13	140
$[Cu(qcb)(OAc)_2]\cdot3H_2O$ **4**	2.23	2.07	167
$[Cu(qcc)(OAc)_2]\cdot3H_2O$ **5**	2.28	2.08	123
$[Cu(qco)(OAc)_2]\cdot H_2O$ **6**	2.31	2.07	153

*The '*A*' values are expressed in units of cm^{-1} multiplied by a factor of 10^{-4}.

EPR spectrum of [Cu(qch)₂(OAc)₂]·2H₂O

EPR spectrum of [Cu₂(qce)₂(OAc)₄]·H₂O

EPR spectrum of [Cu(qcp)(OAc)₂]·2H₂O

EPR spectrum of [Cu(qcb)(OAc)₂]·3H₂O

EPR spectrum of [Cu(qcc)(OAc)₂]·3H₂O

EPR spectrum of [Cu(qco)(OAc)₂]·H₂O

Figure 5.13: EPR spectra of the copper(II) acetate complexes

Table 5.16: EPR spectral data of the copper(II) chloride complexes

Complex	$g_\parallel$	$g_\perp$	g_1	g_2	g_3	$A_\parallel$*
[Cu(qch)Cl$_2$]·2H$_2$O **7**	2.39	2.08				125
[Cu$_2$(qce)$_2$]Cl$_4$·H$_2$O **8**	2.25	2.06				157
[Cu(qcp)ClH$_2$O]Cl·2H$_2$O **9**			2.24	2.10	2.03	
[Cu(qcb)Cl(H$_2$O)]Cl **10**	2.27	2.13				140
[Cu(qcc)Cl$_2$] **11**	2.29	2.10				107
[Cu(qco)Cl$_2$]·H$_2$O **12**	2.30	2.07				118

*The 'A' values are expressed in units of cm^{-1} multiplied by a factor of 10^{-4}.

EPR spectrum of [Cu(qch)Cl₂]·2H₂O

EPR spectrum of [Cu₂(qce)₂]Cl₄·H₂O

EPR spectrum of [Cu(qcp)ClH₂O]Cl·2H₂O

EPR spectrum of [Cu(qcb)Cl(H₂O)]Cl

EPR spectrum of [Cu(qcc)Cl₂]   *EPR spectrum of [Cu(qco)Cl₂]·H₂O*

Figure 5.14: EPR spectra of the copper(II) chloride complexes

Table 5.17: EPR spectral data of the copper(II) nitrate complexes

Complex	$g_\parallel$	$g_\perp$	g_1	g_2	g_3	$A_\parallel$ *
[Cu(qch)NO₃(H₂O)]NO₃ 13			2.374	2.06	2.037	130
[Cu₂(qce)₂](NO₃)₂(OH)₂·9H₂O 14			2.015	2.073	2.381	123
[Cu(qcp)NO₃(H₂O)]NO₃ 15			2.313	2.079	2.024	180
[Cu(qcb)NO₃H₂O]NO₃ 16	2.274	2.073				157
[Cu(qcc)(H₂O)₂](NO₃)₂ 17	2.262	2.060				157
[Cu(qco)(NO₃)₂]·2H₂O 18	2.357	2.073				133

*The '*A*' values are expressed in units of cm⁻¹ multiplied by a factor of 10⁻⁴.

EPR spectrum of [Cu(qch)NO₃(H₂O)]NO₃ *EPR spectrum of [Cu₂(qce)₂](NO₃)₂(OH)₂·9H₂O*

EPR spectrum of [Cu(qcp)NO₃(H₂O)]NO₃   *EPR spectrum of [Cu(qcb)NO₃H₂O]NO₃*

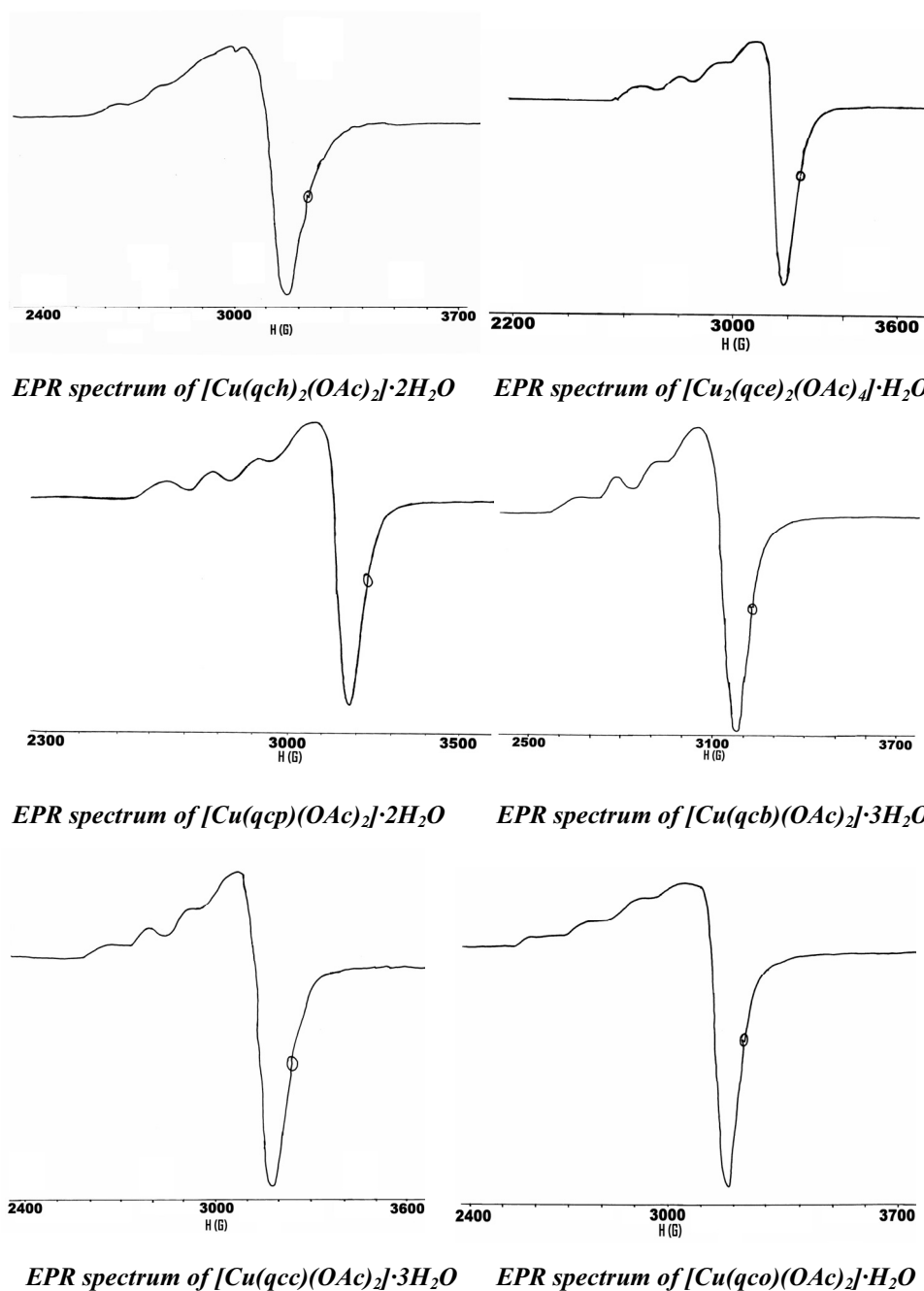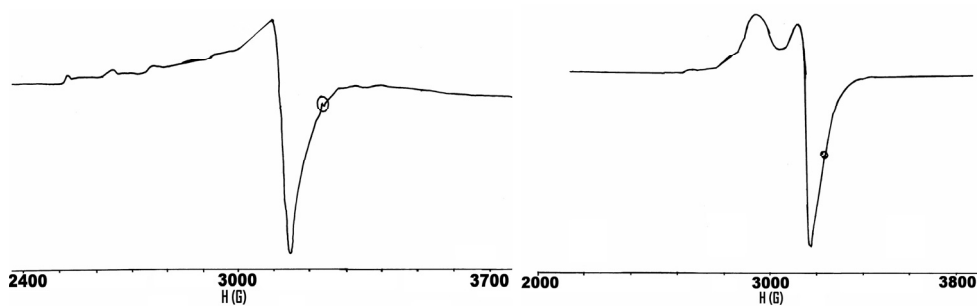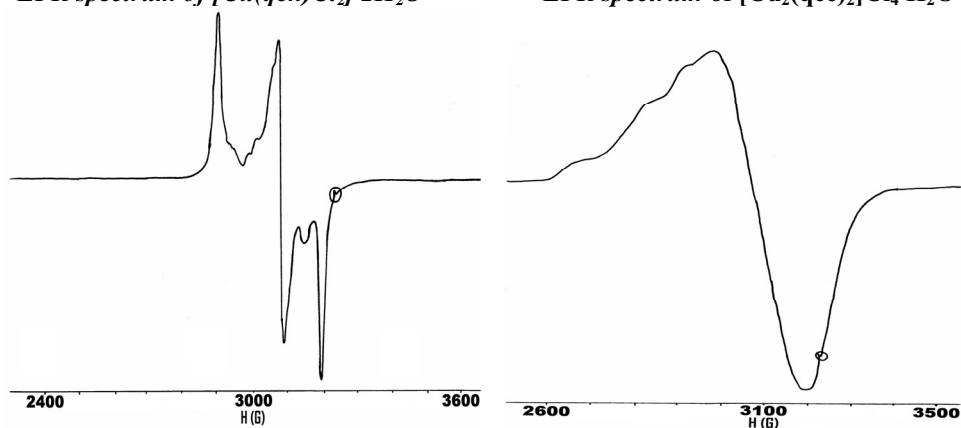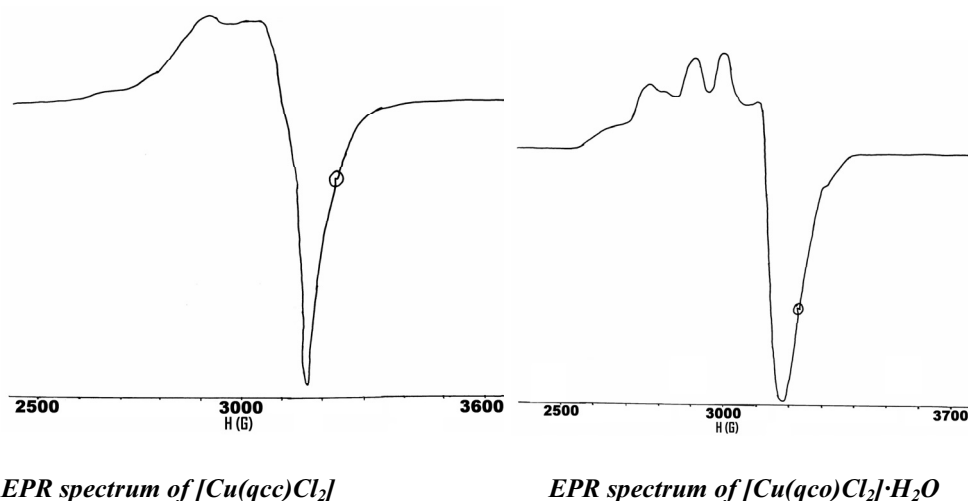*EPR spectrum of [Cu(qcc)(H₂O)₂](NO₃)₂*   *EPR spectrum of [Cu(qco)(NO₃)₂]·2H₂O*
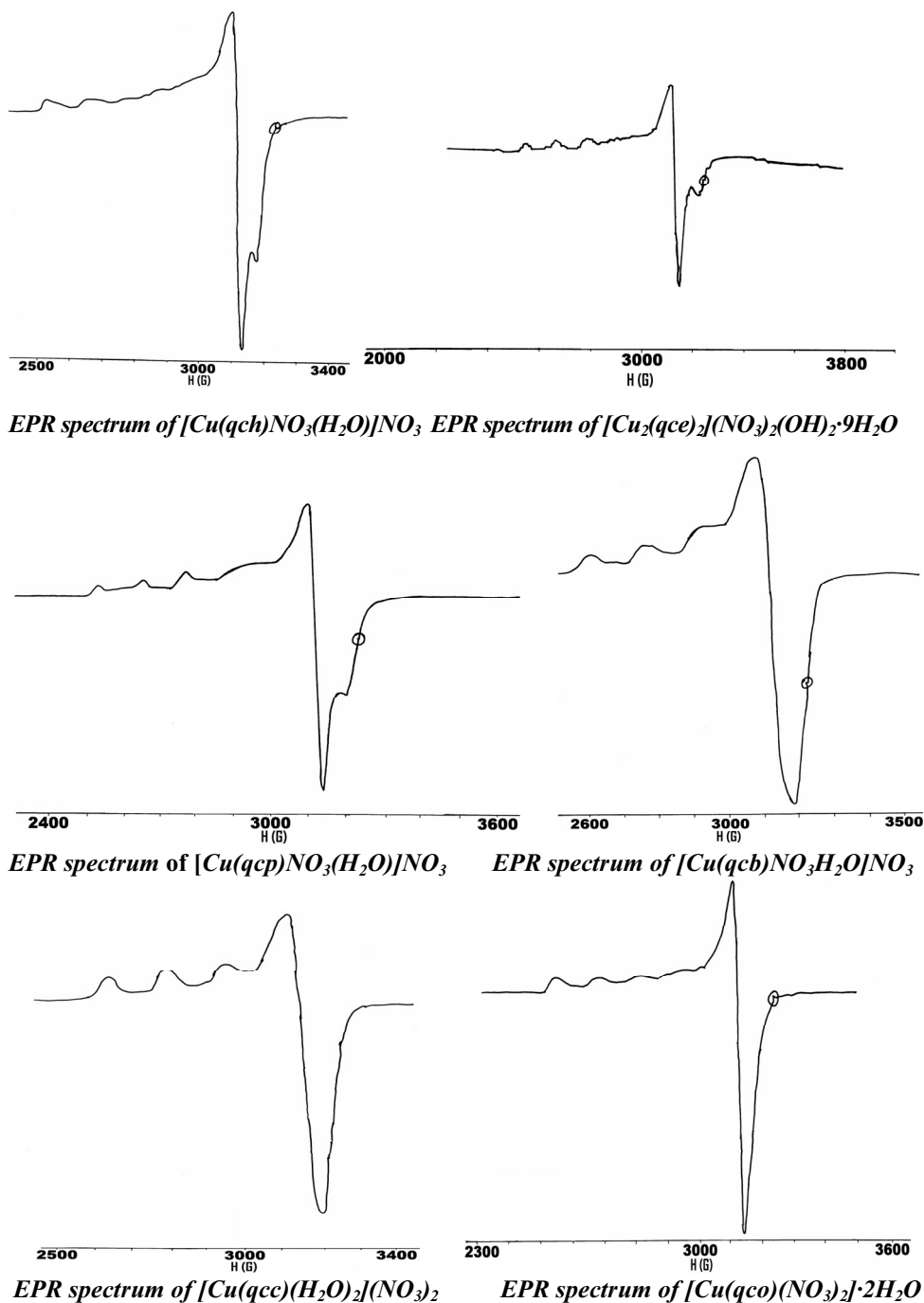
Figure 5.15: EPR spectra of the copper(II) nitrate complexes

Table 5.18: EPR spectral data of the copper(II) complexes

Complex	$g_\parallel$	$g_\perp$	g_1	g_2	g_3	$A_\parallel$*
[Cu(qch)(ClO$_4$)$_2$]·2H$_2$O **19**			2.39	2.06	1.99	120
[Cu$_2$(qce)$_2$](ClO$_4$)$_4$·H$_2$O **20**	2.12	2.05				100
[Cu(qcp)(H$_2$O)$_2$](ClO$_4$)$_2$ **21**	2.28	2.07				180
[Cu(qcb)ClO$_4$(H$_2$O)]ClO$_4$ **22**	2.40	2.083				120
[Cu(qcc)(H$_2$O)$_2$](ClO$_4$)$_2$ **23**	2.266	2.073				150
[Cu(qco)(ClO$_4$)$_2$]·3H$_2$O **24**	2.358	2.073				138

*The '*A*' values are expressed in units of cm^{-1} multiplied by a factor of 10^{-4}.
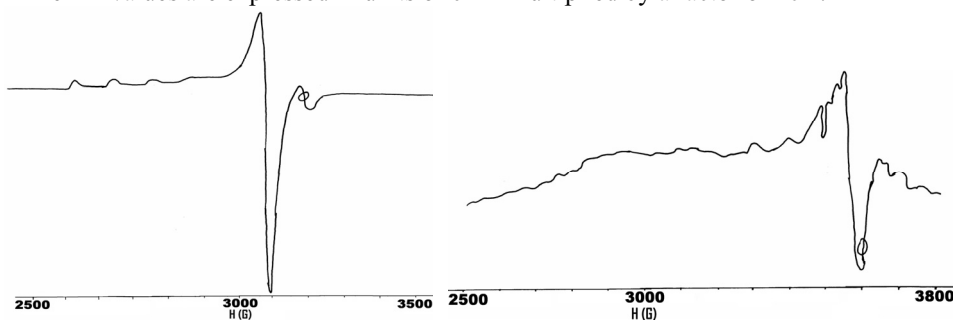
EPR spectrum of [Cu(qch)(ClO$_4$)$_2$]·2H$_2$O

EPR spectrum of [Cu$_2$(qce)$_2$](ClO$_4$)$_4$·H$_2$O
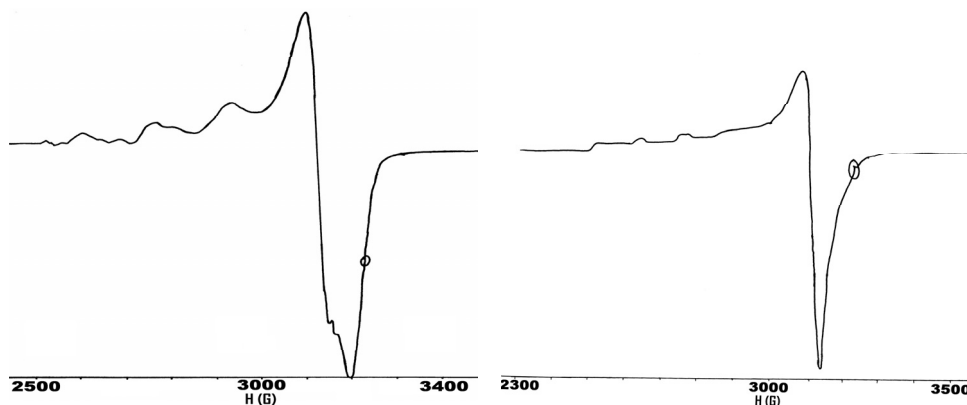
EPR spectrum of [Cu(qcp)(H$_2$O)$_2$](ClO$_4$)$_2$

EPR spectrum of [Cu(qcb)ClO$_4$(H$_2$O)]ClO$_4$
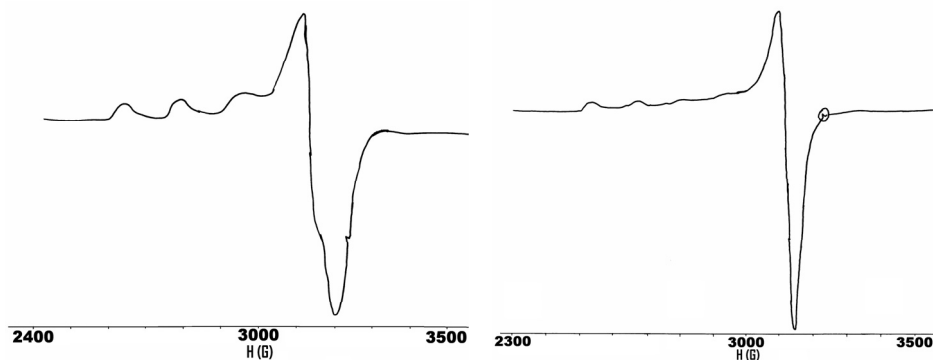
EPR spectrum of *[Cu(qcc)(H₂O)₂](ClO₄)₂*   *EPR spectrum* of *[Cu(qco)(ClO₄)₂]·3H₂O*

Figure 5.16: EPR spectra of the copper(II) perchlorate complexes

5.3.8 Single crystal analysis

The complex, $[Cu_2(qce)_2](NO_3)_2(OH)_2 \cdot 9H_2O$ **14**, [Figure 5.17] was prepared by refluxing ligand *qce* with $Cu(NO_3)_2 \cdot 3H_2O$ in methanol. The complex was formed as violet crystals by slow evaporation of the mother solvent (CH_3OH). These crystals were found to be suitable for X-ray diffraction work.
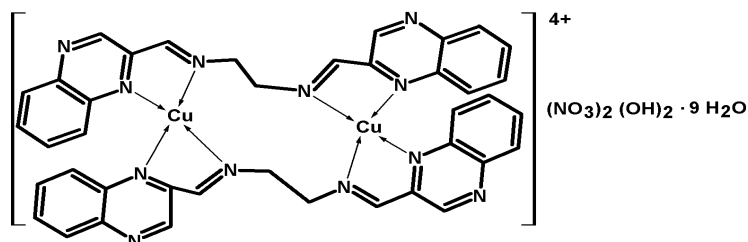
Figure 5.17: $[Cu_2(qce)_2](NO_3)_2(OH)_2 \cdot 9H_2O$ (14)

The complex **14** crystallises in orthorhombic system with the space group *Pbca*. A perspective view of crystal is shown in Figure 5.18. A summary of the crystallographic data and refinement parameters are given in Table 5.19. The crystal of **14** consists of two copper(II) ions with two quadridentate ligands (*qce*), two nitrate anions and eleven oxygen atoms. Unfortunately we could not fix the

hydrogen atoms in this case. Therefore, of the eleven oxygen atom two might belong to the hydroxyl anions and the other oxygen atoms might be the part of nine water molecules. This assumption agrees with the molecular formula derived from elemental analysis, $C_{40}H_{52}Cu_2N_{14}O_{17}$. Each copper(II) ion assumes a tetra coordinated geometry with N_4 donor atoms of the ligand. The symmetrical *qce* ligand is attached to the copper(II) ions in such a way that the half part of the ligand, *qce,* is attached to each copper through one of its azomethine and quinoxaline ring nitrogen.

Table 5.19: Crystallographic and refinement details of complex 14

Empirical formula	$C_{40}H_{32}Cu_2N_{14}O_{17}$	a (Å)	20.444 (2)
Formula weight	1107.88	b (Å)	17.957 (19)
Crystal size (mm)	0.56 x 0.48 x 0.32	c (Å)	27.110 (3)
Crystal system	Orthorhombic	$\alpha = \beta = \gamma =$ 90.00 °	
Space group	*Pbca*	V (Å³)	9952.9 (18)
Z	8	Mo $K\alpha$ radiation	
μ (mm⁻¹)	0.94	λ = 0.71073 Å	
Data collection		**Refinement**	
Brucker SMART APEX CCD area detector diffractometer		Refinement on F^2	
φ and ω scans		$R[F^2 > 2\sigma(F^2)] = 0.089$	
Absorption correction: empirical		$wR(F^2) = 0.223$	
T_{min} = 0.622, T_{max} = 0.753		S = 1.16	
51004 measured reflections		7383 reflections	
9770 independent reflections		658 parameters	
7383 reflections with $I > 2\sigma(I)$		All H atoms parameters refined	
R_{int} = 0.090		$\Delta\rho_{max}$ = 1.92 e Å⁻³	
		$\Delta\rho_{min}$ = -0.90 e Å⁻³	

Table 5.20: Selected Bond lengths (Å) and angles (°) of complex 14

|			
Cu1-N1	2.049 (5)	N1-Cu1-N7	104.67(19)
Cu1-N3	2.007 (5)	N3-Cu1-N1	81.65 (19)
Cu1-N7	2.067 (5)	N9-Cu1-N1	131.81 (19)
Cu1-N9	1.993 (5)	N9-Cu1-N3	131.54(19)
Cu2-N4	2.005 (5)	N9-Cu1-N7	81.00 (19)
Cu2-N6	2.067 (5)	N3-Cu1-N7	129.58 (19)
Cu2-N10	2.018 (5)	N4-Cu2-N10	131.50 (2)
Cu2-N12	2.053 (5)	N4-Cu2-N6	80.90 (2)
N1-C8	1.321 (8)	N4-Cu2-N12	124.60 (19)
N1-C1	1.388 (8)	N12-Cu2-N6	106.50 (19)
N7-C28	1.320 (7)	N10-Cu2-N6	135.10 (19)
N7-C21	1.360 (8)	N10-Cu2-N12	81.42 (19)
N6-C13	1.316 (7)	C11-N4-Cu2	127.90 (4)
N6-C20	1.373 (8)	C12-N4-C11	118.20 (5)
N12-C33	1.328 (7)	C9-N3-C10	116.50(5)
N12-C40	1.369 (8)	C10-N3-Cu1	131.00 (4)
N3-C9	1.286 (8)		
N3-C10	1.464 (7)		
N4-C12	1.288 (7)		
N10-C32	1.297 (7)		
N9-C29	1.289 (7)		
C10-C11	1.516 (8)		
C30-C31	1.518 (8)		
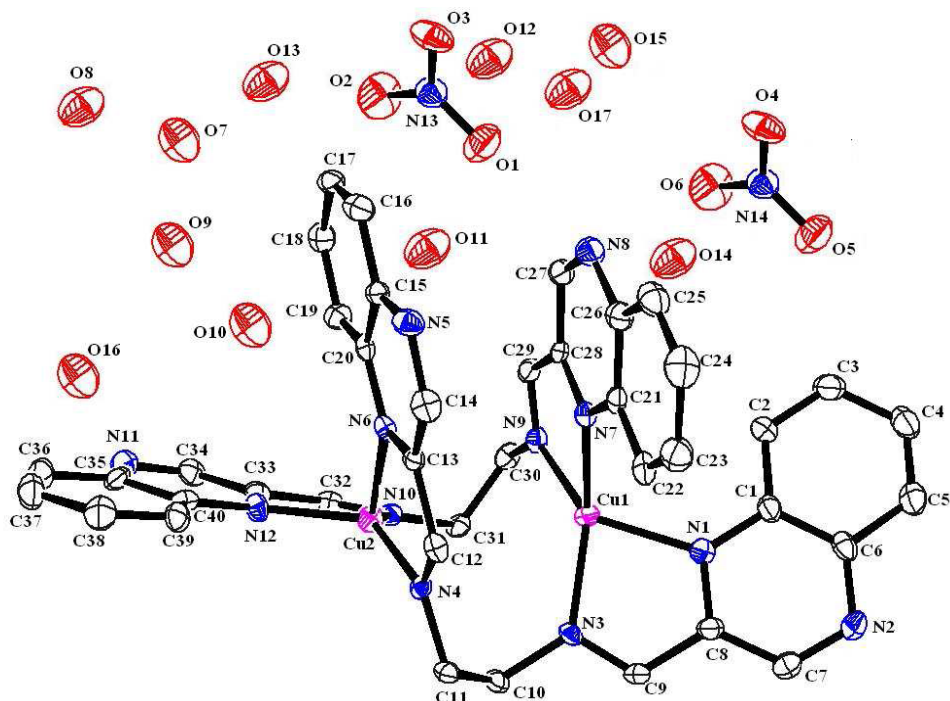
Figure 5.18: ORTEP diagram of complex 14

The geometry of the each CuN$_4$ coordination core is tetrahedral. However, the angle N1-Cu1-N7 is 104.67 (19)° and N12-Cu2-N6 106.50 (19)° suggesting the geometry to be slightly distorted tetrahedral [Table 5.20]. The two copper atoms in the complex are not directly bonded; the distance between Cu1-Cu2 atoms is 3.67 Å. Therefore the metal-metal interaction would be less here. The azomethine (N3-C9) bond length in the ligand *qce* is 1.26 Å (discussed in chapter 2) and that for the complex **14** is 1.29 Å. There is a slight change in the bond lengths of quinoxaline ring nitrogen with adjacent carbon atoms in complex when compared with free Schiff base. Therefore, on coordination both the bond length of azomethine and quinoxaline (C=N) is increased. The two nitrate anions are positioned axially to the copper with a Cu-N distance of 7.5 Å (Cu1-N13) and 5.7 Å (Cu2-N14). Nitrate anions are free from coordination but can be hydrogen-

bonded to the H-atoms of water molecules. There are eleven oxygen atoms axially positioned to the two copper ions. Two of them (O(10) and O(11)) are close to copper ions and these two oxygen atoms may be considered as a part of hydroxyl ions. The distance between Cu1-O10 is 4.7 Å and Cu2-O11 is 5.9 Å. The other nine oxygen atoms are considered as a part of water molecules. The existence of these nine water molecules is also supported by TG-DTG analysis. A layer formed by lattice water molecules in between the [Cu(qce)]$_2$ (sandwich form) is shown in the Figure 5.19. The anions and water molecules in the crystal lattice are stabilised by H-bonds [Figure 5.20]. The crystal structure of this complex is also stabilised by intermolecular hydrogen bonding and π-π stacking interactions.
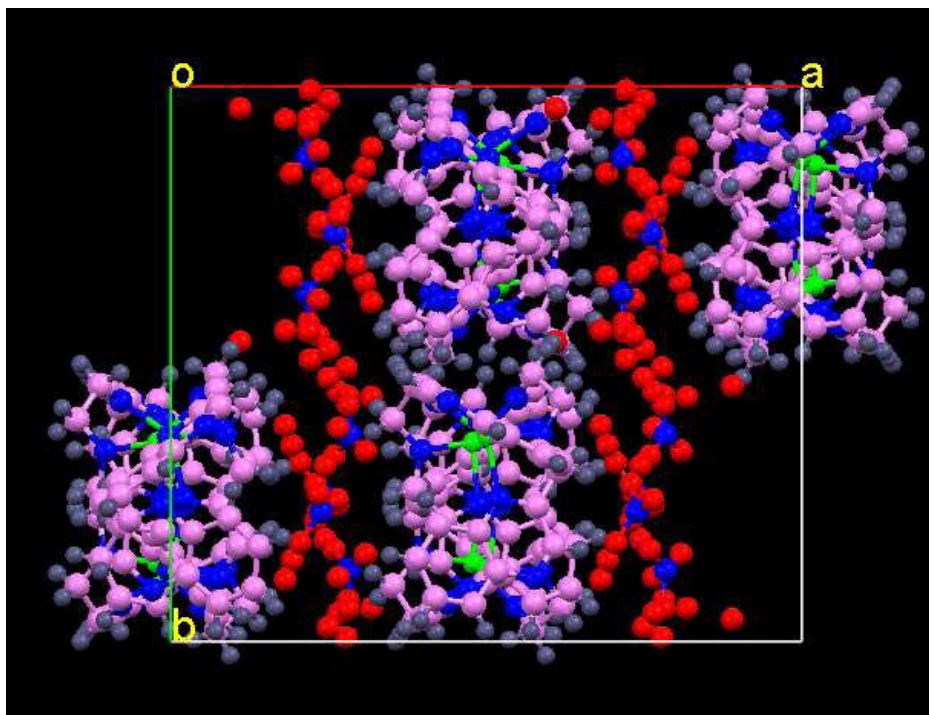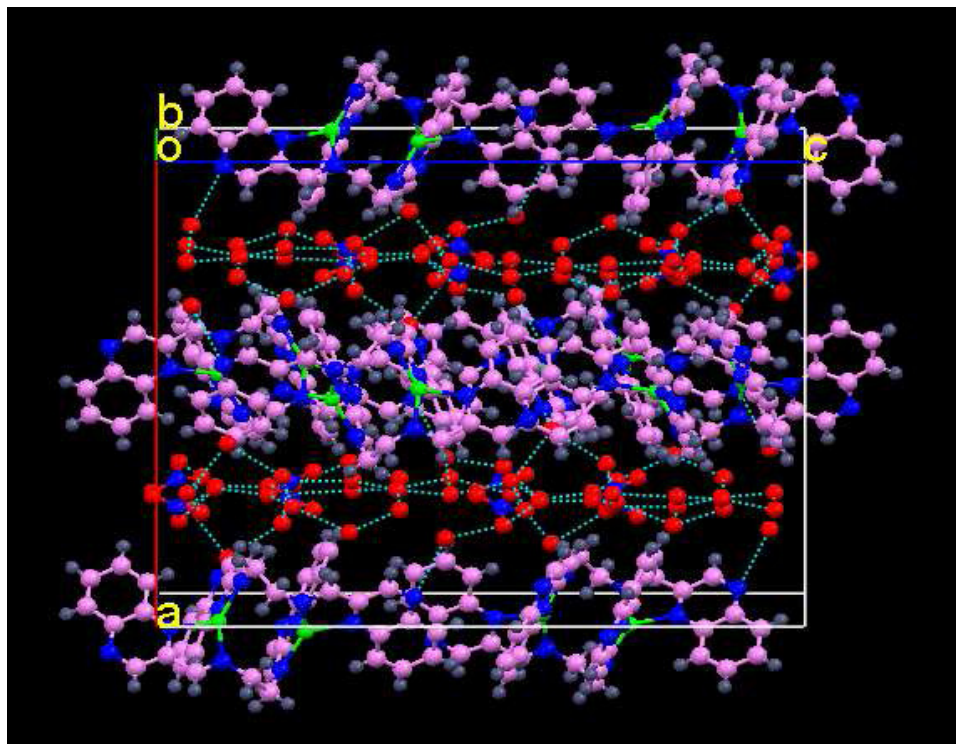

Figure 5.19: Packing diagram of complex 14 along *c* axis

Figure 5.20: Packing diagram of complex 14 showing H-bonding interactions along *b* axis

5.4 CONCLUSIONS

This chapter describes the synthesis and characterisations of a new copper(II) complexes of Schiff bases, *qch*, *qce*, qcp, *qcb*, *qcp* and *qco*. The analytical data suggest that most of the complexes are mononuclear except complexes of *qce*, which is binuclear. The very low molar conductance values observed for **1-7**, **11**, **12**, **18**, **19** and **24**, indicate nonelectrolytic nature of these complexes and all the other complexes are electrolytes. All the copper(II) complexes are found to be thermally stable and exhibit multistage thermal decomposition pattern. Magnetic moments of the complexes under investigation fall in the 1.60-1.92 B.M. range and lie within the range reported for tetrahedral

and tetragonally distorted octahedral structures. The IR data of the complexes reveal that the anions are coordinated to the copper(II) ion in a monodentate way and in some complexes (**8**, **14**, **17**, **20**, **21** and **23**), the anions are not coordinated to the copper(II) ion. The electronic spectrum of copper(II) complexes (**1-7, 9-13, 15-19, 21-24**) in methanol (10^{-3} M) showed d-d bands in the regions 20,000-13,000 cm^{-1} which can be assigned to $^{2}T_{2g} \rightarrow {}^{2}E_{g}$ transition of an octahedral geometry and other complexes exhibit d-d bands corresponding to tetrahedral geometry. EPR spectra of the complexes exhibit axial and rhombic spectra. The complex $[Cu_2(qce)_2](NO_3)_2(OH)_2 \cdot 9H_2O$ **14** crystallises in orthorhombic system with the space group *Pbca*. Each copper(II) ion assumes a tetra coordinated geometry with N_4 donor atoms of the ligand. The geometry of the each CuN_4 coordination core is tetrahedral. The metal-metal interaction is less, as the distance between the Cu(II) ions are greater. The crystal structure of this complex is also stabilised by intermolecular hydrogen bonding and π-π stacking interactions. Based on analytical and physico-chemical data we have proposed the following structure for the other complexes.
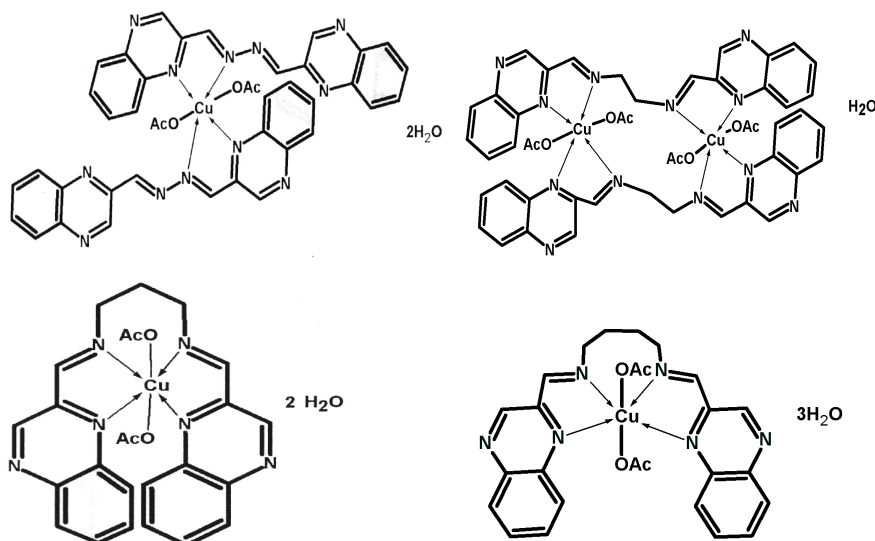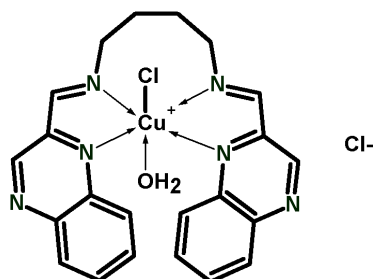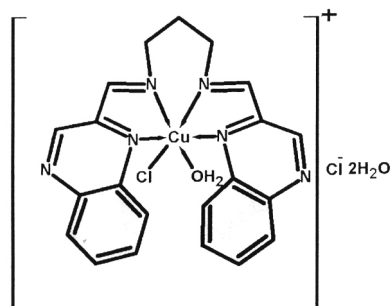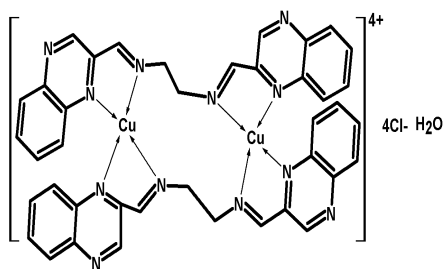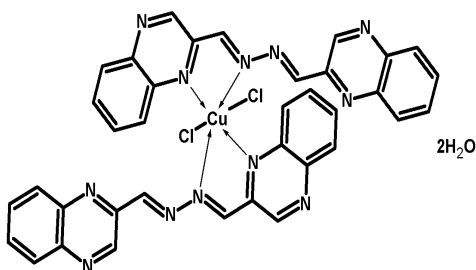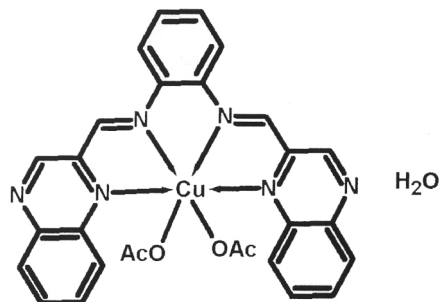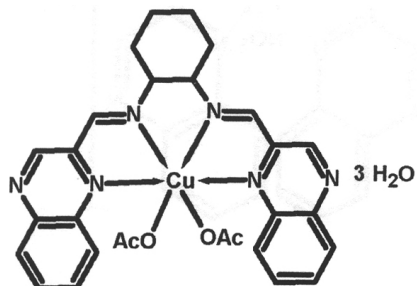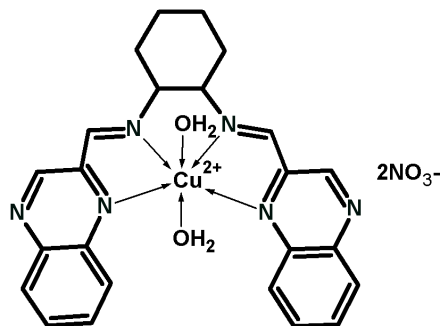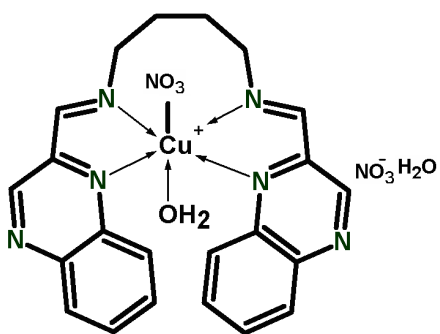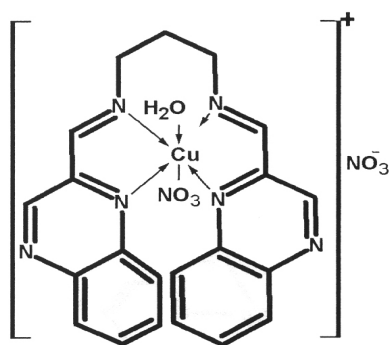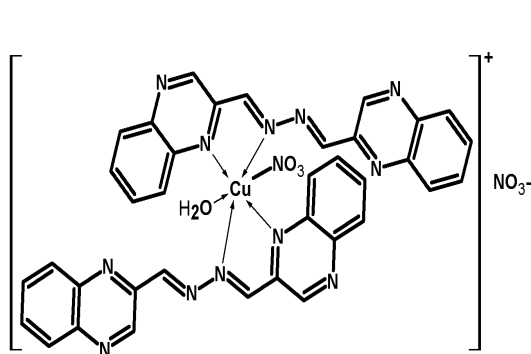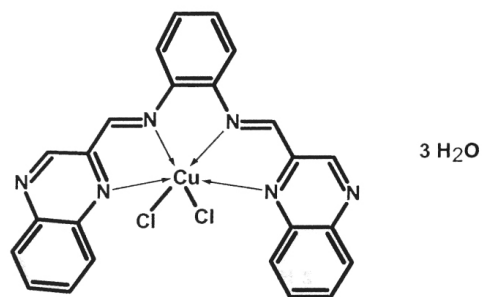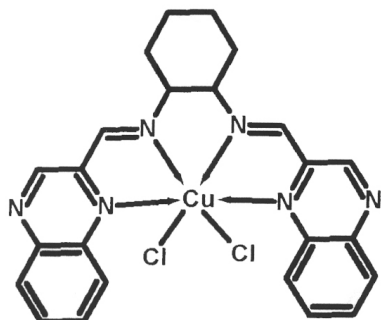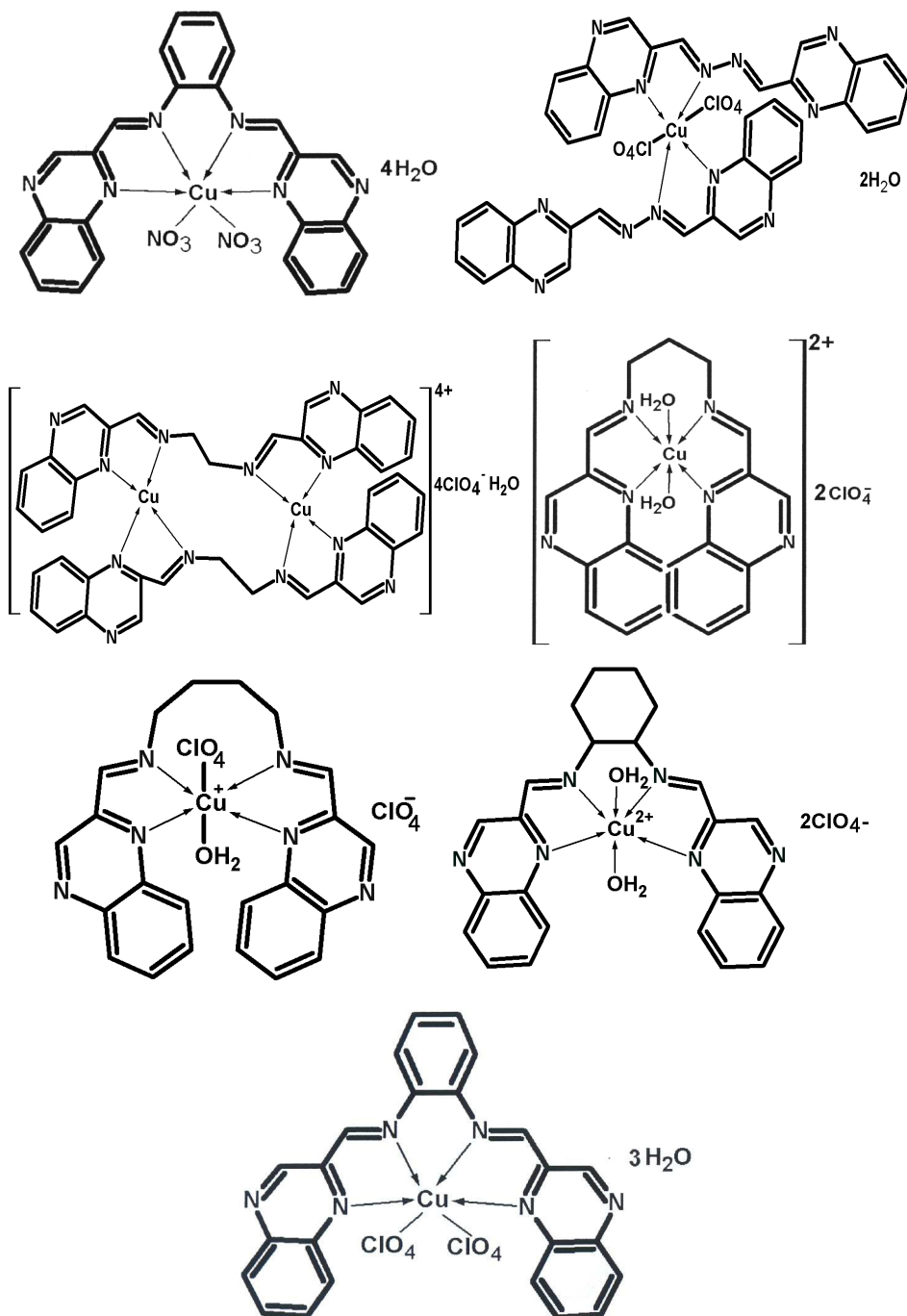
REFERENCES

1. J. G. Haasnoot, *Coord. Chem. Rev.*, 200 (**2000**) 131.

2. M. Alizadeh, F. Farzaneh, M. Ghandi, *J. Mol. Catal. A: Chem.*, 194 (**2003**) 283.

3. H. Dugas, C. Penney, *Bioorganic Chemistry*, Springer, New York, (**1981**) 435.

4. J. D. Mergerum, L. J. Miller, *Photochromism*, Interscience Wiley, 569 (**1971**).

5. L. Que, Jr., W. B. Tolman, *Angew. Chem.*, 114 (**2002**) 1160.

6. B. Dede, I. Ozmen, F. Karipcin, *Polyhedron*, 28 (**2009**) 3967.

7   S. Bunce, R. J. Cross, L. J. Farrugia, S. Kunchandy, L. L. Meason, K. W. Muir, M. O. Donnell, R. D. Peacock, D. Stirling, S. J. Teat, *Polyhedron*, 17 (**1998**) 4179.

8   B. J. Hathaway, *Copper*, 53, 533.

9   D. Reinen, C. Friebel, *Inorg. Chem.*, 23 (**1984**) 791.

10 M. M. Whittaker, W. R. Duncan, J. M. Whittaker, *Inorg. Chem.*, 35 (**1996**) 382.

11 C. E. Ruggiero, S. M. Carrier, W. E Antholine, J. W. Whittaker, C. J. Cramer, W. B. Tolman, *J. Am. Chem. Soc.*, 115 (**1993**) 11285.

12 R. E. P. Winpenny, *Adv. Inorg. Chem.*, 52 (**2001**) 1.

13 V. G. Makhankova, O. Y. Vassilyeva, V. N. Kokozay, B.W. Skelton, J. Reedijk, G. A. Vanalbada, L. Sorace, D. Gatteschi, *New. J. Chem.*, 25 (**2001**) 685.

14 H. Oshio, N. Hoshino, T. Ito, M. Nakano, F. Renz, P. Gotlich, *Angew. Chem.*, 115 (**2003**) 233.

15. A. Caneschi, A. Cornia, S. J. Lippard, *Angew. Chem.*, 107 (**1995**) 511.

16. D. Gatteschi, R. Sessoli, *Angew. Chem.*, 115 (**2003**) 278.

17. W. Wernsdorfer, N. Aliaga-Alcalde, D. N. Hendrickson, G. Christou, *Nature*, 416 (**2002**) 408.

18. M. Thirumavalavan, P. Akilan, M. Kandaswamy, *Inorg. Chem.*, 42 (**2003**) 3308.

19 D. D. Willett, D. Gatteschi, O. Khan, *Magneto-Structural Correlations in Exchange Coupled Systems*, Reidel: Dordrecht, The Netherlands, (**1985**).

20 D. Gatteschi, O. Kahn, J. S. Miller, F. Palacio, *Magnetic Molecular Materials*, NATO ASI Series 198, Kluwer Academic Publishers: Dordrecht, The Netherlands, (**1991**).

21 O. Kahn, Molecular Magnetism; VCH, New York, (**1993**).

22 B. J. Hathaway, G. Wilkinson, R. D. Gillard, J. A. McCleverty, *In Comprehensive Coordination Chemistry*, Eds. Pergamon Press: Oxford, England, 5 (**1987**) 533.

23 D. A. Harvey, C. J. L. Lock, *Acta Cryst*., C42 (**1986**) 799.

24 W. J. Geary. *Coord. Chem. Rev.*, 7 (**1971**) 81.

25 S. A. Sallam, A. S. Orabi, B. A. El-Shetary, A. Lentz, *Transition Met. Chem.*, 27 (**2002**) 447.

26 B. V. Patel, K. Desai, T. Thaker, *Synth. React. Inorg. Met.-Org. Chem.*, 19 (**1989**) 391.

27 M. C. Day, J. Selbin, *Theoretical Inorganic Chemistry*, East-West press, Madras, (**1977**).

28 P. S. N. Reddy, B. V. Agarwala, *Synth. React. Inorg Met.-Org.Chem.*, 17 (**1987**) 585.

29 K. Nakamoto, *Coordination Compounds. In Infrared and Raman Spectra of Inorganic and Coordination Compounds*, 4th Ed.; John Wiley and Sons, Inc.: New York, (**1986**).

30   V. Arun, P. P. Robinson, S. Manju, P. Leeju, G. Varsha, V. Digna, K. K. M. Yusuff, *Dyes and Pigments*, 82 (**2009**) 268.

31   S. Thakurta, J. Chakraborty, G. Rosair, J. Tercero, M. Salah El Fallah, E. Garribba, S. Mitra, *Inorg. Chem.,* 47 (**2008**) 6227.

32   M. Sebastian, V. Arun, P. P. Robinson, P. Leeju, D. Varghese, G. Varsha, K. K. M. Yusuff, *J. Coord. Chem.*, 63 (**2009**) 307.

33   A. B. P. Lever, *Electronic Spectra of Ions. In Inorganic Electronic Spectroscopy*, 2nd Ed., Elsevier, Amsterdam, (**1984**) 555.

34   A. D. Harrish, B. Josasses, R. D. Archer, *Inorg. Chem.*, 4 (**1965**) 147.

35   A. Abragam, B. Bleaney, *Electron Paramagnetic Resonance of Transition Ions*, Clarendon Press, London, (**1970**) 492.

36   G. Wilkinson, R. D. Gillard, J. A. McCleverty, Pergamon Press, U. K., 5 (**1987**) 652.

37   G. J. Anthony, A. Koolhaas, P. M. Van Berkel, S. C. Van Der Slot, G. Mendoza-Diaz, W. L. Driessen, J. Reedijk, H. Kooijman, N. Veldman, A. L. Spek, *Inorg. Chem.*, 35 (**1996**) 3525.

****✿****

Synthesis and characterisation of zeolite encapsulated copper(II) Schiff base complexes

6.1. INTRODUCTION

A variety of transition metal complexes have been successfully encapsulated in zeolites [1-4], and show improved catalytic properties in the oxidation of different types of organic substrates. In this respect, complexes of Schiff bases gained extensive research interest. A number of zeolite encapsulated Schiff base complexes of Co(II), Mn(II), Ni(II) and Cu(II) have been reported in the literature [5-7]. More complex molecules, such as complexes of phthalocyanine and tetramethyl porphyrin could be incorporated in zeolites, without blocking the pore of zeolite host, leading to an increase in the number of active sites. These zeolite encapsulated metal complexes have captured much attention in catalysis and biomimetic chemistry [8-10]. Each catalytic center is separated in these materials and thereby stability of the complex is also enhanced. Zeolite cages protect the molecule from the decomposition and irreversible dimerization by providing the steric constraints around the molecule [11-15].

Due to these features, the zeolite encapsulated metal complexes resemble enzymes. Inorganic complexes encapsulated in such porous systems have therefore been termed as zeozymes.

Transition metal complexes encapsulated in the cavities of zeolites are known to exhibit high catalytic activity in certain oxidation reactions [12]. In general, there have been many attempts to carry out the reactions with high yield and selectivity. We have synthesized zeolite encapsulated copper(II) complexes of Schiff bases *N,N'*-bis(quinoxaline-2-carboxylidene)hydrazine (*qch*), *N,N'*-bis(quinoxaline-2-carboxylidene)-1,2-diaminoethane (*qce*), *N,N'*-bis(quinoxaline-2-carboxylidene)-1,3-diaminopropane (*qcp*), *N,N'*-bis(quinoxaline-2-carboxylidene)-1,4-diaminobutane (*qcb*), *N,N'*-bis(quinoxaline-2-carboxylidene)-1,2-diaminocyclohexane (*qcc*) and *N,N'*-bis(quinoxaline-2-carboxylidene)-1,2-diaminobenzene (*qco*) and studied the catalytic activity of these complexes in the oxidation of cyclohexanol.

In this chapter, studies on the synthesis and characterisation of zeolite Y encapsulated copper(II) complexes of the Schiff bases, *qch*, *qce*, *qcp*, *qcb*, *qcc* and *qco*, are presented.

6.2. EXPERIMENTAL

Details regarding the preparation and characterisation of the Schiff bases are presented in chapter 2. The synthesis and characterisation of their copper(II) complexes are discussed in chapter 5.

6.2.1 Synthesis of zeolite encapsulated copper complexes.

The following general procedure was used for the synthesis of the encapsulated complexes. The copper(II) complexes of *qch*, *qce*, *qcp*, *qcb*, *qcc* and *qco* were entrapped in the cavities of the zeolite by the flexible ligand method [16-18]. The concentration of the ligands for the synthesis was taken to satisfy ~

2:1 ligand to metal ratio. The metal ion exchanged zeolite (CuY, ~1 g) was introduced into a round bottom flask containing the ligand (~1 g) dissolved in methanol/chloroform (50 mL) and the mixture was refluxed on a water bath for 6-12 hours. The zeolite encapsulated complex was filtered and soxhlet extracted with methanol and dichloromethane for a total period of 48 hours until the washings become colourless. The exhaustive extraction process is meant to remove the complexes formed on the surface. Uncomplexed metal ions remaining in the zeolite were removed by back exchange of the zeolite with NaCl (0.01 M) solution for 24 hours. After this, it was repeatedly washed with hot distilled water to remove the chloride ions and then dried in vacuum over anhydrous calcium chloride. The resulting encapsulated complexes are designated as *CuYqch*, *CuYqce*, *CuYqcp*, *CuYqcb*, *CuYqcc* and *CuYqco*.

6.3 RESULTS AND DISCUSSION

Interaction of copper(II) ion with the ligands (*qch*, *qce*, *qcp*, *qcb*, *qcc* and *qco*) inside the zeolite cages results in the formation of encapsulated Schiff base complexes. The metal complexes are too large and can not diffuse out from the zeolite cages. In the transition metal ion exchanged zeolite, the metal ion is surrounded by H_2O, OH^- or oxide ions of the zeolite lattice [19]. The metal oxygen bonds in the lattice are broken during the complexation and might form new bonds with the ligands [20-22]. The encapsulated copper complexes were characterised by elemental analysis, electronic spectra, infrared spectra, EPR spectra, AAS, XRD studies, surface area and pore volume measurement and SEM.

6.3.1 Elemental analysis

The percentage of silica was determined according to the literature procedure [23]. The Si/Al ratio for NaY was found to be 2.6, which correspond to the unit cell formula, $Na_{54}(AlO_2)_{54}(SiO_2)_{138}.nH_2O$ [24,25]. The elemental analysis found for the CuY is Si, 20.77; Al, 7.88; Na, 5.85; Cu, 1.97. The Si to Al ratio for CuY was also found to be 2.6. Retaining of this ratio even after the metal exchange indicates the absence of any dealumination. This result indicates that zeolite framework is unaltered by encapsulation as reported in earlier studies. The percentage of metal in CuY gives the unit cell formula of copper exchanged zeolite as ~ $Na_{46}Cu_4(SiO_2)_{138}(AlO_2)_{54}.nH_2O$. The analytical data [Table 6.1] suggest the purity and stoichiometry of the encapsulated complexes.

Table 6.1: Analytical data of the encapsulated copper(II) Schiff base complexes

Compound	Elemental Analysis (%)						
	Si	Al	Na	Cu	C	H	N
CuY	20.77	7.88	5.85	1.97			
CuYqch	20.45	7.76	5.82	0.91	4.18	2.82	1.20
CuYqce	20.68	7.82	5.86	0.88	3.48	2.88	0.99
CuYqcp	20.53	7.78	5.76	0.76	8.69	2.71	2.87
CuYqcb	20.63	7.80	5.79	0.78	5.85	2.96	2.21
CuYqcc	20.58	7.82	5.69	0.84	5.29	2.76	2.02
CuYqco	20.56	7.76	5.82	0.72	3.36	2.70	0.95

The analytical data of all the encapsulated complexes, *CuYqch*, *CuYqce*, *CuYqcp*, *CuYqcb*, *CuYqcc* and *CuYqco*, show that the Si/Al ratio is 2.64. The Si/Al ratio found for the zeolite encapsulated complexes are in the typical range of zeolite Y. These values suggest that after encapsulation there is no change in the frameworks of zeolite. The maximum complexation was observed in the case of copper exchanged zeolite complexes of *qcp*. The composition of copper in these complexes was not found to agree with that of the neat complexes. This may be due to the presence uncomplexed copper ions found in the surface as well as in the cages of zeolites. Further, the data indicate that the copper ions may still remain in the zeolite cage even after back exchange with NaCl solution. The percentages of carbon, hydrogen and nitrogen in the zeolite encapsulated complexes indicate the presence of the complexes of Schiff bases in the zeolite cages.

6.3.2 Surface area and pore volume

The surface area and pore volume of sodium and copper exchanged zeolites and the encapsulated copper complexes are presented in Table 6. 2. The results of surface area analysis indicate that there is a slight decrease in the surface area of metal exchanged zeolites. However, the surface area decreased drastically in the case of encapsulated complexes of zeolites. The encapsulation of copper ions and copper complexes reduces the surface area and adsorption capacity of zeolite. The lowering of the pore volume and surface area supports the fact that Cu(II) Schiff base complexes are present within the zeolite cages and not on the external surface. Balkus and Gabrielove [18] have reported such extent of reductions in surface area of zeolites due to inclusion of metal complexes in the pores.

Table 6.2: Surface area and pore volume of the ion exchanged zeolites and zeolite encapsulated copper(II) Schiff base complexes

Compound	Surface area (m^2/g)	Pore volume (CC/g)
NaY	690	0.3543
CuY	684	0.3227
CuYqch	416	0.2244
CuYqce	284	0.1522
CuYqcp	470	0.2539
CuYqcb	386	0.2084
CuYqcc	407	0.2199
CuYqco	431	0.2331

6.3.3 Powder X-ray diffraction analysis

The powder XRD pattern of *CuY* and the encapsulated complexes, *CuYqch*, *CuYqce*, *CuYqcp*, *CuYqcb*, *CuYqcc* and *CuYqco*, are given in the Figure 6.1. The XRD patterns of the encapsulated complexes exactly match with that of the *CuY*, and suggest that there is no loss in the crystalline nature of the zeolite [23]. Further more the data does not indicate any dealumination. These results further suggest that the reduction in surface area of the encapsulated complexes is not due to any collapse of the crystalline structure.
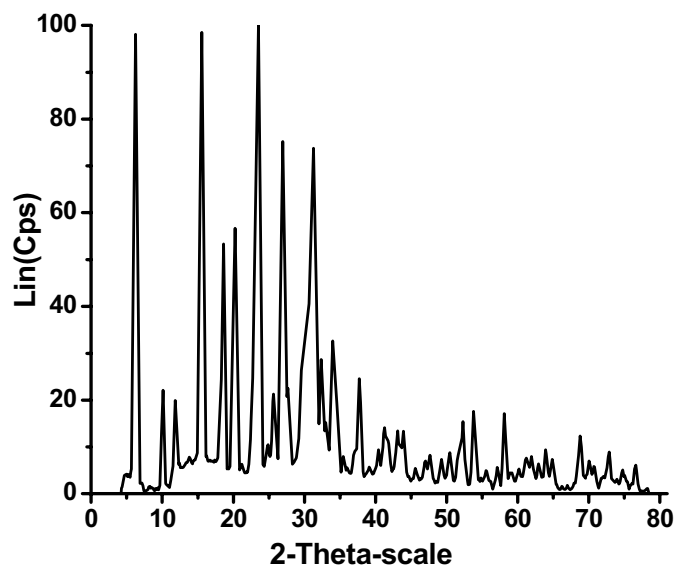
XRD pattern of CuY
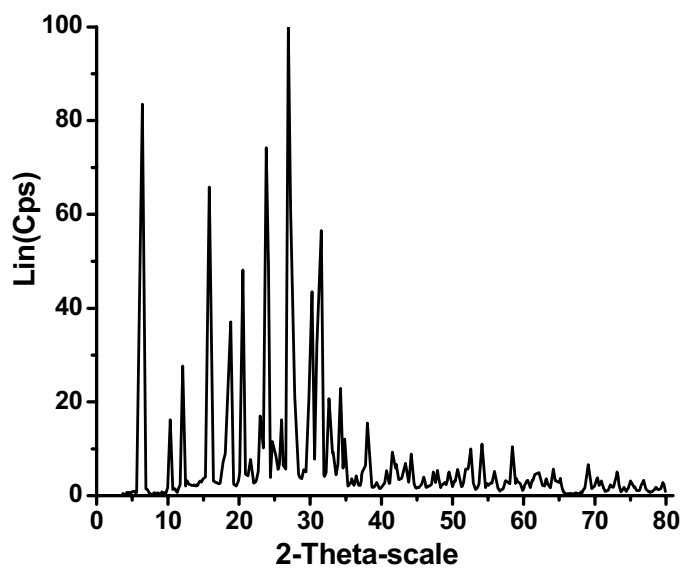
XRD pattern of CuYqch
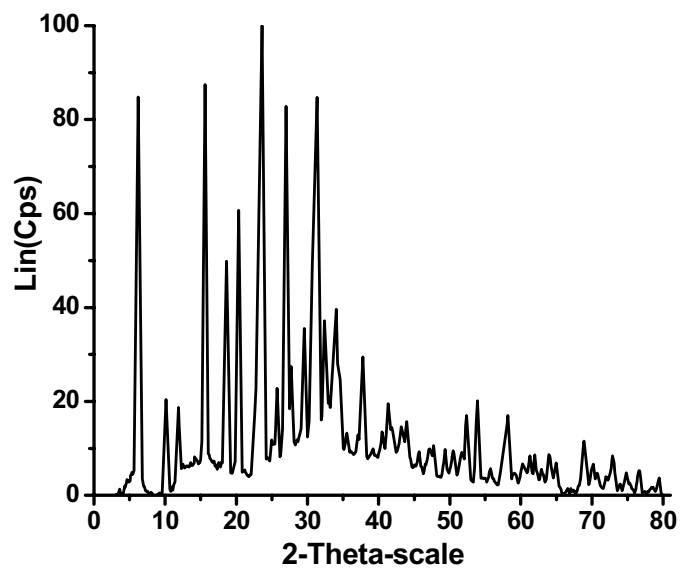
XRD pattern of CuYqce

XRD pattern of CuYqcp

Department of Applied Chemistry
Cochin University of Science and Technology
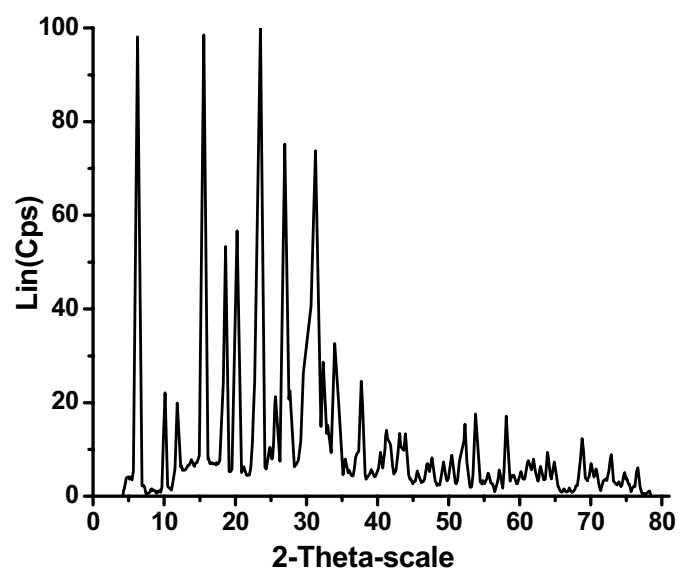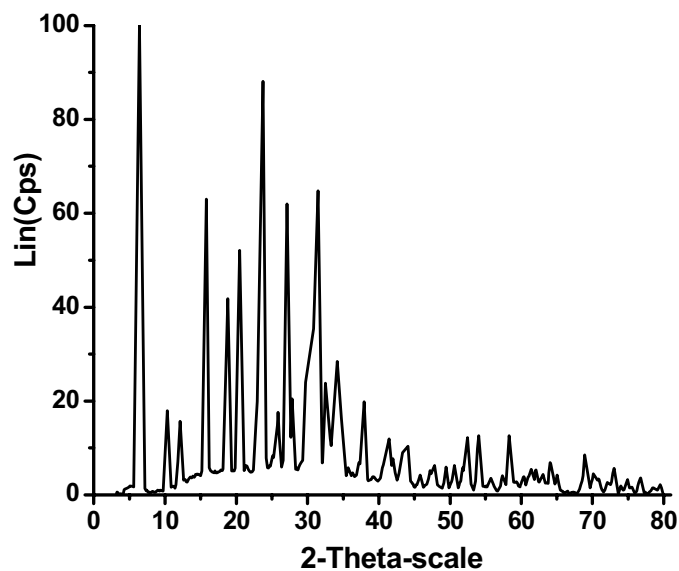
XRD pattern of CuYqcb
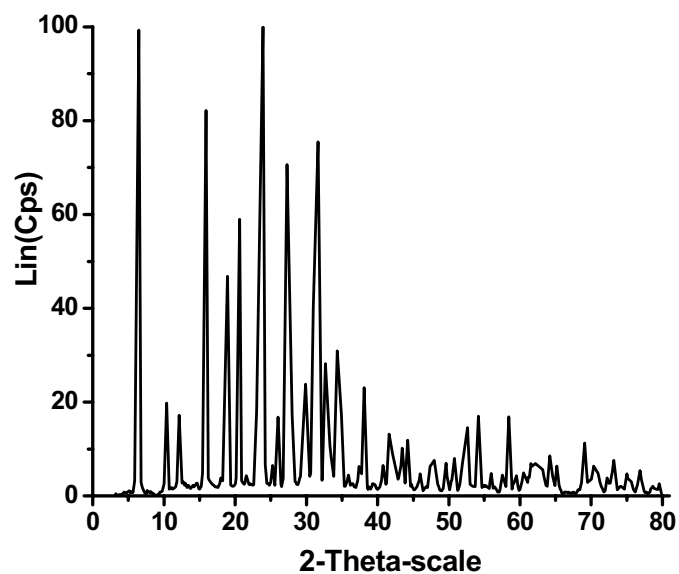
XRD pattern of CuYqcc
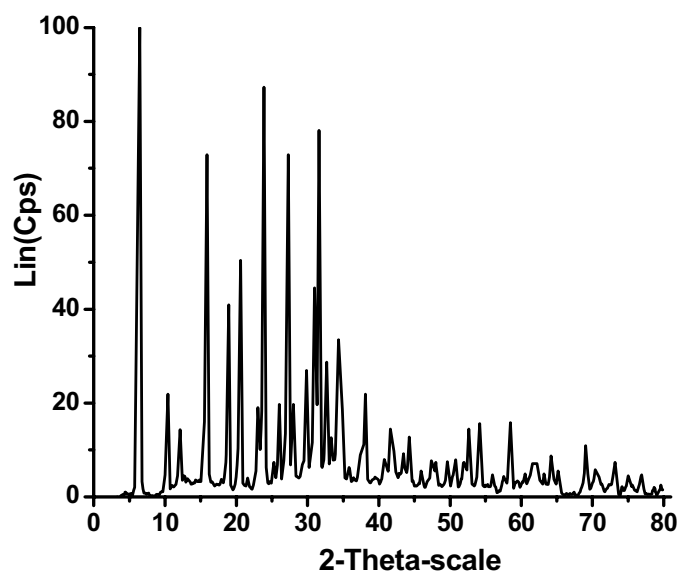
XRD pattern of CuYqco

Figure 6.1: XRD pattern of copper exchanged zeolite and zeolite encapsulated copper(II) Schiff base complexes

6.3.4 SEM analysis

The scanning electron microscopic (SEM) analysis of the zeolite encapsulated complexes is used to find out whether any extraneous material is present on the zeolite. The SEM of the zeolite encapsulated complexes before and after soxhlet extraction was taken. The SEM images are shown in Figure 6.2. The soxhlet extraction was done by using two solvents, such as methanol and dichloromethane. This extraction is necessary to remove any surface adsorbed species. SEM analysis shows that the zeolite encapsulated complexes after soxhlet extraction have well defined crystal structures indicating absence of surface adsorbed species. The SEM further point out that the processes of encapsulation and soxhlet washing during the preparation have no influence on the structure of zeolite [26-28].
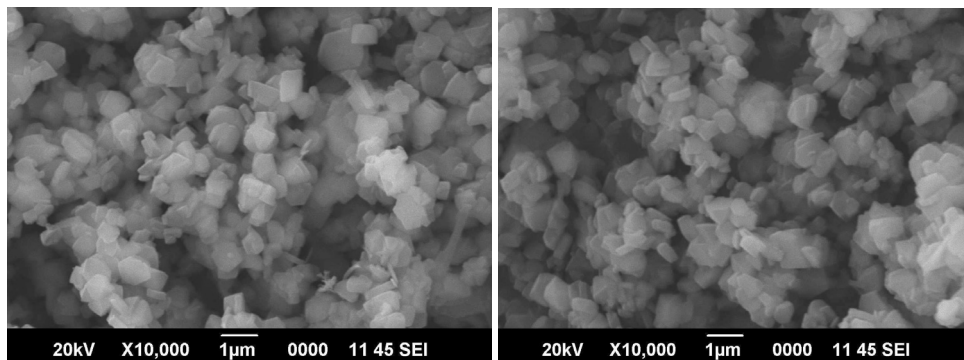
| Before soxhlet extraction | After soxhlet extraction |

Scanning Electron Micrographs of CuYqch
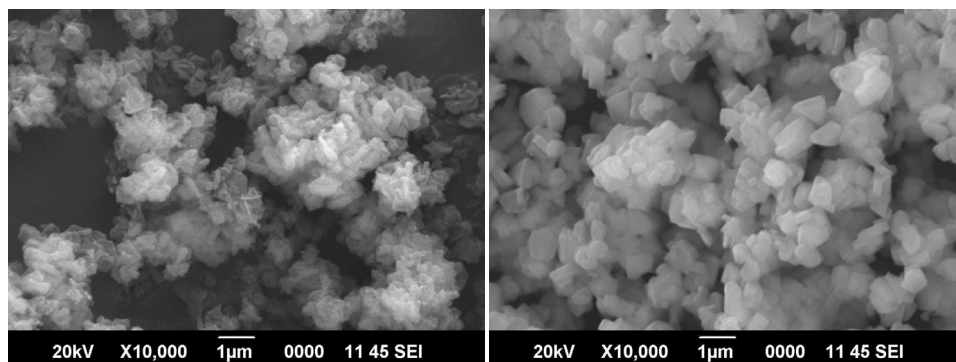
| Before soxhlet extraction | After soxhlet extraction |

Scanning Electron Micrographs of CuYqce
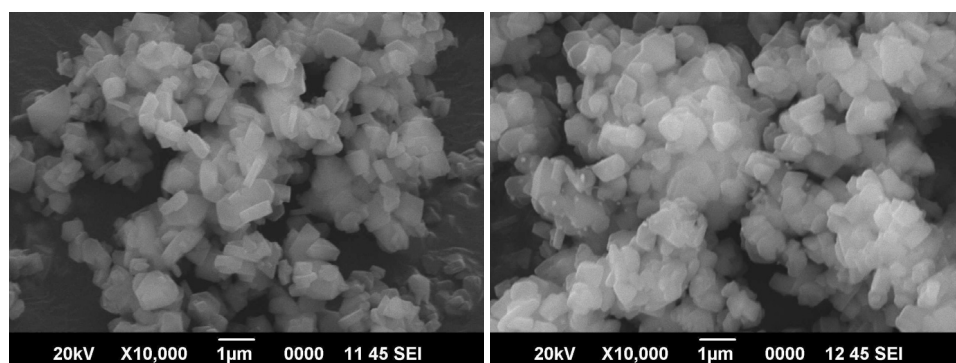
| Before soxhlet extraction | After soxhlet extraction |

Scanning Electron Micrographs of CuYqcp
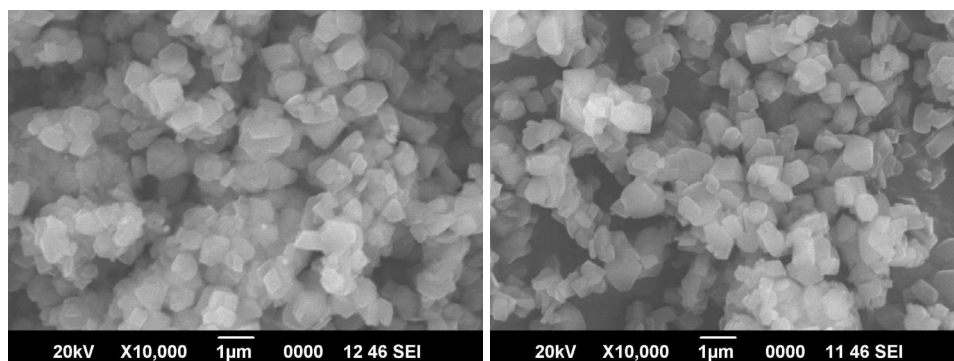
Before soxhlet extraction   **After soxhlet extraction**
Scanning Electron Micrographs of CuYqcb
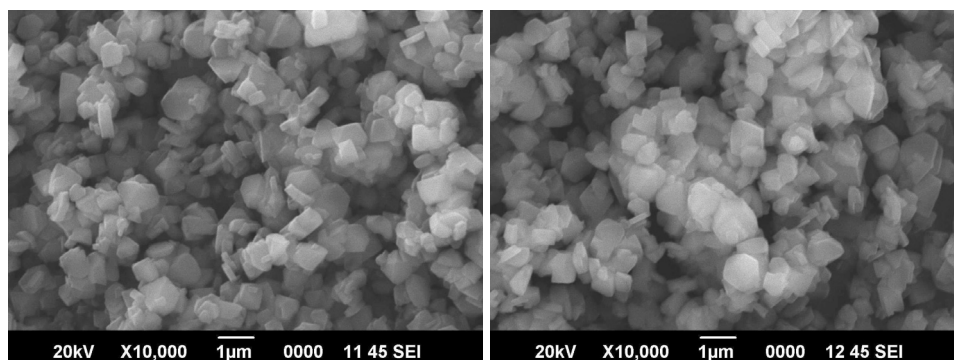
Before soxhlet extraction   **After soxhlet extraction**
Scanning Electron Micrographs of CuYqcc
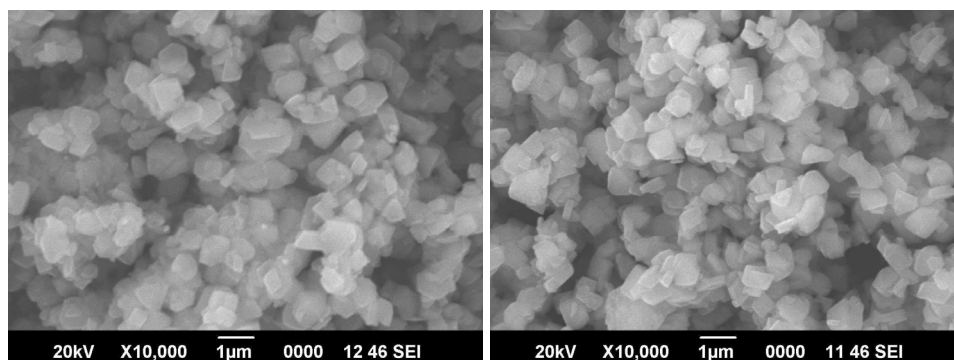
Before soxhlet extraction   **After soxhlet extraction**
Scanning Electron Micrographs of CuYqco

Figure 6.2: SEM of encapsulated copper(II) Schiff base complexes

Department of Applied Chemistry
Cochin University of Science and Technology

6.3.5 Thermal analysis

The thermal properties of the zeolite encapsulated copper complexes were investigated by TG-DTG measurements with a view to compare their thermal stabilities. In the TG run, the encapsulated copper complexes were heated from 50 °C to 1000 °C at a rate of 10° min^{-1} in nitrogen atmosphere. The TG data obtained from these analyses are given in the Table 6.3 and the thermograms are given in Figure 6.3. The TG-DTG curves of encapsulated complexes, *CuYqch*, *CuYqce*, *CuYqcp*, *CuYqcb*, *CuYqcc* and *CuYqco*, are found to be almost similar. The endothermic peak observed at below 200 °C in the TG-DTG curve is due to the desorption of physically adsorbed and occluded water. The exothermic peaks above 200 °C are attributed to the combustion of copper complexes encaged in the host [30]. However, the mass loss in TG curves of the encapsulated complexes was extremely small, due to the very low concentration of metal complexes within the supercages of the zeolite.

Table 6.3: Thermogravimetric analysis data of encapsulated copper(II) Schiff base complexes

Encapsulated complexes	Temperature range (°C)	% Weight loss
CuYqch	50-160	12.82
	160-800	4.50
CuYqce	50-200	19.05
	200-1000	2.41
CuYqcp	50-200	19.16
	200-1000	6.74
CuYqcb	50-180	11.95
	180-800	5.92
CuYqcc	50-170	13.52
	170-800	8.74
CuYqco	50-170	17.60
	170-800	6.16

TG-DTG curve of CuYqch

TG-DTG curve of CuYqce

TG-DTG curve of CuYqcp

TG-DTG curve of CuYqcb

TG-DTG curve of CuYqcc

TG-DTG curve of CuYqco
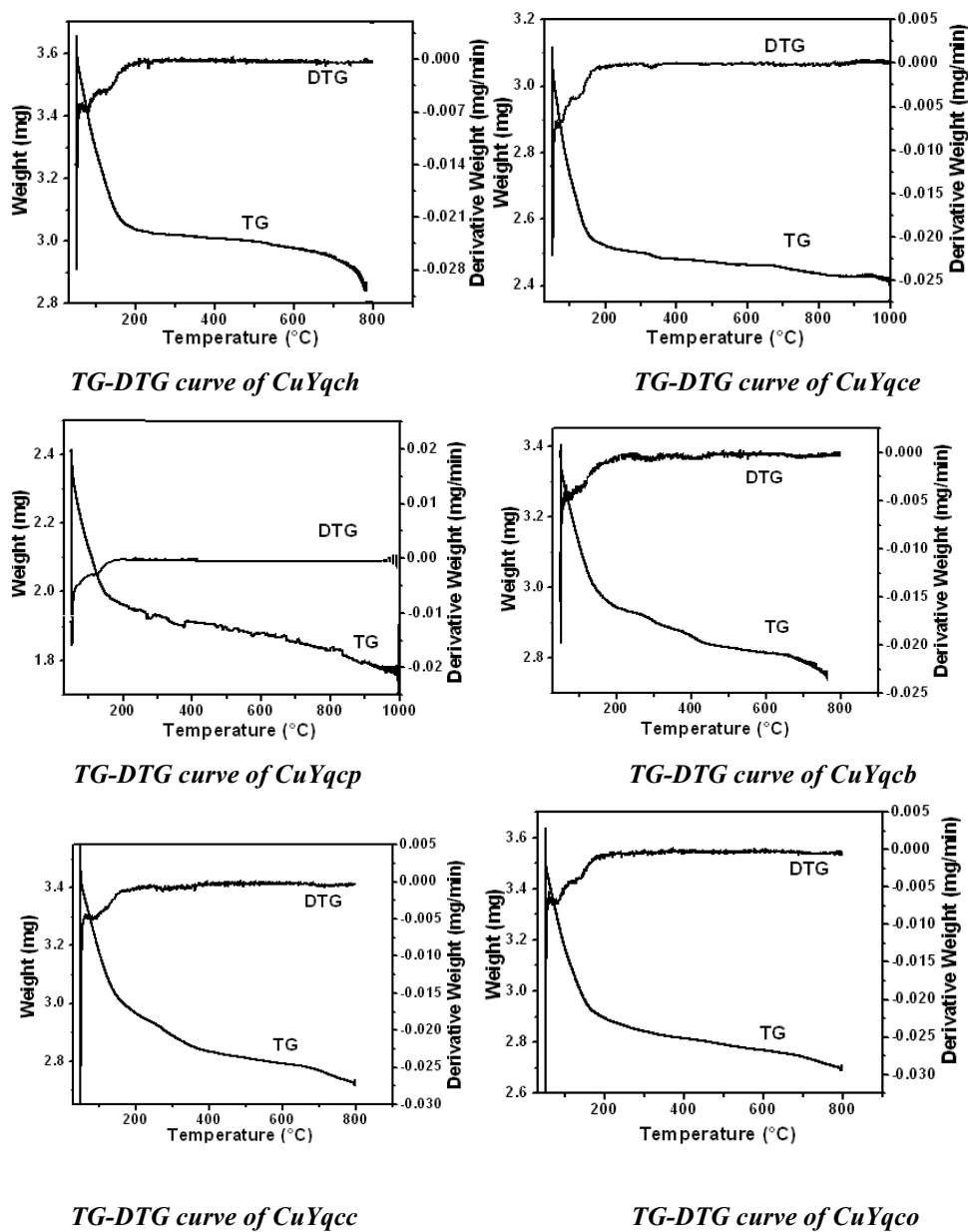
Figure 6.3: TG-DTG curves of encapsulated copper(II) Schiff base complexes

6.3.6 Infrared spectra

The FTIR spectra of the complexes, *CuYqch*, *CuYqce*, *CuYqcp*, *CuYqcb*, *CuYqcc* and *CuYqco*, are shown in Figure 6.4 and the spectral data are presented in Table 6.4. The major IR bands of the zeolite framework are reported to occur in the range of 200-1300 cm^{-1} as it contains the fundamental vibration of framework alumina or silica [23]. The strong and broad band at 1000 cm^{-1} can be attributed to the asymmetric stretching vibrations of $(Si/Al)O_4$ units. The coordination of ligand in the pores can be identified from the bands observed in the 1300-1600 cm^{-1} region where the zeolite has no bands. The broad bands at the region 1650-3500 cm^{-1} are due to lattice water molecules and surface hydroxylic groups.

The IR bands of all encapsulated complexes are weak in comparison with those of the neat complexes due to their low concentrations in zeolite cages. The free Schiff base ligands (*qch*, *qce*, *qcp*, *qcb*, *qcc* and *qco*) shows a strong band at 1610-1640 cm^{-1} (section 2.4.3.3 in chapter 2) due to azomethine group (C=N). On complexation the ν(C=N) band is shifted to lower frequency, in the case of simple complexes. Lowering of the ν(C=N) was also observed for all the encapsulated complexes. The ν(C=N) occurs for the encapsulated complexes in the range 1604-1635 cm^{-1}, suggesting the coordination of nitrogen of azomethine group to the copper. Large numbers of lattice water molecules are present in all the zeolite encapsulated complexes. The presence of water molecules in the lattice are confirmed by the peaks due to –OH vibrations of the zeolites lie in the range from 3600-3300 cm^{-1}. Other major zeolite framework peaks are also seen for all the encapsulated complexes at ~1040, ~780, ~570, ~450 cm^{-1} suggesting the retention of zeolite framework in the complexes. These results are in good agreement with the previously reported results in the literature [23,29,30].

Table 6.4: FTIR data of the encapsulated copper(II) complexes

Encapsulated Complexes	$\nu(OH)_{str}$ (cm^{-1})	$\nu(C=N)_{str}$ (cm^{-1})	Vibrations due to linkages between tetrahedral in zeolite (cm^{-1})
CuYqch	3495	1618	1054, 793, 578, 478
CuYqce	3469	1632	1021, 753, 558, 465
CuYqcp	3482	1630	1048, 793, 578, 445
CuYqcb	3489	1635	1075, 787, 578, 458
CuYqcc	3463	1632	1054, 793, 578, 458
CuYqco	3469	1604	1035, 780, 570, 452
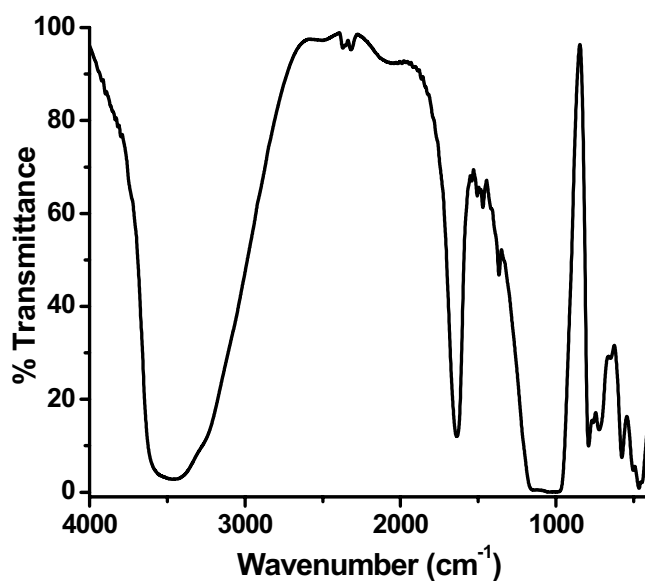
FTIR spectrum of CuYqch
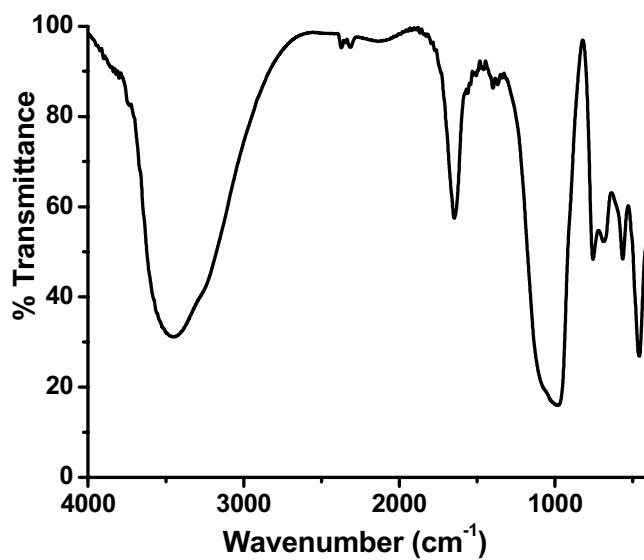
FTIR spectrum of CuYqce
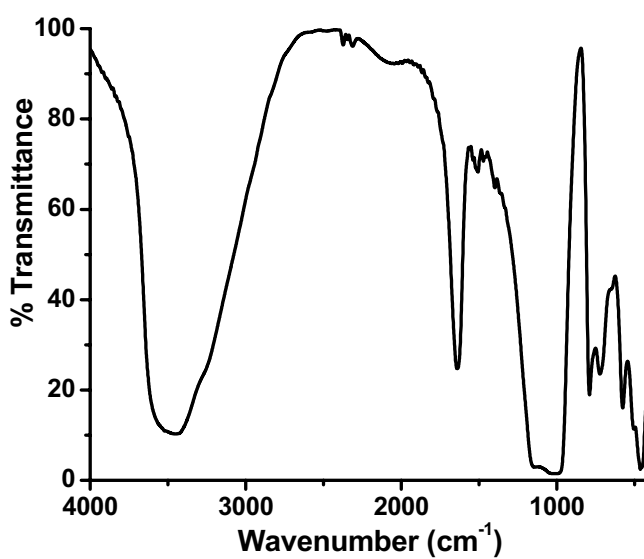
FTIR spectrum of CuYqcp
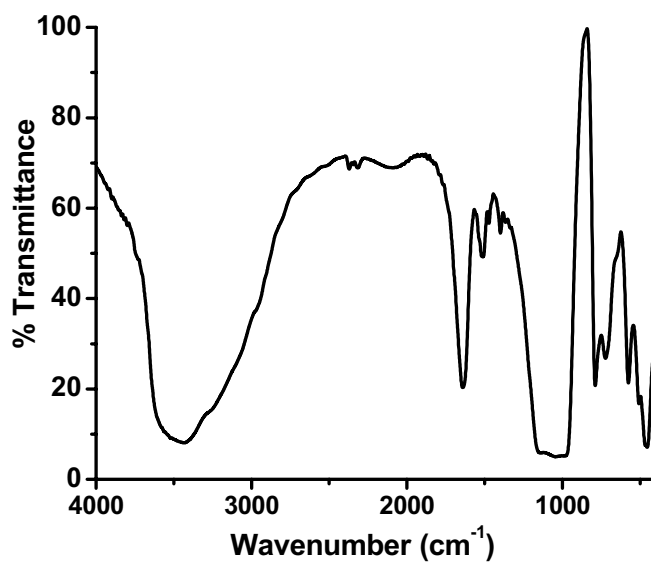
FTIR spectrum of CuYqcb
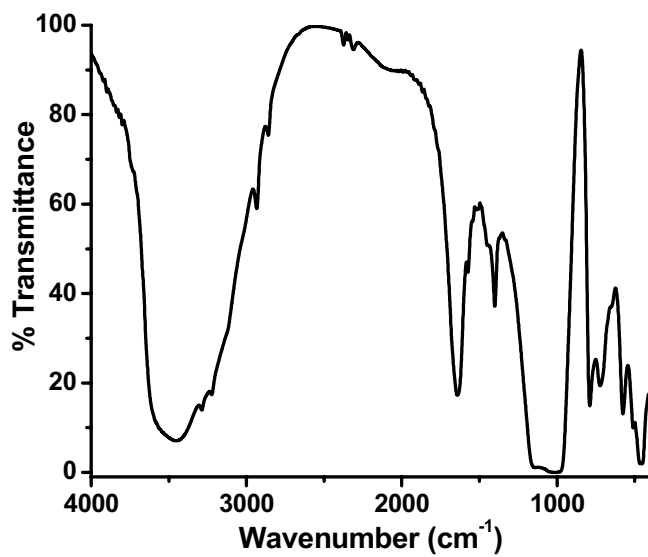
FTIR spectrum of CuYqcc
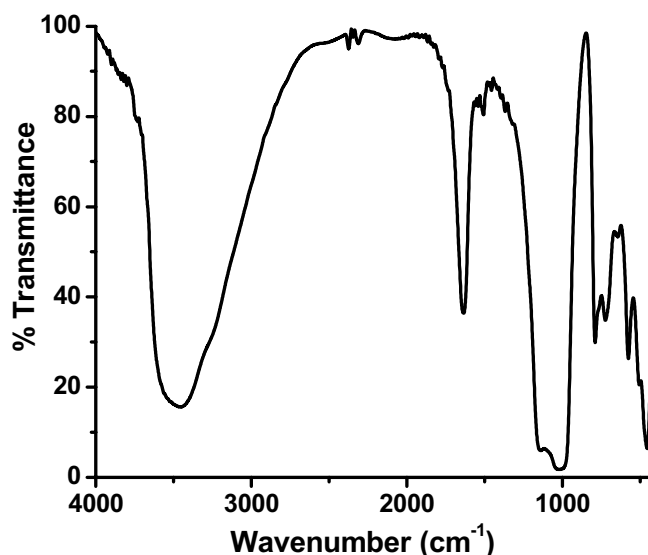
FTIR spectrum of CuYqco

Figure 6.4: FTIR spectra of encapsulated copper(II) Schiff base complexes

6.3.7 Electronic spectra

Electronic spectra of the encapsulated complexes could be carried out only in the diffuse reflectance (DR) mode. Any relevant information in the absorption mode could not be obtained due to scattering of radiation. A Kubelka-Munk equation was used for the data interpretation. The UV-Vis spectra of Figure 6.5 confirm the inclusion of the Cu(II) Schiff base complexes within the zeolite cages. The diffuse reflectance spectral data of the encapsulated complexes are given in Table 6.5. The spectra suggest the existence of Cu(II) Schiff base complex in the cage of zeolite even though the peaks exhibit some shift and broadening, when compared to those for the simple complexes. This might be due to some distortions of the Cu(II) Schiff base complexes happening inside the zeolite cage. A relatively intense absorption band is seen around 300-400 nm in

the DR UV-Vis spectra of all zeolite Y encapsulated Cu(II) Schiff base samples. This band can be attributed to ligand-to-metal charge transfer and gives a strong evidence for the formation of Cu(II) Schiff base complex molecules inside the cavity of zeolite Y.

Table 6.5: Electronic spectral data of the encapsulated complexes

Encapsulated Complexes	Absorption Bands		Tentative Assignments
	(nm)	(cm^{-1})	
CuYqch	203	49260	$\pi \rightarrow \pi^*$
	239	41840	$\pi \rightarrow \pi^*$
	331	30210	CT
	520	19230	$^2T_{2g} \rightarrow {}^2E_g$
	700	14280	$^2T_{2g} \rightarrow {}^2E_g$
CuYqce	237	42190	$\pi \rightarrow \pi^*$
	340	29410	CT
	610	16390	$^2T_{2g} \rightarrow {}^2E_g$
CuYqcp	244	40980	$\pi \rightarrow \pi^*$
	333	30030	CT
	480	20860	$^2T_{2g} \rightarrow {}^2E_g$
	606	16500	$^2T_{2g} \rightarrow {}^2E_g$
CuYqcb	204	49020	$\pi \rightarrow \pi^*$
	254	39370	$\pi \rightarrow \pi^*$
	347	28820	CT
	480	20860	$^2T_{2g} \rightarrow {}^2E_g$
CuYqcc	220	45450	$\pi \rightarrow \pi^*$
	347	28820	$\pi \rightarrow \pi^*$
	470	21270	$^2T_{2g} \rightarrow {}^2E_g$
CuYqco	208	48050	$\pi \rightarrow \pi^*$
	255	39210	$\pi \rightarrow \pi^*$
	404	24750	CT
	520	19230	$^2T_{2g} \rightarrow {}^2E_g$

The diffuse reflectance data for the encapsulated copper complexes suggest a six coordinate structure with a tetragonal distortion. The d-d bands in the case of all zeolite encapsulated complexes occur between 460-700 nm. Their

corresponding neat complexes show bands (section 5.3.6 in chapter 5) around 460-800 nm. The data almost agree with the reported octahedral structure of the complexes [23]. Even though the anions are not present in these encapsulated complexes the axial positions might be occupied by hydroxyl groups present in the zeolite for the charge neutralisation.
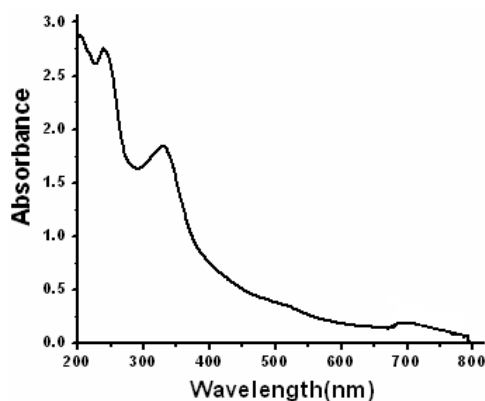
Electronic spectrum of CuYqch
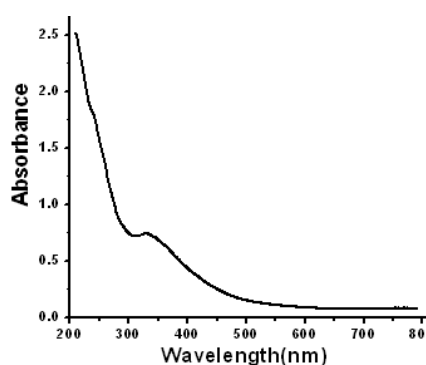
Electronic spectrum of CuYqce
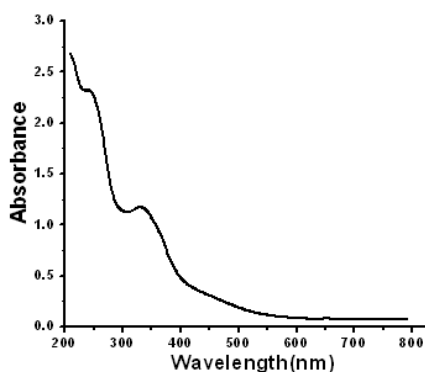
Electronic spectrum of CuYqcp
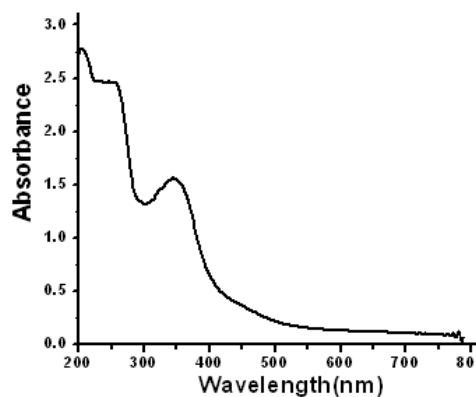
Electronic spectrum of CuYqcb
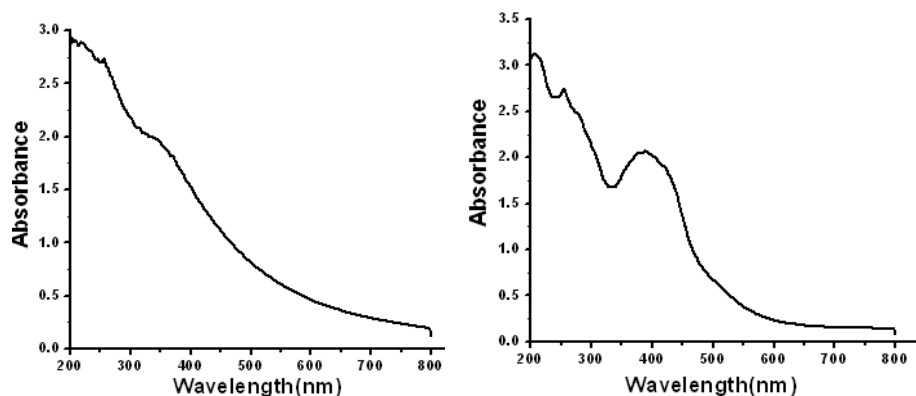
Electronic spectrum of CuYqcc   *Electronic spectrum of CuYqco*

Figure 6.5: Electronic spectra of encapsulated copper(II) Schiff base complexes

6.3.8 EPR spectra

Electron paramagnetic spectroscopy (EPR) is an extremely powerful probe of the electronic structures of the materials with unpaired electrons. The X-band EPR spectra of the encapsulated copper(II) Schiff base complexes were recorded at room temperature and also at 77 K (LNT). The spectra at RT [Figure 6.6] of encapsulated complexes, *CuYqch*, *CuYqce*, *CuYqcp*, *CuYqcb*, *CuYqcc* and *CuYqco*, gave only one *g* value and these values are given in Table 6.6. The EPR spectra of these encapsulated complexes at 77 K [Figure 6.7] exhibit axial spectra ($g_{\parallel} < g_{\perp}$) and their spin Hamiltonian parameters are given in Table 6.6.

Table 6.6: EPR spectral data of encapsulated complexes at RT & LNT

Encapsulated complexes	at RT	at LNT		
	g	$g_\parallel$	$g_\perp$	$A_\parallel$*
CuYqch	2.170	2.404	2.114	130
CuYqce	2.178	2.399	2.114	133
CuYqcp	2.170	2.148	2.107	120
CuYqcb	2.083	2.395	2.089	130
CuYqcc	2.124	2.391	2.044	140
CuYqco	2.170	2.435	2.117	173

*The 'A' values are expressed in units of cm^{-1} multiplied by a factor of 10^{-4}.

EPR spectrum of CuYqch

EPR spectrum of CuYqce

EPR spectrum of CuYqcp

EPR spectrum of CuYqcb

EPR spectrum of CuYqcc   *EPR spectrum of CuYqco*
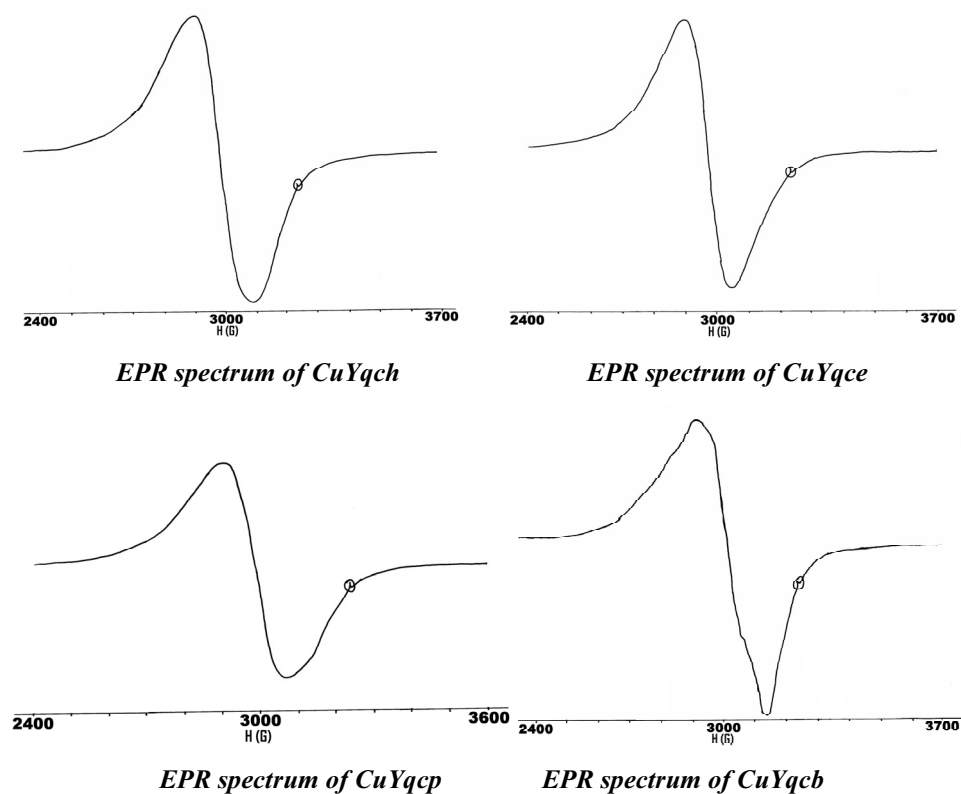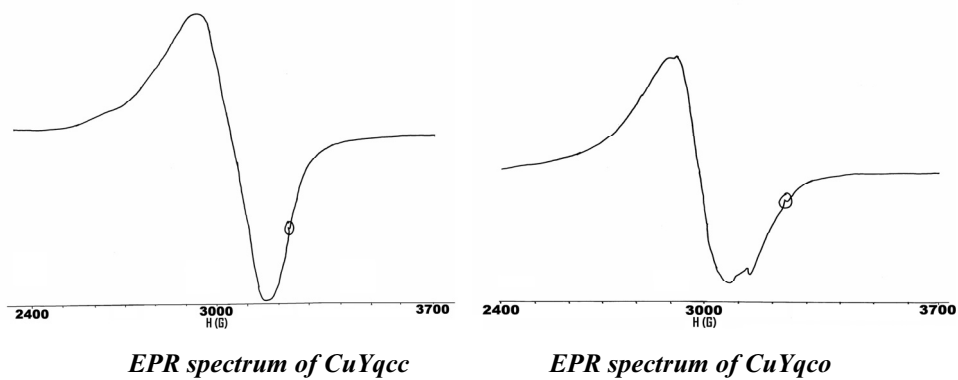
Figure 6.6: EPR spectra of encapsulated copper(II) Schiff base complexes, powder at RT

EPR spectrum of CuYqch   *EPR spectrum of CuYqce*

EPR spectrum of CuYqcp   *EPR spectrum of CuYqcb*

EPR spectrum of CuYqcc   EPR spectrum of CuYqco
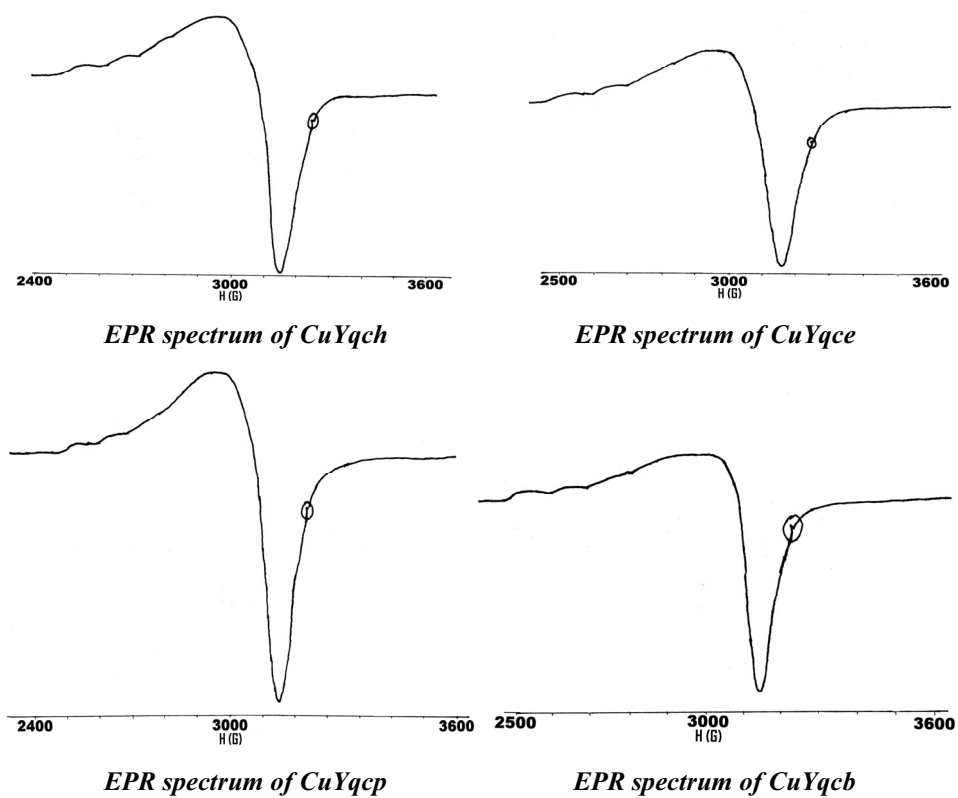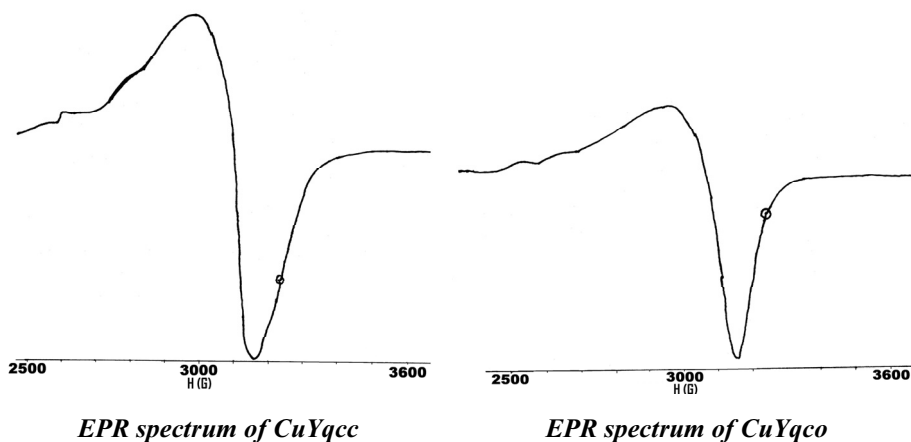
Figure 6.7: EPR spectra of encapsulated copper(II) Schiff base complexes, powder at LNT

6.4 CONCLUSIONS

This chapter presents studies involving the preparation and characterisation of zeolite Y encapsulated complexes, *CuYqch*, *CuYqce*, *CuYqcp*, *CuYqcb*, *CuYqcc* and *CuYqco*. The analytical data shows that the Si/Al ratio is 2.6, which is an indication of the retention of the zeolite framework without any damage after complexation. Reduction in the surface area and pore volume of the zeolite encapsulated complexes supports the inclusion of complexes in the zeolite cages. TG-DTG data gives another evidence for the inclusion of copper(II) Schiff base complexes in the pores of zeolites. XRD patterns and FTIR spectral data suggest that the zeolite structure is retained as such on encapsulation. SEM of the zeolite encapsulated complexes after soxhlet extraction indicates that there is no surface adsorbed species and its crystal structure is clear. Diffuse reflectance spectra indicate that all the zeolite encapsulated Cu(II) complexes have octahedral geometry.

REFERENCES

1. P. P. Knops-Gerrits, M. Labbé, W. H. Leung, A.-M. Van Bavel, G. Langouche, I. Bruynseraede, P. A. Jacobs, *Stud. Surf. Sci. Catal.*, 101 (**1996**) 811.

2. B. Fan, W. Fan, R. Li, *Stud. Surf. Sci. Catal.*, 135 (**2001**) 297.

3. T. M. Salama, I. O. Ali, A. I. Hanafy, W. M. Al-Meligy, *Materials Chemistry and Physics*, 113 (**2009**) 159.

4. B. Fan, W. Cheng, R. Li, *Stud. Surf. Sci. Catal.*, 135 (**2001**) 250.

5. M. Salavati-Niasari, F. Davar, K. Saberyan, *Polyhedron*, 29 (**2010**) 2149.

6. M. Salavati-Niasari, Z. Salimi, M. Bazarganipour, F. Davar, *Inorg. Chim. Acta*, 362 (**2009**) 3715.

7. I. Neves, C. Freire, A. N. Zakharov, B. de Castro, J. k. Figueiredo, *Colloids and Surfaces A: Physicochemical and Engineering Aspects*, 115 (**1996**) 249.

8. P. P. Knops-Gerrits, M. Labbe, P. A. Jacobs, *Stud. Surf. Sci. Catal.*, 108 (**1997**) 445.

9. F. Bedioui, *Coord. Chem. Rev.*, 144 (**1995**) 39.

10. R. F. Parton, I. F. J. Vankelecom, M. J. A. Casselman, C. P. Bezoukhanova, J. B. Utterhoeven, P. A. Jacobs, *Nature*, 370 (**1994**) 541.

11. N. Herron, *Inorg. Chem.*, 25 (**1986**) 4714.

12. R. Ganesan, B. Viswanathan, *J. Mol. Catal. A: Chem.*, 223 (**2004**) 21.

13. D. E. Devos, F. T. Starzyk, P. A. Jacobs, *Angew. Chem.*, 33 (**1994**) 431.

14. D. E. Devos, P. A. Jacobs, *Catal. Today*, 57 (**2000**) 105.

15. R. Ganesan, B. Viswanathan, *J. Mol. Catal. A: Chem.*, 181 (**2002**) 99.

16. Y. Xia, L. Fang, L. He'an, *J. Cent. South Univ. Technol.*, 14 (**2007**) 78.

17. K. J. Balkus Jr., M. Eissa, R. Levado, *J. Am. Chem. Soc.*, 117 (**1995**) 10753.

18. K. J. Balkus Jr., A. G. Gabrielov, *J. Inclusion Phenom. Mol. Recogn. Chem.*, 21 (**1995**) 159.

19. W. H. Quayle, J. H. Lunsford, *Inorg. Chem.*, 21 (**1982**) 97.

20. T. A. Egerton, A. Hagan, F. S. Stone, J. C. Vickerman, *J. Chem. Soc., Faraday Trans.*, 168 (**1972**) 723.

21. E. F. Vansant, J. H. Lunsford, *J. Phys. Chem.*, 76 (**1972**) 2860.

22. J. H. Lunsford, E. F. Vansant, *J. Chem. Soc., Faraday Trans.*, 69 (**1973**) 1028.

23. N. R. Suja, Ph. D Thesis, *Studies on some cobalt(II), Nickel(II) and copper(II) complexes of o-phenylenediamine and Schiff bases derived from 3-hydroxy quinoxaline-2-carboxaldehyde*, Cochin University of Science and Technology, (**2002**).

24. J. Strutz, H. Diegruber, N. I. Jaeger, R. Mosler, *Zeolites*, 3 (**1983**) 102.

25. K. Mizuno, J. H. Luunsford, *Inorg. Chem.*, 22 (**1983**) 3484.

26. N. Öztürk, F. Ucun, A. D. Muhtar, S. Bahçeli, *Journal of Molecular Structure*, 922 (**2009**) 35.

27. R. Raja, P. Ratnasamy, *J. Catalysis*, 170 (**1997**) 244.

28. A. Gu1nesü, O. Bayraktar, S. Yılmaz, *Ind. Eng. Chem. Res.*, 45 (**2006**) 54.

29. K. Nakamoto, *Coordination Compounds. In Infrared and Raman Spectra of Inorganic and Coordination Compounds*, 4th Ed., John Wiley and Sons, New York, (**1986**).

30. K. O. Xavier, J. Chacko, K. K. M. Yusuff, *Appl. Catal. A: Gen.*, 258 (**2004**) 251.

****✿****

Studies on the catalytic activity of zeolite encapsulated copper(II) Schiff base complexes

7.1 INTRODUCTION

A great effort has been devoted to the research and development of new catalysts used for the most important industrial chemical reactions. In most cases, extreme reaction conditions such as high pressure and high temperature are required for the current industrial processes. Development of more efficient catalysts for a required reaction is one of the most important aspects connected with both industrial and academic research. Catalytic oxidation of organic substrates such as alcohols to aldehydes or ketones is a vital reaction in synthetic organic chemistry. Ketones, like cyclohexanone, are important intermediate materials for the manufacture of many important products, such as fiber, drugs and fragrance. Most of such oxidation reactions are still using homogeneous catalysts. From the sustainable and green chemistry point of view, heterogeneous catalysts would be attractive since they offer the advantages of easy catalyst separation, possible catalyst recycle and sometimes high activity and selectivity. Therefore, encapsulation of transition metal complex in zeolites has gained much

interest in the last decade [1-8] since this process can give rise to the materials with both homogeneous catalysis and heterogeneous catalysis characters [9-15].

The need to develop environmentally friendly catalytic oxidations derives not only from the nature and potential toxicity of the metal present in the stoichiometric oxidant, but also from the general principle of green chemistry to reduce the volume of byproducts formed in the overall synthetic route. So in catalytic oxidations, the stoichiometric oxidants used are molecular oxygen, hydrogen peroxide, alkyl hydroperoxide, persulfate, percarbonate, perborate and hypochlorite. Hydrogen peroxide is probably the best terminal oxidant after dioxygen with respect to environmental and economic considerations [16-19]. In certain circumstances, it is better than oxygen as O_2/organic mixtures can sometimes spontaneously ignite. In many oxidation reactions, *tert-*butylhydroperoxide has also been used as oxidant [20].

Oxyfunctionalisation of alcohols to aldehydes and ketones is one of the widely used chemical transformations in industries as these products are important precursors in the synthesis of many drugs, vitamins, and fragrances [21]. In this regard, oxidation products of cyclohexanol to cyclohexanone and adipic acid have been widely used not only as important intermediates in the manufacture of nylon-66 and nylon-6 but also as plasticizers and food additives [22-30]. Other uses of cyclohexanone are as starting materials in the synthesis of insecticides, herbicides, and pharmaceuticals [23]. Therefore, researchers are interested in the development of simple and environmentally friendly methods of their syntheses. Cyclohexanone is manufactured by two processes:- in one process, the cyclohexane is oxidized to cyclohexanol which on dehydrogenation at 400-500 °C and at atmospheric pressure over Zn or Cu catalyst forms cyclohexanone and in the other process phenol is first hydrogenated with nickel catalyst at 140-160 °C and 15 bar pressure to cyclohexanol, which on

hydrogenation yields cyclohexanone. Homogeneous liquid phase catalytic oxidation reactions generally involve the use of soluble salts or transition metal complexes in combination with oxidants like O_2, H_2O_2, or RO_2H (R alkyl, aryl). Despite the good activities and very often excellent selectivities, there are several problems encountered with homogeneous catalysts, particularly in catalyst separation, recovery, and recycling after the reaction. These problem have been claimed to that minimised by using zeolite encapsulated [Cu(salen)] for the oxidation of cyclohexanol to cyclohexanone [31].

In the light of this, we have used the encapsulated copper(II) Schiff base complexes, *CuYqch*, *CuYqce*, *CuYqcp*, *CuYqcb*, *CuYqcc* and *CuYqco* for the oxidation of cyclohexanol. We have also used the simple complexes for this reaction, $[Cu(qch)Cl_2] \cdot 2H_2O$, $[Cu_2(qce)_2]Cl_4 \cdot H_2O$, $[Cu(qcp)ClH_2O]Cl \cdot 2H_2O$, $[Cu(qcb)Cl(H_2O)]Cl$, $[Cu(qcc)Cl_2]$ and $[Cu(qco)Cl_2] \cdot H_2O$, as catalysts for this reaction with a view to compare the efficiency of encapsulated complexes with that of the simple complexes. For convenience, these simple complexes have been designated as *Cuqch, Cuqce, Cuqcp, Cuqcb, Cuqcc* and *Cuqco*. Details regarding the synthesis and characterisation of these simple and their encapsulated complexes are presented in chapter 5 and chapter 6, respectively. This chapter deals with the studies on the efficiency of these simple and supported complexes as catalyst in cyclohexanol oxidation reaction. The results of these studies are discussed in this chapter.

7.2 EXPERIMENTAL

7.2.1 Materials

The materials used for this study are presented in Chapter 2.

7.2.2 Procedure: Catalytic activity measurements

Oxidation of cyclohexanol was carried out in a two-necked glass reactor (50 mL) fitted with a condenser and a septum. Tertiary butylhydroperoxide (70%) was added through the septum to the magnetically stirred solution of cyclohexanol containing catalyst (simple or encapsulated copper(II) complexes). The reaction mixture was kept at the desired reaction temperature and was refluxed with continuous stirring on a water bath. The progress of the reaction was monitored by periodically withdrawing small samples (about 0.5 mL each), which were analysed using a gas chromatograph. The catalyst (the encapsulated copper(II) complexes) after carrying out the oxidation reaction was characterised using physico-chemical techniques. The catalysts were recycled and used to study this oxidation reaction.

7.3 RESULTS AND DISCUSSION

Details of the spectral characterisation of the Schiff base ligands, their simple and encapsulated copper(II) Schiff base complexes are given in Chapters 2, 5 and 6 respectively. As discussed in section 7.1 two major products expected for cyclohexanol oxidation are cyclohexanone and adipic acid. But this oxidation reaction when carried out with our catalysts (*CuYqch*, *CuYqce*, *CuYqcp*, *CuYqcb*, *CuYqcc* and *CuYqco*) yields only one product. The product was cyclohexanone [Scheme 7.1].
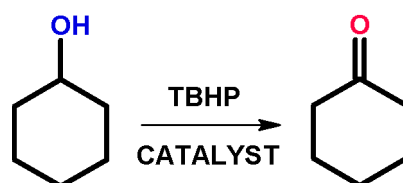
Scheme 7.1: Oxidation of cyclohexanol

A comparative study of the catalytic activity for this reaction was carried out both homogeneously and heterogeneously. For the studies, the simple and encapsulated copper(II) complexes were used as catalysts. Hydrogen peroxide was used as oxidant in this reaction, but no characteristic evolution of oxygen with encapsulated complexes was observed. Therefore, we used a strong oxidant such as *tert*-butylhydroperoxide (TBHP) for this oxidation reaction with simple and encapsulated complexes as catalysts. The first run of the reaction was carried out with these catalysts in solvents like methanol, ethanol, chlorobenzene *etc*. The percentage conversion of cyclohexanol in these cases was found to be approximately similar to that for the reaction carried out without any solvent. As the interaction of organic solvents with *tert*-butylhydroperoxide might result in the contamination of the products and create environmental problems [28,32], we decided to carry out the reactions in the solvent free system. In this reaction cyclohexanone was observed as primary target product and no adipic acid was formed.

7.3.1 Catalytic activity towards the oxidation of cyclohexanol: screening studies

The catalytic performances of the synthesised catalysts for the selective oxidation of cyclohexanol were studied in detail with 70% *tert*-butylhydroperoxide (TBHP) as an oxidant. The reaction was carried without any solvent at 70 °C in a simple glass reactor, keeping the molar ratio of cyclohexanol to *tert*-butylhydroperoxide as two. The products of the oxidation reaction and the percentage conversion were found out using a gas chromatograph (CHEMITO 8510 GC) with carbowax column. The percentage conversion of cyclohexanol was noted after three hours of the reaction, and the data obtained for various catalysts (60 mg each), are given in Table 7.1 and are also represented graphically in Figures 7.1 and 7.2.

Table 7.1 Percentage conversion of cyclohexanol to cyclohexanone in screening studies using simple and encapsulated complexes as catalysts.

Catalyst (Encapsulated complex)	Conversion (%)	Selectivity (%)	Catalyst (Simple complexs)	Conversion (%)	Selectivity (%)
CuYqch	30.58	100	Cuqch	15.22	100
CuYqce	17.64	100	Cuqce	18.90	100
CuYqcp	25.11	100	Cuqcp	13.23	100
CuYqcb	20.85	100	Cuqcb	11.78	100
CuYqcc	23.35	100	Cuqcc	10.56	100
CuYqco	15.42	100	Cuqco	8.25	100

Reaction conditions:	Amount of catalyst: 60 mg
	Oxidant to substrate mole ratio: 2
	Temperature: 70 °C
	Time: 3 hours
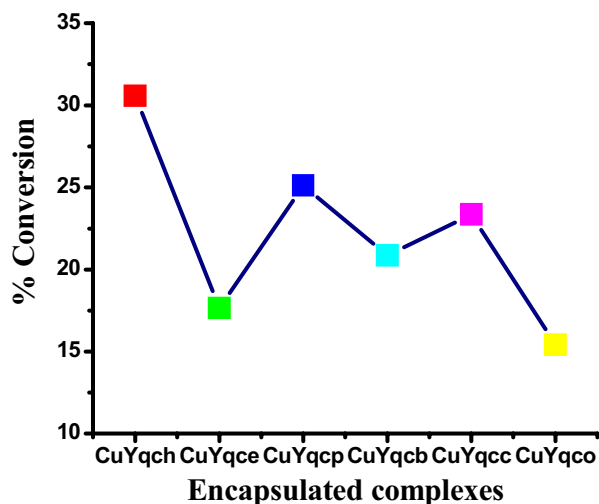
Figure 7.1: Percentage conversion of cyclohexanol with the encapsulated complexes as catalysts.
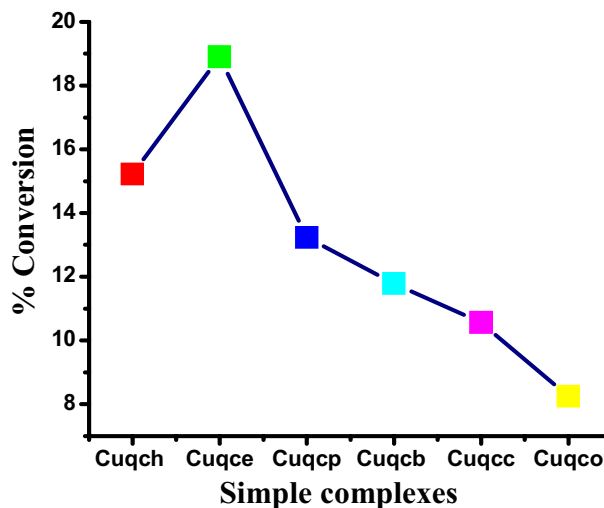
Figure 7.2: Percentage conversion of cyclohexanol with the simple complexes as catalysts.

The product was found to cyclohexanone and there are no other side products. So the reaction is 100% selective and the product of this reaction is industrially useful. It was found that among the encapsulated complexes the *CuYqch* complex was the most active one. The higher catalytic activity of *CuYqch* may be due to the changes of its redox potential on encapsulation. Another reason for higher activity may be due to shape selectivity of the zeolite pore which enhances the decomposition of TBHP. The order of reactivity of encapsulated complexes in the oxidation reaction may be given as *CuYqch > CuYqcp > CuYqcc > CuYqcb > CuYqce > CuYqco*. The same reaction was done with simple complexes as catalysts. The order of reaction is: *Cuqce > Cuqch > Cuqcp> CuYqcb > CuYqcc> CuYqco*. Among the simple complexes, *Cuqce* shows highest percentage conversion, which might be due to its binuclear tetrahedral geometry. The percentage conversion of cyclohexanol for the simple complexes was found to be lesser than that of encapsulated complexes. As in the case of the encapsulated complexes, the product for the simple complexes (as catalysts) is also cyclohexanone and the reaction is 100 % selective.

7.3.2 Blank run

The blank run was conducted in the absence of any catalyst at 70 °C keeping the conditions same as that of screening experiments. There was no conversion occurred even after four hours duration, which indicates that TBHP by itself will not be able to bring about the oxidation of cyclohexanol.

7.3.3 Effect of various parameters on catalysis

A detailed investigation of oxidation of cyclohexanol was carried out to study the influence of various factors. The reaction was performed under solvent free conditions by variation of (1) amount of catalyst (2) reaction time (3) oxidant to substrate ratio and (4) temperature.

7.3.3.1 Influence of the catalyst

To analyse the dependence of amount of catalyst on the oxidation of cyclohexanol, a series of experiments were carried out by varying the amount of catalyst from 20 mg to 80 mg range at 70 °C keeping molar concentration of both the oxidant and substrate and the reaction time constant. A favourable effect of conversion is observed with an increase of amount of catalyst from 20 up to 60 mg [Tables 7.2 and 7.3]. These results are also represented graphically in Figures 7.3 and 7.4. There is no change in the selectivity of product formation with increasing the amount of catalyst. Percentage cyclohexanol conversion is increased to a maximum with 60 mg of catalyst and then decreased with further increase in the amount of catalyst. The reason for the higher conversion may be due to the decomposition of *tert*-butylhydroperoxide with large amount of catalyst.

Table 7.2: Effect of amount of catalyst on the oxidation of cyclohexanol

Catalyst (Encapsulated complex)	% Conversion of cyclohexanol			
	20 mg	40 mg	60 mg	80 mg
CuYqch	18.15	21.75	30.58	25.25
CuYqce	9.42	12.44	17.64	16.76
CuYqcp	11.55	15.21	25.11	19.89
CuYqcb	9.12	14.76	20.85	17.56
CuYqcc	10.90	15.79	23.35	18.35
CuYqco	7.21	11.43	15.42	12.15

Reaction conditions:	Oxidant to substrate mole ratio: 2
	Temperature: 70 °C
	Time: 3 hours
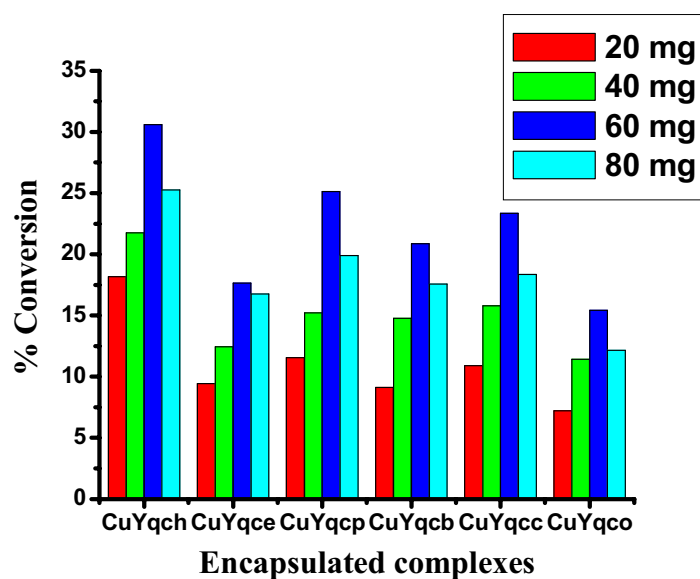
Figure 7.3: Effect of amount of catalyst on the oxidation of cyclohexanol with encapsulated complexes as catalysts

Table 7.3: Effect of amount of catalyst on the oxidation of cyclohexanol

Catalyst (Simple complex)	Conversion of cyclohexanol (%)			
	20 mg	40 mg	60 mg	80 mg
Cuqch	9.89	12.55	15.22	12.40
Cuqce	12.41	16.32	18.90	17.12
Cuqcp	7.85	10.64	13.23	11.04
Cuqcb	6.87	9.35	11.78	8.75
Cuqcc	4.60	6.21	10.56	5.21
Cuqco	3.14	4.98	8.25	3.98

Reaction conditions:	Oxidant to substrate mole ratio: 2
	Temperature: 70 °C
	Time: 3 hours
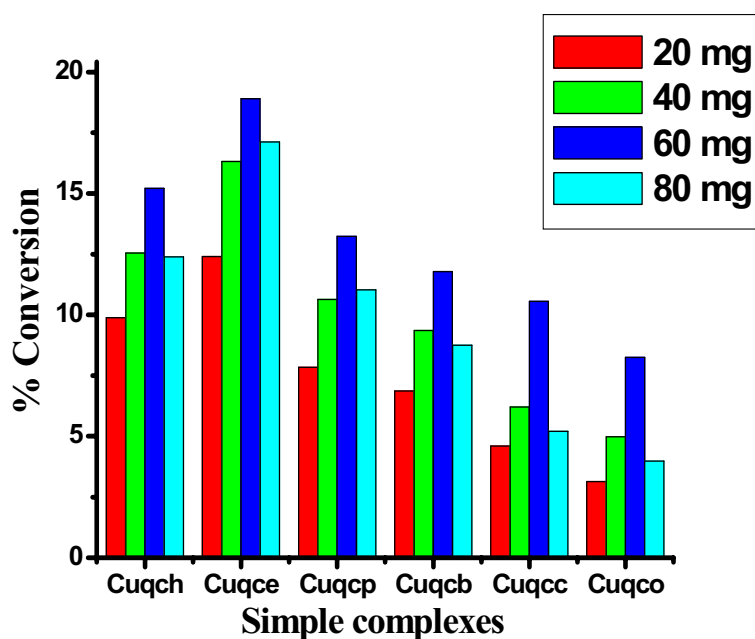
Figure 7.4: **Effect of amount of catalyst on the oxidation of cyclohexanol with simple complexes as catalysts**

7.3.3.2 Influence of the oxidant

The effect of oxidant (*tert*-butylhydroperoxide) on the oxidation of cyclohexanol was studied by varying oxidant to substrate mole ratio in the range 0.5-3 with a constant amount of catalyst (60 mg) at 70 °C and reaction time (3 h) [Tables 7.4 and 7.5]. With increase in the amount of the oxidant to substrate mole ratio, the percentage conversion of cyclohexanol increases. These results are also represented graphically in Figures 7.5 and 7.6. The oxidant efficiency reaches to a maximum in this oxidation reaction at oxidant to substrate mole ratio of 2 and then decreases. No conversion was observed in the absence of *tert*-butylhydroperoxide indicating that the supported catalysts alone could not activate dioxygen at this temperature.

Table 7.4: Effect of oxidant to substrate mole ratio on the oxidation of cyclohexanol

| Catalyst [Encapsulated complex] | Conversion of cyclohexanol (%) | | | |
| | Oxidant to substrate mole ratio | | | |
	0.5	1	2	3
CuYqch	11.67	23.54	30.58	22.79
CuYqce	4.89	11.21	17.64	14.24
CuYqcp	9.23	13.45	25.11	21.12
CuYqcb	5.11	11.21	20.85	13.56
CuYqcc	5.78	12.25	23.35	15.43
CuYqco	3.21	8.13	15.42	12.56

Reaction conditions:	Amount of catalyst: 60 mg
	Temperature: 70 °C
	Time: 3 hours
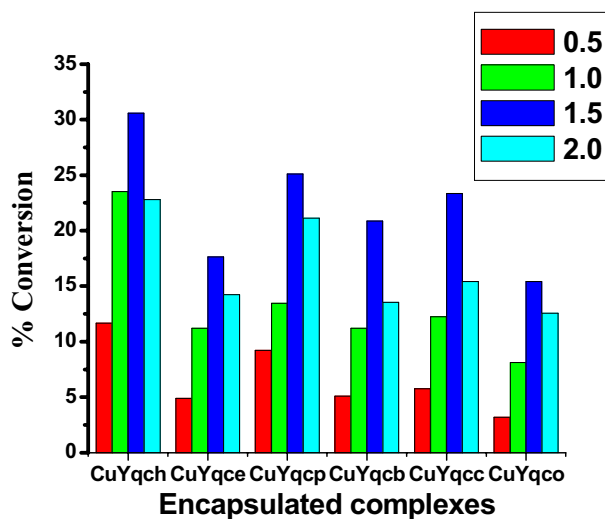
Figure 7.5: Effect of oxidant to substrate ratio on the oxidation of cyclohexanol with encapsulated complexes as catalysts

Table 7.5: Effect of oxidant to substrate mole ratio on the oxidation of cyclohexanol

Catalyst [Simple complex]	Conversion of cyclohexanol (%)			
	Oxidant to substrate mole ratio			
	0.5	1	2	3
Cuqch	4.13	9.42	15.22	10.94
Cuqce	5.55	11.05	18.90	13.31
Cuqcp	4.03	8.25	13.23	10.05
Cuqcb	3.17	6.54	11.78	8.56
Cuqcc	2.10	4.98	10.56	6.98
Cuqco	0.97	3.21	8.25	4.13

Reaction conditions:	Amount of catalyst: 60 mg
	Temperature: 70 °C
	Time: 3 hours

Figure 7.6: Effect of oxidant to substrate ratio on the oxidation of cyclohexanol with simple complexes as catalysts

7.3.3.3 Influence of reaction temperature

The influence of temperature on the conversion of cyclohexanol was studied by the reaction at four different temperatures while keeping the amount of catalyst, oxidant to substrate mole ratio and reaction time constant [Tables 7.6 and 7.7]. The temperature range used on the conversion of cyclohexanol was 30 to 90 °C. As the temperature increases, percentage conversion for cyclohexanol oxidation increases. These results are also represented graphically in Figures 7.7 and 7.8. Selection of this particular temperature range is to avoid the enhanced oxidant decomposition [33]. It was found that the temperature above 80 °C, the reactants converts to a tarry product. So the optimum temperature for the reaction was set as 70 °C.

Table 7.6: Effect of temperature on the oxidation of cyclohexanol

Catalyst [Encapsulated complex]	Conversion of cyclohexanol (%)		
	Temperature (°C)		
	30	50	70
CuYqch	11.25	25.45	30.58
CuYqce	3.45	11.56	17.64
CuYqcp	7.11	13.40	25.11
CuYqcb	4.55	11.05	20.85
CuYqcc	6.10	12.58	23.35
CuYqco	2.25	8.42	15.42

| Reaction conditions:	Amount of catalyst: 60 mg
	Oxidant to substrate mole ratio: 2
	Time: 3 hours
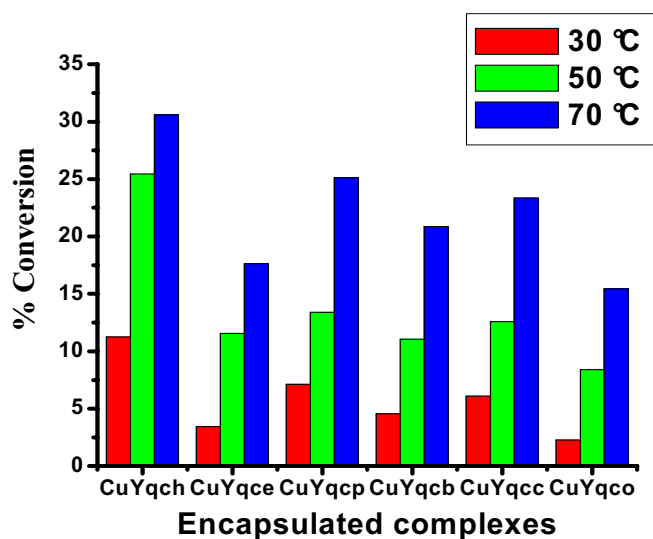
Figure 7.7: Effect of temperature on the oxidation of cyclohexanol with encapsulated complexes as catalysts

Table 7.7: Effect of temperature on the oxidation of cyclohexanol

Catalyst [Simple complex]	Conversion of cyclohexanol (%)		
	Temperature (°C)		
	30	50	70
Cuqch	7.25	10.65	15.22
Cuqce	8.45	11.46	18.90
Cuqcp	5.71	9.50	13.23
Cuqcb	3.55	7.05	11.78
Cuqcc	1.90	5.58	10.56
Cuqco	0.85	3.42	8.25
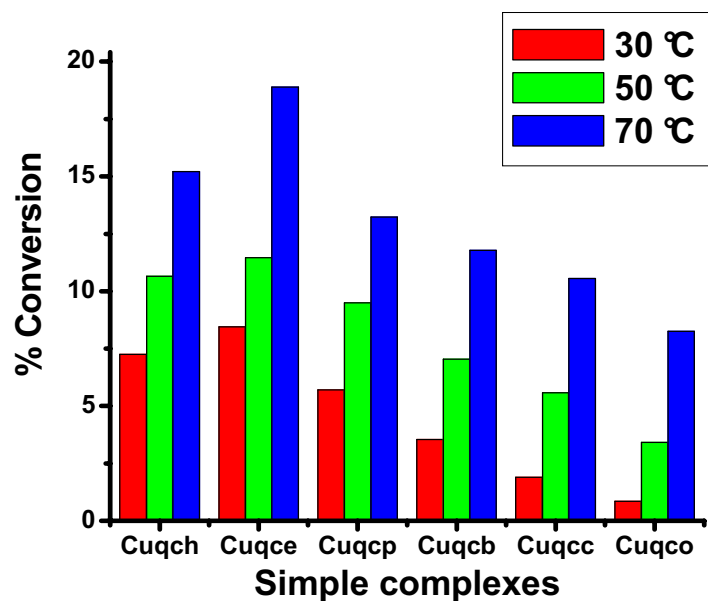
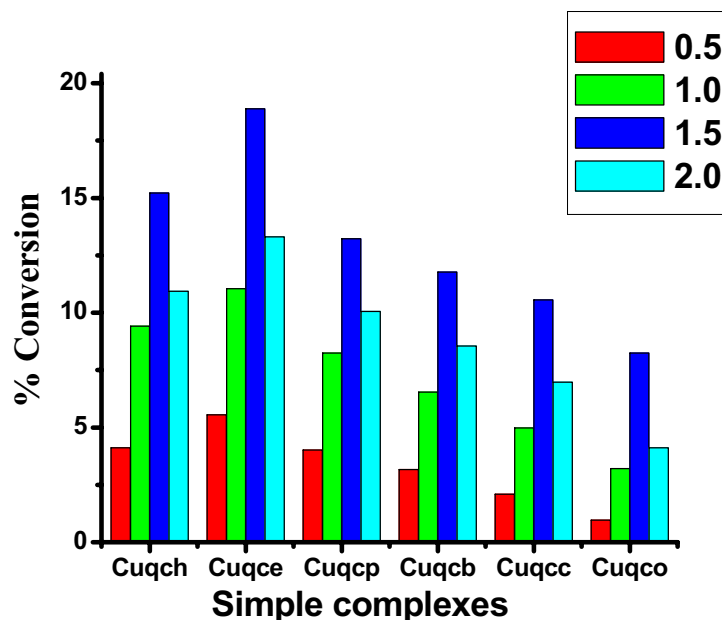**Figure 7.8: Effect of temperature on the oxidation of cyclohexanol with simple complexes as catalysts**

7.3.3.4 Influence of reaction time

The influence of reaction time on the oxidation of cyclohexanol was studied with 60 mg of catalyst with an oxidant to substrate molar ratio is 2 at 70 °C. The percentage conversion of cyclohexanol into cyclohexanone is found to be increase with reaction time [Tables 7.8 and 7.9] and its graphical representation is shown in Figures 7.9 and 7.10. The reaction time was varied from 0 to 4 hours. A longer reaction time is not favourable for this particular reaction as the reaction mixture converts to tar product, when the reaction is carried out for more than 4 hours. The maximum conversion occurred at 3 h and it was selected as the optimum time for reaction.

Table 7.8: Effect of reaction time on the oxidation of cyclohexanol

Catalyst [Encapsulated complex]	Conversion of cyclohexanol (%)		
	Reaction Time (h)		
	1	2	3
CuYqch	12.12	26.54	30.58
CuYqce	5.57	12.38	17.64
CuYqcp	10.22	21.12	25.11
CuYqcb	7.95	15.55	20.85
CuYqcc	9.12	17.43	23.35
CuYqco	4.13	10.11	15.42

| Reaction conditions:	Amount of catalyst: 60 mg
	Oxidant to substrate mole ratio: 2
	Temperature: 70 °C
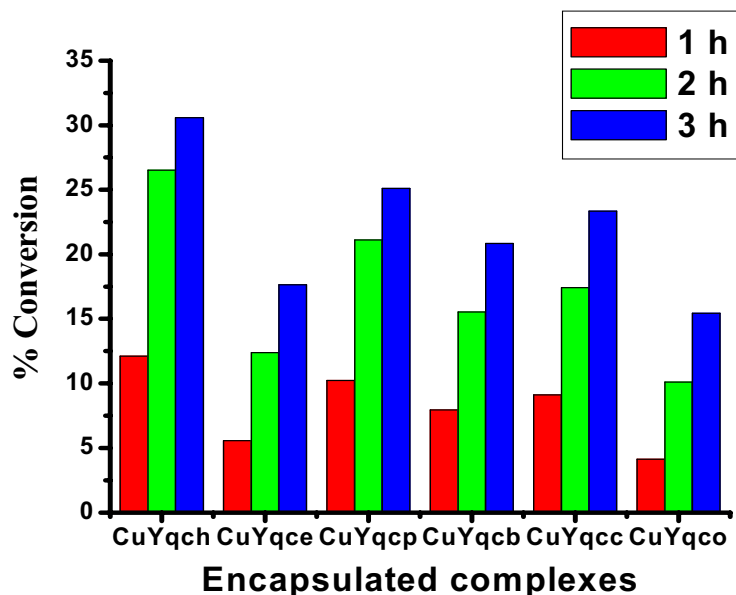
Figure 7.9: Effect of reaction time on the oxidation of cyclohexanol with encapsulated complexes as catalysts

Table 7.9: Effect of reaction time on the oxidation of cyclohexanol

Catalyst [Simple complex]	Conversion of cyclohexanol (%)		
	Reaction Time (h)		
	1	2	3
Cuqch	5.51	10.65	15.22
Cuqce	7.75	12.53	18.90
Cuqcp	4.14	9.48	13.23
Cuqcb	3.57	8.18	11.78
Cuqcc	1.25	6.35	10.56
Cuqco	0.58	4.42	8.25

Reaction conditions:	Amount of catalyst: 60 mg
	Oxidant to substrate mole ratio: 2
	Temperature: 70 °C
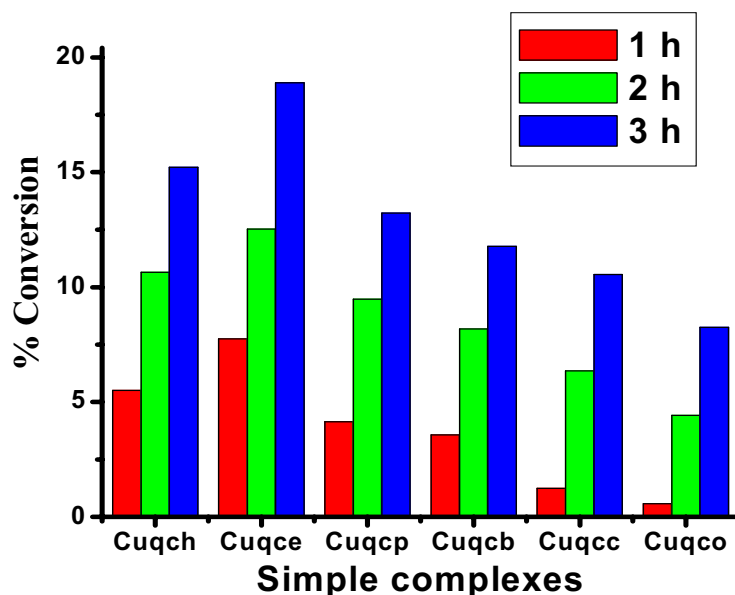
Figure 7.10: Effect of reaction time on the oxidation of cyclohexanol with simple complexes as catalysts

7.3.4 Recycling studies

The encapsulated complexes *CuYqch*, *CuYqce, CuYqcp, CuYqcb, CuYqcc* and *CuYqco,* employed for oxidation of cyclohexanol studies were separated from the reaction mixture, washed with acetone several times and dried in oven to remove the impurities present in the catalyst. The retention of the zeolite structure can be proved from the similar XRD patterns. Then reactions were carried out using recycled catalyst under the same conditions. The percentage conversions of the recycled catalysts are given in Table 7.10. A graphical comparison of the activities of the fresh and recycled samples is presented in Figure 7.11. The similar activity and the spectroscopic properties of the recycled catalyst indicated the preservation of the structural integrity of the synthesised complexes.

Table 7.10: Results of recycling studies

Catalyst [Encapsulated complex]	Fresh sample	Recycled sample First run	Recycled sample Second run
CuYqch	30.58	27.32	22.69
CuYqce	17.64	16.74	12.48
CuYqcp	25.11	23.65	18.35
CuYqcb	20.85	15.98	11.23
CuYqcc	23.35	19.48	12.37
CuYqco	15.42	14.98	12.21

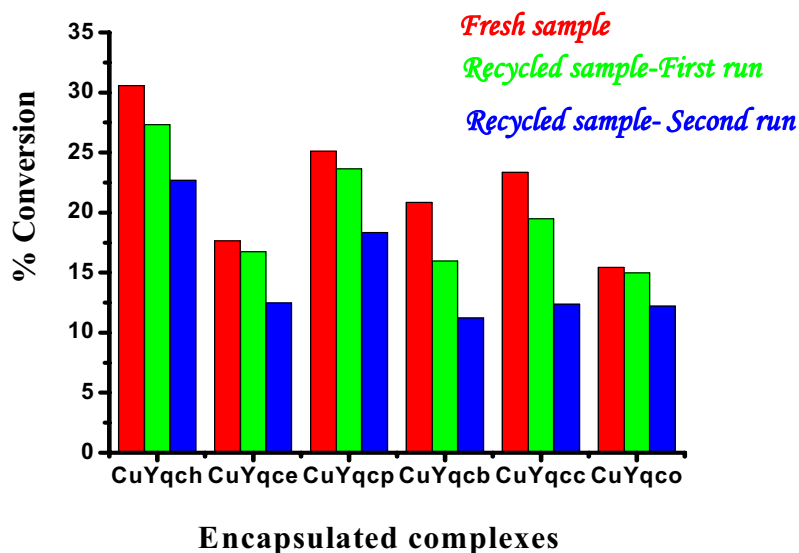| Reaction conditions:	Amount of catalyst: 60 mg
	Oxidant to substrate mole ratio: 2
	Temperature: 70 °C
	Time: 3 hours

Figure 7.11: Comparative studies of the activity of fresh and recycled samples in the oxidation of cyclohexanol using TBHP.

7.4 CONCLUSIONS

The order of the catalytic activity of the simple copper(II) complexes of Schiff bases towards cyclohexanol oxidation with TBHP, as oxidant is *Cuqce > Cuqch > Cuqcp > Cuqcb > Cuqcc > Cuqco*. Among these complexes, *Cuqce* shows highest percentage conversion may be due to its binuclear nature and its tetrahedral geometry. The product of the oxidation reaction is cyclohexanone. Therefore, this oxidation reaction is 100 % selective.

The order of catalytic activity of zeolite encapsulated complexes in the oxidation of cyclohexanol reaction may be given as *CuYqch > CuYqcp > CuYqcc > CuYqcb > CuYqce > CuYqco*. The conversion percentage of about ~ 30% with 100% selectivity toward the formation of cyclohexanone was observed. Only a small amount of the catalyst in mild conditions is able to carry out the oxidation reaction successfully. In addition, *tert*-butylhydroperoxide act as an efficient and environmentally friendly oxidants (as the by-products are only alkyl alcohols). Therefore, this catalysis system is very active and suitable for the oxidation of cyclohexanol.

In summary, the percentage conversion of cyclohexanol was found to be higher for encapsulated complexes than that of their simple complexes. With the increase of reaction time, amount of catalyst, oxidant to substrate mole ratio and temperature, more cyclohexanol is seen to be transformed to cyclohexanone. Optimum values for the reaction were found to be the reaction time (3 h), amount of catalyst (60 mg), oxidant to substrate ratio (2) and temperature (70 °C). Any further increase from these optimum values may result in lower yield of cyclohexanone and in the formation of tarry product. Among the six encapsulated copper(II) complexes *CuYqch* was found to be the very efficient candidate for the conversion of cyclohexanol to cyclohexanone. Finally, the mild conditions, easy working up and the successful one stage oxidation systems are promising for the synthesis of cyclohexanone.

REFERENCES

1. C. R. Jacob, S. P. Varkey, P. Ratnasamy, *Micropor. Mesopor. Mater*, 22 (**1998**) 465.

2. B. Zhan, X. Li, *Chem. Commun.*, (**1998**) 349.

3. K. J. Balkus Jr., M. Eissa, R. Levado, *J. Am. Chem. Soc.*, 117 (**1995**) 10753.

4. T. Kimura, A. Fukuoka, M. Ichikawa, *Catal. Lett.*, 4 (**1990**) 279.

5. B. Fan, W. Fan, R. Li, *Stud. Surf. Sci. Catal.*, 135 (**2001**) 297.

6. B. Fan, W. Cheng, R. Li, *Stud. Surf. Sci. Catal.*, 135 (**2001**) 250.

7. B. Fan, W. Fan, R. Li, *J. Mol. Catal. A*, 201 (**2003**) 137.

8. T. Joseph, S. B. Halligudi, C. Satyanarayan, D. P. Sawant, S. Gopinathan, *J. Mol. Catal. A: Chem.*, 168 (**2001**) 87.

9. P. S. Chittilappilly, N. Sridevi, K. K. M. Yusuff, *J. Mol. Catal. A*: *Chem.*, 286 (**2008**) 92.

10. K. O. Xavier, J. Chacko, K. K. M. Yusuff, *Appl. Catal. A: Gen.*, 258 (**2004**) 251.

11. M. Salavati-Niasari , Z. Salimi , M. Bazarganipour, F. Davar, *Inorg. Chim. Acta*, 362 (**2009**) 3715.

12. M. R. Maurya, A. K. Chandrakar, S. Chand, *J. Mol. Catal. A*: *Chem.*, 263 (**2007**) 227.

13. A. H. Ahmed, Z. M. El-Bahy, T. M. Salam, *Journal of Molecular Structure*, 969 (**2010**) 9.

14. M. Salavati-Niasari, A. Sobhani, *J. Mol. Catal. A*: *Chem.*, 285 (**2008**) 58.

15 M. R. Maurya, A. K. Chandrakar, S. Chand, *J. Mol. Catal. A*: *Chem.*, 274 (**2007**) 192.

16. C. W. Jones, *Applications of Hydrogen Peroxide and Derivatives*, MPG Books Ltd., Cornwall, U.K., (**1999**).

17. K. A. Jorgensen, *Chem. Rev.*, 89 (**1989**) 431.

18. W. Adam, *In Peroxide Chemistry Mechanistic and Preparative Aspects of Oxygen Transfer*, Wiley-VCH, Darmstadt, Germany, (**2000**).

19. W. R. Sanderson, *Pure Appl. Chem.*, 72 (**2000**) 1289.

20. M. H. Peyrovi, V. Mahdavi, M. A. Salehi, R. Mahmoodian, *Catal. Commun.*, 6 (**2005**) 476.

21. M. Salavati-Niasari, E. Zamani, M. R. Ganjali, P. Norouzi, *J. Mol. Catal. A*: *Chem.*, 261 (**2007**) 196.

22. Q. Yi, J. Zhang, W. Huang, X. Liu, *Catal. Commun.*, 8 (**2007**) 1017.

23. A. Sakthivel, P. Selvam, *J. Catalysis*, 211 (**2002**) 134.

24. R. Serpa da Cruz, J. M. de Souza e Silva, U. Arnold, U. Schuchardt, *J. Mol. Catal. A: Chem.*, 171 (**2001**) 251.

25. E. V. Spinacee, U. Schuchardt, D. Cardoso, *Appl. Catal. A: Gen.*, 185 (**1999**) 193.

26. S. Klein, J. A. Martens, R. Parton, K. Vercruysse, P. A. Jacobs, W. F. Maier, *Catal. Lett.*, 38 (**1996**) 209.

27. R. Hutter, T. Mallat, A. Baiker, *J. Catalysis*, 153 (**1995**) 177.

28. R. E. Reim, R. M. Van Effen, *Anal. Chem.*, 58 (**1986**) 3203.

29. X. Zhang, K. Y. Chan, A. C. C. Tseung, *J. Electroanal. Chem.*, 386 (**1995**) 241.

30. J. Wang, Z. Taha, *Anal. Chem.*, 62 (**1990**) 1413.

31. C. Ratnasamy, A. Murugkarand, S. Padhye, *Indian J. Chem.*, 35A (**1995**) 1.

32. G. Qian, D. Ji, G-M. Lu, R. Zhao, Y-X. Qi, J-S. Suo, *J. Catalysis*, 232 (**2005**) 378.

33. A. Dubey, V. Rives, S. Kannan, *J. Mol. Catal. A: Chem.*, 181 (**2002**) 151.

****✿****

Biological studies of copper(II) Schiff base complexes

Contents	**8.1 Introduction** **8.2 Experimental** **8.3 Results and discussion** **8.4 Conclusions** **References**

8.1 INTRODUCTION

Several reviews have appeared discussing the roles of metal ions in biological systems [1-4]. The involvement of metal complex formation in normal life processes has led to reviews such as "The effects of chelating agents on organisms"[5], "Chelation in medicine" [6] "Metal binding in medicine" [7], "Metal chelates in biological systems", [8] and "Structure and bonding in biochemistry" [9]. The aims of these reviews [10] are to draw the attention of coordination chemistry researches to focus upon metal complexes in biological systems. Many Schiff base complexes with transition metals have drawn wide attention because of their diverse biological and pharmaceutical activities [11,12]. The literature survey showed that the chelating Schiff base ligands derived from diamines and various carbonyl compounds encompass a highly remarkable class of compounds having a wide range of applications in clinical [13], biochemical [14,15] and physiological activities [16,17].

Deoxy ribonucleic acid (DNA) is the primary target molecule for most anticancer and antiviral therapies according to cell biologists. Investigations on the interaction of DNA with small molecules are important in the design of new types of pharmaceutical molecules. Since the chemical nuclease activity of transition metal complexes was discovered in the 1980s, there has been a great interest in studying the interaction model and the mechanism of transition metal complexes with DNA. There are metal complexes which interact with DNA and induce the breakage of DNA strands by appropriate methods [18-21]. DNA is an important genetic substance in organisms. Any errors in gene expression can often cause diseases and play a secondary role in the outcome and severity of human diseases. Thus, there is an increasing focus on the binding study of small molecules to DNA during the last decades. A more complete understanding of DNA binding is necessary to design a new drug. There are three DNA binding modes, they are intercalative binding, groove binding and external electrostatic binding. Among these interactions, intercalation and groove binding are the most important DNA binding modes as they invariably lead to cellular degradation. Intercalative binding results when small molecules or the drug intercalate into the nonpolar interior of the DNA helix. Groove binding interactions involve direct interactions of the bound molecule with edges of base pairs in either of the major (G-C) or (A-T) grooves of the nucleic acids. Electrostatic interaction happens in the case of positively charged molecules. They electrostatically interact with the negatively charged phosphate backbone of DNA chain. Geometry of the complexes is mainly responsible for the affinity of the metal complexes to DNA. The geometry of complexes depends on the metal ion type and different functional groups in the ligands. So the investigation on the interaction of the Schiff base transition metal complexes with DNA has a great significance for disease defense, new medicine design and clinical application of drugs.

Copper complexes are of particular interest with regard to DNA cleavage through oxidative pathways [19-22]. Biological activities such as antibacterial and anticancer properties of Cu(II) complexes have been also reported [23-24].

Transition metal complexes with tunable coordination environments and versatile spectral and electrochemical properties offer a great scope for the design of species that are suitable for DNA binding and cleavage activities. Hence, the synthesis of symmetrical and unsymmetrical binuclear Cu(II) complexes has gained more attention in recent years [25].

DNA binding activity of copper(II) complexes of Schiff base, *N,N′*-bis(3,5-*tert*-butylsalicylidene-2-hydroxy)-1,3-propanediamine, has been reported [11]. These complexes bind to DNA by moderate intercalative binding modes. Furthermore, all these complexes can cleave plasmid DNA to nicked DNA in a sequential manner as the concentrations or reaction times are increased. Their cleavage activities are promoted in the presence of hydrogen peroxide. Liu *et al*. [26] reported the cytotoxic and DNA binding activity of Cu(II) Schiff base complexes, which was derived from 2-oxoquinoline-3-carbaldehyde.

Quinoxaline derivatives are present in several biologically active compounds and play an important role in the synthesis of the pharmaceuticals [27,28]. Based on these reports, the synthesized copper(II) Schiff base complexes were screened to know whether these complexes have any cytotoxic and DNA binding activities. The results of the cytotoxicity and DNA cleavage studies are presented in this chapter.

8.2 EXPERIMENTAL

8.2.1 Materials

The materials used for the preparation of Schiff base ligands and their copper(II) complexes are presented in Chapter 2. Dalton Lymphoma Ascites (DLA) cells (Amala Cancer Research Center, Thrissur, Kerala), phosphate buffer saline (PBS) [NaCl 4 g, NaH_2PO_4 0.72 g, KH_2PO_4 0.1 g, KCl 0.1 g, distilled water 500 mL], trypan blue, haemocytometer, agarose gel, ethydium bromide

(Sigma Aldrich), tris-acetate-EDTA buffer and pUC18 DNA (GeNei, Bangalore) were used in this study.

8.2.2 Methods

8.2.2.1 Synthesis of Schiff base ligands

The synthesis of Schiff base ligands, *qch*, *qce*, *qcp*, *qcb*, *qcc* and *qco*, are given in Chapter 2.

8.2.2.2 Synthesis of copper(II) nitrate complexes

The synthesis of copper(II) nitrate complexes are given in Chapter 5.

8.2.2.3 In vitro cytotoxicity studies of copper(II) complexes - *Trypan blue exclusion method*

The predictive value of in vitro cytotoxicity test is based on the idea that toxic chemicals affect basic functions of cells which are common to all cells, and that the toxicity can be measured by assessing cellular damage. The main focus of the research for the development of in vitro cytotoxicity assays is to rapidly evaluate the potential toxicity of large numbers of compounds, to limit animal experimentation whenever possible, and to carry out tests with small quantities of compound. Evidence for the utility of in vitro cytotoxicity tests has led many pharmaceutical companies to screen compound libraries to remove potentially toxic compounds early in the drug discovery process. In the trypan blue exclusion method, a cell suspension is simply mixed with dye and then visually examined to determine whether cells take up or exclude dye. In the protocol presented here, a viable cell will have a clear cytoplasm whereas a nonviable cell will have a blue cytoplasm. Trypan blue exclusion, as described in the above protocol, can be performed in 5 to 10 min [29,30].

In vitro cytotoxicity of the copper(II) nitrate complexes were studied on Dalton Lymphoma Ascites (DLA) cells by trypan blue exclusion method. The principle behind this method is that the drug at toxic concentration damages the cell and makes pores on the membrane through which trypan blue enters. The damaged cells are stained blue by trypan blue stain and can be distinguished from viable cells. Live cells are excluded from staining. The general procedure for this study is given below:

DLA cells were aspirated from the peritoneal cavity of tumour bearing mice. These cells were washed three times using phosphate buffered saline (PBS). The viability of the cells was checked by using trypan blue. Different dilution (10^{-1}, 10^{-2} and 10^{-3} M) of cells was made. The number of cells in the 10^{-3} M dilution was counted by the use of haemocytometer and cell number was adjusted to 1×10^7 cells/mL. The experiment was set up by incubating different concentration of the drug with 1×10^6 cells. The final volume of the assay mixture was made upto 1 mL using PBS and was incubated at 37 °C for about three hours. 1.0 mL of trypan blue was added after incubation and the number of dead cells was counted using a haemocytometer. The percentage of viable cells was calculated as follows:

$$\text{Viable cells (\%)} = \frac{\text{Total number of viable cells per mL of aliquot}}{\text{Total number of cells per mL of aliquot}} \times 100$$

8.2.2.4 DNA Cleavage Studies of Copper(II) Complexes -*Gel electrophoresis*

The cleavage of DNA by metal complexes was studied using agarose gel electrophoresis [31-34]. The ability of the copper(II) nitrate complexes for the DNA cleavage was also checked by agarose gel electrophoresis, which was performed by incubation at 37 °C for 1 h as follows: pUC18 plasmid DNA of 0.25 μg/μL concentration was used for the experiments. Stock solutions of the Cu(II) complexes (10^{-3} M) in demineralised water with DMSO were freshly

prepared before use. Aliquot parts of 3 µL of the Cu(II) complex solutions were added to aliquot parts of 5 µL of the pUC18 DNA in 20 µL of a Tris-acetate EDTA buffer solution. The reaction mixture was incubated at 37 °C for 1 h, and then 4 µL of charge marker were added to aliquots parts of 20 µL of the adduct complex/DNA. The mixtures were electrophoretised in agarose gel (1%) at 80 V for 1 h. After that the DNA was dyed with ethydium bromide solution (0.5 µg/µL in TBE) for 20 min. A sample of free DNA was used as a control. After electrophoresis, bands were visualised by UV light and photographed.

8.3 RESULTS AND DISCUSSION

8.3.1 In vitro cytotoxicity study

The complexes, $[Cu(qch)NO_3(H_2O)]NO_3$ **13**, $[Cu_2(qce)_2](NO_3)_2$ $(OH)_2 \cdot 9H_2O$ **14**, $[Cu(qcp)NO_3(H_2O)]NO_3$ **15**, $[Cu(qcb)NO_3H_2O]NO_3$ **16**, $[Cu(qcc)(H_2O)_2](NO_3)_2$ **17** and $[Cu(qco)(NO_3)_2] \cdot 2H_2O$ **18**, were studied for short term in vitro cytotoxicty using Dalton's Lymphoma Ascites cells. The tumour cells were aspirated from the peritoneal cavity of tumour bearing mice, washed thrice with normal saline and checked for viability using trypan blue dye exclusion method. The cell suspension (1×10^6 cells in 0.1 mL) was added to tubes containing various concentrations of the test compounds and the volume was made upto 1mL using phosphate buffered saline (PBS). In the control tube only cell suspension was taken. These assay mixtures were incubated for 3 hour at 37 °C and percent of dead cells were evaluated by trypan blue exclusion method. Results of this study are given in Table 8.1.

Table 8.1: Effect of copper(II) complexes against DLA cell lines by trypan blue dye exclusion method

Concentration of the complexes µg	Sample					
	Percent cell death (%)					
	13	14	15	16	17	18
200	100	83	100	100	100	100
100	82	64	100	100	100	100
50	63	58	100	78	90	92
20	50	19	98	46	80	86
10	50	12	95	20	78	80

Cells were treated at concentrations ranging from 10-200 µg/mL of the complex for 48 h and then the percentage of cell viability was analysed. Viable cells which remained unstained by trypan blue were counted in a haemocytometer. The percentage cytotoxicity of the DLA cells at different concentrations ranging from 10-200 µg/mL was calculated. Results showed a drug (the copper(II) Schiff base complexes **13-18**) dose dependent inhibition of the growth of DLA cells. The results are also represented in Figure 8.1. All the complexes except **14** produced 100% cytotoxicity at 200 µg/mL. The complexes **15**, **16**, **17** and **18** exhibit 100% cytotoxicity even at 100 µg/mL. Complex **15** $[Cu(qcp)NO_3(H_2O)]NO_3$ was found to have higher cytotoxicity effect than that for the other complexes. Complex **14** $[Cu_2(qce)_2](NO_3)_2(OH)_2 \cdot 9H_2O$ shows slightly lower activity, when compared to that of the other complexes. This study reveal the cytotoxicity nature of copper(II) Schiff base complexes against DLA cells.
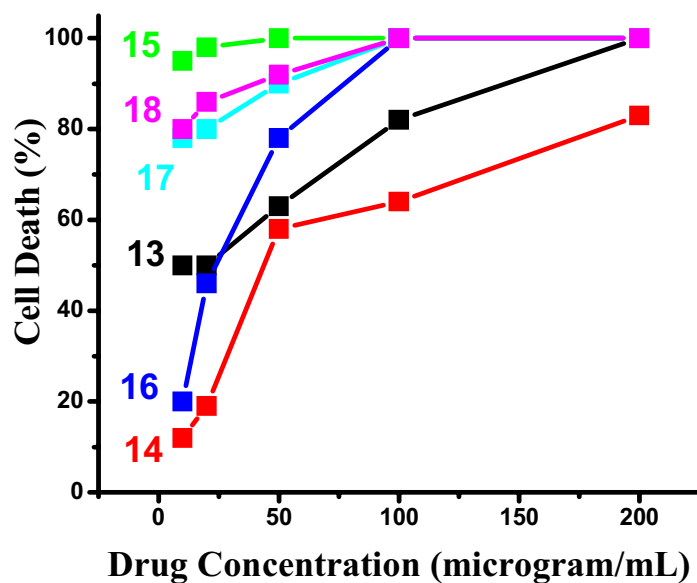
Figure 8.1: Effect of copper(II) complexes against DLA cell lines by trypan blue dye exclusion method

8.3.2 DNA cleavage studies of the copper(II) complexes

The ability of the copper(II) complexes, [Cu(qch)NO$_3$(H$_2$O)]NO$_3$ **13**, [Cu$_2$(qce)$_2$](NO$_3$)$_2$(OH)$_2$·9H$_2$O **14**, [Cu(qcp)NO$_3$(H$_2$O)]NO$_3$ **15**, [Cu(qcb)NO$_3$H$_2$O] NO$_3$ **16**, [Cu(qcc)(H$_2$O)$_2$](NO$_3$)$_2$ **17** and [Cu(qco)(NO$_3$)$_2$]·2H$_2$O **18**, to cleave DNA was tested by gel electrophoresis method. In our study pUC18 DNA was used as the sample. pUC18 is a plasmid DNA of 2686 base pairs. On agarose gel, pUC18 shows three distinct bands corresponding to the three different conformations of the plasmid, namely, open circular, linear and supercoiled forms. The three different conformations interchange, *ie*, supercoiled to open circular and open circular to linear, depending on different physical and chemicals factors. In the present study, the copper(II) complexes were tested for their DNA

binding property. The image of bands obtained after gel electrophoresis is shown in Figure 8.2.
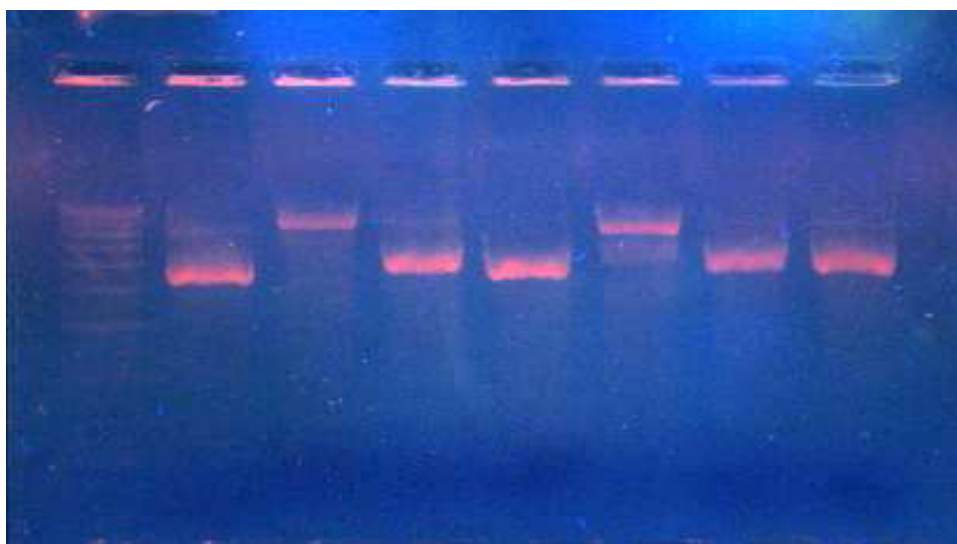
Figure 8.2: *DNA Fragmentation by copper(II) complexes*

The image of DNA cleavage consists of several lanes and it is marked as following:

Lane 1: 500 bp DNA marker

Lane 2: pUC 18 DNA

Lane 3: pUC 18 DNA + [Cu$_2$(qce)$_2$](NO$_3$)$_2$(OH)$_2$·9H$_2$O **14**

Lane 4: pUC 18 DNA + [Cu(qcp)NO$_3$(H$_2$O)]NO$_3$ **15**

Lane 5: pUC 18 DNA + [Cu(qch)NO$_3$(H$_2$O)]NO$_3$ **13**

Lane 6: pUC 18 DNA + [Cu(qcb)NO$_3$H$_2$O]NO$_3$ **16**

Lane 7: pUC 18 DNA + [Cu(qcc)(H$_2$O)$_2$](NO$_3$)$_2$ **17**

Lane 8: pUC 18 DNA + [Cu(qco)(NO$_3$)$_2$]·2H$_2$O **18**

In the above gel photo, two bands are visible for pUC18 DNA (Lane 2) which corresponds to the open circular and supercoiled form of DNA. Only one band is seen in the third and sixth lane, which suggest that the binding of the copper(II) complexes (**14** and **16**) cause a change in the conformation of DNA from supercoiled to open circular form. Likewise, in lanes 4, 5, 7 and 8, only one band is seen which corresponds to supercoiled form of pUC18 DNA. Thus it could be concluded that the binding of the metal complex results in nicking of the DNA strand. Among these complexes, $[Cu_2(qce)_2](NO_3)_2(OH)_2 \cdot 9H_2O$ **14** and $[Cu(qcb)NO_3H_2O]NO_3$ **16**, act as very good DNA cleavagers.

8.4 CONCLUSIONS

Results of the present study suggest that the copper(II) complexes could induce tumor cell death by physiological and pathological means. The potency of complexes, $[Cu_2(qce)_2](NO_3)_2(OH)_2 \cdot 9H_2O$ **14** and $[Cu(qcb)NO_3H_2O]NO_3$ **16** to bring about the cytotoxicity decreases with decrease of dose and they can also cleave the pUC18 plasmid DNA efficiently. Thus, the synthesized Cu(II) complexes exhibit a low DNA cleavage activity together with moderate cytotoxicity against DLA cell lines.

REFERENCES

1   R. J. P. Williams, *Roy. Inst. Chem. Rev.*, 13 (**1968**).

2   R. J. P. Williams, *Quart. Reu. Chem. Soc.*, 24 (**1970**) 331.

3   D. R. Williams, *The Metals of Life*, Van Nostrand, London, (**1971**).

4   H. Sigel, D. B. Mc Cormick, *Accounts Chem. Res.*, 3 (**1970**) 201.

5   A. Albert, *Aust. J. Sci.*, 30 (**1967**) 1.

6   J. Schubert, *Sci. Amer.*, 214 (**1966**) 40.

7   M. J. Seven, L. A. Johnson, *Metal Binding in Medicine*, Lippincott Co., Philadelphia, (**1960**).

8   F. P. Dwyer, D. P. Mellor, *Chelating Agents and Metal Chelates*, Academic Press, London, (**1964**) 383.

9   J. D. Dunitz, *Struct. Bonding*, 8 (**1970**).

10   D. R. Williams, *Chem. Rev.*, 72 (**1972**) 203.

11   S. Padhye, G. B. Kauffman, *Coord. Chem. Rev.*, 63 (**1985**) 127.

12   L. Wang, Y. Zhu, Z. Yang, J. Wu, Q. Wang, *Polyhedron*, 10 (**1991**) 2477.

13   T. Kovelskaya, I. Ganusevich, S. P. Osinsky, I. Levitin, L. Bubnovskaya, A. Sigan, V. Michailenko, *Inorganic cobalt(III) complexes with Schiff bases as a new anticancer agents with radio/thermosensitizing activities*, Poster 33, 6th Internet World Congress for Biomedical Sciences, (**2000**).

14.   C. A. Bolos, G. St Nikolov, L. Ekateriniadou, A. Kortsaris D. A. Kyriakidis, *Metal Based Drugs*, 5 (**1998**) 323.

15.   L. T. Yıldırım, R. Kurtaran, H. Namli ,A. D. Azaz, O. Atakol, *Polyhedron*, 26 (**2007**) 4187.

16.   T. Takeuchi, A. Böttcher, C. M. Quezada, M. I. Simon, T. J. Meade, H. B. Gray, *J. Am. Chem. Soc.*, 120 (**1988**) 8555.

17.   W. Liu, C. Qing, X. Chen, Q. Ye, Y. Yu, S. Hou, *Chem. Pharm. Bull.*, 56 (**2008**) 659.

18.   K. E. Erkkila, D. T. Odom, J. K. Barton, *Chem. Rev.*, 99 (**1999**) 2777.

19.   J. K. Barton, A. L. Raphael, *J. Am. Chem. Soc.*, 106 (**1984**) 2466.

20.   A. Chouai, S. E. Wicke, C. Turro, J. Bacsa, K. R. Dunbar, D. Wang, R. P. Thummel, *Inorg. Chem.*, 44 (**2005**) 5996.

21.   S. Thyagarajan, N. N. Murthy, A. A. N. Sarjeant, K. D. Karlin, S. E. Rokita, *J. Am. Chem. Soc.*, 128 (**2006**) 7003.

22.   M. J. Fernandez. B.Wilson, M. Palacios, M. M. Rodrigo, K. B. Grant, A. Lorente, *Bioconjugate Chem.*, 18 (**2007**) 121.

23   I.-ul-H. Bhat, S. Tabassum, *Spectrochim. Acta Part A*, 72 (**2009**) 1026.

24   V. Uma, M. Kanthimathi, T. Weyhermuller, B. U. Nair, *J. Inorg. Biochem.*, 99 (**2005**) 2299.

25   B. Dede, I. Ozmen, F. Karipcin, *Polyhedron*, 28 (**2009**) 3967.

26   Z.-C. Liu, B.-D. Wang, B. Li, Q. Wang, Z.-Y. Yang, T.-R. Li, Y. Li, *Euro. J. Med. Chem.*, 45 (**2010**) 5353.

27   A. Carta, S. Piras, G. Loriga, G. Paglietti Chemistry, *Mini-Rev Med. Chem.*, 6 (**2006**) 1179.

28   X. Li, K.-H. Yang, W.-L. Li, W.-F. Xu, *Drugs Future*, 31 (**2006**) 979.

29   W. Strober, *Current Protocols in Immunology*, (**1997**) A.3B.1-A.3B.2.

30   H. M. Shapiro, *Practical Flow Cytometry*, 2nd ed., John Wiley & Sons, New York, (**1988**) 129.

31   N. Raman, S. Shobha, A. Thamaraichelvan, *Spectrochim. Acta Part A*, 78 (**2011**) 888.

32   A. Arbuse, M. Font, M. A. Martınez, X. Fontrodona, M. J. Prieto, V. Moreno, X. Sala, A. Llobet, *Inorg. Chem.*, 48 (**2009**) 11098.

33   J. Chen, X. Wang, Y. Shao, J. Zhu, Y. Zhu, Y. Li, Q. Xu, Z. Guo, *Inorg. Chem.*, 46 (**2007**) 3306.

34   N. Raman, J. D. Raja, A. Sakthivel, *J. Chem. Sci.*, 119 (**2007**) 303.

****✿****

Summary and Conclusion

The chelating Schiff bases belong to a highly remarkable class of ligands in coordination chemistry. Multidentate Schiff base ligands can bind one, two, or more metal centers and thus can form homo and/or heteronuclear metal complexes. They have gained increasing attention in recent years due to their applications in various areas such as catalysis, medicine, and material science. Quinoxaline based Schiff bases can be used as an important ligand in coordination chemistry. Details of the studies on the synthesis, single crystal XRD studies, spectral characterisation, catalytic and biological applications of some new transition metal complexes of the Schiff bases derived from quinoxaline-2-carboxaldehyde are presented in this thesis. The thesis is divided into eight chapters. Contents of the various chapters are briefly described as follows:

The chapter 1 presents a general introduction to Schiff bases and their complexes of manganese(II), nickel(II) and copper(II). A brief discussion on the synthetic methodologies, various applications of quinoxalines, the zeolite encapsulated complexes and the advantages of heterogenization of metal complexes are presented. The objectives and scope of the present work are highlighted at the end of this chapter.

Details regarding the materials used in the current study and the various characterisation methods used to study the synthesised ligands and their simple

and encapsulated complexes are presented in chapter 2. Information about synthesis and characterisation of the six Schiff bases, *N,N′*-bis(quinoxaline-2-carboxylidene)hydrazine (*qch*), *N,N′*-bis(quinoxaline-2-carboxylidene)-1,2-diaminoethane (*qce*), *N,N′*-bis(quinoxaline-2-carboxylidene)-1,3-diaminopropane (*qcp*), *N,N′*-bis(quinoxaline-2-carboxylidene)-1,4-diaminobutane (*qcb*), *N,N′*-bis(quinoxaline-2-carboxylidene)-1,2-diaminocyclohexane (*qcc*) and *N,N′*-bis(quinoxaline-2-carboxylidene)-1,2-diaminobenzene (*qco*) is also included in this chapter. Among these, *qce*, *qcp*, *qcb* and *qcc* have been characterised by single crystal X-ray diffraction studies. The *qce* and *qcc* crystallises in triclinic system and *qcp* and *qcb* in monoclinic system. The crystal structures of these are stabilised by intermolecular C—H…N interactions.

Chapter 3 deals with synthesis and characterisation of manganese(II) complexes of *qch, qce, qcp, qcb, qcc* and *qco*. The complexes were prepared by refluxing manganese(II) chloride in methanol and $CH_3OH/CHCl_3$ solution of the Schiff base. Analytical data show that the complexes are formed in 1:1 metal to Schiff base ratio, except for the complex of *qch*, which is formed in 1:2 ratio. The number and nature of water molecules associated with the complexes were estimated by thermogravimetry. Molar conductance measurements suggest that the complexes of *qce* and *qcc* are 1:1 electrolytes, those of *qcp* and *qcb* are 1:2 electrolytes and others are non electrolytes. Based on these studies, the complexes have been assigned the following molecular formula: $[Mn(qch)_2Cl_2]\cdot2H_2O$, $[Mn(qce)Cl(H_2O)]Cl$, $[Mn(qcp)(H_2O)_2]Cl_2$, $[Mn(qcb)(H_2O)_2]Cl_2$, $[Mn(qcc)Cl(H_2O)]$ $Cl\cdot H_2O$, $[Mn(qco)Cl_2]\cdot H_2O$. All the complexes are stable. FTIR spectra of ligands reveal that a $\nu(C=N)$ band occurs for azomethine C=N in the region at 1610-1640 cm^{-1} and for quinoxaline ring in the region at 1550-1580 cm^{-1}. These bands are found to be shifted to lower frequencies in the spectra of complexes indicating coordination of the azomethine nitrogen atoms and quinoxaline ring nitrogen atoms are coordinated to the manganese(II) ion. The presence of water molecules

in these complexes were also confirmed from the IR spectra. Electronic spectra of the manganese complexes exhibit intraligand transitions and also spin forbidden transitions from the ^6A_1g ground state, which indicate octahedral geometry of the complexes. The X-band EPR spectra of the complexes in DMF at LNT display well resolved six-line hyperfine signals. All the complexes exhibit magnetic moment value of ~5.9 B.M. expected for high spin d^5 complexes. The physico-chemical and spectroscopic studies suggest an octahedral geometry for all the complexes.

Details regarding the synthesis and characterisation of nickel(II) complexes of the Schiff bases, *qch, qce, qcp, qcb, qcc* and *qco* are presented in chapter 4. The complexes were prepared by refluxing a $CH_3OH/CHCl_3$ solution of the Schiff base and nickel(II) perchlorate in methanol. Analytical data show that complexes are formed in 1:1 metal to ligand ratio except for the complex of *qch* (1:2 ratio). Complexes of *qch, qce* and *qco* are 1:1 electrolytes and that of *qcb* is 2:1 electrolyte. The complexes of *qcp* and *qcc* are non-electrolytes. The complexes have been assigned the molecular formula: $[Ni(qch)_2(ClO_4)H_2O]ClO_4$, $[Ni(qce)(ClO_4)H_2O]ClO_4$, $[Ni(qcp)(ClO_4)_2]\cdot 2H_2O$, $[Ni(qcb)(H_2O)_2](ClO_4)_2$, $[Ni(qcc)(ClO_4)_2]\cdot H_2O$ and $[Ni(qco)(ClO_4)H_2O]ClO_4$. IR spectral studies reveal that the $\nu(C=N)$ of both azomethine and quinoxaline ring of the Schiff bases were seen to be shifted to lower frequency indicating the coordination of azomethine nitrogen and quinoxaline ring nitrogen to nickel ion. The coordination of the azomethine and quinoxaline ring nitrogen is further supported by the appearance of new bands due to M-N in complexes at 510-540 cm^{-1}. The presence of lattice water/coordinated water in complexes is revealed by the presence of a broad band in the region 3600-3400 cm^{-1}. Furthermore, complexes of *qch, qce, qcc* and *qco* exhibit perchlorate bands in the 1160-1080 cm^{-1} range, suggesting monodentate coordination of perchlorate to the nickel ion. The complex of *qcb* shows a broad unsplit band at 1094 and 627 cm^{-1}, indicates the presence of an ionic perchlorate

group. These are in good agreement with the results of molar conductivity measurements. The electronic spectra of the complexes in methanol show three distinct bands at ~13000 cm^{-1} ($^3A_2g \rightarrow {}^3T_2g$), ~18,000cm^{-1} ($^3A_2g \rightarrow {}^3T_1g$ (F)), and at ~23,000 cm^{-1} ($^3A_2g \rightarrow {}^3T_2g$) which are characteristic for the octahedral Ni(II) coordination. The physico-chemical and spectroscopic measurements show that all the complexes have octahedral geometry.

Chapter 5 deals with a studies on the synthesis and characterisation of the twenty four copper(II) complexes. The complexes were prepared by refluxing a CHCl$_3$/CH$_3$OH solution of ligand (*qch, qce, qcp, qcb, qcc* or *qco*) with copper(II) acetate/chloride/nitrate/perchlorate in methanol. Elemental analysis data show that the complexes of Schiff bases, except those of *qch*, are formed in 1:1 metal ligand ratio. In the case of *qch*, the complexes are formed in 1:2 ratios. They are soluble in common solvents. The presence of lattice and coordinated water in the complexes is confirmed by the FTIR and TG analysis. The complexes have been assigned the molecular formula: [Cu(qch)$_2$(X)$_2$]·2H$_2$O (where X= OAc, Cl or ClO$_4$), [Cu(qch)$_2$NO$_3$(H$_2$O)]NO$_3$, [Cu$_2$(qce)$_2$(OAc)$_4$]·H$_2$O, [Cu$_2$(qce)$_2$]X$_4$·nH$_2$O (where X= Cl or ClO$_4$), [Cu$_2$(qce)$_2$](NO$_3$)$_2$(OH)$_2$·9H$_2$O, [Cu(qcp)(OAc)$_2$]·2H$_2$O, [Cu(qcp)ClH$_2$O]Cl·2H$_2$O, [Cu(qcp)NO$_3$(H$_2$O)]NO$_3$, [Cu(qcp)(H$_2$O)$_2$](ClO$_4$)$_2$, [Cu(qcb)(OAc)$_2$]·3H$_2$O, [Cu(qcb)X(H$_2$O)]X (where X= NO$_3$, Cl or ClO$_4$), [Cu(qcc)(X)$_2$]·nH$_2$O (where X= OAc or Cl), [Cu(qcc)(H$_2$O)$_2$](X)$_2$ (where X= NO$_3$ or ClO$_4$) and [Cu(qco)(X)$_2$]·nH$_2$O (where X= OAc, Cl, NO$_3$ or ClO$_4$). The infrared spectral data show that Schiff base ligands are coordinated to copper ion through the azomethine nitrogen and quinoxaline nitrogen. The unidentate coordination of acetate ion in these complexes is supported by the IR spectra. The IR spectra of nitrate complexes showed bands corresponding to the free nitrate ion and the unidentate coordination of nitrate groups in complexes. The IR spectra of the perchlorate complexes showed bands at around ~1094 cm^{-1} and 627 cm^{-1} suggesting that the perchlorate ions are not coordinated to the copper ions.

The split perchlorate bands in the IR spectra at ~ 1120, 1098 and 1025 cm^{-1} are indicative of the presence of coordinated perchlorate. These results are in good agreement with the molar conductivity values. The electronic spectra of the copper(II) complexes in methanol show d-d bands in the region 20,000-13,000 cm^{-1} which can be assigned to $^2Eg \rightarrow {}^2T_2g$ transition of an octahedral geometry. Low temperature X-band EPR spectra of the copper(II) complexes show axial spectra having $g_\parallel > g_\perp > 2.0023$ and rhombic spectra. From the physico-chemical and spectroscopic studies, a tetrahedral geometry was assigned for complexes [Cu$_2$(qce)$_2$]X$_4$·nH$_2$O (where X= Cl or ClO$_4$) and [Cu$_2$(qce)$_2$](NO$_3$)$_2$(OH)$_2$· 9H$_2$O and for all the other complexes, an octahedral geometry was assigned.

The chapter 6 presents studies involving the preparation and characterisation of zeolite Y encapsulated complexes, *CuYqch*, *CuYqce*, *CuYqcp*, *CuYqcb*, *CuYqcc* and *CuYqco*. The analytical data show that the Si/Al ratio is 2.6, which is an indication of the retention of the zeolite framework without any damage after complexation. Reduction in the surface area and pore volume of the zeolite encapsulated complexes supports the inclusion of complexes in the zeolite cages. The quinoxaline C=N stretching frequency of the ligands was found to be shifted to lower frequency on complexation indicating that this nitrogen atom is also involved in coordination to copper ions. XRD patterns and FTIR spectral data suggest that the zeolite structure is retained as such on encapsulation. SEM of the zeolite encapsulated complexes after soxhlet extraction indicates that there is no surface adsorbed species. Diffuse reflectance spectra exhibit d-d bands, which indicate that all the zeolite encapsulated Cu(II) complexes have octahedral geometry. As compared to the corresponding neat complex, the thermal stability of the encapsulated complexes is greatly enhanced.

Chapter 7 deals with the studies on the catalytic activity of the simple and zeolite encapsulated copper complexes in cyclohexanol oxidation reactions. The

order of the catalytic activity of the simple complexes is *Cuqce > Cuqch > Cuqcp > Cuqcb > Cuqcc > Cuqco*. Among these complexes, *Cuqce* shows highest percentage conversion, which may be due to its binuclear nature and tetrahedral geometry.   The only product of the oxidation reaction is cyclohexanone. Therefore, this oxidation reaction is 100 % selective.   The order of catalytic activity of zeolite encapsulated complexes is *CuYqch > CuYqcp > CuYqcc > CuYqcb > CuYqce > CuYqco*. The percentage conversion of cyclohexanol was found to be higher for encapsulated complexes than that of the simple complexes. Detailed study of the catalytic activity of the complexes was carried out by changing different parameters like the, amount of catalyst, oxidant to substrate ratio, temperature and reaction time.

Details on the biological activity studies of the complexes, obtained by the interaction of copper(II) nitrate with the Schiff base, *qch, qce, qcp, qcb, qcc* or *qco*, are presented in chapter 8. The methods used for carrying out biological studies are also included in this chapter. These complexes were checked for cytotoxicity and DNA cleavage studies. In vitro cytotoxicity was done by Trypan blue exclusion method. Cytotoxic activity was found to be higher for the complex of *qcp*. Gel electrophoresis method was used for DNA cleavage studies. Binding of the complexes of the ligands *N,N′*-bis(quinoxaline-2-carboxylidene)-1,2-diaminoethane (*qce*), and *N,N′*-bis(quinoxaline-2-carboxylidene)-1,4-diaminobutane (*qcb*), with DNA results in the nicking of DNA and in the change of its conformation.

****✿****

List of research publications

1   Two novel bis-azomethines derived from quinoxaline-2-carbaldehyde, **Digna Varghese**, V. Arun, P. P. Robinson, Manju Sebastian, P. Leeju, G. Varsha, K. K. M. Yusuff, Acta Cryst., C65 (2009) o612–o614.

2   N,N′-Bis[(E)-quinoxalin-2-ylmethylidene]ethane-1,2-diamine,   **Digna Varghese**, V. Arun, Manju Sebastian, P. Leeju, G. Varsha, K. K. M. Yusuff, Acta Cryst., E65 (2009) o435.

3*   N-[(E)-Quinoxalin-2-ylmethylidene]-1-Hindazol-5-amine, P. Leeju, V. Arun, Manju Sebastian, G. Varsha, **Digna Varghese**, K. K. M. Yusuff, Acta Cryst., E65 (2009) o1981.

4*   (Z)-2-Amino-3-[(E)-benzylideneamino]but-2-enedinitrile, G. Varsha, V. Arun, Manju Sebastian, P. Leeju, **Digna Varghese**, K. K. M. Yusuff, Acta Cryst., E65 (2009) o919.

5*   A   novel   fluorescent   bisazomethine   dye   derived   from   3-hydroxyquinoxaline-2-carboxaldehyde and 2,3-diaminomaleonitrile, V. Arun, P. P. Robinson, Manju Sebastian, P. Leeju, G. Varsha, **Digna Varghese**, K. K. M. Yusuff, Dyes and Pigments, 82 (2009) 268–275.

6*   Synthesis, characterization, and structure of a new cobalt(II) Schiff-base   complex   with   quinoxaline-2-carboxalidine-2-amino-5-methylphenol, Manju Sebastian, V. Arun, P. P. Robinson, P. Leeju, **Digna Varghese**, G. Varsha, K. K. M. Yusuff, Journal of Coordination Chemistry, 63 (2009) 307-314.

7*   Two new fluorescent heterocyclic perimidines: first synthesis, crystal structure and spectral characterisation, G. Varsha ,V. Arun, P. P. Robinson, Manju Sebastian, **Digna Varghese**, P. Leeju, V. P. Jayachandran, K. K. M. Yusuff, Tetrahedron Letters, 51 (2010) 2174-2177.

* Not related to the work presented in this thesis.

Assurance of God's Protection

"You who live in the shelter
of the Most High,
who abide in the shadow of the Almighty,
will say to the Lord, "My refuge and my fortress;
my God, in whom I trust."
For He will deliver you from the
snare of the fowler
and from the deadly pestilence;
he will cover you with his pinions
and under His wings you will find refuge;
his faithfulness is a shield and buckler.
You will not fear the terror of the night,
or the arrow that flies by day,
or the pestilence that stalks in darkness,
or the destruction that wastes at noonday.
A thousand may fall at your side,
ten thousand at your right hand,
but it will not come near you.
You will only look with your eyes
and see the punishment of the wicked,
Because you have made the Lord your refuge,
the most high your dwelling place,
no evil shall befall you,
no scourge come near your tent.
For he will command his angels concerning you
to guard you in all your ways.
On their hands they will bear you up,
so that you will not dash your foot against a stone.
You will tread on the lion and the adder,
the young lion and the serpent you will trample under foot.
Those who love me, I will deliver;
I will protect those who know my name.
When they call to me, I will answer them;
I will be with them in trouble,
I will rescue them and honor them.
With long life I will satisfy them,
And show them my salvation."

(The Holy Bible- Psalm 91/1-16)